1986

Irreversible stochastic processes on lattices

Ross Stewart Nord
Iowa State University

INFORMATION TO USERS

This reproduction was made from a copy of a manuscript sent to us for publication and microfilming. While the most advanced technology has been used to photograph and reproduce this manuscript, the quality of the reproduction is heavily dependent upon the quality of the material submitted. Pages in any manuscript may have indistinct print. In all cases the best available copy has been filmed.

The following explanation of techniques is provided to help clarify notations which may appear on this reproduction.

1. Manuscripts may not always be complete. When it is not possible to obtain missing pages, a note appears to indicate this.

2. When copyrighted materials are removed from the manuscript, a note appears to indicate this.

3. Oversize materials (maps, drawings, and charts) are photographed by sectioning the original, beginning at the upper left hand corner and continuing from left to right in equal sections with small overlaps. Each oversize page is also filmed as one exposure and is available, for an additional charge, as a standard 35mm slide or in black and white paper format.*

4. Most photographs reproduce acceptably on positive microfilm or microfiche but lack clarity on xerographic copies made from the microfilm. For an additional charge, all photographs are available in black and white standard 35mm slide format.*

***For more information about black and white slides or enlarged paper reproductions, please contact the Dissertations Customer Services Department.**

U·M·I Dissertation Information Service

University Microfilms International
A Bell & Howell Information Company
300 N. Zeeb Road, Ann Arbor, Michigan 48106

Nord, Ross Stewart

IRREVERSIBLE STOCHASTIC PROCESSES ON LATTICES

Iowa State University PH.D. 1986

PLEASE NOTE:

In all cases this material has been filmed in the best possible way from the available copy. Problems encountered with this document have been identified here with a check mark __✓__.

1. Glossy photographs or pages _____
2. Colored illustrations, paper or print _____
3. Photographs with dark background _____
4. Illustrations are poor copy _____
5. Pages with black marks, not original copy ✓
6. Print shows through as there is text on both sides of page _____
7. Indistinct, broken or small print on several pages ✓
8. Print exceeds margin requirements _____
9. Tightly bound copy with print lost in spine _____
10. Computer printout pages with indistinct print _____
11. Page(s) _____ lacking when material received, and not available from school or author.
12. Page(s) _____ seem to be missing in numbering only as text follows.
13. Two pages numbered _____. Text follows.
14. Curling and wrinkled pages _____
15. Dissertation contains pages with print at a slant, filmed as received _____
16. Other _____

_____

_____

Irreversible stochastic processes on lattices

by

Ross Stewart Nord

A Dissertation Submitted to the
Graduate Faculty in Partial Fulfillment of the
Requirements for the Degree of
DOCTOR OF PHILOSOPHY

Department: Chemistry
Major: Physical Chemistry

Approved:

Signature was redacted for privacy.

In Charge of Major Work

Signature was redacted for privacy.

For the Major Department

Signature was redacted for privacy.

For the Graduate College

Iowa State University
Ames, Iowa
1986

TABLE OF CONTENTS

GENERAL INTRODUCTION

Many processes in chemistry and physics can be modeled by one or more types of events occurring effectively irreversibly and, in general, cooperatively at the sites of a lattice. The event distributions for these models never attain their equilibrium forms (even at the completion of the process) since there are no equilibrating mechanisms operating. The events are "frozen" into place once they have occurred. Consequently, equilibrium statistics, as obtained from the usual equilibrium models, are inappropriate for describing these systems. Therefore, kinetic models have been developed in order to model these types of processes. The aim of these models is to describe the time evolution of the event distribution given an appropriate set of rates of the events.

The time evolution of the event distribution over the entire lattice is given by a master equation[1,2]:

$$\frac{dF_{\underline{A}}}{dt} = \sum_{\underline{B}} \{W_{\underline{B} \to \underline{A}} F_{\underline{B}} - W_{\underline{A} \to \underline{B}} F_{\underline{B}}\} \tag{1.1}$$

Here $\underline{A}$ and $\underline{B}$ are states of the entire lattice, occurring with probabilities $F_{\underline{A}}$ and $F_{\underline{B}}$, and $W_{\underline{A} \to \underline{B}}$ is the transition probability for going from state $\underline{A}$ to state $\underline{B}$.

Thus the first term on the right side of (1.1) describes the increase in $F_{\underline{A}}$ due to state $\underline{B}$ undergoing a transition to state $\underline{A}$, this is summed over all possible states $\underline{B}$. The second term describes the loss in $F_{\underline{A}}$ due

to transitions from state $\underline{A}$ to all possible states $\underline{B}$. The time evolution of $F_{\underline{A}}$ is completely described by the solution of (1.1). Note that (1.1) pertains to reversible, as well as irreversible, processes.

It is often more convenient (and for an infinite lattice more appropriate) to rewrite the master equations in hierarchial form. This can be done by formally summing (1.1) over all states in which the particular subconfiguration of sites of interest appears (the hierarchy of rate equations for the probabilities of various subconfigurations of sites can also be written down intuitively).

Consider a specific irreversible filling process $o \to a$ at single sites. For a particular subconfiguration $\underset{\sim}{\sigma}$ one can write the rate equation[3]

$$\frac{d}{dt} f_{\underset{\sim}{\sigma}} = \sum_{\substack{j \in \underset{\sim}{\sigma} \\ \sigma_j = a}} \sum_{\underset{\sim}{\sigma}^j_*} \tau_{\underset{\sim}{\sigma}^j} f_{\underset{\sim}{\sigma}}(\sigma_j \to o) + \underset{\sim}{\sigma}^j_*$$

$$- \sum_{\substack{j \in \underset{\sim}{\sigma} \\ \sigma_j = o}} \sum_{\underset{\sim}{\sigma}^j_*} \tau_{\underset{\sim}{\sigma}^j} f_{\underset{\sim}{\sigma}} + \underset{\sim}{\sigma}^j_* \quad . \tag{1.2}$$

Here $f_{\underset{\sim}{\sigma}}$ is the probability of finding a configuration $\underset{\sim}{\sigma}$, $\underset{\sim}{\sigma}^j_*$ denotes the configuration of sites which influence the filling rate of j but are not in the configuration $\underset{\sim}{\sigma}$, $\tau_{\underset{\sim}{\sigma}^j}$ is the rate for filling site j (note that the rate is a function of $\underset{\sim}{\sigma}^j_*$), and the sums over j are over all sites j in $\underset{\sim}{\sigma}$ which are filled 'a' and empty 'o', respectively. This equation is easily understood intuitively. The first term in (1.2) corresponds to the

creation of $\underset{\sim}{\sigma}$ by filling the jth site in the configuration $\underset{\sim}{\sigma}(\sigma_j \to 0)$, which has the jth site empty, summed over all such possible sites j, and the second term corresponds to the destruction of $\underset{\sim}{\sigma}$ by filling any of its empty sites. The generalization of (1.2) to cases where more than one site simultaneously fills is straightforward.

Equation (1.2) is quite general and is easily written in explicit form for a specific choice of lattice (size, connectivity, and site-type distribution) and rates. Note that the initial conditions (empty or partially filled lattice) are also arbitrary. For an infinite lattice (1.2) has an infinite number of coupled equations (and for large, finite lattices the number of equations is effectively infinite).

In this work we will be presenting some refinements in the solution techniques which have been used to obtain results from equation (1.2), extensions of previous results, and also extensions of tne models to some new processes. A brief discussion of the solution methods follows.

It is often convenient to perform some preliminary manipulations on the hierarchy in order to display more clearly features that can be exploited in obtaining solutions.

All of the possible equations of the form (1.2) are not independent. It is possible, through conservation of probability, to express any subconfiguration containing filled sites in terms of those containing only empty sites. The advantages of this will become apparent shortly. If we decompose $\underset{\sim}{\sigma}$ into the subset of its filled sites, $\{n\}_a$, and the subset of its empty sites, $\{m\}_o$ we have $\underset{\sim}{\sigma} = \{n\}_a + \{m\}_o$. It then follows that [1,3,4]

$$f_{\{n\}_a + \{m\}_o} = \sum_{\{\ell\}\in\{n\}} (-1)^{\ell} f_{\{m\}_o + \{\ell\}_o} \quad . \tag{1.3}$$

Instead of using the entire hierarchy (1.2), we can consider an equivalent subhierarchy for f's containing only empty sites. Note that equivalently we could also express the hierarchy in terms of f's containing only filled sites.

In certain cases, a subset of the hierarchy can be written which is independent of the other equations in the hierarchy. Thus, for the filling of single, adjacent pairs, triples, ... or any connected group of sites, with arbitrary finite blocking range (range R blocking means that filling cannot occur at a site if there are one or more filled sites within R lattice vectors), one can show that the minimal closed hierarchy involves only $f_{\{m\}_0}$, where $\{m\}_0$ are connected clusters of empty sites, if the filling events have nearest-neighbor cooperative effects or the events are random (i.e., the probability of filling a site or a group of sites is independent of the states of the neighboring sites). This structure was first realized by Plate *et al.*[5] and then by Wolf[1]. This further reduces the size and complexity of the hierarchy. Nevertheless, for an infinite lattice this minimal hierarchy is still infinite.

One way to obtain closed form solutions, in certain cases, is to recast this reduced hierarchy in terms of conditional probabilities $q_{\underset{\sim}{\sigma}\,\underset{\sim}{\bar{\sigma}}'}$ ($\equiv f_{\underset{\sim}{\sigma}+\underset{\sim}{\sigma}'}/f_{\underset{\sim}{\sigma}'}$) of $\underset{\sim}{\sigma}$ given $\underset{\sim}{\sigma}'$. In keeping with the above discussion, we take $\underset{\sim}{\sigma}$ to be a subconfiguration containing only empty sites. These conditional probability equations can then be truncated (in some cases exactly) in order to obtain solutions. This truncation is based upon the following fundamental shielding property which states for a translationally invariant system[4]: Suppose that a wall of empty sites separates the

lattice into two disconnected regions, and is sufficiently thick that any event on the lattice is not simultaneously affected by (the state of) sites on both sides; then sites on one side are shielded from the effect of those on the other. Proof of this property is via self-consistency with the hierarchial equations[4]. Hence, for one-dimensional N-mer filling with range R cooperative effects, we need a wall of empty sites of width N + 2R - 1 to shield sites on one side from the influence of those on the other. As an example, if we consider monomer (1 site) filling with range 1 (nearest-neighbor) cooperative effects, we need a shielding wall of width 2. In two or higher dimensions this wall either closes upon itself or (for an infinite lattice) contains an infinite number of sites, however, in one dimension (1D) two adjacent empty sites will shield. In terms of conditional probabilities this means $q_{o\phi\phi} = q_{o\phi\phi\phi} = q_{o\phi\phi\phi\phi} = q_{o\phi_n}$, $n \geq 2$, (assuming a compatible set of initial conditions) where $\phi(\equiv \bar{o})$ represents a single conditioning site and ϕ_n indicates a string of n conditioning sites. Consequently, we are able to truncate exactly and solve the hierarchy of equations. In general, even in 1D, exact solution is not possible and the shielding property is used to obtain approximate solutions by applying various orders of truncation to the conditional probabilities. Note that only empty sites shield, which explains why it was advantageous to express the hierarchy in terms of the $f_{\{o\}_m}$.

As an alternate method to truncation for solving the hierarchial equations we also consider formal density expansions. In this method we write the hierarchy in terms of probabilities of subconfigurations containing only filled sites (we also confine ourselves to the case of the

initially empty lattice). We are then able (through simple, but tedious manipulations) to express the $f_{\underset{\sim}{\sigma}}$'s in terms of expansions in the density. However, the complexity in calculating the coefficients increases rapidly as the order in the density increases. Therefore, these expansions are most useful at low density (coverage), altnough a resummation procedure can be implemented which allows accurate results to be obtained even at saturation.

Before discussing the solution and results obtained in this work it is appropriate to review the literature concerning other kinetic lattice models. We also will review applications of these models to physical processes. Previous reviews, which are updated here, have been provided by Wolf[1] and Burgess[3].

A. Review of Random Filling

The first statistical treatment of a lattice filling problem was by Flory[6] in 1939 where he analyzed the 1D random filling of adjacent pairs of sites (dimers). He used recursion relations based upon the observation that each event which took place reduces the original problem into two smaller ones. He used this model to describe the condensation of ketone groups of poly(methyl vinyl)ketone.

E. S. Page[7] solved the 1D random dimer problem by using generating function techniques. He was motivated by a problem where molecular hydrogen is absorbed upon two adjacent sites on a surface and is subsequently absorbed by mercury. He was the first to observe that the results depend upon the manner in which the adjacent sites are chosen,

simultaneously (conventional filling) or by first picking one site and then randomly filling one of its unoccupied neighbor sites (end-on filling). We will be concerned with conventional filling here unless it is specified otherwise.

Cohen and Reiss[8] solved the kinetic equations for the probabilities of empty strings of sites through the use of transform techniques. They considered 1D random dimer filling on finite rings and linear lattices as well as the infinite lattice. They were the first to discover the empty site shielding property, discussed earlier, which allows for exact truncation and solution of the infinite hierarchy for this problem.

This problem has also been treated by other authors by recursion techniques[9-10], density expansions[11], use of Markov chains[12], and generating function techniques[13-15]. Using the master equation approach outlined earlier and an exact truncation based on the shielding property discovered by Cohen and Reiss[8], Vette et al.[16] were able to exactly solve the dimer problem as well. Based on this technique Wolf[1] and Evans et al.[17] were able to determine the two-point correlations.

The more general case of 1D random N-mer filling (where N denotes the number of consecutive lattice sites filled by the species) has been considered by several authors through the use of recurrence relations and/or generating functions[18-22]. Wolf et al.[23] were able to exactly analyze these processes through hierarchy truncation. Proposed applications include the binding of large ligands to polynucleotides or polypeptides[21] and modeling the crystallization of linear polymer chains[24].

The first analytical treatment of a higher-dimensional random filling process was by Jackson and Montroll[25] who considered random dimer filling in 3D. This was motivated by a study of the recombination of free radicals in a quasicrystalline matrix. They used a simplified statistical model where they average over all possible configurations.

Barron et al.[14], in considering the dehydration of poly(acrylic acid) and of poly(methacrylic acid), proposed that the carboxyl groups pair randomly, which leads to 1D dimer filling if both carboxyl groups are on the same chain. However, they also proposed a model where groups on neighboring chains pair (represented by a 2 x M lattice) such that only diagonal-nearest-neighbor filling is allowed.

Downton[15] considered briefly the 2D random dimer problem. He approximated the square lattice by parallel 1D lattices such that the 1D lattices each filled to saturation and only then could the pairs of empty sites in adjacent 1D lattices fill (see Figure 1).

There have been numerous Monte Carlo simulations of the 2D random dimer filling problem[26-33]. Roberts[26] suggested it in 1935 as a model for O_2, H_2 or N_2 adsorption onto a single crystal of W. Other applications included γ-alumina dehydroxylation[28], dehydration of silica gels[29], desorption of N from W[30], water sorption to form hydroxyls on metal ion sites[32], and β-CO adsorption onto metals[33]. In their work on CO Hayden and Klemperer[33] also consider coadsorption of β-CO (two-point or dimer filling) and α-CO (one-point or monomer filling) onto binary metal alloy surfaces. Their alloys consisted of random mixtures of active and inactive sites, so the effect of inactive sites was considered as well.

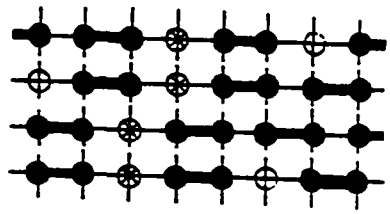

Figure 1: Dimer filling of parallel 1D linear lattices which each fill to saturation prior to filling between lattices (which can occur on sites marked by x)

McQuistan et al.[34] motivated by the CO coadsorption problem did a statistical analysis for small rectangular lattices (of 12 sites or less). They counted all possible configurations using recursion relations.

Vette et al.[16] approximated the solution to 2D random dimer filling on triangular, square, and hexagonal lattices through approximate truncation of the infinite hierarchy.

Blaisdell and Solomon[35] have performed Monte Carlo simulations in two and higher dimensions in order to test the generalized Palasti conjecture (which states that if, for N-mer filling of a 1D lattice with the saturation coverage, θ^{sat} equal to c, then θ^{sat} for N^d-mer filling of a d-dimensional lattice is c^d). They have performed simulations for variously sized squares of sites filling finite square lattices, cubes of sites filling cubic lattices, and a few smaller 4D trials. Given their results on finite lattices they extrapolated to find the infinite lattice results. These simulations represent the only previous attempt to obtain results for species larger than a dimer in 2D.

Thus, a need exists to expand upon the limited modeling which has been done for random filling in higher dimensions. The first half of this thesis addresses that need. In particular we extend the truncation scheme of Vette et al.[16] to higher orders for random dimer filling of hexagonal, square and triangular lattices. From these calculations we are able to obtain highly accurate results and provide sufficient insight into the shielding propensity of subconfigurations of empty sites so as to justify a more sophisticated refinement of the truncation procedure. We also provide the first results for 2D trimer and tetramer filling. Additionally, we

demonstrate how coadsorption or a random distribution of defects can be handled giving explicit results for two- and three-dimensional problems, respectively. These complications occur in problems such as the CO adsorption modeled by Hayden and Klemperer[33], where both occur, or the free-radical-recombination model proposed by Jackson and Montroll[25], where there can be inactive sites. We also present the first 3D example of solution using formal density expansions (coupled with resummation) and explicitly demonstrate how to consider a random distribution of inactive sites for this method, as well.

B. Review of Cooperative Filling

There has been a considerable amount of work done on cooperative models in 1D. Keller[36], Alfrey and Lloyd[37], and Arends[38] were the first to consider the simplest such cooperative process, monomer filling with nearest-neighbor (NN) cooperative effects (here cooperative means that different, but nonzero, filling rates apply for sites which have different numbers of filled neighboring sites). They considered it in the context of reactions such as the dehydrochlorination of polyvinyl chloride or the quaternization of poly(4-vinyl pyridine). Each of these sets of authors were able to solve their rather similar models exactly.

McQuarrie et al.[39] presented an exact solution to the NN cooperative monomer problem for a model which is the kinetic analog of the Zimm-Bragg equilibrium model[40]. They were able to solve the hierarchy of equations for consecutive n-tuples of empty sites in terms of incomplete gamma functions. They used this model to describe the denaturation of polypeptides.

This same application was studied by Gō[41] who developed a formalism to describe chemical kinetics based on the path integral model of Kikuchi[42]. Schwarz[43] later attempted a general solution for the nonequilibrium behavior of a linear Ising lattice which was similar in spirit to Gō's work. In particular, the solutions were not exact and the approximations used were equivalent. Schwarz called his the "triplet closure rule" and it amounted to a 2^{nd}-order Markovian truncation where any two sites shield. However, as we have discussed, to truncate exactly, for this case, both sites must be empty[1,4,23]. This exact truncation, described earlier, has been used in more recent statistical treatments[5,44,45] and will exploited later in this work.

Other methods for obtaining exact solutions include the generating function techniques of Boucher[20], directly solving the hierarchy through guessing the solution form[46] and a "principle of independence" of unreacted neighbors[47] which is related to the exact shielding truncation.

The extension to N-mer filling with NN cooperative effects has been made by several authors[1,20,21,46]. Wolf et al.[23] exactly solved the N-mer problem for arbitrary (finite) range N cooperative effects. Some additional complications which have been investigated include consecutive reaction problems[47-49] and lattices with periodic or stochastic site distributions[23,47,49,50] which arise in the context of the study of copolymers. Other problems addressed include filling in stages[4,34,51,52], competitive filling[21,53], longer, range 2, cooperative effects[52], and mobility[55].

Evans et al.[4] showed how approximate hierarchy truncation could be applied to more general problems involving cooperativity. Specifically, they looked at monomer filling with nearest-neighbor cooperative effects on a square lattice (see ref. (3) also). They later also calculated spatial correlations for this more general problem as well as for random dimer filling[17]. Evans found that this truncation can lead to exact solution on Bethe lattices (lattices with no closed loops) and he showed this in solving the NN cooperative monomer and the random dimer problems[56].

Evans and Hoffman[57] found that exact solutions could be obtained for "almost random" filling (where the filling rate is independent of the surrounding sites except when all NN sites are filled) of a lattice with arbitrary dimension or coordination number. The mechanism proposed by Rosei et al.[58] to deposit carbidic carbon on Ni(110) from dissociative adsorption of CO conforms to the conditions of 2D "almost random" filling.

As an alternate method to truncation for solution of the infinite hierarchy, Hoffman[59] and Evans[60] proposed formal density expansions. Hoffman considered cooperative dimer filling of a square lattice. These results, however, are also applicable to more general irreversible processes on uniform, infinite lattices with Arrhenius rates and pairwise additive activation energy (they provide a diagrammatic characterization for terms in the expansions). Evans[60] considered general cooperative processes on uniform, periodic or defective lattices of arbitrary size (finite, semi-infinite, or infinite). He also considered coadsorption as well as resummation procedures. Formal resummations of density expansions have been also considered by Knodel and Hoffman[61].

Some additional applications for 2D cooperative models include the chemisorption of water vapor onto Fe(001) to form an immobile oxide (or hydroxyl group). Dwyer et al.[62] proposed that this could be modeled by monomer adsorption with NN blocking (sites with one or more NN sites filled cannot fill) on a square lattice.

Similar to the above problem, nitrogen appears to chemisorb on W(100) as a monomer with NN blocking and a longer range cooperative effect. Wolf et al.[63] modeled it as 1D monomer filling with NN blocking. The true surface geometry of W(100) is a square lattice and the modifications due to this are discussed.

The majority of the above references are concerned only with solving for the probabilities of finding clusters of empty sites. The additional problem of obtaining probabilities of clusters of filled sites is discussed by several authors[1,5,14,20,64,65]. Platé et al.[5] first solved this problem exactly for the 1D NN cooperative monomer process on the infinite lattice and Wolf[1] first solved it on the semi-infinite lattice. However, only the values for very small clusters were obtained. There had been no analyses of the entire cluster-size distribution or, in particular, its asymptotic behavior.

Therefore, the second half of this thesis is concerned with determination of the cluster-size distribution for a lattice process. We are able to solve for the exact cluster-size distribution for cluster sizes up to the asymptotic regime and thus estimate the asymptotic decay rate for 1D monomer filling with NN cooperative effects or NN blocking and 2^{nd}-NN cooperative effects. Furthermore, indication is given as to how asymptotic properties can be extracted directly from the hierarchial equations.

C. Cluster Growth Via Random Walks

A second method for studying cluster growth is also discussed. In this method the growth of a single cluster is modeled by the aggregation of random walkers about some nucleation center. A random walker is introduced onto a finite lattice and walks until it encounters a trap site where it is irreversibly trapped. By specifying all sites adjacent to a cluster to be trap sites this process corresponds to irreversible cluster growth (Witten-Sander irreversible particle-cluster aggregation[66]). From calculating the probabilities of being caught by particular traps, it is possible to determine the shape distribution of the clusters formed. Differently sized and shaped clusters will have different growth rates associated with them and these growth rates can be related to (reciprocals of) the associated average walk lengths. Rates, determined in this manner, can then be used as input into the kinetic hierarchial equations for determining the cluster-size distribution, as a function of time, for a Brownian aggregation process (a process where a gas of random walkers irreversibly aggregate to form immobile clusters).

D. Explanation of Dissertation Format

In Paper I we consider random N-mer filling of 2D lattices. In particular, dimer and trimer filling of hexagonal, square, and triangular lattices and square tetramer filling of a square lattice are considered with special emphasis on dimer filling of a square lattice. Various

truncation techniques are developed and contrasted. Particular emphasis is given to the saturation coverage. Paper II extends the methods of the first paper to consider competitive random filling of 2D lattices. The behavior of these processes are displayed by plotting "filling trajectories" of the partial coverages for different ratios of the two competing species filling rates. The competing species may be of the same size or different sizes. Examples are also given for the competition of more than two species. In Paper III, random dimer filling of a cubic lattice is considered. Besides the truncation techniques developed previously, techniques involving formal density expansions (coupled with resummation) and spectral analysis are described. The effect of a random distribution of inactive sites is also considered.

In the fourth and fifth papers, a cooperative problem is studied. 1D monomer filling with NN cooperative effects is considered with emphasis upon determination of the cluster-size distribution. Paper VI discusses random walks on finite lattices with completely adsorbing traps and their relationship to the shape of clusters formed by irreversible aggregation. It also indicates, for a Brownian aggregation process, how cluster-size distributions can be determined from the average walk lengths calculated above.

In the Monte Carlo Simulations section we compare certain of our approximate truncation results (from Papers I and III) with those obtained from direct simulation. A description of the simulation technique is also given. A summary is presented in the Conclusion section along with a brief discussion of future work.

The arrangement of this dissertation follows the alternate style format. The six papers presented here are collaborative efforts, primarily with Dr. J. W. Evans. Certain components of these papers are predominantly the work of Dr. Evans. In particular, these include the formal analysis in Papers III and VI, and the formal asymptotic cluster-size distribution analysis in Papers IV and V. Paper I, "Irreversible immobile random adsorption of dimers, trimers, ... on 2D lattices", was published in volume 82 of the Journal of Chemical Physics on pages 2795-2810. Paper II, "Competitive irreversible random one-, two-, three-, ... point adsorption on two-dimensional lattices", was published in volume 31 of Physical Review B on pages 1759-1769. Paper III, "Random Dimer Filling of Lattices: Three-Dimensional Application to Free Radical Recombination Kinetics", was published in volume 38 of the Journal of Statistical Physics on pages 681-705. Paper IV, "Cluster-size distributions for irreversible cooperative filling of lattices. I. Exact one-dimensional results for coalescing clusters", was published in volume 31 of Physical Review A on pages 3820-3830. Paper V, "Cluster-size distributions for irreversible cooperative filling of lattices. II. Exact one-dimensional results for noncoalescing clusters", was published in volume 31 of Physical Review A on pages 3831-3840. Paper VI, "Random walks on finite lattices with multiple traps: Application to particle-cluster aggregation", was published in volume 32 of Physical Review A on pages 2926-2943. All of the papers were published in 1985.

PAPER I:

IRREVERSIBLE IMMOBILE RANDOM ADSORPTION OF DIMERS, TRIMERS, ••• ON 2D LATTICES

IRREVERSIBLE IMMOBILE RANDOM ADSORPTION OF DIMERS, TRIMERS, ... ON 2D LATTICES

R. S. Nord and J. W. Evans

Ames Laboratory and Department of Chemistry
Iowa State University
Ames, Iowa 50011

ABSTRACT

Models where pairs, triples, or larger (typically connected) sets of sites on a 2D lattice "fill" irreversibly (described here as dimer, trimer, ... filling or adsorption), either randomly or cooperatively, are required to describe many surface adsorption and reaction processes. Since filling is assumed to be irreversible and immobile (species are "frozen" once adsorbed), even the stationary, saturation state, which is nontrivial since the lattice cannot fill completely, is not in equilibrium. The kinetics and statistics of these processes are naturally described by recasting the master equations in hierarchial form for probabilities of subconfigurations of empty sites. These hierarchies are infinite for the infinite lattices considered here, but approximate solutions can be obtained by implementing truncation procedures. Those used here exploit a shielding property of suitable walls of empty sites peculiar to irreversible filling processes. Accurate results, including saturation coverage estimates, are presented for random filling of dimers, and trimers of different shapes, on various infinite 2D lattices, and of square tetramers on an infinite square lattice.

I. INTRODUCTION

Consider processes where adjacent pairs of (empty) sites on a uniform lattice are filled irreversibly ("dimer filling"), either randomly or cooperatively. In the former case, a single rate, k, characterizes the process, whereas in the latter, rates must be prescribed for each possible configuration of the environment influencing filling of an empty pair. Since, by assumption, the dimers are frozen once adsorbed (they cannot desorb or hop), the resulting distribution of filled sites is not described by equilibrium statistics even in the stationary, saturation state. Furthermore, the lattice does not completely fill here since isolated empty sites are created which can never fill (see Fig. 1a). Clearly these distributions, even for random dimer filling, incorporate nontrivial spatial correlations (unlike random monomer filling). More generally, one could consider processes where adjacent triples, or other sets of sites (of fixed relative configuration), fill irreversibly ("trimer or N-mer filling") either randomly or cooperatively. Again, the resulting nonequilibrium distributions of filled sites are spatially correlated and the lattice is not completely filled at saturation (where a variety of isolated empty clusters now remain, as shown in Fig. 1).

The quantities of interest here are proabilities, $P_{\underset{\sim}{\sigma}}$, for subconfigurations of sites, $\underset{\sim}{\sigma}$, specified either empty 'o' or filled 'a'. Equations for the time evolution of these can be obtained by rewriting the master equations in hierarchial form (the latter can be written down directly from intuition)[1-9]. For infinite, uniform lattices, of interest

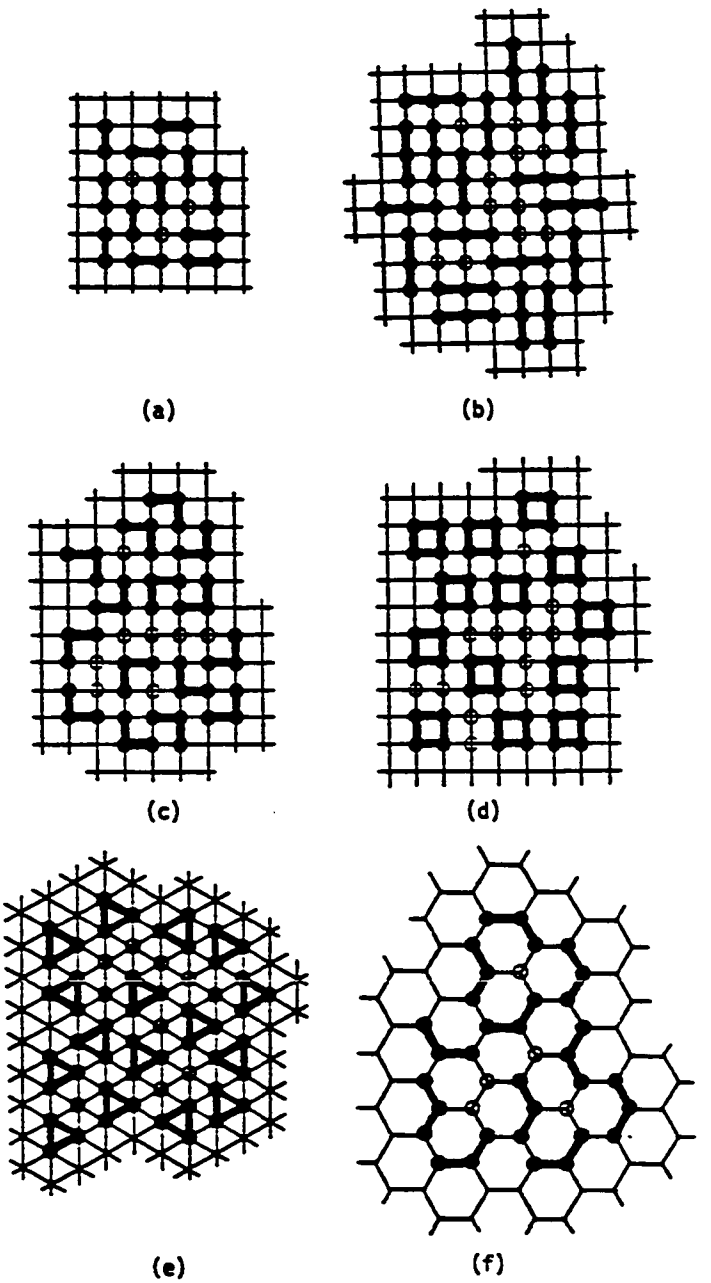

Figure 1: Irreversible filling of a square lattice by (a) dimers, (b) linear trimers, (c) bent trimers, (d) square tetramers, (e) of a triangular lattice by triangular trimers, and (f) of a hexagonal lattice by bent trimers. A site labeled with an 'o' can never fill

here, these hierarchies are infinite making their solution nontrivial. We restrict our attention to initially empty lattices in which case time evolution preserves invariance of the $P_{\underset{\sim}{g}}$ under all lattice group operations (e.g., translation and rotation). Thus we often naturally consider the $P_{\underset{\sim}{g}}$ as functions of coverage, $\theta \equiv P_a \equiv 1 - P_0$, rather than time 't'. Of course, the infinite time values of the $P_{\underset{\sim}{g}}$ provide complete information about the saturation state. The saturation coverage is the quantity of prime importance here but, nontrivial spatial correlations and, for trimer and N-mer filling, nonzero probabilities of various empty clusters, described in the following paragraph, can also be determined.

For filling on a 1D lattice by dimers, only isolated empty sites remain at saturation[9,10] (so $P_{aoa} = P_o$ here), but for filling by N-mers (taking N consecutive sites at a time), isolated empty sites and empty pairs, triples, ..., (N-1)-tuples remain at saturation[2-4]. As indicated above, for dimer filling on any lattice, only isolated empty sites remain at saturation[5], so here, e.g., $P_{\substack{a\\ a\,o\,a\\ a}} = P_o$ for a 2D square lattice (Fig. 1a). However the saturation state is more complicated for trimer, etc., filling as indicated by the following 2D square lattice examples. For linear trimer filling (Fig. 1b), one finds at saturation, isolated empty sites, empty pairs, empty bent triples, ..., so $P_{\substack{a\\ a\,o\,a\\ a}}$, $P_{\substack{a\,a\\ a\,o\,o\,a\\ a\,a}}$, $P_{\substack{a\\ a\,o\,a\\ a\,o\,o\,a\\ a\,a}}$, ... and therefore P_o, P_{oo}, $P_{\substack{o\\ o\,o}}$, $P_{\substack{o\,o\\ o\,o\,o}}$, $P_{\substack{o\,o\\ o\,o\,o}}$, ... (i.e., empty staircase configurations) have nonzero saturation values, as does $P_{\substack{o\,o\\ o\,o}}$. For bent

trimer filling (see Fig. 1c), $P_{\substack{a\\a\square a}}$, $P_{\substack{aa\\a\square\square a}}$, $P_{\substack{aaa\\a\square\square\square a}}$, ••• and therefore P_o, P_{oo}, P_{ooo}, P_{oooo}, ••• have nonzero saturation values. For square tetramer filling (see Fig. 1d), we similarly see that P_o, P_{oo}, $P_{\substack{o\\o\square}}$, P_{ooo}, ••• all have nonzero saturation values. A number of these quantities are determined in this work.

For 1D lattices, these models have an important application in describing irreversible reaction on polymer chains[9]. Dimer filling typically models a cyclization reaction where adjacent groups link[9,10]. N-mer filling models the binding to N consecutive sites of large ligands[2-4,9]. Here we are primarily interested in these models for 2D lattices where they are essential in the analysis of certain irreversible immobile chemisorption processes as well as various irreversible reactions between groups on surfaces[11-16]. There is increasing evidence that, for chemisorption processes, often surface mobility (and desorption) are negligible[15-17]. Consequently equilibrium statistical mechanics is inappropriate for describing the filled site distribution since it relies on these mechanisms to achieve equilibration. The first specific application of the 2D random dimer filling model was by Roberts[11] to O_2 and N_2 adsorption on W. Other more recent applications include description of (i) desorption of nitrogen adatoms in adjacent pairs[13], i.e., adsorption of dimer holes; (ii) dehydration of γ-Alumina where adjacent hydroxyl (ion) groups combine to form water molecules[14]; (iii) water sorption at adjacent pairs of metal ion sites (bridged by oxygen atoms) to create two hydroxyl groups; this study is in part motivated by desire to understand more complex dehydration-hydration processes on hydrotreating

catalysts[15]; and (iv) adsorption of CO at adjacent sites on W (two-point β-CO)[16]. Obviously the more general N-mer filling models will be required for the adsorption of larger molecules (the number of sites filled, e.g., three for trimer filling, need not, however, correspond to the number of atoms in the adsorbate)[18]. Sometimes steric hindrance will require that filling is blocked within a certain range of a previously adsorbed species. Recent studies of hydrocarbon adsorption provide examples of such irreversible binding[19].

Before describing the contribution of this work, we briefly review previous analyses of these models. The earliest exact results come from Flory's[10] statistical analysis of saturation coverages for random dimer filling on 1D lattices. For an infinite lattice, a value of $1-e^{-2}$ was obtained. More extensive statistical analyses have also been given[20]. In addition, for the infinite 1D lattice, a number of treatments involving exact hierarchy truncation based on a shielding property of a single empty site provide information on the time dependence of n-tuples of empty sites, and recover the above mentioned saturation value[1,5]. Two-point spatial correlations have also been analyzed and shown to determine all spatial correlations[21,22]. Statistical analyses have also been given for random N-mer filling on finite 1D lattices[18,23], and exact solution, via hierarchy truncation (exploiting a shielding property of empty (N-1)-tuples), is again possible for filling of an infinite, uniform 1D lattice. Saturation coverage values have been tabulated for various N[3]. More generally exact solution via hierarchy trunction is possible for N-mer filling with, not just nearest neighbor[3], but also range N cooperative

effects[4]. Exact solution via hierarchy truncation is also possible for dimer, trimer, ••• filling on Bethe lattices, either randomly, or with nearest-neighbor cooperative effects[24].

A statistical analysis has been presented for random dimer filling on several small finite lattices[25]. For random dimer, trimer, ••• filling on infinite 2D (or higher dimensional) lattices, exact closed form solution of the hierarchy is not possible (although there still exists a shielding property of suitable walls of empty sites[6]). An approximate truncation scheme has been implemented previously for random dimer filling[5], and will be developed further here. Formal coverage (density) expansions are available even for cooperative filling[7,8] and a resummation scheme, exploiting exact Bethe lattice results, has been developed for random dimer filling[8]. There have been numerous Monte Carlo simulations of random dimer filling, concentrating on determination of the saturation coverage[12-16]. The trimer filling model has been mentioned recently in the context of surface adsorption, but no analysis has been given[18]. In fact, apart from monomer and dimer filling, the only other 2D filling process considered previously is random square N^2-mer filling on a square lattice[25]. Here, according to the generalized Palásti conjecture, the saturation coverage for an infinite lattice is the square of that for random N-mer filling on an infinite 1D lattice, e.g., $(1-e^{-2})^2$ for random square tetramer filling.

In this work, we analyze and present results for several random filling processes on a variety of infinite, uniform 2D lattices. Approximate solutions are obtained for the infinite, closed hierarchies of

rate equations satisfied by probabilities for subconfigurations of empty sites. The approximate truncation procedure implemented here is motivated by hierarchial structure, in particular, a shielding property of suitable walls of empty sites (rather than inappropriately borrowing, e.g., Kirkwood-style factorizations, or Bethe-type approximations from equilibrium theory). The 1D analogues of these schemes recover exact results. For random dimer filling, the simplest truncation scheme, which corresponds to that used previously by Vette et al.[5], is extended to higher orders for square, hexagonal and triangular lattices. Extremely accurate results are obtained for the probabilities of various small compact subconfigurations. These benchmark calculations also provide valuable insight into the structure of the hierarchy solutions and, in particular, into the shielding propensity of various subconfigurations of empty sites. Furthermore they suggest corresponding natural refinements of the truncation procedure. By solving appropriately truncated equations to various orders, we also provide the first results for random filling of linear and bent trimers on a square lattice, bent trimers on a hexagonal lattice, and triangular trimers on a triangular lattice. We also treat random square tetramer filling on a square lattice, the results from which can be compared with numerical simulations and the generalized Palásti conjecture.

The hierarchial rate equations for random dimer, trimer, ••• filling are described in Section II, first for probabilities, $P_{\bullet\bullet}$, of empty subconfigurations, and then for corresponding conditional probabilities, $Q_{\bullet\bullet}$. In Section III, after reviewing the shielding property for suitable

walls of empty sites, we describe a truncation procedure for the Q hierarchies which follows naturally from this. Refinements are indicated with emphasis on the random dimer filling case. Results from various levels of truncation are described in Section IV for the random filling processes listed above. Some interesting isomorphisms between different filling processes are described in Section V. Finally some conclusions and comparisons with previous work are given in Section VI, together with a discussion of extensions of these analyses.

II. THE HIERARCHIAL RATE EQUATIONS

Let {m} represent some subset of m sites and $P_{\{m\}}$ denote the probability that these are empty. The $P_{\{m\}}$ can be regarded as functions of time, t, or lattice coverage, $\theta \equiv 1 - P_{\{1\}}$ (assuming translational invariance). Hereafter we set the filling rate, k, equal to unity without loss of generality (this simply corresponds to transforming to a chemical time scale $t' \equiv kt$).

In presenting the hierarchial rate equations for the $P_{\{m\}}$, it is convenient to define $n_{\{m\}}$ to be the number of ways that the adsorbing species can land entirely within {m}, and $n_{\{k\},\{m\}} \equiv n_{\{k\}+\{m\}} - n_{\{m\}}$. Thus for <u>random dimer filling</u>, $n_{\{m\}}$ is the number of adjacent pairs in {m}, and[5,27]

$$d/dt\ P_{\{m\}} = - n_{\{m\}}\ P_{\{m\}} - \sum_{j \notin \{m\}} n_{j,\{m\}}\ P_{j+\{m\}} \quad , \tag{2.1}$$

where $n_{j,\{m\}} = n_{j+\{m\}} - n_{\{m\}}$ is the number of sites in {m} adjacent to j. These terms correspond to destruction of the empty configuration {m} from dimers landing completely within, and partly overlapping {m}, respectively. For <u>random N-mer filling</u>, a configuration, {p}, is called sub-N-mer if it contains $p<N$ sites and can be filled by adsorption of a single N-mer (thus {p} consists of single sites and adjacent pairs of sites for trimer filling). Here the hierarchy equations have the form

$$d/dt\ P_{\{m\}} = - n_{\{m\}}\ P_{\{m\}} - \sum_{\substack{\{p\} \cap \{m\} = \phi \\ \{p\}\ \text{sub-N-mer}}} n_{\{p\},\{m\}}\ P_{\{p\}+\{m\}} \quad , \tag{2.2}$$

where these terms correspond to destruction of empty {m} from N-mer landing completely within, and partly overlapping {m}, respectively. Note that (2.2) includes (2.1) as a special case and that, for N-mers which fill connected sets of sites, (2.1,2) include infinite closed subhierarchies for probabilities of connected empty clusters.

Here we consider only filling of infinite, uniform, initially empty lattices (i.e., $P_{\{m\}} = 1$ for all {m} at t = 0) where the hierarchial equations clearly preserve the invariance of the $P_{\{m\}}$ under all lattice group operations. In particular these are translationally invariant which allows us to denote the probability of an empty site, an empty pair, ••• by P_o, P_{oo}, ••• respectively. With this notation, it is elucidating to consider tne following examples of (2.1,2) for filling of a 2D square lattice (where all lattice symmetries have been exploited to simplify these equations):

<u>dimer filling</u>:

$$d/dt\ P_o = -4P_{oo}$$

$$d/dt\ P_{oo} = -P_{oo} - 2P_{ooo} - 4P_{o\overset{o}{\overset{|}{o}}}$$

$$d/dt\ P_{ooo} = -2P_{ooo} - 2P_{oooo} - 2P_{o\overset{o}{\overset{|}{o}}o} - 4P_{oo\overset{o}{\overset{|}{o}}}$$

$$\vdots \qquad (2.3a)$$

<u>linear trimer filling</u>:

$$d/dt\ P_o = -6P_{ooo}$$

$$d/dt\ P_{oo} = -\ 2P_{ooo} - 2P_{oooo} - 2P_{o8} - 4P_{o8}$$

$$d/dt\ P_{ooo} = -\ P_{ooo} - 2P_{oooo} - 2P_{ooooo}$$
$$-\ P_{o8o} - 4P_{o8o} - 4P_{oo8}$$

$$d/dt\ P_{o8} = -\ 2P_{oo8} - 2P_{o8o} - 4P_{88}$$
$$-\ 2P_{ooo8} - 2P_{o8oo} - 2P_{o8oo}$$

$$\vdots \qquad (2.3b)$$

<u>bent trimer filling:</u> $d/dt\ P_{o} = -\ 12P_{o8}$

$$d/dt\ P_{oo} = -\ 4P_{o8} - 4P_{oo8} - 4P_{o8o} - 4P_{88} - 4P_{o8o}$$

$$\vdots \qquad (2.3c)$$

<u>square tetramer filling:</u> $d/dt\ P_{o} = -\ 4P_{88}$

$$d/dt\ P_{oo} = -\ 2P_{88} - 4P_{88o}$$

$$\vdots \qquad . \qquad (2.3d)$$

The truncation procedures discussed in the next section deal directly with the conditional probabilities $Q_{\{n\},\{m\}} = P_{\{n\}+\{m\}}/P_{\{m\}}$ for n conditioned sites {n} to be empty given the m conditioning sites {m} are empty. Thus it is convenient to recast (2.2) in an equivalent form which involves these Q's explicitly (rather than P's). One obtains straightforwardly from (2.2),

$$d/dt\ \ell n\ Q_{\{n\},\{m\}} = S(\{n\}+\{m\}) - S(\{m\}) \quad , \tag{2.4a}$$

$$\text{where } S(\{r\}) = d/dt\ \ell n\ P_{\{r\}} = -\ n_{\{r\}} - \sum_{\substack{\{p\}\cap\{r\}=\phi \\ \{p\}\ \text{sub-N-mer}}} n_{\{p\},\{r\}}\ Q_{\{p\},\{r\}} \tag{2.4b}$$

Note that only for random dimer filling does (2.4a) involve a closed subhierarchy for Q's with a single conditioned site. This simplification has ramifications for the implementation of truncation. In the following, 'o' denotes empty conditioned, and 'ϕ' empty conditioning sites, so $Q_o \equiv P_o$, $Q_{o\phi} \equiv P_{oo}/P_o$, $\cdots$. Then, for the 2D square lattice examples described in (2-3), the following Q hierarchies are obtained:

<u>dimer filling</u>:

$$\begin{aligned} d/dt\ \ell n\ Q_o &= -\ 4Q_{o\phi} \\ d/dt\ \ell n\ Q_{o\phi} &= -\ 1 - 2Q_{o\phi\phi} - 4Q_{\substack{o \\ \phi\phi}} + 4Q_{o\phi} \\ d/dt\ \ell n\ Q_{o\phi\phi} &= -\ 1 - 2(Q_{o\phi\phi\phi} - Q_{o\phi\phi}) - 4(Q_{\substack{o \\ \phi\phi\phi}} - Q_{\substack{o \\ \phi\phi}}) - 2Q_{\substack{o \\ \phi\phi\phi}} \\ &\ \ \vdots \end{aligned} \tag{2.5a}$$

linear trimer filling:

$$d/dt\ \ell n\ Q_{o} = -\ 6Q_{oo\phi}$$

$$d/dt\ \ell n\ Q_{o\phi} = -\ 2Q_{o\phi\phi} - 2Q_{\phi\overset{o}{\phi}\overset{o}{o}} - 2(Q_{oo\phi\phi} - Q_{oo\phi}) - 4(Q_{oo\overset{\phi}{\phi}} - Q_{oo\phi})$$

$$d/dt\ \ell n\ Q_{o\phi\phi} = -\ 1 - 2(Q_{o\phi\phi\phi} - Q_{o\phi\phi}) - 2(Q_{oo\phi\phi\phi} - Q_{oo\phi\phi}) - 2(Q_{\phi\phi\overset{o}{\phi}\overset{o}{o}} - Q_{\phi\overset{o}{\phi}\overset{o}{o}}) - 4(Q_{\phi\phi\overset{o}{\phi}\overset{o}{o}} - Q_{\phi\overset{o}{\phi}\overset{o}{o}}) - Q_{\phi\phi\overset{o}{\phi}\overset{o}{o}} - 2Q_{\phi\overset{o}{\phi}\overset{o}{\phi}}$$

$$\vdots$$

$$d/dt\ \ell n\ Q_{oo\phi} = S(ooo) - S(o)$$
$$= (S(ooo) - S(oo)) + (S(oo) - S(o))$$
$$= d/dt\ \ell n\ Q_{o\phi\phi} + d/dt\ \ell n\ Q_{o\phi}$$

$$\vdots \qquad (2.5b)$$

bent trimer filling:

$$d/dt\ \ell n\ Q_{o} = -\ 12Q_{o\overset{\phi}{o}}$$

$$d/dt\ \ell n\ Q_{o\phi} = -\ 4Q_{\phi\overset{o}{\phi}} - 4Q_{\phi\phi\overset{o}{o}} - 4Q_{\phi\overset{o}{\phi}o} - 4Q_{\overset{o}{\phi}\overset{o}{\phi}} - 4Q_{\phi\phi o} + 12Q_{o\overset{\phi}{o}}$$

$$\vdots \qquad (2.5c)$$

square tetramer filling: $d/dt\ \ell n\ Q_o = -4Q_{\substack{oo\\ \phi\phi}}$

$$d/dt\ \ell n\ Q_{o\phi} = -2Q_{\substack{oo\\ \phi\phi}} - 4(Q_{\substack{oo\\ o\phi\phi}} - Q_{\substack{oo\\ \phi\phi}})$$

$$\vdots \qquad . \tag{2.5d}$$

Here one should note obvious equalities such as $Q_{oo\phi} \equiv Q_{o\phi o}$, $Q_{\substack{o\\ o\phi}} \equiv Q_{\substack{o\\ o\phi}}$, $Q_{oo\phi\phi} \equiv Q_{o\phi\phi o}$, ••• . There are various other equalities imposed on the Q's from physical constraints. For dimer filling, since it is not possible to have a filled site surrounded by empty sites (filled sites must occur in pairs), clearly $Q_{o\phi\frac{\phi}{\phi}-\phi} \equiv Q_{o\phi\frac{\phi}{\phi}\phi\phi}$ etc. (here '-' represents an unspecified site). Similarly, for linear trimer filling, $Q_{o\phi\frac{\phi\phi\phi}{\phi}-\phi} \equiv Q_{o\phi\frac{\phi\phi\phi}{\phi}\phi\phi}$ since there is no way that the left unspecified site could be filled given its environment (tnis identity does not hold for bent trimer filling).

We note that the hierarchies (2.5b,c,d) can be written in an equivalent form involving only Q's with a single conditioned site 'o', since Q's with several conditioned sites can be simply factorized in terms of these. For example,

$$\begin{aligned} Q_{oo\phi\phi} &\equiv P_{oooo}/P_{oo} \equiv (P_{oooo}/P_{ooo})(P_{ooo}/P_{oo}) \equiv Q_{o\phi\phi\phi}\ Q_{o\phi\phi} \\ &\equiv (P_{oooo}/P_{o-oo})(P_{o-oo}/P_{oo}) \equiv Q_{\phi o\phi\phi}\ Q_{o-\phi\phi} \end{aligned}$$

$$Q_{\substack{o\\ \phi\phi o}} \equiv Q_{\substack{\phi\\ \phi\phi o}}\ Q_{\substack{o\\ \phi\phi}} \equiv Q_{\substack{o\\ \phi\phi\phi}}\ Q_{\phi\phi o} \tag{2.6}$$

which also illustrates exact product relationships between these Q's tnat are obviously consistent with the Q hierarchy (cf. (2.5b)). Various other nontrivial identities will be indicated in the discussion of shielding in the following section.

Once the Q hierarchy equations are solved, values for the P's can be obtained from such identities as

$$P_o \equiv Q_o,\ P_{oo} \equiv Q_o\, Q_{o\phi},\ P_{ooo} \equiv Q_o\, Q_{o\phi}\, Q_{o\phi\phi},$$

$$P_{o\overset{o}{\phi}o} \equiv Q_o\, Q_{o\phi}\, Q_{o\phi\phi}\, Q_{\overset{o}{\phi}\phi\phi} \equiv Q_o\, Q_{o\phi}\, Q_{\overset{o}{\phi}\phi}\, Q_{o\overset{\phi}{\phi}\phi}$$

$$\vdots \qquad \cdot \qquad (2.7)$$

III. THE EMPTY SITE SHIELDING PROPERTY AND HIERARCHY TRUNCATION

In this section, we first describe a shielding property of suitable walls of empty sites, then introduce various truncation schemes based straightforwardly on this property. Finally, for random dimer filling, we introduce a refined truncation scheme which exploits this shielding property to the fullest.

A. The Empty Site Shielding Property

The most general statement of this property applicable to general irreversible filling processes, including the ones of interest here, is as follows[6]: consider a wall of sites specified empty which divides the lattice into two disconnected regions, and is sufficiently thick that a filling event occuring on the lattice is not simultaneously affected by the state of sites on both sides of the wall; then such a wall completely shields sites on one side from the influence of those on the other.

Thus for random dimer filling (random N-mer filling, taking N consecutive sites at a time) on a 1D lattice, a single empty site (a block of N-1 empty sites) shields sites on one side from the influence of those on the other[3,4]. For example with random N-mer filling, if P_m denotes the probability of finding 'm' consecutive empty sites, the conditional probabilities $Q_m = Q_{o\underbrace{\phi\phi\cdots\phi}_{m}} \equiv Q_{\underbrace{\phi\phi\cdots\phi}_{m}o} \equiv P_{m+1}/P_m$ are equal to Q_{N-1}, for $m > N-1$. For a two-dimensional lattice, the shielding wall must either close on itself or extend to infinity in order to separate the lattice into two disconnected parts. Some examples of shielding walls on a square lattice,

for random dimer, linear and bent trimer, and square tetramer filling are shown in Fig. 2.

Mathematically, shielding is expressed through equality of various conditional probabilities and proof follows from observation of self-consistency with respect to the Q hierarchy[6]. We do not give details here but refer the reader to Ref. (27) for a discussion of the random dimer filling case (the treatment for general random N-mer filling is more complicated in detail, but the same in spirit). As a simple example, for random dimer filling of a square lattice, we have that

$$Q_{\cdots\phi\phi\underset{\phi}{o}\phi\phi\cdots} \equiv Q_{\cdots\phi\phi o\phi\phi\cdots} \tag{3.1}$$

(where the dots indicate an infinite string of 'ϕ' sites) and thus expect the difference between corresponding Q's with finite segments of shielding wall, e.g., $Q_{\underset{\phi}{o}\phi\phi\phi}$ and $Q_{o\phi\phi\phi}$, to be "relatively small". (This will be verified later.)

B. Hierarchial Truncation Schemes

For random N-mer filling of 1D lattices, the shielding property described above and, in particular, the equality $Q_m = Q_{N-1}$ for $m > N-1$, enables exact truncation and solution of the hierarchy equations[1-5]. This, however, is not the case in 2D.

For random dimer filling on 2D lattices, Vette et al.[5] proposed a series of (n^{th}-shell) truncation schemes wherein one obtains from the hierarchy for Q's with a single 'o' site, a closed set of equations for a

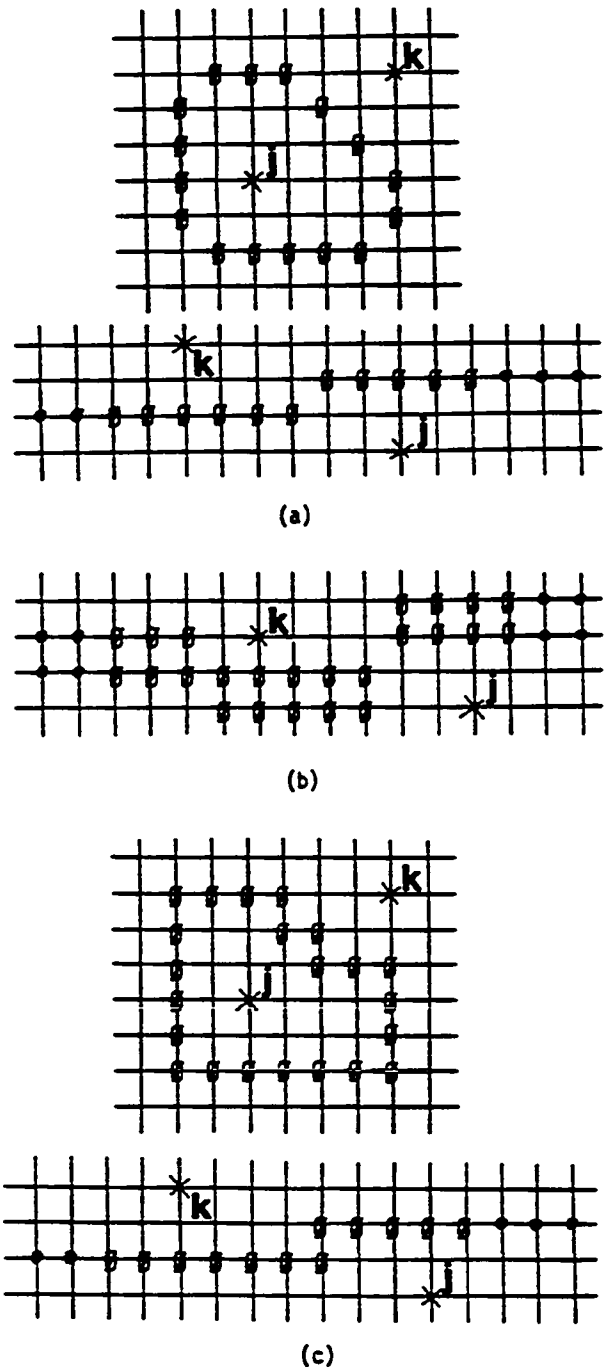

Figure 2: Shielding walls for random filling on a square lattice (a) dimers, (b) linear trimers, (c) bent trimers and square tetramers, which shield site j from the influence of k and vice versa

finite subset of these Q's by neglecting 'ϕ' sites further than n-lattice vectors from the single 'o' site. This scheme has also been used for 3D lattices[27]. As an example, consider the 1st-shell approximation for random dimer filling on a square lattice. Since, here, $Q_{o\phi\phi}$, $Q_{\phi\phi o} \to Q_{o\phi}$, the second equation in (2.5a) is replaced by

$$d/dt \, \ell n \, Q_{o\phi} = -1 - 2Q_{o\phi} \tag{3.2}$$

which closes with the first equation. These may be integrated using the initial conditions $Q_o = 1$, $Q_{o\phi} = 1$. An analogous pair of equations for Q_o and $Q_{o\phi}$ is obtained, in the 1st-shell approximation, for random dimer filling on a lattice with coordination number $c > 2$, and no closed loops of length three (thus excluding, e.g., a 2D triangular lattice). Integration of these yields[5,27]

$$Q_{o\phi} = \frac{1}{c-2}\left[(c-1)\, Q_o^{\frac{c-2}{c}} - 1\right] \quad . \tag{3.3}$$

Since P_{oo}, and hence $Q_{o\phi}$, is zero at saturation, the 1st-shell estimate of the saturation value of $P_o \equiv Q_o$ is $Q_o^s = \left(\frac{1}{c-1}\right)^{\frac{c-2}{c}}$. The case of the triangular lattice is more complex since $Q_{\phi\phi o}$ is also included in the 1st-shell equations[5].

As the order of the truncation increases, we shall see that the number of Q's involved in the minimal closed set increases dramatically. For a square lattice, Vette et al. also gave results for 2nd-shell (a closed set

of equations is obtained here for Q_{o}, $Q_{o\phi}$, $Q_{o\phi\phi}$, $Q_{o\phi\atop\phi}$, $Q_{o\phi\atop\phi\phi}$, $Q_{\phi o\phi\phi}$, $Q_{\phi\atop\phi o\phi\phi}$, $Q_{o\phi\atop\phi\phi}$) and for a simplified 3rd-shell truncation (neglecting any disconnected 'ϕ' sites after truncation). Here we give the more accurate (full) 3rd-shell, as well as 4th-shell results. The accuracy of truncation results is expected to increase dramatically with increasing order, since neglected 'ϕ' sites are further from the 'o' site and may often be obscured from the 'o' site by other 'ϕ' sites. Since separating empty walls of thickness one shield here, this process should be a better candidate for truncation, especially at low orders than, say, linear trimer filling (requiring a shielding wall of thickness two). We shall use the high order truncation results as the basis for a detailed analysis of the shielding propensity of finite sections of shielding wall. Finally we remark that solutions of the truncated equations exhibit <u>product consistency</u>, i.e., satisfy relationships of the form (2.6) (see Ref. (6)). This is important since it guarantees that $P_{\bullet\bullet}$'s can be reconstructed uniquely as products of these $Q_{\bullet\bullet}$'s (cf. (2.7)).

For <u>random N-mer filling</u>, there is considerable arbitrariness in the choice of truncation scheme associated with the appearance of Q's with more than one conditioned 'o' site. Two simple choices, which we term <u>severe</u> (<u>mild</u>) n^{th}-order truncations, neglect conditioning 'ϕ' sites in the Q's further than n-lattice vectors from <u>any</u> (<u>all</u>) conditioned 'o' sites. Thus for a square lattice in the 2nd-order,

$$Q_{o\phi\phi\phi},\ Q_{o\phi\atop\phi},\ \cdots \rightarrow Q_{o\phi\phi} \text{ (severe and mild)}$$

$$Q_{oo\phi\phi\phi},\ Q_{oo\phi\phi\atop\phi},\ Q_{oo\phi\phi},\ \cdots \to Q_{oo\phi}\ \text{(severe) and}\ Q_{oo\phi\phi}\ \text{(mild)}$$

$$Q_{\phi\phi\phi\atop o} \to Q_{oo\phi}\ \text{(severe)},\ Q_{\phi\phi\phi\atop o}\ \text{(mild)},\ \text{etc.}\quad . \tag{3.4}$$

For linear trimer filling on a square lattice, some examples of severe 2^{nd}-order equations, following from (2.5b), are

$$d/dt\ \ell n\ Q_o = -\ 6Q_{o\phi\phi}\quad ,\quad \text{unchanged from (2.5b)}\quad ,$$

$$d/dt\ \ell n\ Q_{o\phi} = -\ 2Q_{o\phi\phi} - 2Q_{\phi\phi\atop o}$$

$$d/dt\ \ell n\ Q_{o\phi\phi} = -\ 1 - Q_{\phi\phi\phi\atop o} - 2Q_{oo\phi}$$

$$d/dt\ \ell n\ Q_{o\phi\atop\phi} = -\ 2Q_{\phi\phi o\atop\phi} - 4Q_{o\phi\atop\phi\phi} + 2Q_{\phi\phi\atop o}$$

$$\vdots \tag{3.5}$$

whereas, in contrast, the mild 2^{nd}-order equations are

$$d/dt\ \ell n\ Q_o \text{ and } d/dt\ \ell n\ Q_{o\phi} \text{ are unchanged from (2.5b),}$$

$$d/dt\ \ell n\ Q_{o\phi\phi} = -\ Q_{\phi\phi\phi\atop o} - 2Q_{\phi\phi\phi\atop o}$$

$$d/dt\ \ell n\ Q_{o\phi} = -2(Q_{\phi\phi oo} - Q_{\phi oo}) - 2Q_{\phi\phi o} - 4Q_{\substack{o\\ \phi\phi}} + 2Q_{\substack{o\\ \phi\phi}}$$

$$\vdots \qquad\qquad \cdot \qquad\qquad (3.6)$$

From (3.4,5,6) we see that the severe truncation does indeed have a more severe effect on the hierarchy equations (hence the name). It is also apparent that fewer Q's will be included in the minimal closed set for severe truncation. Again solutions of the truncated equations exhibit product consistency[6].

Other truncation schemes for <u>random N-mer filling</u> are based on the observation that Q's with more than one conditioned 'o' site can be <u>factorized</u> as in (2.6). If one first truncates the Q hierarchy severely (to n^{th}-order) and then factorizes to obtain a closed set of equations for a finite number of Q's with a single 'o' site (the T.nF truncation of Ref. (6)), then it is possible to show that the resulting approximate solutions do not depend on the choice of factorization. Furthermore they agree with the solutions of the corresponding nonfactorized severe truncation equations[6]. Thus we do not discuss this scheme further. An obvious alternative is to start by factorizing Q's with several conditioned 'o' sites in (2.5b,c,d) to thus obtain an infinite closed hierarchy for Q's with a single conditioned 'o' site. Truncation can then be employed by neglecting 'ϕ' sites further than n-lattice vectors from the 'o' site, just as for random dimer filling (such truncations are referred to as FT.n in Ref. (6) and will be described as <u>factorizing</u> here). One shortcoming of

this scheme is that the solution depends (presumably weakly) on the choice of factorization. For example, if n = 2,

$$Q_{\phi\phi oo} \equiv Q_{\phi\phi\phi o}\, Q_{\phi\phi o} + (Q_{\phi\phi o})^2 \quad , \quad Q_{\substack{\phi\phi\\ \phi\phi}\, o} \equiv Q_{\substack{\phi\phi\\ \phi\phi\\ \phi\phi}\, o}\, Q_{\substack{\phi\phi\\ \phi\phi}\, o} + Q_{\substack{\phi\\ \phi\phi}\, o}\, Q_{\substack{\phi\phi\\ \phi\phi}\, o}$$

$$\equiv Q_{\phi\phi o\phi}\, Q_{\phi\phi - o} + Q_{\phi\phi o\phi}\, Q_{\phi - o} \qquad \equiv Q_{\substack{\phi\phi\\ \phi\phi\\ \phi\phi}\, o}\, Q_{\substack{\phi\\ \phi\phi}\, o} + Q_{\substack{\phi\phi\\ \phi\phi\\ \phi\phi}\, o}\, Q_{\phi\phi o} \qquad (3.7)$$

after truncation, and since, e.g., $(Q_{\phi\phi o})^2$ and $Q_{\phi\phi o\phi}\, Q_{\phi - o}$ are not equal for exact Q's, solutions of the truncated equations associated with these particular choices will differ. It is important to use a consistent factorization procedure (where a particular Q is always factorized in the same way) since one can then show that the solutions of the truncated equations still exhibit product consistency[6]. The details of the factorization choice used here are described in Appendix A. Examples of the factorized and truncated equations with n = 2 (FT.2) for linear trimer filling on a square lattice are

$$d/dt\ \ell n\ Q_o = -\,6Q_{o\phi\phi}\, Q_{o\phi}$$

$$d/dt\ \ell n\ Q_{o\phi} = -\,2Q_{o\phi\phi} - 2Q_{\substack{o\\ \phi\phi\\ \phi}}\, Q_{\substack{o\\ \phi\phi}} - 2Q_{o\phi\phi}(Q_{o\phi\phi} - Q_{o\phi})$$

$$- 4Q_{o\phi\phi}(Q_{\substack{o\\ \phi\\ \phi}} - Q_{o\phi})$$

$$d/dt\ \ell n\ Q_{o\phi\phi} = -\,1 - Q_{\substack{o\\ \phi\phi\\ \phi\phi}}\, Q_{\substack{o\\ \phi\phi}} - 2Q_{o\phi\phi}\, Q_{\substack{o\\ \phi\phi}}$$

$$\vdots \qquad \cdot \qquad (3.8)$$

In closing this subsection, we remark that the factorized truncation scheme does have the advantage of having a smaller minimal closed set of equations (at each order) than the corresponding mild (unfactorized) truncation (see the next section).

C. A Refined Truncation Scheme for Random Dimer Filling

Here we exploit the fact that a separating wall of empty sites of thickness one shields. In the standard Vette et al. 2^{nd}-shell truncation, the difference $Q_{o\phi\phi\phi} - Q_{o\phi\phi}$ is set identically zero whereas $Q_{o\phi\phi\atop\phi} - Q_{o\phi\phi}$ is determined from the truncated equations. However, this is somewhat inconsistent with our expectation that, for the corresponding exact Q's, the second difference should be slightly smaller since the 'o' site must "look" further around the pair of 'ϕ' sites in $Q_{o\phi\phi}$ (four lattice vectors compared with three) to see the third 'ϕ' site (3^{rd}- and 4^{th}-shell truncation results are consistent with this expectation). Similarly, setting $Q_{o\phi\phi\phi\phi} - Q_{o\phi\phi\phi}$ to zero but evaluating $Q_{o\phi\phi\phi\atop\phi} - Q_{o\phi\phi\phi}$, from 2^{nd}-shell truncated equations, is not so much inconsistent as unnecessary, since these equations automatically set the second quantity to zero.

These observations motivate the development of a truncation scheme exploiting the shielding propensity of 'ϕ' sites in a more refined fashion. We use the concept of the shortest path between an (exterior) 'ϕ' site and the single 'o' site which does not cross over other 'ϕ' sites, e.g., 3(4) for the right most 'ϕ' site in $Q_{o\phi\phi\phi}$ ($Q_{o\phi\phi}$ and $Q_{o\phi\phi}$). In the n^{th}-order truncation, now all 'ϕ' sites with such a shortest unshielded path of

length greater than 'n' are truncated. The slight reduction in accuracy from the less severe n^{th}-shell truncation of Vette et al., for $n > 1$, is expected to be compensated for by the substantial reduction in the number of Q's retained in the minimal closed set at each order. Some mathematical justification for the use of this shortest unshielded path concept, based on the structure of the Q hierarchy equations, is given in Appendix B together with an indication of the appropriate extension for random N-mer filling. (Here we must clearly take into account the shape and larger size of the N-mer in determining path length and the requirement, in some cases, of a thicker empty shielding wall.)

IV. RESULTS FROM HIERARCHY TRUNCATION

In this section, we present results for random dimer and trimer filling on various 2D lattices, and for random square tetramer filling on a square lattice, obtained from implementation of the hierarchial truncation procedures discussed in Section III. We are interested in comparison of results from various order truncations and in obtaining accurate results from truncations of higher order. However, for the cases analyzed here, the latter typically involve hundreds, and sometimes thousands, of Q's in their minimal closed sets. Consequently, computer routines were written to generate, truncate (to various orders), and then numerically integrate these coupled sets of Q equations. Here we first give a general discussion of results and then concentrate on the random dimer filling case.

A. General Remarks and Results

Saturation coverage estimates for the various random filling processes considered here are displayed in Table I for various types and orders of trunction. The corresponding minimum numbers of Q equations, required to close around the $Q_0 \equiv P_0$ equation after truncation, are also given. One observes a dramatic increase in these numbers for higher order truncations. As expected, for trimer and tetramer filling, typically at each order the severe truncation gives the poorest results (but has the smallest number of equations), and the other two truncation schemes exhibit comparable accuracy (but the factorizing scheme has fewer equations). The difference is most significant for spreadout N-mers (e.g., the linear trimer). A

Table I: Saturation Coverage Estimates for Random Dimer and N-mer Filling on Different Lattices for Various Orders and Types of Truncation (V = Vette et al., SUP = Shortest Unshielded Path, S = Severe, M = Mild, F = Factorizing). The minimum number of equations to close the set for each order of truncation is also shown (* indicates that one or more Q's "blowup" just before saturation so values given are obtained from extrapolation)

			SATURATION COVERAGE (Number of Equations) ORDER			
ADSORBATE	LATTICE	TRUNCATION	1st	2nd	3rd	4th
Dimer						
	Square	V	0.88889(2)	0.90215(8)	0.90634(114)	0.9068(4650)*
		SUP	0.88889(2)	0.90187(4)	0.90357(24)	0.9064(766)*
	Triangular	V	0.91239(3)	0.91363(42)		
	Cubic	V	0.91056(2)	0.91546(14)		
	Hexagonal	V	0.87500(2)	0.87500(4)	0.87889(20)	
Triangular Trimer						
	Triangular	F	0.79263(3)	0.79712(38)		
Bent Trimer						
	Square	S		0.82892(12)	0.83381(173)	
		M	0.80237(8)	0.83415(112)		
		F		0.83431(19)	0.83334(697)	
	Hexagonal	F		0.83939(8)		
Linear Trimer						
	Square	S		0.79823(7)	0.83268(96)	
		M	0.78508(3)	0.83321(240)		
		F		0.82653(9)	0.8366(1177)*	
Square Tetramer						
	Square	S		0.73640(3)	0.74803(17)	0.74835(180)
		M	0.73640(3)	0.74804(15)	0.7483(491)*	
		F		0.74817(9)	0.7482 (78)*	0.7482(2010)*

measure of the success of our truncation methods is provided by the rapid convergence and stabilization of the saturation coverage estimates for increasing truncation order. Note that the 1^{st}-order results are given only for the mild truncation because, in 1^{st}-order, the more severe truncations affect even the Q_0 equation, leading to unreliable results.

The most obvious trend in the saturation coverage results is the decrease in the saturation coverage (estimates) with increasing N-mer size (N), just as observed for the 1D linear lattice[3,4,23]. For random dimer filling, we see that the saturation coverage increases as the lattice coordination number 'c' increases (from hexagonal to square to triangular lattices). This is not surprising since the number of ways that a dimer can land on a site (with empty local environment) equals 'c' suggesting that this site is more likely to be filled eventually as 'c' increases. In terms of our hierarchial equations, this is expressed by

$$d/dt\ P_0 = -\ c\ P_{00} \quad . \tag{4.1}$$

Finally we remark that for Bethe lattices, where exact solution for random dimer filling is possible, this trend is also observed (saturation coverage values here can be obtained from (3.3) with $Q_{0\phi} = 0$)[24].

The situation for random N-mer filling is more complex. It is appropriate here to introduce a generalized coordination number, $c_{\{N\}}$, for an N-mer, {N}, which gives the number of different ways that the N-mer can land covering some site (with empty local environment). For N fixed, we expect the saturation coverage to increase with increasing $c_{\{N\}}$, since

$$d/dt\ P_0 = -\ c_{\{N\}}\ P_{\{N\}} \quad , \tag{4.2}$$

where $P_{\{N\}}$ is the probability for an N-mer shaped cluster of sites to be empty. We have checked that this is true in an exact treatment of random trimer filling on Bethe lattices of coordination number 2($c_{\{N\}} = 3$), 3($c_{\{N\}} = 9$), and 4($c_{\{N\}} = 18$) where one has saturation coverages of 0.82365, 0.83809, and 0.85682 respectively (see Appendix C). However, for 2D lattices one observes some anomalous behavior. Consider <u>bent</u> trimer filling on hexagonal ($c_{\{N\}} = 9$) and square ($c_{\{N\}} = 12$) lattices where one has saturation coverages of ≈ 0.839 and ≈ 0.834 respectively. This anomaly occurs since, at saturation, empty sites are either isolated or in isolated empty pairs on the hexagonal lattice, but can <u>also</u> occur in longer strings of empty sites with probability 0.019 (Table II) on a square lattice. The latter clearly more than compensates for the influence of the differing $c_{\{N\}}$.

As mentioned previously, probabilities of various clusters of empty sites can be determined as products of Q's (clearly the number of empty clusters whose probabilities can be thus determined, without further approximation, increases with the order of the truncation). Here we consider only P_{oo} for random dimer filling, and $P_{\{N\}}$ for random N-mer, {N}, filling which are needed to determine the sticking coefficient behavior as functions of coverage or time. Differences $P_{\{N\}} - P_o^N$ are plotted in Fig. 3. Probabilities for subconfigurations involving both empty and filled sites can be determined from conservation of probability, e.g., on a square lattice, $P_{\substack{a\\ a\square a\\ a}} = P_o - 4P_{oo} + 2P_{ooo} + 4P_{\substack{\square\\ o\square o}} - 4P_{\substack{\square\\ o\square\\ o}} + P_{\substack{\square\\ o\square o\\ \square}}$. Of particular interest are the probabilities of an isolated empty site, P_1 (say), an isolated empty pair, P_2 (say), ... and the probabilities, P^n (say), that a

Table II: Saturation Estimates of Various Quantities for Random N-mer Filling. P^n denotes the probability for a site to be in a cluster of >n empty sites, so $P^1 \equiv P_o$

SQUARE LATTICE	TRUNCATION	SATURATION VALUE ESTIMATES $P_{\substack{a\\ao_a\\a}}$	$P_{\substack{aa\\ao_a\\aa}}$	p^1	p^2	p^3
Linear Trimer	2F	0.0437	--	0.1735	0.1298	--
	3F	0.0547	0.0148	0.1638	0.1091	0.0499
Bent Trimer	2F	0.0878	--	0.1657	0.0779	--
	3F	0.0882	0.0148	0.1666	0.0784	0.0192
Square Tetramer	2F	0.0129	--	0.2518	0.2389	--
	3F	0.0079	0.0120	0.2518	0.2439	0.1959
	4F	0.0093	0.0114	0.2518	0.2425	0.1969
HEXAGONAL LATTICE		$P_{\substack{\\ao_a^a}}$	$P_{\substack{a\\a^{oo}_a}}$	p^1	p^2	p^3
Bent Trimer	2F	0.0874	0.0244	0.1606	0.0732	0.00
TRIANGULAR LATTICE		$P_{\substack{\\a^{aa}_{aa}a}}$		p^1	p^2	
Triangular Trimer	2F	0.0421		0.2029	0.1608	

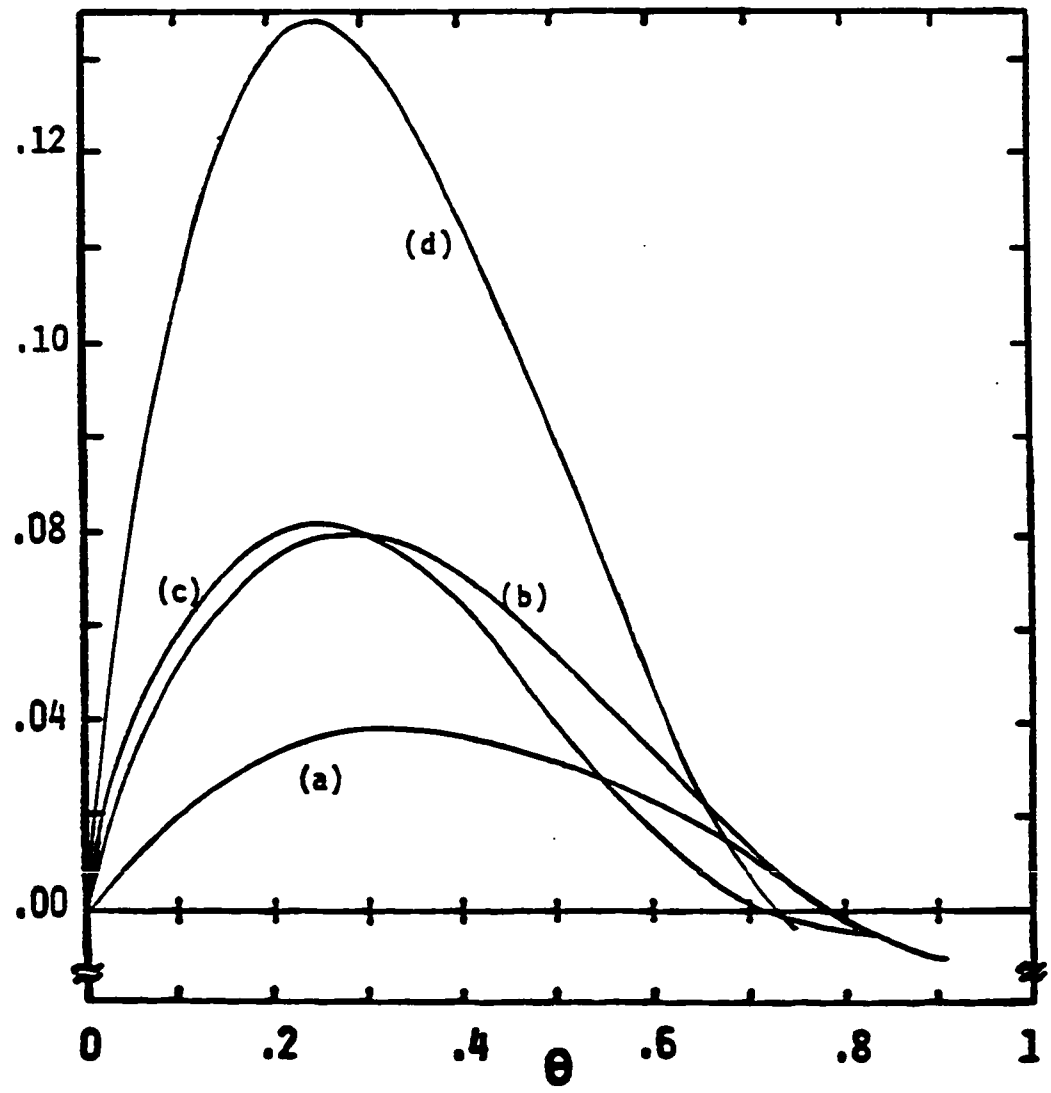

Figure 3: Coverage dependence of (a) $P_{oo}-P_o^2$ for dimer, (b) $P_{ooo}-P_o^3$ for linear trimer, (c) $P_{\substack{o\\oo}}-P_o^3$ for bent trimer, (d) $P_{\substack{oo\\oo}}-P_o^4$ for square tetramer random filling on a square lattice

site is in an empty cluster of 'n' or more sites. Clearly $P^1 \equiv P_0 \equiv P_1 + P^2$, $P^2 \equiv c\,P_2 + P^3$, ... where 'c' is the lattice coordination number. Saturation values of some of these quantities are presented in Table II for several random filling processes. Some examples of other identities which hold at saturation are: $P^2 = 0$ for dimer filling; $P_{\substack{aa\\ a\bigcirc\bigcirc a\\ aa}}$ equals $P_{\substack{aa\\ \bigcirc\bigcirc\\ aa}}$ (P_{aooa}) for linear (bent) trimer filling on a square lattice; $P^3 = 0$ for bent trimer filling on a hexagonal lattice.

B. Detailed Analysis for Random Dimer Filling on a Square Lattice

The higher order truncation results available here allow a detailed and accurate analysis of various features of this process which are expected to be indicative of behavior in more general irreversible processes. The difference between the best two estimates of saturation coverage is 0.0004, and we shall later give arguments which suggest that the exact value is above 0.9068 by no more than ~ 0.0002. In Fig. 4, we have plotted some probabilities for small connected empty configurations as functions of coverage, and similarly in Figs. 5 and 6, some two-point and three-point correlations, respectively. The only significant variation between the best two truncations occurs near saturation for the three-point correlations (e.g., ~ 10% for $c_{\substack{o\\ o-o}}$) where their magnitude is relatively small. In Fig. 7, we compare 2^{nd}-shell with (essentially exact) higher order truncation estimates for various Q's. It is clear that, in the 2^{nd}-shell, various natural pairs of Q's, e.g., $Q_{o\phi\phi}$ and $Q_{o\phi}$, $Q_{\substack{\phi\\ o\phi\phi}}$ and $Q_{\substack{\phi\\ o\phi}}$, are artificially close (in fact $Q_{\substack{\phi\\ o\phi\\ \phi}}$ and $Q_{\substack{\phi\\ o\phi}}$ are identically equal here as is

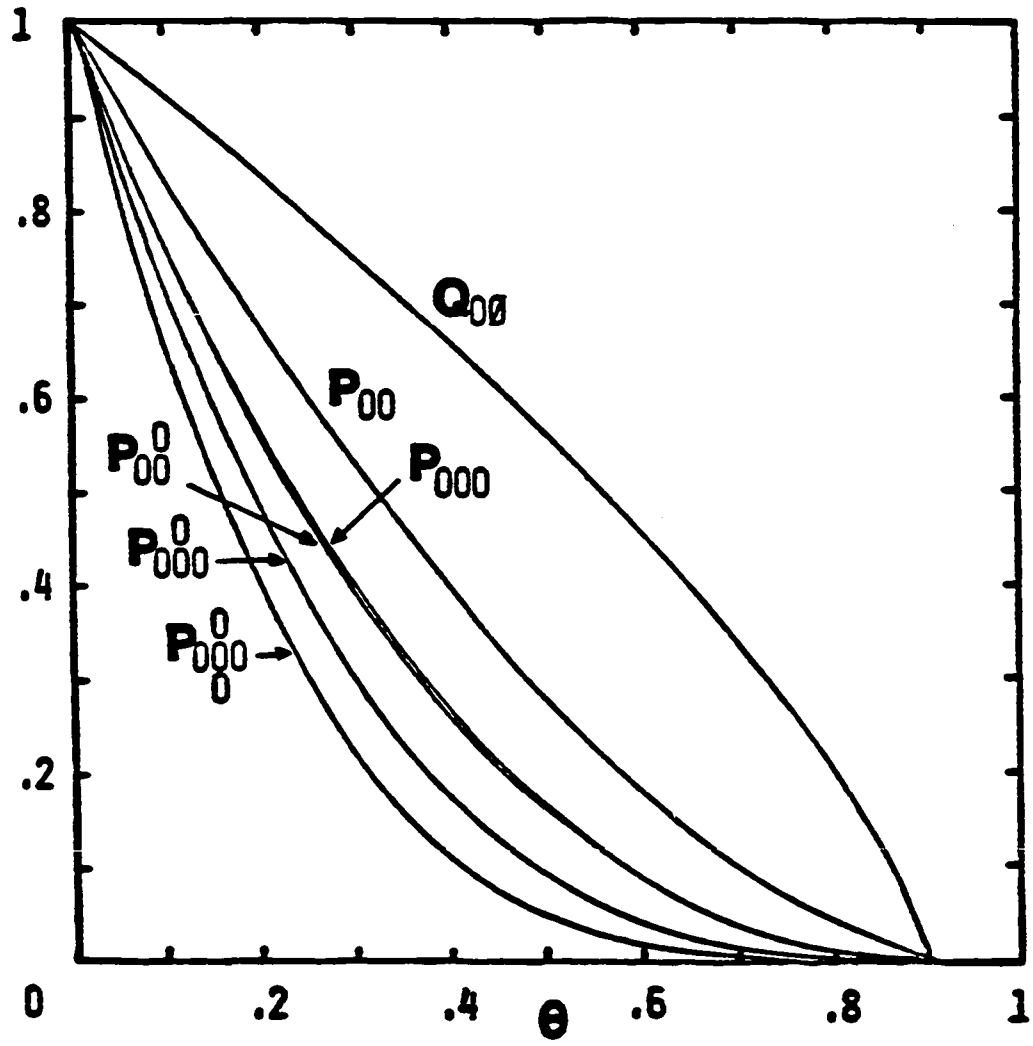

Figure 4: Coverage dependence of probabilities for several small connected empty clusters for random dimer filling on a square lattice

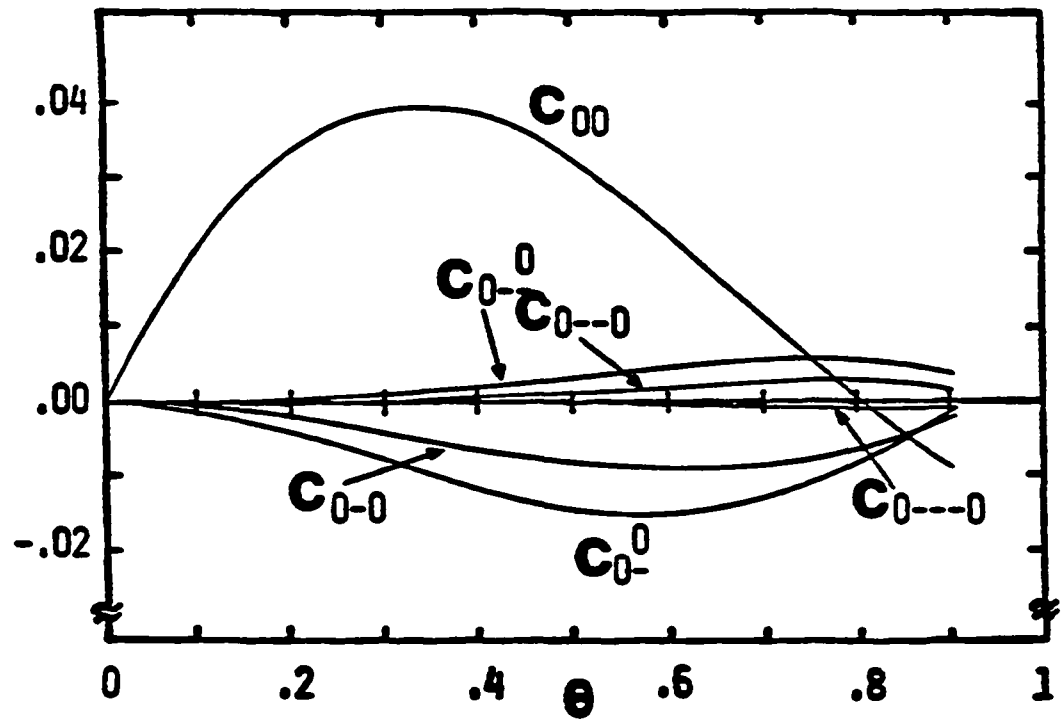

Figure 5: Coverage dependence of short separation two-point correlations $C_{o\text{—}o} = P_{o\text{—}o} - P_o^2$ for random dimer filling on a square lattice

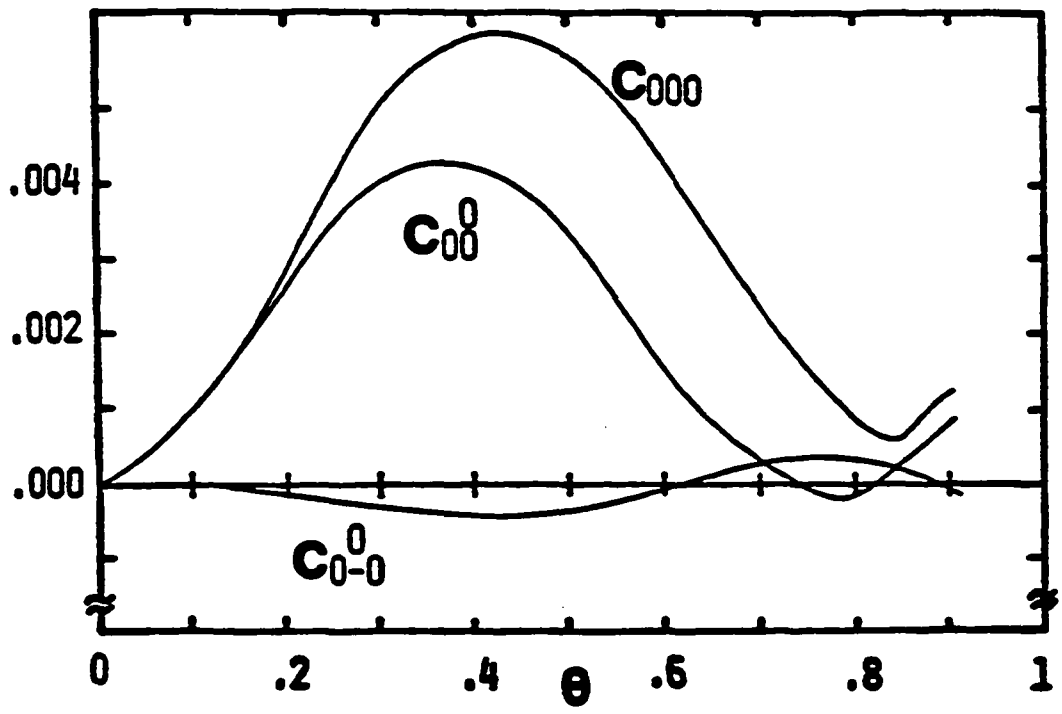

Figure 6: Coverage dependence of three-point correlations C_{000}, C_{00}^{0}, C_{0-0}^{0} where $C_{000} = P_{000} - 2P_{00}P_{0} - P_{0-0}P_{0} + 2P_{0}^{3}$, etc.

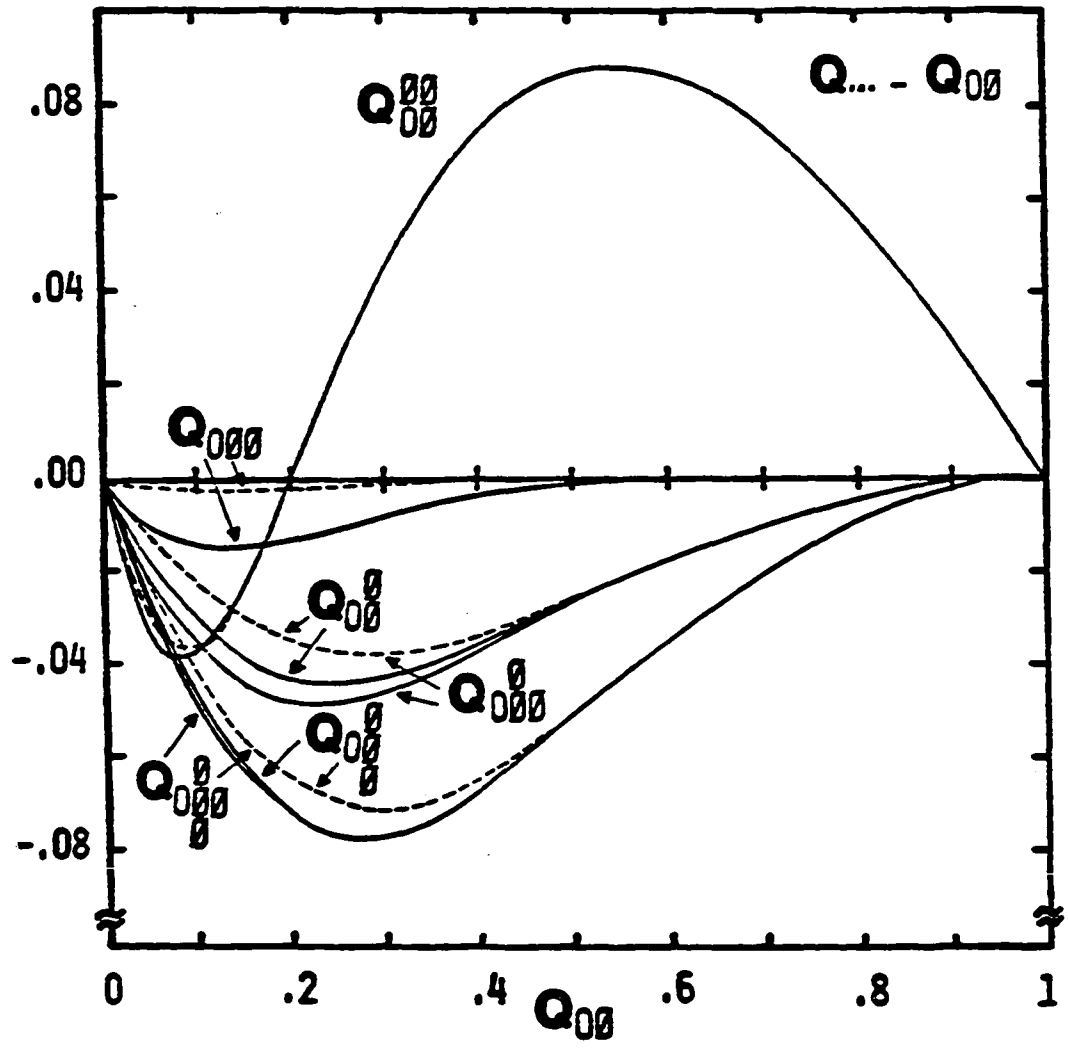

Figure 7: Comparison of 2^{nd}-shell (dotted line) and 4^{th}-shell/effectively exact (solid line) behavior of deviations of several 2^{nd}-shell Q's from $Q_{0\phi}$ for random dimer filling on a square lattice

obvious from the corresponding truncated equations given in Ref. (5)), but in 3rd- and higher-order truncations these differences become larger and stabilize. The 4th-shell estimates of various other Q's are plotted in Fig. 8 illustrating the shielding propensity of strings of three and four empty sites. Deviations between "similar" Q's achieve their maximum shortly before saturation indicating that, at lower coverages, even severe truncations should give accurate results.

Next we investigate the validity of the principles underlying the shortest unshielded path truncation method where it is assumed that the influence of a 'ϕ' site is primarily determined by the length of the shortest unshielded path between it and the 'o' site. Thus, using 4th-shell truncation results, we naturally compare $Q_{o\phi}-Q_{o}$, $Q_{o\overset{\phi}{\phi}}-Q_{o\phi}$, $Q_{o\overset{\phi}{\overset{\phi}{\phi}}}-Q_{o\overset{\phi}{\phi}}$, $Q_{o\phi\phi}-Q_{o\phi}$, $Q_{o\overset{\phi}{\phi\phi}}-Q_{o\phi\phi}$, $Q_{o\phi\phi\phi}-Q_{o\phi\phi}$, $Q_{o\overset{\phi}{\phi}\phi}-Q_{o\overset{\phi}{\phi}}$, $Q_{o\overset{\phi}{\phi\phi}}-Q_{o\overset{\phi}{\phi}}$, $Q_{o\overset{\phi}{\overset{\phi}{\phi}}\phi}-Q_{o\overset{\phi}{\overset{\phi}{\phi}}}$, ••• where the length and number of such shortest unshielded paths between 'o' and the additional 'ϕ' are given by the (length, number) pairs (1,1), (2,1), (3,1), (4,2), (4,1), (5,2), (5,1), (6,2) •••, respectively. As anticipated, there is (roughly speaking) a monotonic decrease in the maximum magnitude of these differences (see Table III). An exact assessment of the influence of any 'ϕ' site, must of course sum contributions from all unshielded paths between it and the 'o' site, but the above results indicate that the dominant influence is associated with the shortest such patn(s).

It is also possible to give simple physical arguments explaining whether each additional connected 'ϕ' site increases or decreases the value of those Q's with a single 'o' site and connected cluster of 'ϕ' sites.

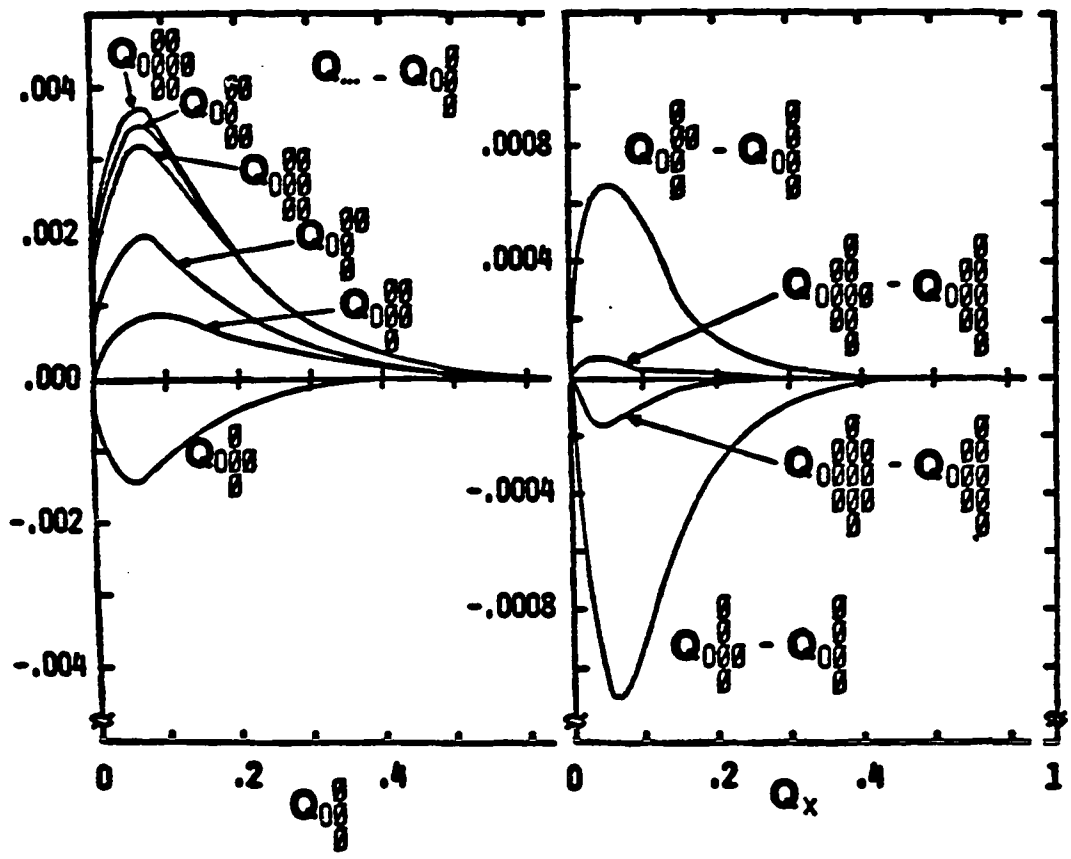

Figure 8: Shielding propensity for strings of three and four shielding sites: differences in corresponding pairs of Q's as functions of the Q with the fewer conditioning sites

Table III: Crude Estimate of Maximum Change in Magnitude for Q's with a single 'o' site from adding a 'ϕ' site with various lengths (and numbers) of shortest unshielded paths from the 'o' site for random dimer filling on a square lattice (4^{th}-shell results were used)

Length(number) of Shortest Unshielded Paths	(1,1)	(2,1)	(3,1)	(4,2) (4,1)	(5,2) (5,1)	(6,2) (6,1)	(7,2) (7,1)	(8,2)	(9,2)
Maximum Magnitude of Q-Deviation	0.12	0.045	0.02	0.015 0.005	0.007 0.0025	0.002 0.0011	0.00065 0.00045	0.0004	0.0001

These, of course, all have initial values of unity and saturation values of zero (excepting Q_o). We first observe, from Fig. 4, that $Q_{o\phi} > Q_o \equiv 1 - \theta$ for all but high coverages. This follows since the given empty site in $Q_{o\phi}$ means there are only three instead of four ways that a dimer could land on the 'o' site (Note that the hierarchy equations imply $d/d\theta\ Q_{o\phi} = -3/4$ when $\theta = 0$). However, near saturation it becomes increasingly likely that sites around 'ϕ' will be filled and, in fact, $Q_{o\phi} \to 0$ whereas $Q_o \to 0.093$. In Table IV, we indicate whether values of various Q's are increased or decreased by additional 'ϕ' sites. Comparing $Q_{o\overset{\phi}{\phi}}$ with $Q_{o\phi}$, we anticipate that the additional 'ϕ' site enhances the probability of a dimer landing adjacent to $\overset{\phi}{\phi}$ (see Table IV), thus filling the 'o' site and lowering $Q_{o\overset{\phi}{\phi}}$ cf. $Q_{o\phi}$. Similarly the additional 'ϕ' site in $Q_{o\overset{\phi}{\phi}\overset{\phi}{\phi}}$ cf. $Q_{o\overset{\phi}{\phi}}$ should enhance the probability of a dimer landing adjacent to the top $\overset{\phi}{\phi}$ pair, reducing the number of ways that the 'o' site can be filled and thus increasing $Q_{o\overset{\phi}{\phi}\overset{\phi}{\phi}}$ cf. $Q_{o\overset{\phi}{\phi}}$. Thus, in general, additional 'ϕ' sites enhance probabilities for certain dimer fillings (various examples are shown in the Table) which either inhibit or enhance the probability for the 'o' site to be empty. In summary we can say that: <u>additional 'ϕ' sites increase (decrease) the Q value for a corresponding shortest unshielded path of odd (even) length.</u>

We can now give a reasonable explanation for the observed monotonic increase in saturation coverage estimates (to the exact value) with increasing truncation order. First we recall the form of the Q hierarchy equations (2.5a), in particular,

Table IV: Magnitude Relationships between Q's and Enhanced Configurations due to Additional 'ϕ' Sites

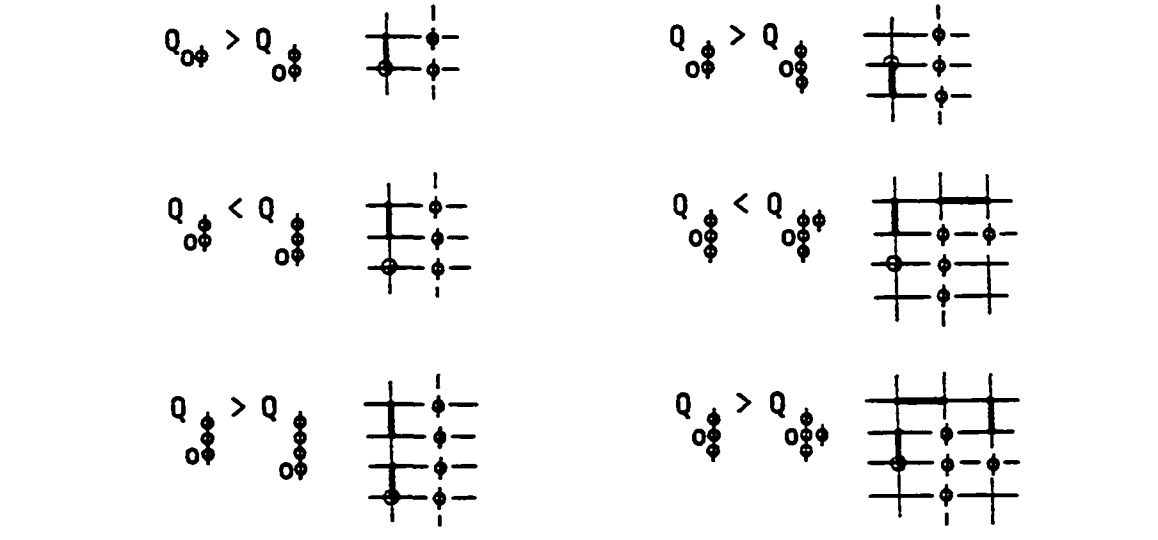

$$d/dt\ \ell n\ Q_{O} = -4Q_{O\phi} \tag{4.3a}$$

$$d/dt\ \ell n\ Q_{O\phi} = -1 - 4Q_{O\overset{\phi}{\phi}} - 2Q_{O\phi\phi} + 4Q_{O\phi} \tag{4.3b}$$

$$d/dt\ \ell n\ Q_{O\overset{\phi}{\phi}} = -1 - 2(Q_{O\phi\overset{\phi}{\phi}} - Q_{O\phi\phi}) - 2(Q_{\overset{\phi}{\phi}\overset{\phi}{\phi}} - Q_{\overset{\phi}{\phi}\phi}) - 2(Q_{\phi\overset{\phi}{\phi}\overset{\phi}{\phi}} - Q_{\phi\overset{\phi}{\phi}\phi}) - 2Q_{O\overset{\phi}{\phi}\overset{\phi}{\phi}}$$

$$\vdots \qquad . \tag{4.3c}$$

In the 1^{st}-shell truncation, $Q_{O\overset{\phi}{\phi}}$ and $Q_{O\phi\phi}$ in (4.3b) are replaced by the larger $Q_{O\phi}$, so d/dt $\ell n\ Q_{O\phi}$ is more negative and therefore $Q_{O\phi}$ decreases to zero faster than the 2^{nd}- or higher-shell truncation or exact values. Consequently the saturation coverage estimate is lower since the source term in (4.3a), driving Q_{O} to decrease, is reduced in magnitude. In the 2^{nd}-shell truncation $Q_{O\overset{\phi}{\phi}\overset{\phi}{\phi}}$ is replaced by the smaller $Q_{O\phi\phi}$, and $Q_{\overset{\phi}{\phi}\overset{\phi}{\phi}}$ by the smaller $Q_{\overset{\phi}{\phi}\phi}$, so in (4.3c), d/dt $\ell n\ Q_{O\overset{\phi}{\phi}}$ is less negative and therefore $Q_{O\overset{\phi}{\phi}}$ is larger than the 3^{rd}- and higher-shell truncation or exact values (2^{nd}-shell truncation has the same effect on $Q_{O\phi\phi}$). Consequently here d/dt $\ell n\ Q_{O\phi}$ is still more negative than the 3^{rd}- and higher-shell truncations or its exact value, so the saturation coverage estimate is correspondingly lower (but, from the above analysis, higher than the 1^{st}-shell). This argument extends in the obvious way to suggest that the n^{th}-shell saturation coverage estimate is lower than the $(n+1)^{th}$-shell and exact values.

V. ISOMORPHIC FILLING PROCESSES

Consider first the random (dissociative) dimer filling of diagonally-nearest-neighbor sites on a square lattice (with both NE-SW and NW-SE orientation). Such a process has been considered by Fuller et al.[15] in the context of water sorption on metal oxides, i.e., hydroxylation. It is clear that this process decomposes into two completely independent dimer filling processes on the ± sublattices shown in Fig. 9. Since each of these is a $\pi/4$-rotated square lattice, each of the independent subprocesses is equivalent to horizontal/vertical dimer filling of nearest-neighbor sites on a square lattice discussed previously in great detail. Thus, e.g., the saturation coverage for diagonal filling equals that for horizontal/vertical filling. Furthermore if $\underset{\sim}{\sigma}_{\pm}$ represents a subconfiguration of sites entirely on the ± sublattice, then $P_{\underset{\sim}{\sigma}_+ \underset{\sim}{\sigma}_-} = P_{\underset{\sim}{\sigma}_+} P_{\underset{\sim}{\sigma}_-}$, e.g., $P_{oo} = P_{o_+o_-} = P_{o_+} P_{o_-} = P_o^2$, for diagonal filling and each of $P_{\underset{\sim}{\sigma}_{\pm}}$ can be determined from corresponding quantities for horizontal/vertical dimer filling. This factorization property is self-evident in the hierarchical rate equations for diagonal filling. If one continues to consider the corresponding (dissociative) diagonal filling of linear and bent trimers, square tetramers, etc., on a square lattice, one finds a decomposition into independent filling processes on the same ± sublattices as shown in Fig. 9, where again each of these independent subprocesses is equivalent to the corresponding horizontal/vertical filling process on a square lattice described previously.

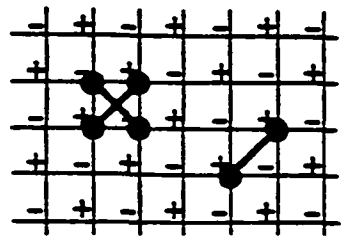

Figure 9: Independent ± sublattices associated with diagonal dimer filling

Another class of isomorphisms can be demonstrated by simply comparing different descriptions of the same process. From Fig. 10, we see that random filling of a hexagonal lattice by hexagonal hexamers is equivalent to monomer filling of a triangular lattice with nearest-neighbor blocking (i.e., the monomer cannot land at a site which has one or more occupied nearest neighbor). Similarly from Fig. 11, one can see that random square tetramer filling of a square lattice is equivalent to monomer filling of a square lattice with both nearest-neighbor and diagonal nearest-neighbor blocking. Other more complex examples of such isomorphisms can, of course, be given. In previous work[7,8], the description of N-mer filling used here (where each N-mer fills N lattice sites) was termed the "atomic lattice" picture. The alternative description where an adsorbing species is represented by the filling of a single site on a "dual lattice" (cf. Figs. 10 and 11) was termed the "event lattice" picture. The latter in general contains more information[8] since, e.g., knowing which sites are filled for dimer filling on a square lattice does not necessarily tell us where the dimers landed.

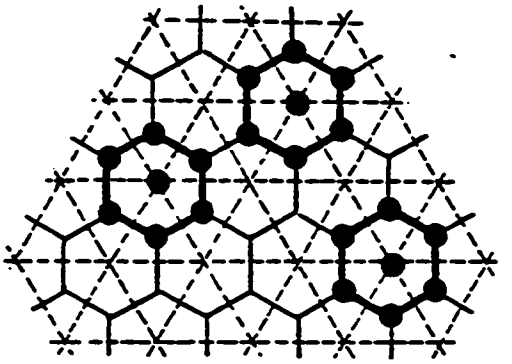

Figure 10: Equivalence of filling of hexagonal hexamers on a hexagonal (atomic) lattice and monomers with nearest-neighbor blocking on a triangular (event) lattice

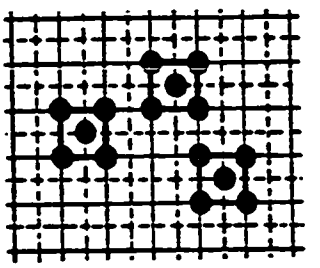

Figure 11: Equivalence of filling of a square tetramer on a square (atomic) lattice and monomers with nearest-neighbor and diagonal nearest-neighbor blocking on a square (event) lattice

VI. CONCLUSIONS AND EXTENSIONS

For random dimer or N-mer filling of infinite 2D lattices, we have demonstrated that the hierarchial truncation techniques presented here can produce accurate estimates of the time or coverage dependence of probabilities for various small subconfigurations including saturation coverage estimates. For random dimer filling, our results should be compared with those of several Monte Carlo simulations listed in Table V. By extending Vette et al.'s analysis to generate the most extensive and accurate results available for this process, we have provided sufficient insight into the underlying structure to motivate and justify a "shortest unshielded path" truncation procedure. This has ramifications for general irreversible cooperative processes. Our analysis of various random trimer filling processes is the first available. Results should be most accurate for a bent trimer (and square tetramer) on a square lattice and a triangular trimer on a triangular lattice, where a shielding wall thickness of one suffices, and for a bent trimer on a hexagonal lattice whose "large" loops make it "Bethe lattice like". Results for the linear trimer on a square lattice, requiring a shielding wall thickness of two, should be less accurate. For random square tetramer filling of a square lattice, Monte Carlo simulation of Solomon[26] on a 100 x 100 lattice obtained a saturation coverage estimate of 0.7468 compared with our best estimate of 0.7482 ± 0.0002, and the generalized Palasti conjecture value of $(1-e^{-2})^2 \sim 0.74765$. In later work, we will provide our own more extensive Monte Carlo simulation results for most of these processes.

Table V: Estimates of Saturation Coverage for Random Dimer Filling on a Square Lattice from Various Monte Carlo Simulations with Cyclic Lattice Boundary Conditions [cf. our best estimate for an infinite lattice of slightly (no more than ~ 0.0002) above 0.9068]

LATTICE SIZE	NUMBER OF SIMULATIONS	AVERAGE SATURATION COVERAGE	STANDARD DEVIATION	REF.
10x10	unknown	0.90	0.024	12c
100x100	201	0.9085	0.0025	12b
22x22	100	0.9049	0.0102	15
30x30	100	0.9066	0.0092	15
36x36	100	0.9066	0.0076	15

In all of the above, the treatment discussed centers on determination of probabilities for small compact empty subconfigurations, which do not provide us with information as to, e.g., the large separation behavior of the two-point correlations. Determination of the latter involves consideration and appropriate treatment of further hierarchial rate equations which couple back to the minimal set for connected empty subconfigurations analyzed here. Some limited development along these lines, for random dimer filling on a square lattice, can be found in Ref. (22).

Treatment of many physical processes leads to several natural extensions of the models presented here. We can consider the irreversible coadsorption of various dimer and N-mer species[28]. If one is interested in a statistical treatment describing only which sites are filled and empty (rather than which species fill the various sites) then, for random filling (only), again one obtains a closed hierarchy for probabilities of connected clusters of empty sites which can be straightforwardly treated by the methods presented here[28,29]. Epstein has discussed the analogous 1D processes[3]. Partial coverages can be obtained simply by adding the appropriate rate equations which close with this set[28]. A further natural extension is to cases where there are several types of sites, e.g., periodic lattices or lattices with a stochastic distribution of "inactive" nonadsorptive sites[27]. Application of our analytic methods to such extended models provides a powerful tool for treating, e.g., competitive α- and β-CO on binary alloy surfaces (for which Monte Carlo simulations have been performed recently[16]).

Finally we comment on a rather subtle variation of the dimer filling problem which we characterize as "end-on dimer filling". We describe only the random filling case here. Instead of randomly sampling pairs of empty sites on which to adsorb (as in the model treated above), one could randomly sample single empty sites (with one end of the dimer), testing to see if any adjacent sites are empty. Then if this is the case, one of these is picked at random and the other end of the dimer attached (at which point the dimer becomes irreversibly adsorbed), and if not, the dimer desorbs. In later work we detail the statistical differences between these dimer filling models (which seem not to have been appreciated in previous treatments).

ACKNOWLEDGEMENTS

Ames Laboratory is operated for the U.S. Department of Energy by Iowa State University under Contract No. W-7405-ENG-82. This work was supported by the Office of Basic Energy Sciences.

APPENDIX A: FACTORIZING TRUNCATION SCHEMES

The choice of factorization for Q's with several conditioned 'o' sites used in the n^{th}-order factorizing (FT.n) truncation scheme is briefly described here. Consider first Q's which have one or more 'ϕ' sites further than n-lattice vectors from at least one 'o' site (and so are affected by truncation). We choose the factorization in which the 'o' site with the most (truncated) 'ϕ' sites greater than n-lattice vectors from it is in the Q with the most 'ϕ' sites, e.g., in the 3^{rd}-order,

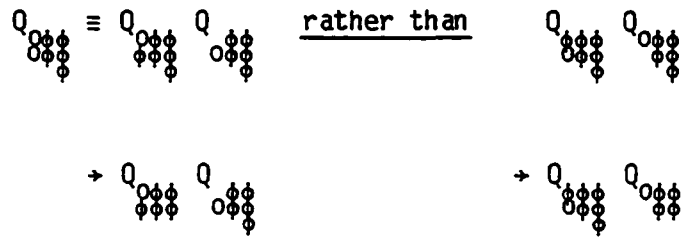

This choice creates an additional 'ϕ' site near the 'o' site with the most truncated 'ϕ' sites, thus maximizing shielding from these. If two or more 'o' sites have the same (maximum) number of 'ϕ' sites greater than n-lattice vectors from them, then the 'o' in the largest Q is chosen as the one with the most 'ϕ' sites at distance n+1 (or if this does not distinguish between the 'o' sites, then at distance n+2, and so on). For example, in the 2^{nd}-order,

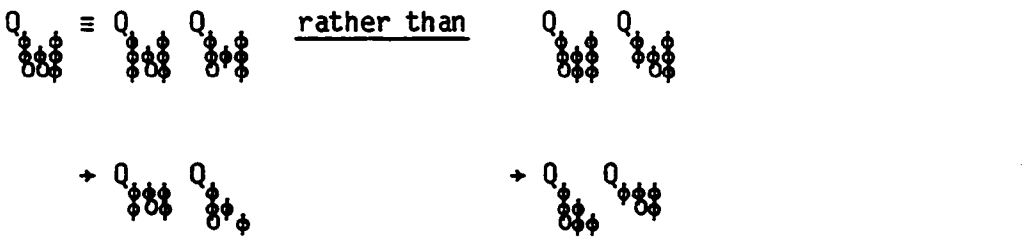

If none of these rules distinguish between 'o' sites, then we factorize in an arbitrary, but consistent, fashion.

For other Q's (where no 'ϕ' sites are truncated), the choice of factorization does not affect the solution. For if two different choices are made and the resulting truncated sets of equations extended, if necessary, to include the same Q's, then the only difference between the two sets is that different but "compatible" products of Q's appear in some places (i.e., these products are equal for exact Q's). It then follows that solutions of the two sets will agree by virtue of product consistency (cf. Ref. 6). For completeness, we give the following examples of the choice, written into our computer routine, for 3rd- or higher-order truncation:

APPENDIX B: THE SHORTEST UNSHIELDED PATH

We first analyze the source of the difference between $Q_{\phi\phi\phi}$ and $Q_{\phi\phi\phi}$ for random dimer filling on a 2D square lattice. This will substantiate the appropriateness of our concept of the shortest unshielded path and definition of its length in determining the influence of the bottom 'ϕ' site in the first Q. One has from (2.4),

$$- d/dt \ln Q_{\phi\phi\phi} - 1 = (Q_{\phi\phi\phi} - Q_{\phi\phi\phi}) + 2(2Q_{\phi\phi\phi} - Q_{\phi\phi\phi})$$

$$+ 2(Q_{o\phi\phi\phi} - Q_{o\phi\phi\phi}) + 2(Q_{\phi\phi\phi} - Q_{\phi\phi\phi}) + (Q_{\phi\phi\phi} - Q_{\phi\phi\phi}) \quad (B1)$$

$$- d/dt \ln Q_{\phi\phi\phi} - 1 = (Q_{\phi\phi\phi} - Q_{\phi\phi\phi}) + 2(2Q_{\phi\phi\phi} - Q_{\phi\phi\phi})$$

$$+ 2(Q_{o\phi\phi\phi} - Q_{o\phi\phi\phi}) + 2(Q_{\phi\phi\phi} - Q_{\phi\phi\phi}) + (Q_{\phi\phi\phi} - Q_{\phi\phi\phi}). \quad (B2)$$

The differences between (B1) and (B2) values for corresponding terms on the r.h.s. are given by:

5^{th} and 1^{st} terms: $(Q_{\phi\phi\phi} - Q_{\phi\phi\phi}) - (Q_{\phi\phi\phi} - Q_{\phi\phi\phi})$

$(1/2)4^{th}$ [2^{nd}] terms: [2] ($Q_{o\phi\phi\phi\phi}$ - $Q_{o\phi\phi\phi}$) - ($Q_{o\phi\phi\phi}$ - $Q_{o\phi\phi}$)

$(1/2)3^{rd}$ terms: ($Q_{o\phi\phi\phi\phi}$ - $Q_{o\phi\phi\phi}$) - ($Q_{o\phi\phi\phi}$ - $Q_{o\phi\phi\phi}$)

$= Q_{o\phi\phi\phi\phi} - 2Q_{o\phi\phi\phi} + Q_{o\phi\phi\phi}$.

Clearly the 5^{th} and 1^{st} terms contribute less than the 4^{th} and 2^{nd} where the 'o' site is closer to the additional 'ϕ' site. In the 3^{rd} terms, the 'o' site is even closer to the additional 'ϕ' site(s) but we have a second-order rather than first-order difference in Q's and thus anticipate that the contribution will be of the same order as from the 2^{nd} and 4^{th} terms. This is verified from high-order truncation results. (The generalization of this argument requires that a (first-order) difference in Q's with the additional 'ϕ' site at shortest unshielded path (s.u.p.) distance 2N is of the same order as a second-order difference in Q's with additional 'ϕ' site(s) at s.u.p. distance N.)

Thus in analyzing the difference between $Q_{\phi\phi\phi\phi}$ and $Q_{\phi\phi\phi}$, we are naturally lead to consider the difference between corresponding Q's associated with the $2^{nd}/4^{th}$ and 3^{rd} terms. Here we consider only the former, which is easier to analyze, and thus to compare $Q_{o\phi\phi\phi\phi}$ with $Q_{o\phi\phi\phi}$ (and $Q_{\phi\phi\phi}$ with $Q_{\phi\phi\phi}$). The rate equations for these display a similar, but somewhat less precise, correspondence of terms and, for the former,

motivate us to compare $Q_{\phi\phi\phi\phi\phi\phi\phi}$ with $Q_{\phi\phi\phi\phi\phi\phi\phi}$. These in turn motivate us to compare $Q_{\phi\phi\phi\phi\phi\phi\phi}$ with $Q_{\phi\phi\phi\phi\phi\phi\phi}$, and then $Q_{\phi\phi\phi\phi\phi\phi\phi}$ with $Q_{\phi\phi\phi\phi\phi\phi\phi}$ where a somewhat weaker correspondence of terms can still be made. However, when naturally continuing to compare $Q_{\phi\phi\phi\phi\phi\phi\phi}$ with $Q_{\phi\phi\phi\phi\phi\phi\phi}$, one observes a fundamental structural difference in the rate equations, i.e.,

$$-d/dt\ \ell n\ Q_{\phi\phi\phi\phi\phi\phi\phi} = 3 + \cdots, \quad d/dt\ \ell n\ Q_{\phi\phi\phi\phi\phi\phi\phi} = 2 + \cdots \tag{B3}$$

This substantial difference is propagated back through the coupled sequence of six pairs of Q's (as the 'o' site travels around the shielding wall segment $\phi\phi\phi$) to cause deviation between $Q_{\phi\phi\phi\phi}$ and $Q_{\phi\phi\phi\phi}$. Compatibility with our choice of corresponding shortest unshielded path length of six should be clear.

Similarly one could consider equations for these Q's for random bent trimer and square tetramer filling. Here one "gets around" the end of the shielding wall segment $\phi\phi\phi$ with fewer steps (couplings) and hence obtains lower shortest unshielded path length values. Finally for random linear trimer filling (where the wall segment $\phi\phi\phi$ is not thick enough to shield), one has a substantial difference in structure in the $Q_{\phi\phi\phi\phi}$ and $Q_{\phi\phi\phi\phi}$ equations, i.e.,

$$-d/dt\ \ell n\ Q_{\phi\phi\phi\phi} = 1 + (Q_{\phi\phi\phi\phi} - Q_{\phi\phi\phi\phi}) + \cdots$$

$$- d/dt \, \ell n \, Q_{\phi\phi\phi} = (Q_{\phi\phi\phi} - Q_{\phi\phi\phi}) + \cdots$$

giving a corresponding shortest unshielded path length of one.

APPENDIX C: RANDOM TRIMER FILLING ON BETHE LATTICES

It is possible to obtain exact solutions (and thus, e.g., saturation coverage values) for random dimer and N-mer filling of Bethe lattices[24]. This provides a useful intuitive tool for analyzing trends in corresponding processes on physical lattices. For random dimer filling on physical lattices with no closed loops of length three (so excluding, e.g., the triangular lattice), it has been shown that the 1^{st}-shell truncation solutions correspond to the exact solution for random dimer filling on a Bethe lattice of the same coordination number[24]. In fact this correspondence has been used as the basis for resummation of corresponding formal coverage expansions[8,27].

In considering random trimer filling of Bethe lattices, we note first that all connected triples of sites are equivalent for a Betne lattice of (arbitrary) coordination number c. Thus we expect that random trimer filling on a Bethe lattice with c=3 and a hexagonal lattice should exhibit certain similarities (these have the same generalized coordination number for trimer filling). However, random trimer filling on a Bethe lattice with c=4 in a sense corresponds to simultaneous random linear and bent trimer filling of a square lattice (the generalized coordination number for the former is the sum of those for the latter). The procedure of Ref. (24) leads straightforwardly to the following exact closed sets of equations for random trimer filling of a Bethe lattice with

A. c=3

$$d/dt\ P_o = -\ 9P_{oo}\ Q_{o\phi\phi}$$

$$d/dt\ P_{oo} = -\ P_{oo}\ Q_{o\phi}\ (4 + 8Q_{o\phi\phi} + 2Q_{o\phi\overset{\phi}{\underset{\phi}{\phi}}})$$

$$d/dt\ \ell n\ Q_{o\phi\phi} = -\ 1 - 2Q_{o\phi\overset{\phi}{\underset{\phi}{\phi}}} - 2Q_{o\phi\phi}\ Q_{o\phi\overset{\phi}{\underset{\phi}{\phi}}}$$

$$d/dt\ \ell n\ Q_{o\phi\overset{\phi}{\underset{\phi}{\phi}}} = -\ 2 - 2Q_{o\phi\phi} - (Q_{o\phi\phi})^2 + 2Q_{o\phi\overset{\phi}{\underset{\phi}{\phi}}} + Q_{o\phi\phi}\ Q_{o\phi\overset{\phi}{\underset{\phi}{\phi}}}$$

B. c=4

$$d/dt\ P_{o} = -\ 18P_{oo}\ Q_{o\phi\phi}$$

$$d/dt\ P_{oo} = -\ P_{oo}\ Q_{o\phi\phi}\ (6 + 18Q_{o\phi\phi} + 6Q_{o\overset{\phi}{\underset{\phi}{\overset{\phi}{\underset{\phi}{\phi}}}}})$$

$$d/dt\ \ell n\ Q_{o\phi\phi} = -\ 1 - 4Q_{o\overset{\phi}{\underset{\phi}{\overset{\phi}{\underset{\phi}{\phi}}}}} - 6Q_{o\phi\phi}\ Q_{o\overset{\phi}{\underset{\phi}{\overset{\phi}{\underset{\phi}{\phi}}}}} - Q_{o\overset{\phi}{\underset{\phi}{\overset{\phi}{\underset{\phi}{\phi}}}}}\ Q_{o\overset{\phi}{\underset{\phi}{\overset{\phi}{\underset{\phi}{\phi\phi}}}}}$$

$$d/dt\ \ell n\ Q_{o\overset{\phi}{\underset{\phi}{\overset{\phi}{\underset{\phi}{\phi}}}}} = -\ 2 - 3Q_{o\overset{\phi}{\underset{\phi}{\overset{\phi}{\underset{\phi}{\phi\phi}}}}} - 3Q_{o\phi\phi} - 9(Q_{o\phi\phi})^2 - 3Q_{o\phi\phi}\ Q_{o\overset{\phi}{\underset{\phi}{\overset{\phi}{\underset{\phi}{\phi\phi}}}}}$$
$$+ 4Q_{o\overset{\phi}{\underset{\phi}{\overset{\phi}{\underset{\phi}{\phi}}}}} + 3Q_{o\phi\phi}\ Q_{o\overset{\phi}{\underset{\phi}{\overset{\phi}{\underset{\phi}{\phi}}}}} + Q_{o\overset{\phi}{\underset{\phi}{\overset{\phi}{\underset{\phi}{\phi}}}}}\ Q_{o\overset{\phi}{\underset{\phi}{\overset{\phi}{\underset{\phi}{\phi\phi}}}}}$$

$$d/dt\ \ell n\ Q_{o\overset{\phi}{\underset{\phi}{\overset{\phi}{\underset{\phi}{\phi\phi}}}}} = -\ 3 - 3Q_{o\phi\phi} - 9(Q_{o\phi\phi})^2 - 3Q_{o\phi\phi}\ Q_{o\overset{\phi}{\underset{\phi}{\overset{\phi}{\underset{\phi}{\phi}}}}}$$
$$+ 3Q_{o\overset{\phi}{\underset{\phi}{\overset{\phi}{\underset{\phi}{\phi\phi}}}}} + 3Q_{o\phi\phi}\ Q_{o\overset{\phi}{\underset{\phi}{\overset{\phi}{\underset{\phi}{\phi\phi}}}}}$$

Saturation coverage values are simply obtained from integration of these equations.

REFERENCES

1. E. R. Cohen and H. Reiss, J. Chem. Phys. 38, 680 (1963); T. H. K. Barron and E. A. Boucher, Trans. Faraday Soc. 65, 3301 (1969).
2. E. A. Boucher, J. Chem. Phys. 59, 3848 (1973).
3. E. A. Boucher, Chem. Phys. Lett. 17, 221 (1972); Faraday Trans. II 69, 1839 (1973); J. J. Gonzalez, P. C. Hemmer and J. S. Høye, Chem. Phys. 3, 228 (1974); I. R. Epstein, Biopolymers 18, 765 (1979).
4. N. O. Wolf, J. W. Evans, D. K. Hoffman, J. Math. Phys. 25, 2519 (1984).
5. K. J. Vette, T. W. Orent, D. K. Hoffman and R. S. Hansen, J. Chem. Phys. 60, 4854 (1974).
6. J. W. Evans, D. R. Burgess and D. K. Hoffman, J. Chem. Phys. 79, 5011 (1983).
7. D. K. Hoffman, J. Chem. Phys. 65, 95 (1976).
8. J. W. Evans, Physica 123A, 297 (1984).
9. N. A. Plate and O. V. Noah, Adv. Polym. Sci. 31, 133 (1979); E. A. Boucher, Prog. Polym. Sci. 6, 63 (1978).
10. P. J. Flory, J. Am. Chem. Soc. 61, 1518 (1939).
11. J. K. Roberts, Nature 135, 1037 (1935); Proc. Camb. Phil. Soc. 34, 399 (1938).
12. a) J. K. Roberts, Proc. R. Soc. A 152, 473 (1935); Proc. R. Soc. A 161, 141 (1937).
    b) D. R. Rossington and R. Borst, Surf. Sci. 3, 202 (1965).
    c) W. D. Dong, Surf. Sci. 42, 609 (1974).
13. P. T. Dawson and Y. K. Peng, Surf. Sci. 33, 565 (1972).

14. J. B. Peri, J. Chem. Phys. 69, 220 (1965).

15. E. L. Fuller, S. Ebey, and V. R. R. Uppuluri, "Statistical Modelling of Adsorption Processes on Catalyst Surfaces: Preliminary Report", ORNL-5231, Oak Ridge National Laboratory (1976); E. L. Fuller and P. A. Agron, Oak Ridge National Laboratory Report 5129 (1976).

16. B. E. Hayden and D. F. Klemperer, Surf. Sci. 80, 401 (1979) and references therein.

17. R. Gomer, Disc. Faraday Soc. 28, 540 (1959); Solid State Physics 30, 94 (1975).

18. A. Maltz and E. Mola, Surf. Sci. 115, 599 (1982); J. Chem. Phys. 79, 5141 (1983).

19. T. E. Madey and J. T. Yates, Surf. Sci. 76, 397 (1978); F. M. Hoffmann, T. E. Felter, P. A. Thiel and W. H. Weinberg, Surf. Sci. 130, 163, 173 (1983); P. D. Szuromi, J. R. Eystrom and W. H. Weinberg, J. Chem. Phys. 80, 508 (1984).

20. E. S. Page, J. R. Stat. Soc. B 21, 364 (1959); F. Downton, J. R. Stat. Soc. B 23, 207 (1961); R. B. McQuistan and D. Lichtman, J. Math. Phys. 9, 1680 (1968); T. H. K. Barron, R. J. Bawden, and E. A. Boucher, J. Chem. Soc. 70, 651 (1979).

21. N. O. Wolf, Ph.D. Thesis, Iowa State University, 1979.

22. J. W. Evans, D. R. Burgess and D. K. Hoffman, J. Math. Phys. 25, 3051 (1984).

23. J. K. Mackenzie, J. Chem. Phys. 37, 723 (1962); E. A. Boucher, Chem. Phys. Lett. 17, 221 (1972).

24. J. W. Evans, J. Math. Phys. 25, 2527 (1984).

25. R. B. McQuistan, D. Lichtman and L. P. Levine, Surf. Sci. 20, 401 (1970).

26. B. E. Blaisdell and H. Solomon, J. Appl. Prob. 7, 667 (1970); H. Solomon, in Proc. Fifth Berkeley Symp. on Math. Stat. and Prob. 3, 119 (1967), Univ. of California Press;
The $N\to\infty$ limit of the generalized Palásti conjecture recovers the Palásti conjecture that the saturation coverage for random filling of the plane with nonoverlapping, identical squares (of some fixed orientation) equals the square of the saturation coverage for the car parking problem (random filling of the infinite line with nonoverlapping equal-length intervals).

27. J. W. Evans and R. S. Nord, J. Stat. Phys. 38, 681 (1985).

28. J. W. Evans and R. S. Nord, Phys. Rev. B 31, 1759 (1985).

29. J. W. Evans, D. K. Hoffman and D. R. Burgess, J. Chem. Phys. 80, 936 (1984).

PAPER II:

COMPETITIVE IRREVERSIBLE RANDOM ONE-, TWO-, THREE-, ••• POINT ADSORPTION ON TWO-DIMENSIONAL LATTICES

COMPETITIVE IRREVERSIBLE RANDOM ONE-, TWO-, THREE-, ... POINT ADSORPTION ON TWO-DIMENSIONAL LATTICES

J. W. Evans and R. S. Nord

Ames Laboratory and Department of Chemistry
Iowa State University
Ames, Iowa 50011

ABSTRACT

An analytic treatment of competitive, irreversible (immobile) random one-, two-, three-, ••• point adsorption (or monomer, dimer, trimer, ••• filling) on infinite, uniform 2D lattices is provided by applying previously developed truncation schemes to the hierarchial form of the appropriate master equations. The behavior of these processes for two competing species is displayed by plotting families of "filling trajectories" in the partial-coverage plane for various ratios of adsorption rates. The time or coverage dependence of various subconfiguration probabilities can also be analyzed. For processes where no one-point (monomer) adsorption occurs, the lattice cannot fill completely; accurate estimates of the total (and partial) saturation coverages can be obtained.

I. INTRODUCTION

Irreversible immobile adsorption or reaction at specific sites on a 1D polymer chain, or 2D substrate has been modeled as the irreversible (immobile) filling of either single sites, or pairs, or triples, ••• of sites on a lattice. In general such processes are cooperative, i.e., the adsorption rates depend on the state of sites surrounding those being filled. These rates are the input to the master equations which are naturally recast in hierarchial form for processes on infinite lattices (of interest here)[1]. In 1D, exact results are available for all such random filling processes as well as a variety of cooperative processes[2]. The same is true for Bethe lattices[3] and other branching media. Except for random and "almost random" filling[1,4], no exact closed form solutions are available for processes on 2D lattices[1]. However formal coverage (density) expansions for subconfiguration probabilities are always available[5]. In this work, we shall exploit a recent analysis, via approximate hierarchial truncation to various orders, of the random filling of pairs, or of certain triples, or 4-tuples of sites on various infinite 2D lattices[6]. Even for these simple random filling processes, the occupation statistics are nontrivial, the most obvious indication here being that the lattice is not completely filled at saturation.

Here we consider processes involving <u>competitive, irreversible (immobile) filling</u> of single sites and/or pairs, triples, ••• of lattice sites. Physically this could correspond to irreversible coadsorption of several different molecular species or, alternatively, adsorption of a single type of molecule with different binding configurations. The latter

is proposed for CO adsorption on several metal surfaces. This process involves competition between two-point binding of β-CO at pairs of sites and one-point binding of α-CO at single sites[7]. Other examples can be cited. For unification, here we shall describe such processes in terms of competitive adsorption of monomers, dimers, trimers, ••• (i.e., of various N-mers). Here the term, N-mer, indicates the number (N) of lattice sites filled by this adsorbing species, rather than the number of atoms contained therein.

A hierarchy of rate equations for the probabilities, $P_{\underset{\sim}{\sigma}}$, of various subconfigurations of sites, $\underset{\sim}{\sigma}$, specified filled and/or empty, can be written down intuitively even for such cooperative processes[1,8]. In these subconfigurations, we must, in general, specify which species occupy the various filled sites. Here we note that the following fundamental shielding property is embedded in these equations[1]: <u>suppose that a wall of empty sites separates the lattice into two disconnected regions, and is sufficiently thick that any event on the lattice is not simultaneously affected by (the state of) sites on both sides; then sites on one side are shielded from the effect of those on the other</u>. Proof is via self-consistency with the hierarchial equations[1,8]. This property leads to exact truncation and solution of the hierarchy for various competitive, irreversible, random and cooperative processes on 1D lattices[8] (as well as on Bethe lattices and other branching media), and motivates our approximate hierarchial truncation procedures in 2D.

A significant simplification in these hierarchial equations occurs if the adsorption rates depend <u>at most</u> on whether the influencing sites are

filled or empty, and not on the particular species adsorbed there[8,9]. Here one can obtain a closed subhierarchy for probabilities of various subconfigurations of empty sites, using conservation of probability (just as for adsorption of a single type of species). One such important case, to which we restrict our attention henceforth, is the competitive, irreversible, immobile, random filling of monomers, dimers, trimers, ... Furthermore, we shall consider only infinite, uniform lattices, which are initially empty, so that subconfiguration probabilities are invariant under all space group operations on the lattice, including translation. It has been observed previously that, in 1D, these simpler equations are readily amenable to exact solution[8,9] (again by virtue of the above mentioned shielding property), so here we concentrate on the 2D case.

The general form of the hierarchial rate equations, appropriate to these processes, is presented in Section II, together with a brief discussion of the hierarchial truncation procedure. Results for a variety of competitive, irreversible, random filling processes, concentrating on the "filling trajectories" characterizing partial-coverage behavior, are presented in Section III. The special case of competitive random filling of two distinct dimer species is described in Section IV, and some concluding remarks are given in Section V.

II. HIERARCHIAL RATE EQUATIONS AND THEIR TRUNCATION

Here we consider competitive, random filling of a mixture of monomers (m), dimers (d), various trimers (e.g., linear (ℓt) and bent (bt) trimers on a square lattice), ••• with rates κ_m, κ_d, $\kappa_{\ell t}$, κ_{bt}, ••• respectively. In general, we refer to an N-mer species 's' (with $N=N_s$) adsorbing with rate κ_s, where κ_s dt denotes the probability of filling a specific 's'-shaped cluster of sites prescribed empty in an (infinitesimal) time interval dt. If $\{n\}_o$ denotes a subconfiguration of 'n' empty sites, {n}, and $P_{\{n\}_o}$ the corresponding probability, then one can write

$$d/dt\ P_{\{n\}_o} = -\kappa_m D^m_{\{n\}} - \kappa_d D^d_{\{n\}} - \kappa_{\ell t} D^{\ell t}_{\{n\}} - \cdots \quad , \tag{2.1}$$

Here the quantity $D^s_{\{n\}}$ takes account, through a sum over appropriate empty subconfiguration probabilities, of all possible ways that an adsorbing species 's' can destroy $\{n\}_o$ by landing completely within or partly overlapping {n}. Specifically one has

$$D^m_{\{n\}} = n\ P_{\{n\}_o} \quad , \tag{2.2a}$$

$$D^d_{\{n\}} = n_{\{m\}}\ P_{\{n\}_o} + \sum_{j \notin \{n\}} n_{j,\{n\}}\ P_{j_o+\{n\}_o} \quad , \tag{2.2b}$$

⋮

where $n_{\{n\}}$ is the number of pairs of adjacent sites in $\{n\}$ and $n_{j,\{n\}} = n_{j+\{n\}} - n_{\{n\}}$ (10) (see Ref. (6) for $D^s_{\{n\}}$ for a general N-mer species 's'). Modification to include several distinct monomer species, dimer species, ••• is straightforward and, in fact, (2.1) can still be used if κ_m, κ_d, ••• are reinterpreted as the sums of adsorption rates for all monomers, dimers, ••• respectively.

Our truncation procedure, however, operates directly on the conditional probabilities $Q_{j_o,\{n\}_o} = P_{j_o+\{n\}_o}/P_{\{n\}_o}$ for the (conditioned) site 'j' to be empty <u>given</u> that the (conditioning) sites in $\{n\}$ are empty. These satisfy equations of the form

$$d/dt\ \ell n\ Q_{j_o,\{n\}_o} = (d/dt\ P_{j_o+\{n\}_o})/P_{j_o+\{n\}_o} - (d/dt\ P_{\{n\}_o})/P_{\{n\}_o}$$

$$= -\kappa_m R^m_{j,\{n\}} - \kappa_d R^d_{j,\{n\}} - \kappa_{\ell t} R^{\ell t}_{j,\{n\}} - \cdots , \quad (2.3)$$

where

$$R^m_{j,\{n\}} = D^m_{j+\{n\}}/P_{j_o+\{n\}_o} - D^m_{\{n\}}/P_{\{n\}_o} = 1 \quad , \quad (2.4a)$$

$$R^d_{j,\{n\}} = D^d_{j+\{n\}}/P_{j_o+\{n\}_o} - D^d_{\{n\}}/P_{\{n\}_o}$$

$$= n_{j,\{n\}} + \sum_{k\notin j+\{n\}} n_{k,j+\{n\}}\, Q_{k_o,j_o+\{n\}_o} - \sum_{\ell\notin\{n\}} n_{\ell,\{n\}}\, Q_{\ell_o,\{n\}_o} \quad .$$

$$\vdots \quad (2.4b)$$

The $R^{s}_{j,\{n\}}$ for trimer, tetramer, ••• species 's' are more complex, involving products of Q's, and are described in detail elsewhere[6]. Our n^{th}-shell (or n^{th}-order) truncation procedure operates directly on the r.h.s. of these by neglecting conditioning sites further than 'n' lattice vectors from the conditioned site, thus obtaining a closed set of equations for a finite subset of Q's. We thus take advantage of the shielding propensity of closer empty conditioning sites. (On 1D and Bethe lattices, and on more general branching media, this procedure, suitably implemented, produces exact results).

As mentioned in the Introduction, we consider here only adsorption on infinite, uniform, initially empty lattices. Consequently the subconfiguration probabilities are invariant under all lattice space group operations, and $\{n\}_0$, in $P_{\{n\}_0}$, is naturally interpreted as representing a class of subconfigurations related by space group operations. Since, in particular, probabilities are translationally invariant, in the following we use the obvious notation P_0, P_{00}, P_{000}, ••• to denote probabilities of an empty site, adjacent pair of sites, linear triple of sites (e.g., on a square lattice), ••• respectively. Thus $\theta \equiv 1-P_0$ gives the lattice coverage.

In our previous treatment of the random filling of single types of N-mer species, computer routines were written to generate the $R^{s}_{j,\{n\}}$ and apply truncation to various orders. This allowed treatment and comparison of various orders of truncation where many coupled Q equations are

involved. It should be clear that treatment of competitive random filling involves simple combination of these individual routines (for each order of truncation). In general, more Q's will be required to close the set of truncated equations, at each order, than for the random filling of any of the individual species. Modification to consider competitive random filling of monomers with a single type of N-mer species is particularly simple since $R^{m}_{j,\{n\}}=1$, for all $\{n\}$. The numerical results presented in the next section follow from estimates of probabilities of empty subconfigurations obtained via these truncation procedures.

For competitive adsorption, knowledge of probabilities of empty subconfigurations only provides limited information about the distribution of adsorbed species (in contrast to single species adsorption). For example, partial coverages θ_m, θ_d, $\theta_{\ell t}$, ••• for monomers, dimers, linear trimers (for an appropriate lattice), •••, which satisfy $\theta \equiv \theta_m + \theta_d + \theta_{\ell t} + \cdots$, are not included. However, the partial coverage, θ_s, for any N-mer species 's', adsorbing with rate κ_s, can be simply determined by integrating the additional equation

$$d/dt\ \theta_s = \kappa_s D^s_0 \quad , \quad \text{where } D^s_0 \equiv D^s_{\{1\}} \equiv c_s P^s_0 \quad . \tag{2.5}$$

Here P^s_0 is the probability of an 's'-shaped subconfiguration of empty sites, and the "generalized coordination number", c_s, for the species 's', gives the number of ways that this species can be placed on the lattice to cover a particular site. Thus, in particular, $c_m = 1$, and $c_d = c$, the standard lattice coordination number. On a square lattice, for example,

one has

$$d/dt\ \theta_m = \kappa_m P_o,\ d/dt\ \theta_d = \kappa_d c_d P_{oo},\ d/dt\ \theta_{\ell t} = \kappa_{\ell t} c_{\ell t} P_{ooo} \quad ,$$

$$d/dt\ \theta_{bt} = \kappa_{bt} c_{bt} P_{oo} \quad ,\quad d/dt\ \theta_{sq} = \kappa_{sq} c_{sq} P_{oo},\ \cdots \quad , \tag{2.6}$$

where 'sq' denotes square tetramers, and $c_d=4$, $c_{\ell t}=6$, $c_{bt}=12$, and $c_{sq}=4$. It is important to note that, provided the truncation scheme does not affect the d/dt P_o equation, we are guaranteed that the <u>truncation solutions</u> satisfy the "conservation of probability" condition $1-P_o \equiv \theta = \theta_m + \theta_d + \cdots$.

Since the probabilities on the r.h.s. of (2.5,6) equal unity when t=0, we have that $\theta_s \sim \kappa_s c_s t$, as $t\to 0$, and so for two species 's' and 's*', one has that $\theta_s/\theta_{s*} \sim (\kappa_s c_s)/(\kappa_{s*} c_{s*})$, as $t\to 0$. This motivates introduction of the modified rates

$$K_s \equiv \kappa_s c_s \quad , \tag{2.7}$$

where $K_s dt$ gives the probability that the species 's' will adsorb covering some particular site, with local environment prescribed empty, in an (infinitesimal) time interval dt (so $\theta_s/\theta_{s*} \sim 1$, as $t\to 0$, when $K_s = K_{s*}$). These rates will be used later in presenting results. The enhancement of K_s over κ_s by a factor of c_s (or of θ_s over θ_m, as $t\to 0$, when $\kappa_s = \kappa_m$) occurs since there are c_s ways that a species 's' can adsorb covering any site (with empty local environment). <u>Often</u> one can write $c_s = N_s \nu_s$ (for an

N-mer 's' with $N = N_s$), and interpret ν_s as the number of different orientations that the species 's' can assume on the lattice [e.g., on a square lattice, ν_d=2, $\nu_{\ell t}$=2 (horizontal and vertical), ν_{bt}=4 and ν_{sq}=1]. This equality reflects the fact that any of the N_s atoms of the N_s-mer 's' can fill a particular site, and that this filling can occur via ν_s differently oriented processes (e.g., horizontal and vertical for dimers and linear trimers on a square lattice). Note that this decomposition is <u>not</u> always appropriate since ν_s can be nonintegral, e.g., $\nu_d \equiv c/2$ equals 3/2 for a hexagonal lattice.

Determination of probabilities of more general subconfigurations involving sites specified filled with various species is more complicated. Consider, for example, competitive random filling of monomers $o \to m$ (with rate κ_m), and dimers $oo \to dd$ (with rate κ_d), at the sites of a square lattice. To determine the probability of an adjacent m-filled and empty site, P_{mo}, we must consider the infinite coupled set of equations (exploiting all lattice symmetries),

$$d/dt\ P_{mo} = \kappa_m(P_{oo} - P_{mo}) - \kappa_d(P_{moo} + 2P_{m\overset{o}{\underset{o}{}}}) \quad ,$$

$$d/dt\ P_{moo} = \kappa_m(P_{ooo} - 2\ P_{moo}) - \kappa_d(P_{moo} + P_{mooo} + 2P_{m\overset{o}{\underset{oo}{}}} + 2P_{m\overset{oo}{\underset{o}{}}}) \quad ,$$

$$\vdots \qquad (2.8)$$

for probabilities of subconfigurations with a single m-filled site adjacent to all possible connected clusters of empty sites. A natural 2^{nd}-order

truncation (measuring distance from the m-filled site) of these equations would, for example, make the approximation

$$P_{mooo} \equiv Q_{m\phi\phi\phi} P_{ooo} \approx Q_{m\phi\phi} P_{ooo} \equiv P_{moo} P_{ooo} / P_{oo} \quad , \tag{2.9}$$

where 'ϕ' denote empty conditioning sites. A similar set of equations must be considered when determining, e.g., P_{do}. More generally, rate equations for probabilities of subconfigurations involving a number of filled sites couple to P's for configurations with one or more of the filled sites replaced by empty sites, and to P's for configurations with the same set of filled sites but more empty sites. For example

$$d/dt\ P_{mdo} = \kappa_m (P_{odo} - P_{mdo}) + \kappa_d (2P_{m\partial o} - P_{mdoo} - 2P_{md\partial}) \quad . \tag{2.10}$$

Systematic estimation of such quantities from sufficiently high order truncation approximations is clearly possible. Analogous remarks can be made regarding the estimation of probabilities of subconfigurations involving sites specified filled with various species for more general random competitive filling processes. Such an example is presented in Section IV, where a modified version of this truncation procedure is illustrated for the special case of competitive random filling of two distinct dimer species.

III. RESULTS FOR COMPETITIVE RANDOM FILLING OF DIFFERENT SPECIES

We first consider several irreversible, random filling processes involving just two distinct species, 's' and 's*', say. The process is naturally described by a "filling trajectory" in the (θ_s, θ_{s*}) partial coverage plane. We assume that the lattice is initially empty so that this trajectory starts at the origin and is confined, in the positive quadrant, to the triangle $0 < \theta \equiv \theta_s + \theta_{s*} < 1$. It is natural to generate a continuous one-parameter family of such trajectories by varying the ratio of the adsorption rates, K_s/K_{s*}, for the two species. The nontrivial trajectory curves presented in this section should be contrasted with those from "standard" treatments of the kinetics of 1^{st}-order competitive processes (which correspond to competitive <u>random monomer filling</u>)[11]. There trajectories are trivially straight lines with slopes given by the rate ratios.

Results for processes where a monomer is involved (so the lattice fills completely) are very accurate since we have used, here, the previously generated $R^s_{j,\{m\}}$ of high (3^{rd}-) order for the appropriate competing species. For competitive, <u>random monomer and dimer filling</u>, we show in Fig. 1, filling trajectories for both hexagonal and square lattices. These are naturally compared with the exact filling trajectories for the corresponding processes on Bethe lattices of coordination numbers c=3 and 4, respectively. The latter coincide, here, with 1^{st}-order truncation results for the physical lattices, and differ little from higher-order (and exact) physical lattice behavior. A detailed assessment

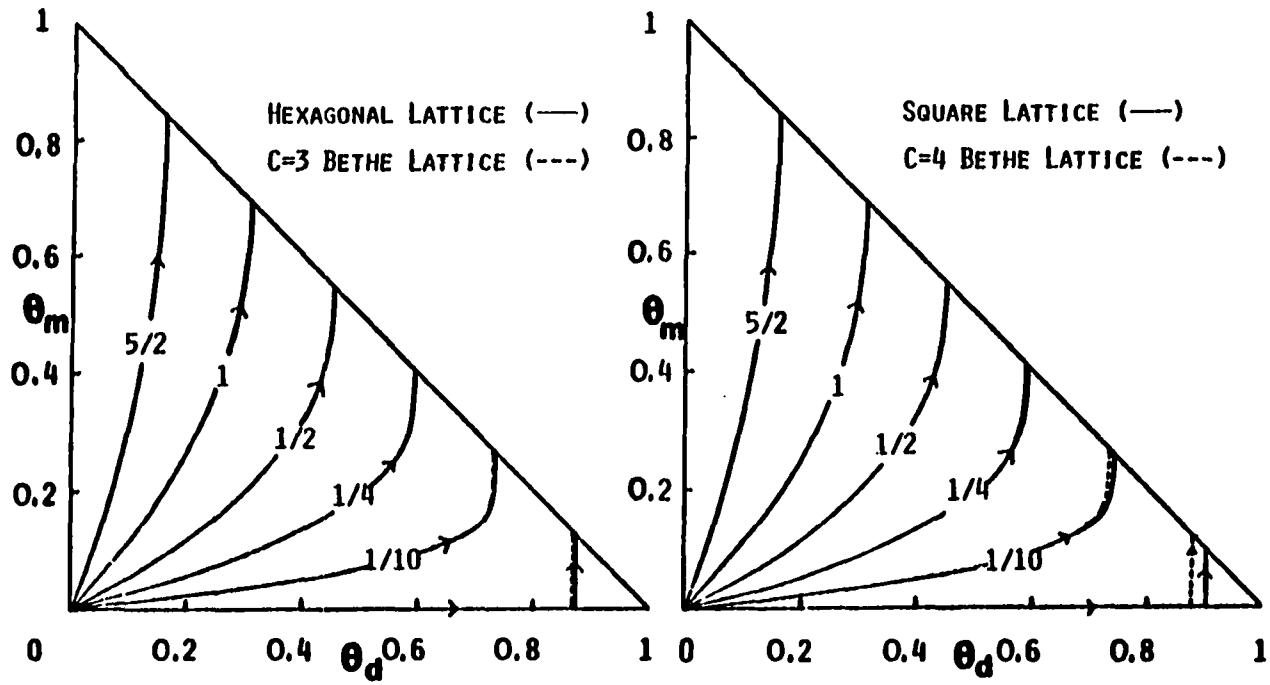

Figure 1: Filling trajectories for competitive, random monomer and dimer filling, for various ratios K_m/K_d (shown). Results are given for hexagonal and square lattices and for the corresponding Bethe lattices

of the accuracy of our procedures, for the square lattice case, can be obtained from Table I where we have shown θ_m^{sat} for various ratios of K_m/K_d, and compared 2^{nd}- and 3^{rd}-order results, and also exact results for random monomer and dimer filling on a Bethe lattice with c=4, and on a square cactus. Accuracy of the 2^{nd}- and 3^{rd}-order truncation results clearly increases dramatically with increasing K_m/K_d, as might be expected since monomer filling contributions to the Q equations are unaffected by truncation. (See the Appendix for a presentation of these Bethe lattice and square cactus analyses, and a discussion of the correspondence with physical lattice behavior.) Corresponding plots for competitive, random filling of monomers and either linear trimers, bent trimers, or square tetramers, are shown in Fig. 2.

In Fig. 3, we have shown the filling trajectories for three cases where dimers, and one type of N-mer species 's' with N>3, compete randomly filling the sites of a square lattice. The 2^{nd}-order truncation approximation was used here. The saturation coverage, θ^{sat} (which is less than unity), is listed in Table II, for several values of K_d/K_s. These saturation coverages are clearly discontinuous as functions of K_d/K_s at zero, since when $K_d/K_s=0$, the process simply involves random N-mer filling, but when $K_d/K_s=0+$, the process continues through an (infinitely slower) second stage where dimers randomly fill some of the remaining empty pairs of sites. Note that the saturation coverage for these processes is continuous as a function of K_s/K_d at zero since, after random dimer filling to saturation, there remain only isolated empty sites (on which N-mers cannot adsorb). It is particularly interesting to note that the effect of

Table I. Monomer saturation coverages, θ_m^{sat}, for competitive random monomer and dimer filling; 1^{st}-, 2^{nd}- and 3^{rd}-order truncation estimates are given for a square lattice, and exact values for a square cactus and c=4 Bethe lattice, for various values of K_m/K_d

K_m/K_d	3^{rd}-order	2^{nd}-order	Square Cactus	Bethe Lattice (1^{st}-order)
0+	0.093660	0.097853	0.105385	0.111111
1/10	0.257451	0.258199	0.261223	0.263866
1/4	0.403483	0.403612	0.404745	0.405806
1/2	0.545354	0.545371	0.545718	0.546056
1	0.689318	0.689319	0.689388	0.689455
5/2	0.839623	0.839623	0.839628	0.839632

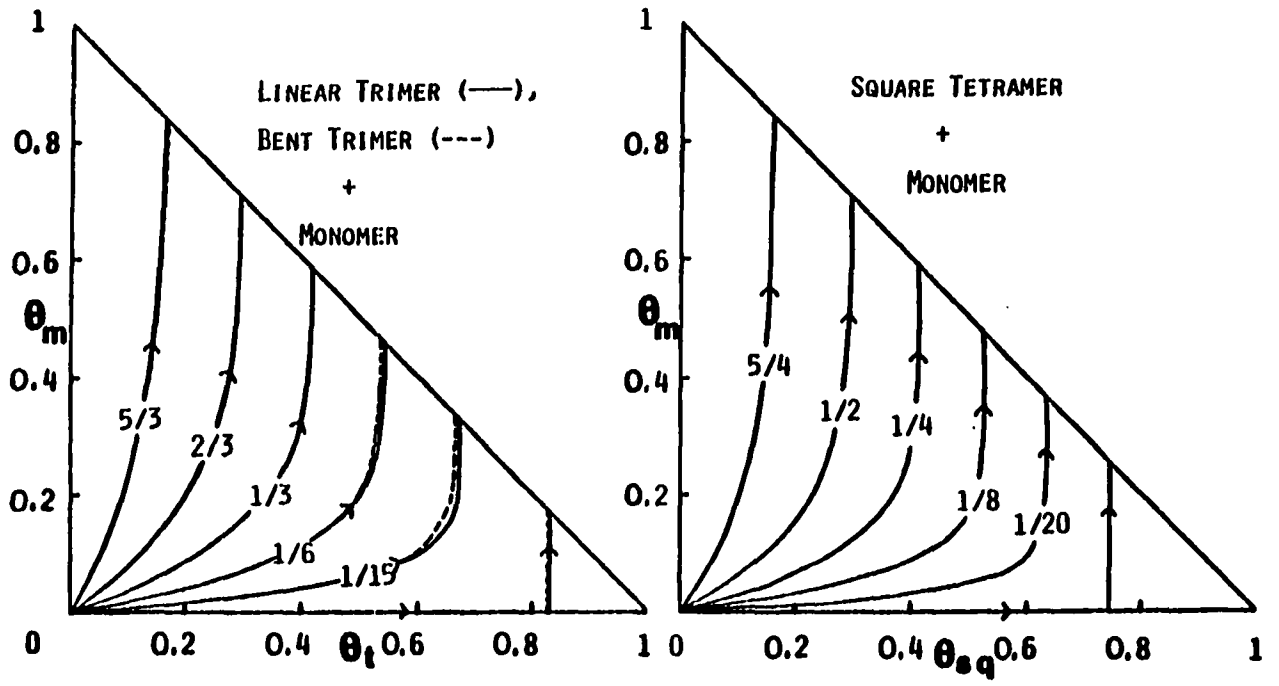

Figure 2: Filling trajectories for competitive, random filling of monomers and N-mer species 's' on a square lattice, for various ratios of K_m/K_s (shown). The N-mers are either linear or bent trimers, or square tetramers

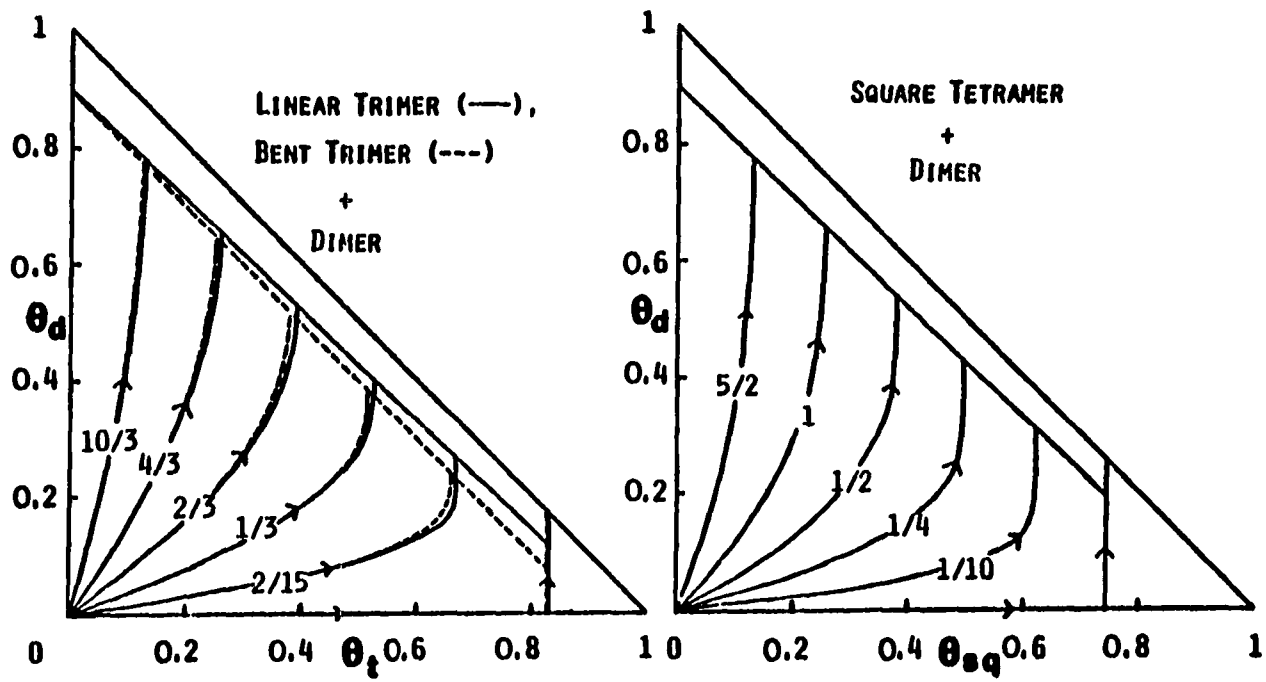

Figure 3: Filling trajectories for competitive, random filling of dimers and N-mer species 's' on a square lattice, for various ratios of K_d/K_s (shown). The N-mers are either linear or bent trimers, or square tetramers

Table II. Saturation coverages for competitive, random dimer and N-mer filling on a square lattice, for various values of K_s/K_d (from 2^{nd}-order truncation). The N-mers are either linear or bent trimers, or square tetramers

K_s/K_d	Linear Trimer	Bent Trimer	Square Tetramer
0	0.90215	0.90215	0.90215
1/5	0.90602	0.90065	0.90564
1/2	0.91062	0.89935	0.90979
1	0.91624	0.89843	0.91481
2	0.92334	0.89827	0.92102
3	0.92770	0.89871	0.92473
5	0.93286	0.89980	0.92893
10	0.93852	0.90171	0.93327
20	0.94234	0.90347	0.93602
100	0.94616	0.90560	0.93855
2000	0.94721	0.90626	0.93923

adding some N-mer coadsorption to the random dimer filling problem (i.e., consider K_s/K_d increasing from zero) is to <u>increase</u> the saturation coverage for linear trimers and square tetramers, but to initially <u>decrease</u> it for bent trimers. We expect that this is because of the relatively high probability of isolating empty sites in the "elbow" of the bent trimer (see Fig. 4).

For competitive, random filling on a square lattice of linear and bent trimers, and of linear trimers and square tetramers, filling trajectories (from 2^{nd}-order truncation) are shown in Fig. 5. Discontinuities in the saturation coverage obviously occur at both ends of the (infinite) range of rate ratios since, infinitesimally close to either end, two stage filling occurs.

Let us now analyze, in more detail, the limiting rate regimes described above where filling occurs in two stages. Since 2^{nd}-order truncation is used to analyze these competing processes, for consistency, the saturation values quoted below for many quantities, for various single species random filling processes, are also taken from 2^{nd}-order analyses (detailed in Ref. 6). Limited accuracy is expected especially when linear trimers are involved.

For competitive, random filling of dimers and bent trimers, when $K_d/K_{bt}=0+$, bent trimer filling proceeds to coverage ≈ 0.834, at which point isolated linear strings of empty sites (of length one or more) remain[6]. The process then continues with random dimer filling on the empty strings of length two or more to coverage ≈ 0.906, so the saturation partial coverage of dimers is ≈ 0.072. For random bent trimer filling, at

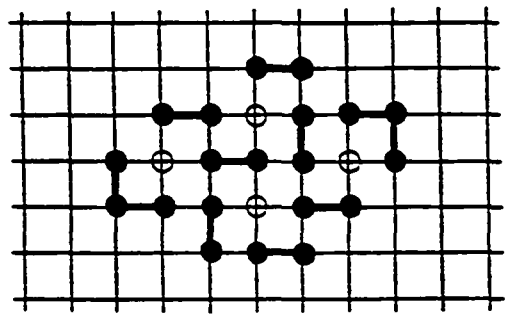

Figure 4: Isolation of empty sites for competitive, random filling of dimers and bent trimers on square lattice

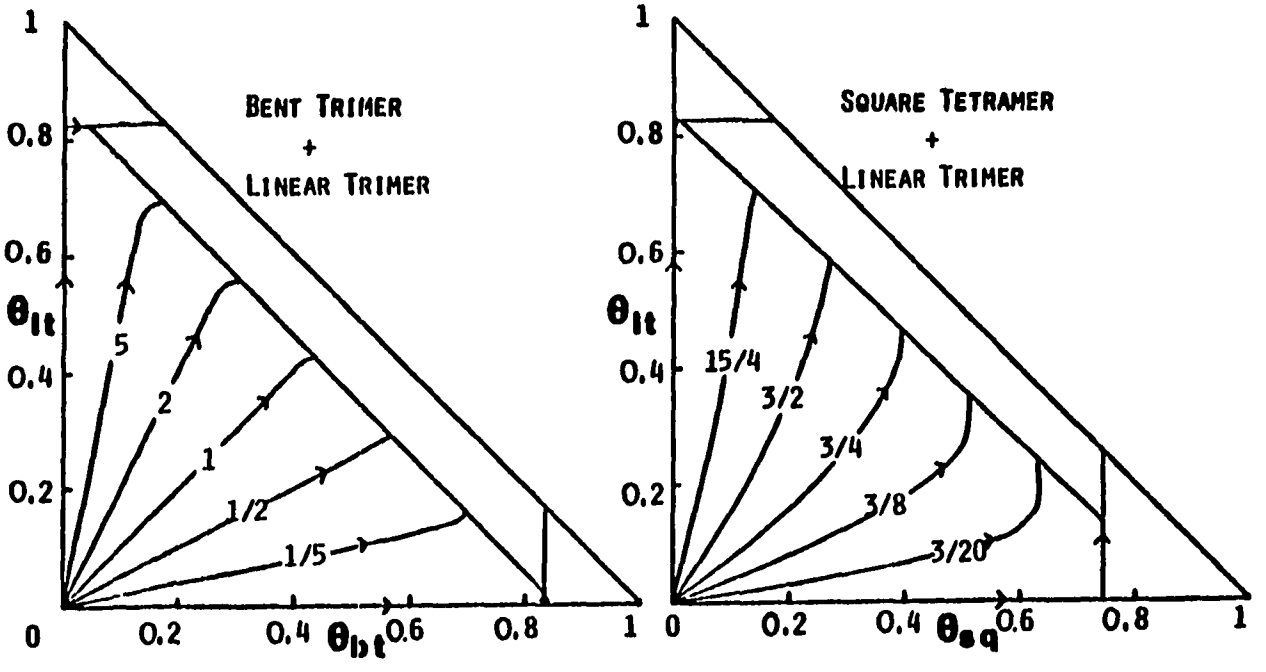

Figure 5: Filling trajectories for competitive, random filling, on a square lattice, of linear trimers and bent trimers [square tetramers], for various ratios of $K_{\ell t}/K_{bt}[K_{\ell t}/K_{sq}]$

saturation, the fraction of empty sites in linear strings of length two or more is 0.078, of which, the fraction in strings of exactly length two (i.e., in isolated empty pairs) is 0.058 (determined, in the 2^{nd}-order, using the approximation $P_{oooo} \equiv Q_{o\phi\phi\phi}P_{ooo} \approx Q_{o\phi\phi}P_{oo}$). The latter, of course, are all filled by dimers. We thus conclude that $\sim \frac{0.014}{0.020}$ or ~70% of the sites in linear empty strings of length three or more are filled. Exact calculations for random dimer filling on finite linear lattices produce mean saturation coverages of 2/3, 5/6, 4/5 for lengths 3, 4, 5 respectively and, thereafter, a monotonic increase to infinite length value of $1-e^{-2} \approx 86.5\%$[12]. Thus our results indicate that, of the empty strings of length three or more remaining after random bent trimer filling, most have length three (which is not unreasonable).

Similar remarks apply for competitive, random filling of dimers and linear trimers when $K_d/K_{\ell t}=0+$. Random linear trimer filling proceeds to coverage ≈0.827 where isolated empty sites, pairs oo, quadruples $\overset{o}{o}\overset{o}{o}$, and staircase configurations $o\overset{o}{o}$, $o\overset{o}{o}\overset{o}{o}$, $o\overset{o}{o}\overset{o}{o}\overset{o}{o}$, ... remain[6]. Random dimer filling then continues to a saturation partial coverage of 0.121, filling ≈93% of the available 0.130 sites in empty clusters of two or more sites, including <u>all</u> 0.087 in isolated empty pairs (determined, in 2^{nd}-order, using the approximation $P_{o\overset{o}{o}\overset{o}{o}} \equiv Q_{o\phi\phi}P_{\overset{o}{o}\overset{o}{o}} \approx Q_{o\phi}P_{\overset{o}{o}\overset{o}{o}}$), and <u>all</u> 0.014 in empty quadruples. This implies that $\sim \frac{0.020}{0.029}$ or ~69% of the sites in empty stair cases are filled (which, from the above 1D remarks, indicates that most of these have length three). For competitive, random dimer and square tetramer filling when $K_d/K_{sq}=0+$, similar analysis shows that ~80% of the

complicated network of nonisolated empty sites (remaining after square tetramer filling) are filled by dimers. This seems reasonable.

For competitive, random filling of bent and linear trimers, a list of saturation coverages for various $K_{\ell t}/K_{bt}$ is given in Table III. When $K_{\ell t}/K_{bt}=0+$, random bent trimer filling first occurs to coverage ≈ 0.834, and then linear trimer filling occurs on remaining 0.020 empty sites in linear strings of length three or more. Since most of these strings have length three (see above), we anticipate that the (total) saturation coverage should be $\approx 0.834+0.020=0.854$, in reasonable agreement with Table III. When $K_{bt}/K_{\ell t}=0+$, random linear trimer filling first occurs to coverage ≈ 0.827, and then bent trimer filling occurs on the remaining 0.014 empty sites in isolated empty quadruples $\begin{smallmatrix} \bullet\bullet \\ \bullet\bullet \end{smallmatrix}$, and on the remaining 0.029 sites in empty staircases of length three or more. Since most of the latter have length three, we anticipate that the (total) saturation coverage should be $\approx 0.827+3/4\times 0.014+0.029=0.867$ also in reasonable agreement with Table III.

Finally, to demonstrate the flexibility of our methods, we give results for the saturation coverage for a competitive, random filling process on a square lattice involving dimers, and both linear and bent trimers. In Fig. 6, we have shown the constant saturation coverage contours in "rate space". The saturation coverage is continuous at the dimer vertex, and along the two edges extending from it (dimer and linear trimer filling; dimer and bent trimer filling), but <u>not</u> at the lower edge (bent and linear trimer filling) where the extent of discontinuity can be determined from Table III.

Table III. Saturation coverages, θ^{sat}, for competitive, random linear and bent trimer filling on a square lattice, for various values of $K_{bt}/K_{\ell t}$ (from 2^{nd}-order truncation)

$K_{bt}/K_{\ell t}$	θ^{sat}
< 0.002	0.86754
0.02	0.86740
0.2	0.86567
0.4	0.86374
1	0.85985
2	0.85698
4	0.85500
10	0.85367
20	0.85323
200	0.85284
>2000	0.85279

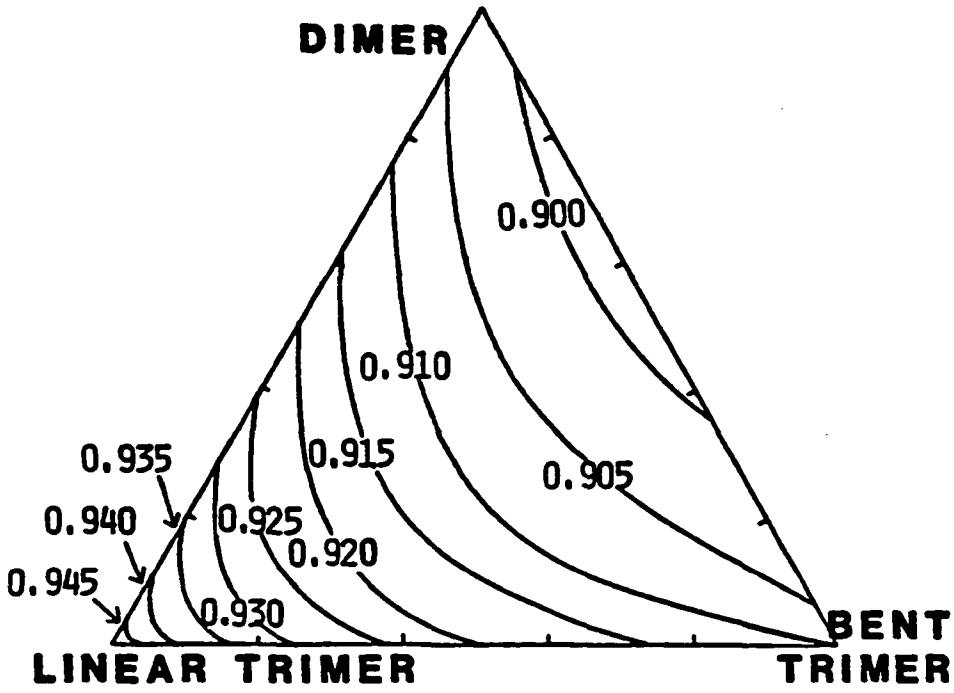

Figure 6: Constant saturation coverage contours for competitive, random filling on a square lattice, of dimers and both bent and linear trimers. For any point inside the triangle, the κ_s rates for various species are in proportion to the distances from that point to the edges opposite the appropriate species vertex

IV. COMPETITIVE RANDOM FILLING OF TWO DISTINCT DIMER SPECIES

As mentioned previously, one can straightforwardly derive hierarchial equations for irreversible random filling of several monomer species (where they are trivial), or several dimer species, or several linear trimer species (e.g., on a square lattice), ... These processes have the simplifying feature that the "filling trajectories" are straignt lines with slopes determined by the rate ratios. Consider, e.g., random filling of two dimer species oo→dd, with rate κ_d, and oo→d'd', with rate $\kappa_{d'}$. Clearly one has for $\theta_d \equiv P_d$, $\theta_{d'} \equiv P_{d'}$,

$$d/dt\ \theta_d = \kappa_d\ P_{oo} \quad , \quad d/dt\ \theta_{d'} = \kappa_{d'}\ P_{oo} \quad , \tag{4.1}$$

so $\theta_d/\theta_{d'} = \kappa_d/\kappa_{d'} = K_d/K_{d'}$. Furthermore, we have also indicated that the probabilities of empty subconfigurations for this process are identical to those for random filling of a single type of dimer with rate κ, if we make the identification $\kappa = \kappa_d + \kappa_{d'}$.

In this section, we shall restrict our attention to this competitive dimer filling process for the case of an initially empty square lattice. We then have

$$\kappa^{-1}\ d/dt\ P_o = -\ 4\ P_{oo} = -\ 4\ P_o\ Q_{o\phi} \quad , \tag{4.2}$$

where 'ϕ' denotes an empty conditioning site so $Q_{o\phi} \equiv P_{oo}/P_o$. In the 1^{st}-order truncation approximation[6,10]

$$\kappa^{-1}\, d/dt\, \ell n\, Q_{o\phi} = -1 - 2Q_{o\phi} \quad , \tag{4.3}$$

which allows (4.2) and (4.3) to be integrated with (4.1). Some quantities for this process cannot be trivially determined from those for standard random dimer filling (cf. Section II). The simplest such example is the probability P_{do} (or $P_{d'o}$) of a d- (or d'-) filled site adjacent to an empty site. We must use that

$$d/dt\, P_{do} = \kappa_d\, (P_{ooo} + 2P_{\underset{\delta o}{\delta}}) - \kappa\, (P_{doo} + 2P_{\underset{d\delta}{\delta}})$$

$$= \kappa_d\, (Q_{o\phi\phi} + 2Q_{\underset{\phi\phi}{o}})\, P_{oo} - \kappa\, (Q_{d\phi\phi} + 2Q_{\underset{d\phi}{\phi}})\, P_{oo}$$

$$\longrightarrow 3\, \kappa_d\, Q_{o\phi}\, P_{oo} - 3\, \kappa\, Q_{d\phi}\, P_{oo}$$

$$= 3\, (\kappa_d\, P_{oo} - \kappa\, P_{do})\, P_{oo}/P_o \quad , \tag{4.4}$$

in the 1^{st}-order approximation (allowing integration with the above equations). Now we can also determine P_{dd} from

$$d/dt\, P_{dd} = \kappa_d\, (P_{oo} + 2P_{doo} + 4P_{\underset{d\delta}{\delta}}) = \kappa_d\, (1 + 2Q_{d\phi\phi} + 4Q_{\underset{d\phi}{\phi}})\, P_{oo}$$

$$\longrightarrow \kappa_d\, (1 + 6Q_{d\phi})\, P_{oo} = \kappa_d\, (P_o + 6P_{do})\, P_{oo}/P_o \quad , \tag{4.5}$$

in the 1^{st}-order approximation. Using conservation of probability, one can now also determine 1^{st}-order estimates of such quantities as $P_{d'o} \equiv P_o$ -

$P_{oo} - P_{do}$, $P_{dd'} \equiv P_d - P_{do} - P_{dd}$ and $P_{d'd'} \equiv 1 - P_{oo} - 2P_{do} - 2P_{d'o} - 2P_{dd'} - P_{dd} \equiv P_{d'} - P_{d'o} - P_{dd'}$. It is important to note that these identities are consistent with the truncation solutions obtained from integrating additional equations for $P_{d'o}$, $P_{dd'}$ and $P_{d'd'}$. For example, one obtains from the 1st-order truncated $P_{d'o}$, P_{do} and P_{oo} equations, after some rearrangement,

$$\kappa^{-1} \, d/dt \, (P_{oo} + P_{do} + P_{d'o}) = - [1 + 3(P_{oo} + P_{do} + P_{d'o})/P_o] \, P_{oo} \, , \qquad (4.6)$$

which should be compared with (4.2) to demonstrate that $P_{oo} + P_{do} + P_{d'o} \equiv P_o$.

For comparison, we now consider the 2nd-order truncation estimates of these quantities. It is natural to start with P_{do} which couples to P_{doo} and $P_{d\underset{\sim}{o}\underset{\sim}{o}}$ which are retained in the 2nd-order. These then couple to $P_{d\underset{\sim}{o}\underset{\sim}{o}o}$, $P_{d\underset{\sim}{o}\underset{\sim}{o}\underset{\sim}{o}}$ and $P_{d\underset{\sim}{o}\underset{\sim}{o}}$. Other quantities are truncated, e.g., $P_{dooo} \to P_{doo} \, P_{ooo}/P_{oo}$ in the 2nd-order, according to the prescription in Section II. If we continue according to this prescription, we clearly obtain a closed coupled set of equations for (the large set of) P's with a single 'd' and adjacent connected clusters of empty sites where each is within two lattice vectors of the 'd'. This observation motivates the introduction of a modified 2nd-order truncation, based on Q equations, which involves far fewer equations with only a slight reduction in accuracy.

Here we deal with the $Q_{\underset{\sim}{\sigma}\underset{\sim}{\sigma}'} \equiv P_{\underset{\sim}{\sigma}+\underset{\sim}{\sigma}'}/P_{\underset{\sim}{\sigma}'}$ where either none or one of the specified sites in the subconfiguration $\underset{\sim}{\sigma} + \underset{\sim}{\sigma}'$ is d-filled, and the rest

are empty. It is easy to see that an exact closed set of equations can be obtained for these (with $\underset{\sim}{\sigma}$ either 'o' or 'd') using

$$d/dt\ \ell n\ Q_{\underset{\sim}{\sigma}\underset{\sim}{\sigma}'} = S(\underset{\sim}{\sigma} + \underset{\sim}{\sigma}') - S(\underset{\sim}{\sigma}') \quad , \tag{4.7}$$

where $S(\underset{\sim}{\sigma}'') = d/dt\ \ell n\ P_{\underset{\sim}{\sigma}''}$, which can be expressed in terms of these Q's. For example, one has

$$S(\underset{\circ\circ}{d\circ}) = 2\kappa_d\, P_{\underset{\circ\circ}{\circ\circ}\circ}/P_{\underset{\circ\circ}{d\circ}} - 2\kappa(P_{\underset{\circ\circ}{d\circ}} + P_{\underset{\circ\circ\circ}{d\circ}} + P_{\underset{\circ\circ}{d\circ}\circ} + P_{\underset{\circ\circ}{d\circ}})/P_{\underset{\circ\circ}{d\circ}}$$

$$= 2\kappa_d\, Q_{\underset{\phi\phi}{\circ\phi\phi}}\, Q_{\underset{\phi\phi}{\circ\phi}}/Q_{\underset{\phi\phi}{d\phi}} - 2\kappa(1 + Q_{\underset{\circ\phi}{\delta\phi}} + Q_{\underset{\phi\phi\circ}{\delta\phi}} + Q_{\underset{\phi\phi}{\delta\circ}}) \quad , \tag{4.8}$$

where 'ϕ' ('δ') denote empty (d-filled) conditioning sites. In the 2^{nd}-order truncation, we neglect conditioning sites in these Q's further than two lattice vectors from the single 'o' or 'd' conditioned site so, e.g., $Q_{\underset{\phi\phi}{o\phi\phi}}, Q_{\underset{\phi\phi}{o\phi\delta}} \longrightarrow Q_{\underset{\phi\phi}{o\phi}}, Q_{\underset{\phi\phi}{\delta\phi}} \longrightarrow Q_{\underset{\circ\phi}{\delta\phi}}, Q_{\underset{\phi\phi}{\delta\circ}} \longrightarrow Q_{\underset{\phi}{\delta\circ}}$. A potential deficiency of this approach is seen in these last two examples where we draw on the shielding propensity of a d-filled site (which is less than that of an empty site), but these approximations are no worse than others made in 2^{nd}-order.

By evaluating 2^{nd}-order expressions for S(do), S(doo), $S(_{d\circ}{}^{\circ})$, $S(_{d\circ\circ}{}^{\circ})$, $S(_{\circ\circ\circ}{}^{d})$, $S(\underset{\circ\circ}{d\circ})$ and $S(_{d\circ\circ}{}^{\circ}{}_{\circ})$, one obtains a closed set of equations for $Q_{d\phi}$, $Q_{o\phi\delta}$, $Q_{\underset{\phi\delta}{\circ}}$, $Q_{\underset{\delta\phi\phi}{\circ}}$, $Q_{\underset{\circ\phi}{\delta\phi}}$, $Q_{\underset{\circ\phi\delta}{\phi}}$, $Q_{\underset{\circ\phi\phi}{\delta}}$, $Q_{\underset{\phi\phi\phi}{d}}$, $Q_{d\phi\phi}$, $Q_{\underset{\phi\phi}{d\phi}}$, $Q_{o\phi\underset{\phi}{\delta}}$, $Q_{\underset{\phi\phi}{\delta\phi}\circ}$, $Q_{\underset{\phi\phi\phi}{d}}$ and the

"standard" 2^{nd}-order empty Q's[6,10]. We note that Q's with a d-filled conditioning site 'δ' are given by indeterminate forms at $t = \theta = 0$, e.g., $Q_{o\phi}^{\ \ \delta} = P_{od}/P_{\delta}$. Furthermore, one finds terms in their d/dt Q equations which are singular at $t = \theta = 0$, e.g., S(do) includes a term $P_{ooo}/P_{do} \equiv Q_{o\phi\phi}Q_{o\phi}/Q_{d\phi}$. However using straightforward formal density- (coverage-) expansion techniques (described in Ref. 5), one can determine initial values, and demonstrate the cancellation of singularities from terms of 1^{st}-order in the coverage, and determine initial slopes from terms of 2^{nd}-order in the coverage. The closed set of equations can then be integrated to provide 2^{nd}-order estimates of such quantities as P_o, P_d, P_{oo}, P_{do}, ... It is now a trivial matter to determine the 2^{nd}-order estimate of P_{dd} from

$$d/dt\ P_{dd} = \kappa_d\ (P_{oo} + 2Q_{o\phi\delta}\ Q_{d\phi}\ P_o + 4Q_{o\ \ \ \delta}\ Q_{d\phi}\ P_o) \quad . \tag{4.9}$$

In Fig. 7, we have plotted resulting probabilities for various configurations of an adjacent pair of sites, as function of the total coverage, $\theta = \theta_d + \theta_{d'}$.

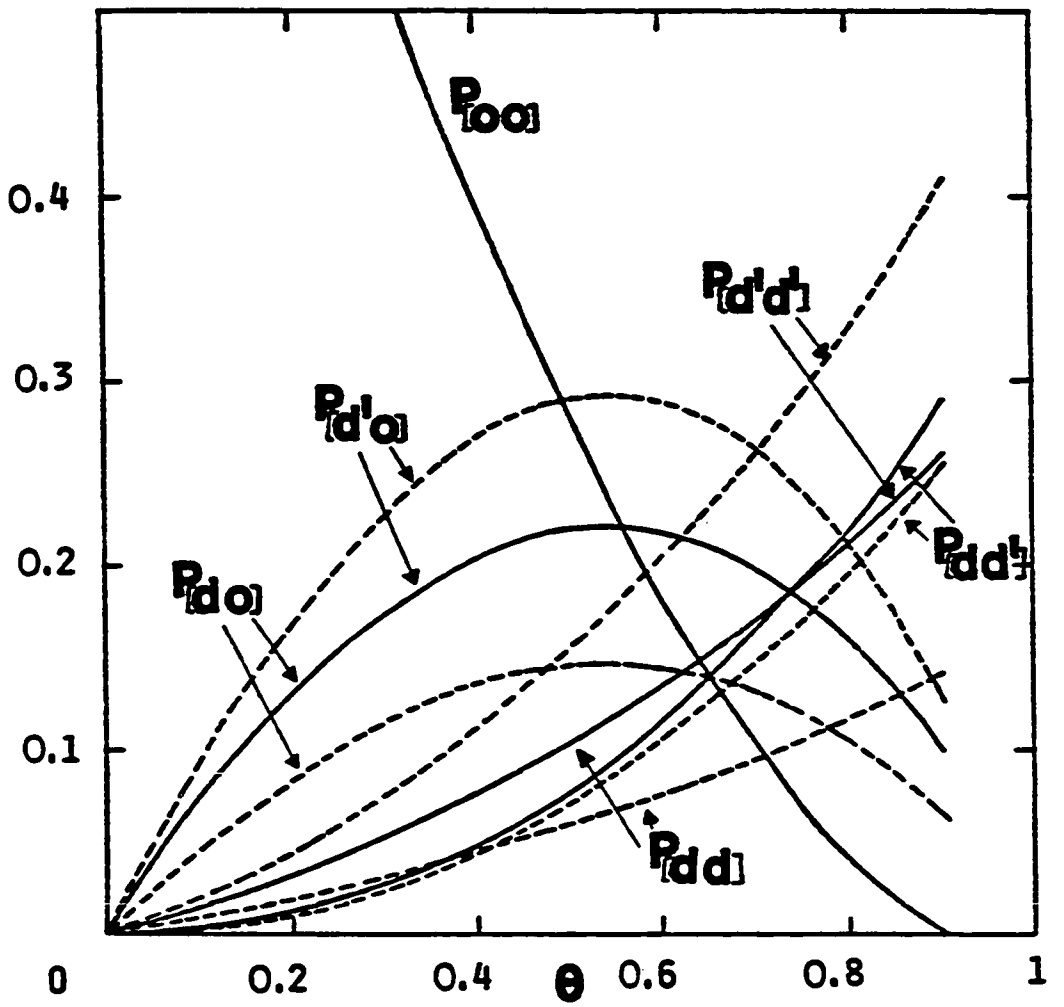

Figure 7: Total coverage dependence of probabilities for various configurations of an adjacent pair of sites, for competitive random filling of two distinct dimer species, d and d'. Behavior for $K_{d'} = K_d$ (——) and $K_{d'} = 2K_d$ (---) is shown

V. DISCUSSION

We have exploited sophisticated hierarchial truncation techniques here to obtain accurate results for the kinetics and statistics of processes involving competitive, irreversible (immobile), random filling of monomers, dimers, ••• on 2D lattices (the first such results for nontrivial competitive, irreversible 2D-lattice processes). "Filling trajectories" for various ratios of species filling rates are used to conveniently characterize these filling processes. For comparison, we again recall that in standard analyses of the kinetics of competitive 1^{st}-order processes, i.e., competitive random monomer filling, one trivially obtains straight line filling trajectories with slopes determined by the rate ratio. We have shown that this is also the case for various nontrivial competitive filling processes where only dimers, or only linear trimers, ••• are involved (cf. Section IV).

It is appropriate to indicate, here, a subtle variation of the random dimer filling mechanism, which we characterize as "end-on dimer filling". Instead of randomly sampling empty <u>pairs</u> of sites on which to adsorb (as implicit in the above treatment), one could randomly sample <u>single</u> empty sites (with one end of the dimer) and then either attach the other end to a randomly chosen adjacent empty site (should one exist) or, otherwise, desorb. We shall elaborate on the statistical difference between the models in later work[13], where it will be shown that the saturation coverage for random end-on dimer filling (cf. random dimer filling) is 87.668% (cf. 86.466%) from exact calculations on a 1D lattice, and 92.1%

(cf. 90.7%) from approximate calculations on a 2D square lattice. These results indicate that Hayden and Klemperer's[7] Monte Carlo simulations, modeling random adsorption on metal surfaces of two-point β-CO, in competition with one-point α-CO, refer to the end-on dimer filling model (they obtained saturation coverage estimates, for dimer filling with no monomers present, of 88.0% on a 1D lattice, and 92.1% on a 2D square lattice). For further comparison of the models, one can consider, e.g., the saturation coverage of β-CO (dimers) for various ratios of the β-CO (dimer) to α-CO (monomer) adsorption rate κ_d/κ_m. For κ_d/κ_m = 3/2 (5/3), Monte Carlo estimates in Ref. (7) for end-on dimer filling yield 65.8±1.5% (67.4±1.5%), which should be compared with our accurate 3^{rd}-order truncation results for "conventional" dimer filling with κ_d/κ_m = 3/4 (5/6) of 53.969±0.005% (56.096±0.005%). Ratios κ_d/κ_m are doubled in the end-on dimer filling case to ensure corresponding short time partial coverage behavior for the two processes. Detailed discussion of this point, and confirmation of the above Monte Carlo results, will be presented in later work[13], but we note here the potential for using results from these models to assertain the underlying dimer filling mechanism.

Finally we remark that our method is readily adapted to consider the effect of a stochastic, e.g., random, distribution of inactive (nonadsorptive) sites on competitive filling processes[14]. This would allow an accurate analytic treatment of competitive β-CO and α-CO adsorption on binary alloys (as simulated in Ref. (7)).

ACKNOWLEDGEMENTS

Ames Laboratory is operated for the U.S. Department of Energy by Iowa State University under Contract No. W-7405-ENG-82. This work was supported by the Office of Basic Energy Sciences.

APPENDIX: COMPETITIVE IRREVERSIBLE RANDOM FILLING ON BETHE LATTICES AND OTHER BRANCHING MEDIA

Exact solution of the hierarchial equations is possible for competitive, irreversible, random, and sometimes cooperative, filling of monomers, dimers, ••• on Bethe lattices (infinite, regular lattices with no closed loops) and on more general branching media[15] (see Fig. 8). The key to exact solution is the empty site shielding property described in the Introduction (cf. Ref. 3). For competitive random filling involving monomers and dimers only, this property implies that any site which separates the lattice into two, or more disconnected parts (i.e., an articulation point), when specified empty, shields sites in one part from the influence of those in the others. It is natural to use these results to gain insight into the behavior of corresponding processes on physical lattices of the same coordination number. For Bethe lattices, we expect significant similarities when the size of the adsorbing species (extended by the range of the cooperative effects) is smaller than the (smallest) closed loops on the physical lattice. Here we consider only competitive random monomer and dimer filling.

For this process on a Bethe lattice of coordination number $c(>2)$, we have that

$$- d/dt\ P_o = \kappa_m P_o + c\,\kappa_d P_{oo} \quad , \tag{1a}$$

$$- d/dt\ P_{oo} = 2\kappa_m P_{oo} + \kappa_d P_{oo} + 2(c-1)\,\kappa_d P_{ooo} \quad , \tag{1b}$$

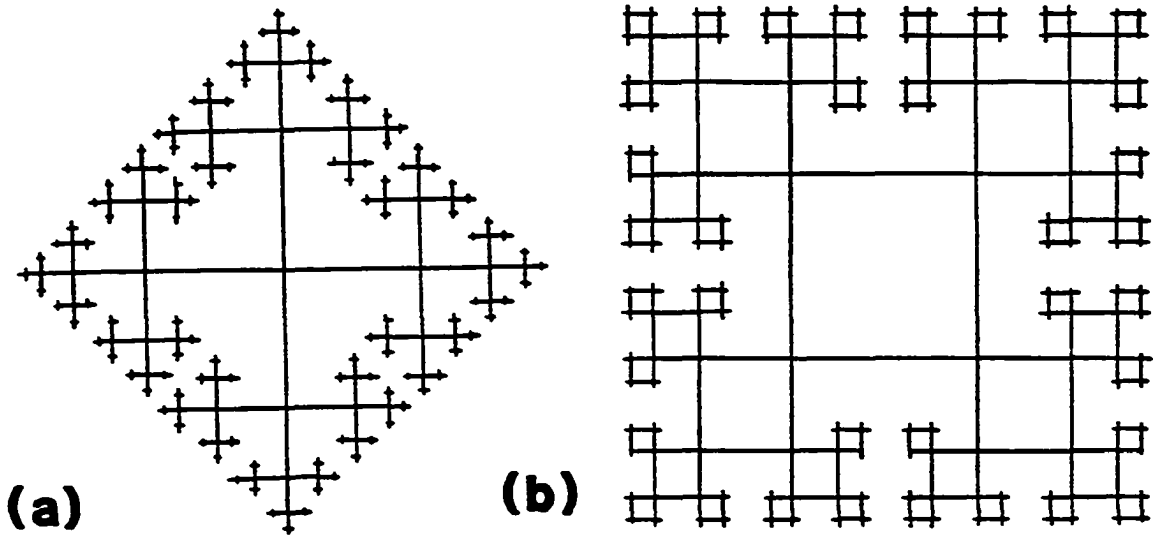

Figure 8: Examples of infinite, regular lattices for which exact solution of the hierarchial equations is sometimes possible

(a) a Bethe lattice with c=4; (b) a square cactus. Here the length of the bonds (connecting sites) has no significance, i.e., the lattices should be interpreted as graphs where only connectivity is relevant. Thus, for (a) and (b), all sites are equivalent

where ooo represents a string of three connected empty sites. These equations can be rewritten as

$$- d/dt \ln P_o = \kappa_m + c \kappa_d Q_{o\phi} \quad , \tag{2a}$$

$$- d/dt \ln Q_{o\phi} = \kappa_m + \kappa_d + 2(c-1) \kappa_d Q_{o\phi\phi} - c \kappa_d Q_{o\phi}$$

$$= \kappa_m + \kappa_d + (c-2) Q_{o\phi} \quad , \tag{2b}$$

where $Q_{o\phi} \equiv P_{oo}/P_o$, $Q_{o\phi\phi} = P_{ooo}/P_{oo}$ and, in (2b), we have used that $Q_{o\phi\phi} \equiv Q_{o\phi}$ since, here, any (single) <u>empty</u> site shields[1,3]. Integration of (2b) yields immediately

$$Q \equiv Q_{o\phi} = \frac{(\kappa_m+\kappa_d) \exp[-(\kappa_m+\kappa_d)t]}{(\kappa_m+\kappa_d) + (c-2) \kappa_d [1-\exp[-(\kappa_m+\kappa_d)t]]} \quad . \tag{3}$$

Dividing (2a) into (2b) and integrating, one obtains

$$P_o = \frac{(\kappa_m+(c-1) \kappa_d) Q}{\kappa_m+\kappa_d + (c-2) \kappa_d Q} \left(\frac{\kappa_m}{\kappa_m+\kappa_d}\right) \left(\frac{\kappa_m+\kappa_d + (c-2) \kappa_d Q}{\kappa_m + (c-1) \kappa_d}\right)^{\frac{c}{c-2}} \quad , \tag{4}$$

which, together with (3), yields the explicit time dependence of P_o. Note that the first factor on the r.h.s. of (4) equals $\exp(-\kappa_m t)$.

Partial coverages can now be obtained through integration of the equations

$$d/dt\ \theta_m = \kappa_m P_o\ ,\ d/dt\ \theta_d = c\ \kappa_d P_{oo} = c\ \kappa_d P_o Q_{o\phi}\ , \qquad (5)$$

(or we can use $\theta_m+\theta_d+\theta_o\equiv 1$, and drop one of the equations (5)). The physical requirement that $\theta_m=1-P_o$ when $\kappa_d=0$ and $\theta_m<1-P_o$ when $\kappa_d>0$ and $t>0$ is guaranteed since the second factor in (4) is identically equal to unity when $\kappa_d=0$ and between zero and unity when $\kappa_d>0$ and $0<q<1$.

It is interesting to note here that the above results coincide with the 1^{st}-order truncation approximation on a physical lattice of coordination number, c, provided this lattice has no closed loops of length three. Clearly the 1^{st}-order approximation on, e.g., square and hexagonal lattices cannot "see" that these lattices have closed loops. For a hexagonal lattice (which has larger loops, and is thus more "Bethe lattice like"), the 2^{nd}-order approximation also coincides with the c=3 Bethe lattice results[3]. Thus the similarity between hexagonal and c=3 Bethe lattice behavior is greater than that between square and c=4 Bethe lattice behavior (see Fig. 1).

It is natural to consider these filling problems on brancning structures, having some closed loops, which resemble the physical lattice more closely than the corresponding Bethe lattice, but for which exact solution is still possible. In this context, we consider competitive, random monomer and dimer filling on a square cactus (see Fig. 8). Using the fact that, here, any site specified empty separates the lattice into two disconnected parts and shields sites in one part from the influence of those in the other, one can straightforwardly obtain the following closed set of equations

$$- d/dt \, \ell n \, P_o = \kappa_m + 4\kappa_d \, Q_{o\phi} \quad ,$$

$$- d/dt \, \ell n \, Q_{o\phi} = \kappa_m + \kappa_d(1 + 2Q_{\substack{o \\ \phi\phi}}) \quad ,$$

$$- d/dt \, \ell n \, Q_{\substack{o \\ \phi\phi}} = \kappa_m + \kappa_d(1 + 2Q_{o\phi} + 2Q_{\substack{\phi \\ \phi\phi}} - 2Q_{\substack{o \\ \phi\phi}}) \quad ,$$

$$- d/dt \, \ell n \, Q_{\substack{\phi \\ \phi\phi}} = \kappa_m + 2\kappa_d(1 + Q_{o\phi} - Q_{\substack{\phi \\ \phi\phi}}) \quad . \tag{6}$$

Here sites in the configurations $\substack{o \\ \phi\phi}$ and $\substack{\phi \\ \phi\phi}$ should be interpreted to lie on a single loop. Integrating these equations together with (5) produces the results shown in Table I. As might be anticipated, these lie between the c=4 Bethe lattice and square lattice values.

REFERENCES

1. J. W. Evans, D. R. Burgess and D. K. Hoffman, J. Chem. Phys. 79, 5011 (1983).
2. See for example: E. A. Boucher, Prog. Polym. Sci. 6, 63 (1978); N. A. Plate and O. V. Noah, Adv. Polym. Sci. 31, 133 (1979); E. A. Boucher, Faraday Trans. II 69, 1839 (1973); J. J. Gonzalez, P. C. Hemmer and J. S. Høye, Chem. Phys. 3, 228 (1974); N. O. Wolf, J. W. Evans and D. K. Hoffman, J. Math. Phys. 25, 2519 (1984).
3. J. W. Evans, J. Math. Phys. 25, 2527 (1984).
4. J. W. Evans and D. K. Hoffman, J. Stat. Phys. 36, 65 (1984).
5. D. K. Hoffman, J. Chem. Phys. 65, 95 (1976); J. W. Evans, Physica 123A, 297 (1984).
6. R. S. Nord and J. W. Evans, J. Chem. Phys. 82, 2795 (1985).
7. B. E. Hayden and D. F. Klemperer, Surf. Sci. 80, 401 (1979).
8. J. W. Evans, D. K. Hoffman and D. R. Burgess, J. Chem. Phys. 80, 936 (1984).
9. I. R. Epstein, Biopolymers 18, 765 (1979).
10. K. J. Vette, T. W. Orent, D. K. Hoffman and R. S. Hansen, J. Chem. Phys. 60, 4854 (1974).
11. See, e.g., E. N. Yeremin, "The Foundations of Chemical Kinetics", MIR, Moscow (1979).
12. P. J. Flory, J. Am. Chem. Soc. 61, 1518 (1939); E. R. Cohen and H. Reiss, J. Chem. Phys. 38, 680 (1963).
13. R. S. Nord and J. W. Evans, Ames Laboratory Preprint (1986).
14. J. W. Evans and R. S. Nord, J. Stat. Phys. 38, 681 (1985).
15. J. W. Essam, in "Phase Transition and Critical Phenomena", Volume 2, edited by C. Domb and M. S. Green (Academic, New York, 1972).

PAPER III:

RANDOM DIMER FILLING OF LATTICES: THREE-DIMENSIONAL APPLICATION TO FREE RADICAL RECOMBINATION KINETICS

RANDOM DIMER FILLING OF LATTICES: THREE-DIMENSIONAL APPLICATION TO FREE RADICAL RECOMBINATION KINETICS

J. W. Evans and R. S. Nord

Ames Laboratory and Department of Chemistry
Iowa State University
Ames, Iowa 50011

ABSTRACT

The recombination of nearest neighbors in a condensed matrix of free radicals was modeled by Jackson and Montroll as irreversible, sequential, random dimer filling of nearest-neighbor sites on an infinite, 3D lattice. Here we analyze the master equations for random dimer filling recast as an infinite hierarchy of rate equations for subconfiguration probabilities using techniques involving truncation, formal density expansions (coupled with resummation), and spectral theory. A detailed analysis for the cubic lattice case produces, e.g., estimates for the fraction of isolated empty sites (i.e., free radicals) at saturation. We also consider the effect of a stochastically specified distribution of nonadsorptive sites (i.e., inert dilutents).

I. INTRODUCTION

It is possible to condense free radicals of, e.g., O, H or N, as a quasicrystalline matrix in which recombination and a subsequent release of energy can occur[1]. Jackson and Montroll, and others[2] have modeled this process assuming nearest-neighbor (n.n.) free radicals (sequentially) recombine randomly and irreversibly leaving an isolated fraction of free radicals at the end of the process. The effect of a stochastically specified, time-independent distribution of inert dilutents on the latter quantity is also of interest. This model is clearly equivalent to the irreversible (sequential) random dimer filling of n.n. sites of a 3D lattice.

Random dimer filling of n.n. sites on lattices has received the most thorough attention of any (nontrivial) irreversible process on a lattice. The saturation fraction of isolated empty sites, P_0^S, is the prime quantity of interest here (see Fig. 1). The earliest analyses were for 1D lattices in the context of pairing/cyclization reactions on polymer chains[3-7] beginning with Flory's[3] work in 1939 which showed that $P_0^S = e^{-2}$ for an infinite 1D lattice. The 2D lattice case has been the subject of several studies in the context of two-point surface adsorption and reaction[8-13]. Combinatorial techniques have been used for finite 1D[3,6,7] and 2D[9] lattices and several Monte Carlo simulations have been performed for the 2D case[8]. The analytic approach implemented here is based on the hierarchial form of the master equations describing the time evolution of probabilities for various subconfigurations of filled and/or empty sites.

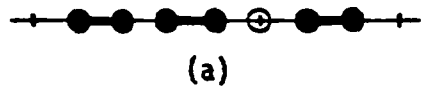

(a)

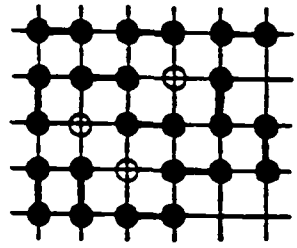

(b)

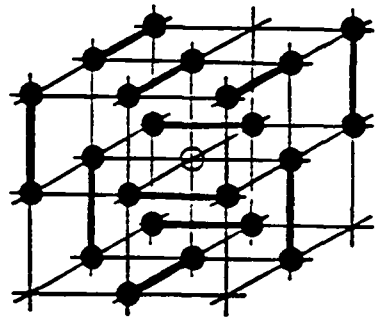

(c)

Figure 1: Dimer filling of a (a) 1D linear, (b) 2D square, (c) 3D cubic lattice creating isolated empty sites (indicated by 'o') which never fill

These can be written down intuitively even for reversible nonrandom adsorption[10,14,15] (where the adsorption/desorption rates depend on the state of a finite region around the sites being filled). They are particularly simple for irreversible random dimer filling (see Refs. (4,5) for 1D and Ref. (10,13) for 2D). Solution of these hierarchial equations gives complete information about not only the time evolution of the process but also the nonequilibrium saturation state including, e.g., P_0^S. (Equilibrium is not achieved since the dimer adsorption is irreversible and immobile.)

In this work, we consider random dimer filling on infinite lattices and implement various techniques to analyze the corresponding (infinite) hierarchy of rate equations. We first present a simple spectral analysis which exploits the special linear structure of these equations. Next a hierarchial truncation technique, approximate except in 1D, is discussed. We adopt a scheme used by Vette et al.[10] in 2D which deals directly with conditional probabilities for a site to be empty given various other sites are empty. This technique is tailored to the special structure of the hierarchy, associated with irreversibility, which leads to a shielding property of suitable walls of empty sites (see Ref. (15) for a discussion in the context of general irreversible cooperative processes). A third alternative is to obtain formal density (coverage) expansions of solutions [11,12]. These are readily available even for complicated cooperative irreversible processes but typically suffer from convergence problems particularly for high, e.g., saturation, coverages. Consequently, here we also implement a resummation procedure which incorporates our knowledge of

nonanalyticity (outside the physical range of coverage) explicit in the lowest order truncation solution.

In Section II we analyze the kinetics of irreversible random dimer filling of n.n. sites of an infinite uniform lattice (i.e., free radical recombination in the absence of inert dilutents). The nature of the approach to the final state is first elucidated through a simple spectral analysis. Next the truncation and density expansion resummation techniques described above are implemented. Most of the detailed results presented are for the case of a cubic lattice. Estimates for the final fraction of isolated empty sites (i.e. free radicals) demonstrate good agreement between the two techniques. The truncation and density expansion techniques are extended straightforwardly in Section III to analyze the effect of a stochastically specified distribution of nonadsorptive inactive sites (i.e., inert dilutents).

II. DIMER FILLING OF INFINITE UNIFORM LATTICES (RECOMBINATION IN THE ABSENCE OF INERT DILUTENTS)

A. General Theory

For convenience we shall use the terminology of adsorption. Thus we consider the irreversible random dimer filling of nearest neighbor (n.n.) sites of an infinite, uniform lattice. One can intuitively write down an infinite hierarchy of rate equations for the probabilities $P_{\{m\}}$ that groups $\{m\}$ of 'm' sites are empty (evaluated with respect to an appropriate ensemble of irreversible fillings). Specifically (cf. Refs. (10,13),

$$\kappa^{-1}\, d/dt\, P_{\{m\}} = - n_{\{m\}}\, P_{\{m\}} - \sum_{j \notin \{m\}} n_{j,\{m\}}\, P_{\{m\}+j} \quad , \tag{2.1}$$

where κ is the (single) adsorption rate, $n_{\{m\}}$ is the number of n.n. pairs in $\{m\}$, and $n_{j,\{m\}} \equiv n_{j+\{m\}} - n_{\{m\}}$ is the number of sites in $\{m\}$ adjacent to j. These terms correspond to destruction of $\{m\}$ through dimer adsorption on sites completely within and partly overlapping $\{m\}$, respectively. In the 2^{nd} term, $P_{\{m\}+j}$ rather than $P_{\{m\}}$ appears, since site j must be empty for the dimer to land in the described fashion. Note that (2.1) contains an infinite closed subhierarchy for connected clusters of empty sites.

The equations (2.1) do not assume any invariance of the $P_{\{m\}}$'s and thus apply for any choice of initial conditions. Here, however, we assume that the $P_{\{m\}}$ are invariant under all space group operations on the lattice, as for example with an initially empty lattice, i.e., $P_{\{m\}} = 1$ at t =

0 for all {m}. Thus {m} in (2.1) will be interpreted, henceforth, as representing the infinite class of subconfigurations of sites equivalent to {m} after translation. For example, for a 1D lattice, if P_m denotes the probability of any m-tuple of empty sites, then (2.1) includes the infinite subhierarchy[4,5,10]

$$\kappa^{-1} \, d/dt \, P_m = -(m-1) \, P_m - 2 \, P_{m+1} \quad , \quad m \geq 1 \quad , \tag{2.2}$$

where these terms correspond to destruction of an empty m-tuple by a dimer adsorbing completely within and partly overlapping the m-tuple, respectively.

In this work we invoke spectral theoretic, hierarchial truncation[10,15] and formal density expansion (with subsequent resummation)[11,12] techniques to analyze various equivalent forms of these equations. The former two are now described for a (general) lattice with coordination number c, and the latter two are implemented in the next subsection to treat the cubic lattice case.

Exploiting the fact that (2.1) is linear and thus can be written in (infinite) matrix form, one can readily extract some understanding of the nature of the approach to the final stationary state. Let $\underline{P}(m)$ be the <u>finite</u> dimensional vector constructed from $P_{\{m\}}$ for connected {m} (modulo translations) and <u>fixed</u> m. We may or may not choose to reduce the dimension of $\underline{P}(m)$ through other symmetries. Thus, e.g., $\underline{P}(1) \equiv P_{\{1\}} \equiv P_0$, the probability that any site is empty. Next we construct the infinite dimensional vector $\underline{P}$, say, from these, which satisfies the time evolution

equation (2.1) in the form

$$d/dt \begin{bmatrix} \underline{P}(1) \\ \underline{P}(2) \\ \underline{P}(3) \\ \vdots \end{bmatrix} = -\kappa \begin{bmatrix} \underline{0} & \underline{n}^{+}(1) & \underline{0} & \underline{0} & & \\ \underline{0} & \underline{n}(2) & \underline{n}^{+}(2) & \underline{0} & & \\ \underline{0} & \underline{0} & \underline{n}(3) & \underline{n}^{+}(3) & \underline{0} & \\ & & \underline{0} & \underline{n}(4) & \underline{n}^{+}(4) & \underline{0} \\ & & & \underline{0} & \ddots & \ddots \end{bmatrix} \begin{bmatrix} \underline{P}(1) \\ \underline{P}(2) \\ \underline{P}(3) \\ \vdots \end{bmatrix}$$

$$\equiv \underline{\underline{K}} \begin{bmatrix} \underline{P}(1) \\ \underline{P}(2) \\ \underline{P}(3) \\ \vdots \end{bmatrix} . \qquad (2.3)$$

Here $(\underline{\underline{n}}(j))_{\{j\},\{j\}'} = \delta_{\{j\},\{j\}'}\, n_{\{j\}}$ and $(\underline{\underline{n}}^{+}(j))_{\{j\},\{j+1\}}$ is an integral multiple of $\delta_{\{j+1\}-\{j\},k}$ where the Kronecker delta here means that $\{j\} \subset \{j+1\}$ and the only site of $\{j+1\}$ not in $\{j\}$ is k. In a rigorous setting, $\underline{\underline{K}}$ should be regarded as the unbounded generator of time evolution in the infinite dimensional ℓ^{∞}-type Banach space naturally associated with the vectors $\underline{P}$.

The infinite dimensional rate matrix $\underline{\underline{K}}$ on the r.h.s. of (2.3) generating time evolution is upper triangular and consequently its eigenvalues are given by its diagonal components $-\kappa n_{\{j\}}$. Furthermore the eigenvector corresponding to the nondegenerate eigenvalue $-\kappa n_{\{1\}} = 0$ can be chosen to have unity in the first component and zeroes elsewhere. This result should be anticipated since, in the final stationary state, clearly $P_{\{m\}}$ (in $\underline{P}$) = 0 for $m > 2$, but $P_{\{1\}} \equiv P_0 \neq 0$. It is also useful to calculate the corresponding biorthogonal dual eigenvector $(1, \underline{a}(2)^{T}, \underline{a}(3)^{T}, \cdots)$, say. A

simple recursive analysis shows that

$$\underline{a}(j)^T = -\,\underline{a}(j-1)^T \cdot \underline{\underline{n}}^+(j-1) \cdot \underline{\underline{n}}(j)^{-1}$$
$$= (-1)^{j-1}\, \underline{\underline{n}}^+(1) \cdot \underline{\underline{n}}(2)^{-1} \cdot \underline{\underline{n}}^+(2) \cdot \underline{\underline{n}}(3)^{-1} \cdot \ldots \cdot \underline{\underline{n}}^+(j-1) \cdot \underline{\underline{n}}(j)^{-1} \,. \quad (2.4)$$

Now since $n(2) = 1$ and $n(j) > 1$ for $j > 2$, and for an initially empty lattice $\underline{P}|_{t=0} = \underline{1}$ (a vector with every component unity), it follows that

$$\underline{P}(t) = e^{+\underline{\underline{K}}t}.\underline{1} = \begin{bmatrix} 1 \\ \underline{0}(2) \\ \underline{0}(3) \\ \vdots \end{bmatrix} (1,\, \underline{a}(2)^T,\, \underline{a}(3)^T,\, \ldots) \cdot \underline{1} + O(e^{-\kappa t}), \text{ as } t \to \infty \,, \quad (2.5)$$

where, for each j, all components of $\underline{0}(j)$ are zero. Consequently the saturation value, P_0^S, of $P_0 \equiv P_{\{1\}}$ (i.e., the final fraction of isolated empty sites) is given by

$$P_0^S = (1,\, \underline{a}(2)^T,\, \underline{a}(3)^T,\, \ldots) \cdot \underline{1} \quad . \quad (2.6)$$

For a 1D lattice, it follows immediately from (2.2) that $n(j) = j-1$, $n^+(j) = 2$ for $j>1$, and (2.4,6) readily yield $P_0^S = e^{-2}$ recovering the well known result of Flory[3]. However, difficulty in obtaining accurate estimates of P_0^S from (2.6) increases dramatically as the lattice dimension increases.

We can, of course, extend $\underline{P}$ to include disconnected configurations $\{m\}$ as well. Since disconnected configurations, loosely speaking, couple only

to those with the same or shorter separations, we can, by restricting our attention to a finite range of separations, still choose finite-dimensional vectors $\underline{P}(n)$. However there is no need for this. It is interesting to note that if $\underline{P}$ includes $P_{\{m\}}$ where all 'm' points are separated (so $n_{\{m\}} = 0$), then the corresponding rate matrix $\underline{\underline{K}}$ has a zero-eigenvalue eigenvector with all components zero except the $\{m\}^{th}$. After constructing biorthogonal dual eigenvectors corresponding to all zero eigenvalue eigenvectors, the nonzero saturation values of such $P_{\{m\}}$ can be calculated analogous to (2.5,6). However, even in one dimension, such a construction is complicated.

Finally, we remark that the upper triangular structure of the hierarchial rate equations for probabilities of empty subconfigurations is generic to all irreversible random and cooperative processes. The zero eigenvalue dual eigenvector construction can be extended, in principle, to determine saturation coverages, e.g., for random polyatomic filling or for monomer filling with some degree of blocking. However, a more detailed treatment is left till later work.

We next consider (2.1) in a modified form more suited to implementation of our truncation scheme and again restrict our attention to an initially empty lattice. Define the conditional probability $Q_{j,\{m\}} = P_{j+\{m\}}/P_{\{m\}}$ of j being empty <u>given</u> the sites in {m} are empty (the sites in {m} are referred to as <u>conditioning</u> sites). From (2.1), one immediately obtains an infinite closed hierarchy for these Q's, specifically (cf. Refs. (10,13),

$$\kappa^{-1}\, d/dt\, \ell n\, Q_{j,\{m\}} = \kappa^{-1}\, d/dt\, P_{j+\{m\}}/P_{j+\{m\}} - \kappa^{-1}\, d/dt\, P_{\{m\}}/P_{\{m\}}$$

$$= -\left(n_{\{m\}+j} - n_{\{m\}}\right) - \sum_{k\notin\{m\}+j} n_{k,\{m\}+j}\, Q_{k,\{m\}+j} + \sum_{k\notin\{m\}} n_{k,\{m\}}\, Q_{k,\{m\}} \quad . \tag{2.7}$$

Note that (2.7) also contains an infinite closed subhierarchy for $Q_{j,\{m\}}$ with $j+\{m\}$ connected. Again subconfigurations labels can and will be interpreted to refer to classes equivalent after translations. A shielding property of empty sites embodied, e.g., in (2.7), has been discussed elsewhere in a more general context[15]. For random dimer filling, this property states that if a wall of empty sites of thickness one separates the lattice into disconnected regions, then the sites in any one region are not influenced by those in the other regions.

In one dimension, it follows that a single site specified empty shields sites on one side from those on the other. Thus, for example, $Q_m \equiv P_{m+1}/P_m \equiv Q_{\underbrace{\circ\phi\phi\cdots\phi}_{m}} \equiv Q_{\underbrace{\phi\phi\cdots\phi\circ}_{m}}$ (where ϕ denotes a conditioning site specified empty) are equal to $Q(\equiv P_2/P_1 \equiv P_{oo}/P_o)$, say, for all $m>1$. This result follows immediately after simply recasting (2.2) in the form (2.7) to obtain[10]

$$\kappa^{-1}\, d/dt\, \ell n\, Q_m = -1 - 2\,(Q_{m+1} - Q_m) \quad , \quad m>1 \quad . \tag{2.8}$$

Furthermore, (2.8) implies that, for an initially empty lattice[4,5,10],

$$\kappa^{-1}\, d/dt\, \ell n\, Q = -1 \text{ so } Q = e^{-\kappa t}, \tag{2.9}$$

which can be used to exactly truncate the hierarchy (2.2) noting that $P_2 = QP_1$. In two and three dimensions, the separating shielding wall of sites specified empty must either be closed or extend to infinity (some 2D square lattice examples are displayed in Fig. 2). Proof of this shielding property again follows from observation of self-consistency with (2.7) after noting various cancellations analogous to those in (2.8). Some further discussion is given in the Appendix. Although this property does not allow exact truncation and solution of the hierarchy, it indicates the shielding propensity of empty sites and adds credence to the following truncation procedure which recovers exact results in 1D (Since filled sites do not have as great a shielding propensity, we avoid more standard Markovian-style truncations which, in any case, would not recover exact 1D results).

We obtain approximate finite, closed, coupled sets of equations for various subsets of Q's by adopting the n^{th}-shell truncation approximations of Vette et al.[10]. Here conditioning sites in the $Q_{k,\{r\}}$ further than 'n' lattice vectors from 'k' are neglected. To illustrate this procedure, consider the 1^{st}-shell approximation. If $P_o = Q_o$ denotes the probability for any site to be empty, P_{oo} for an adjacent pair to be empty, ... and $Q_{o\phi} \equiv P_{oo}/P_o$, ... then for a lattice with coordination number c, (2.7) becomes

$$\kappa^{-1} \, d/dt \, \ell n \, P_o = - c \, Q_{o\phi} \tag{2.10a}$$

$$\kappa^{-1} \, d/dt \, \ell n \, Q_{o\phi} = - 1 - \sum_{n.n.} Q_{j,\phi\phi} + c \, Q_{o\phi} \tag{2.10b}$$

$$\vdots$$

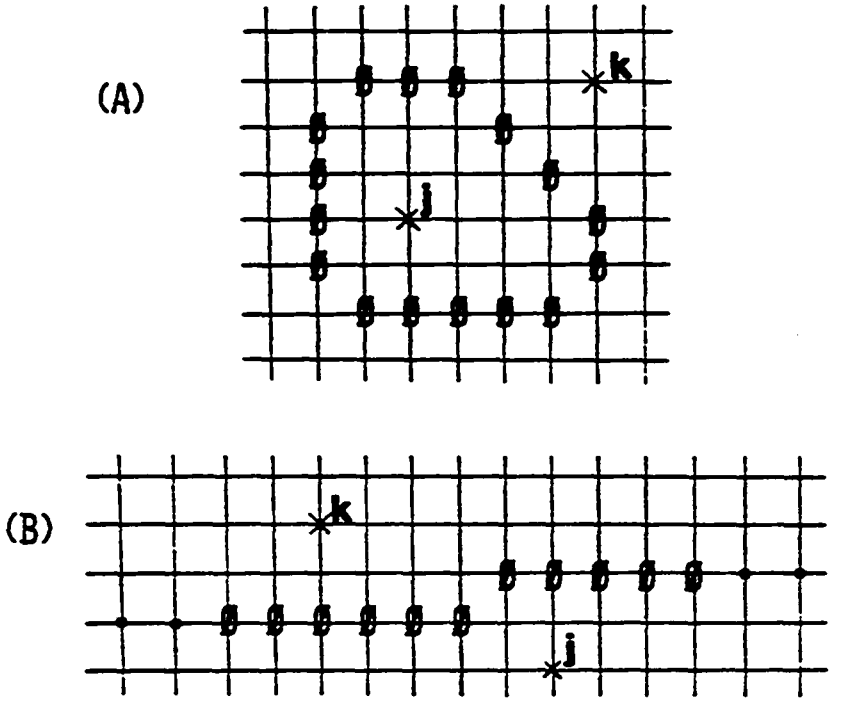

Figure 2: Closed (A) and infinite (B) shielding walls, for random dimer filling on a 2D square lattice, which shield site j from the influence of k and visa versa (where Ø represents an empty conditioning site and the dots indicate that the wall of Ø sites extends to infinity)

where the sum on the r.h.s. of (2.10b) is over all empty sites j adjacent to the empty conditioning pair $\phi\phi$. If there are no closed loops of length three (so excluding, e.g., a 2D triangular lattice), then this sum consists of 2(c-1) terms. Furthermore, here, in the 1^{st}-shell truncation approximation $Q_{j,\phi\phi} \to Q_{o\phi}$ and so (2.10b) is replaced by

$$\kappa^{-1} \, d/dt \, \ell n \, Q_{o\phi} = - 1 - (c-2) \, Q_{o\phi} \quad . \tag{2.11}$$

Integration of (2.10a) and (2.11) for c>2 using the initial conditions $P_o = 1$, $Q_{o\phi} = 1$, yields

$$Q_{o\phi} = \frac{1}{c-2} \left[(c-1) \, P_o^{\frac{c-2}{c}} - 1 \right] \quad . \tag{2.12}$$

Since clearly P_{oo} and hence $Q_{o\phi}$ are zero at saturation, the 1^{st}-shell estimate of the saturation value of P_o is $P_o^s = (\frac{1}{c-1})^{\frac{c}{c-2}}$. It has been noted elsewhere that (2.10a,11,12) constitute the exact solution for random dimer filling on a Bethe lattice (i.e., a lattice with no closed loops) of coordination number c[16].

Higner order truncation approximations, of course, retain more Q's (see the cubic lattice example below) and should be more accurate since neglected 'ϕ' sites are further from the 'o' site and often will be obscured from the latter by several other 'ϕ' sites (which will have

substantial shielding propensity). An estimate of accuracy can be obtained by comparison of results from different order approximations. We mention that the random dimer filling equations should be more amenable to truncation (especially at low orders) than those for other irreversible cooperative processes which typically require a shielding wall thickness greater than one[15].

B. The Cubic Lattice

Here we consider only the case where the lattice is initially empty. Exploiting all lattice symmetries, (2.1) becomes

$$\kappa^{-1}\, d/dt\, P_o = -\,6\, P_{oo}$$

$$\kappa^{-1}\, d/dt\, P_{oo} = -\,P_{oo} - 2\, P_{ooo} - 8\, P_{o\overset{o}{\overset{|}{o}}}$$

$$\kappa^{-1}\, d/dt\, P_{ooo} = -\,2\, P_{ooo} - 2\, P_{oooo} - 8\, P_{oo\overset{o}{\overset{|}{o}}} - 4\, P_{o\overset{o}{\overset{|}{o}}o}$$

$$\vdots \qquad (2.13)$$

where o, oo, ooo, ••• denotes a single, pair, triple, ••• of empty sites, respectively. From (2.13), one immediately obtains the following specific form of (2.7) for $Q_o \equiv P_o$, $Q_{o\phi} \equiv P_{oo}/P_o$, $Q_{o\phi\phi} \equiv P_{ooo}/P_{oo}$, ...

$$\kappa^{-1}\, d/dt\, \ell n\, P_o = -\,6\, Q_{o\phi} \qquad (2.14a)$$

$$\kappa^{-1}\, d/dt\, \ell n\, Q_{o\phi} = -1 - 2\, Q_{o\phi\phi} - 8\, Q_{\phi\overset{o}{\phi}} + 6\, Q_{o\phi} \tag{2.14b}$$

$$\kappa^{-1}\, d/dt\, \ell n\, Q_{o\phi\phi} = -1 - 2\,(Q_{o\phi\phi\phi} - Q_{o\phi\phi}) - 8\,(Q_{\phi\phi\overset{o}{\phi}} - Q_{\phi\overset{o}{\phi}}) - 4\, Q_{\phi\overset{o}{\phi}\phi} \tag{2.14c}$$

$$\vdots$$

We have already discussed the 1^{st}-shell truncation approximation wherein, e.g., $Q_{o\phi\phi}$, $Q_{\phi\overset{o}{\phi}} \to Q_{o\phi}$ in (2-14b) which then closes together with (2.14a). From (2.12) with c=6, one obtains a 1^{st}-shell estimate of the fraction of (isolated) empty sites at the end of the process of $P_o^s = \frac{1}{5\sqrt{5}} =$ .08944 (corresponding to a saturation coverage $\theta^s = .91056$). Here $P_{oo} = P_o\, Q_{o\phi}$ can also be calculated without further approximation unlike probabilities for larger configurations, e.g., the probability for any connected cluster of m empty sites, $P_{\{m\}} = P_o\, Q_{o\phi}^{m-1}$.

In the 2^{nd}-shell approximation one neglects 'ϕ' sites, in the above Q's, further than two lattice vectors from the 'o' site so, e.g., $Q_{o\phi\phi\phi} \to Q_{o\phi\phi}$, $Q_{\phi\phi\overset{o}{\phi}} \to Q_{\phi\overset{o}{\phi}}$. Thus (2.14a,b) are unaffected by this truncation but, here, e.g., (2.14c) is replaced by

$$\kappa^{-1}\, d/dt\, \ell n\, Q_{o\phi\phi} = -1 - 4\, Q_{\phi\overset{o}{\phi}\phi} \,. \tag{2.15}$$

Continuing in this fashion, one obtains a minimal closed set of equations for the 14 Q's shown in Table I. These allow the determination of probabilities for several connected empty configurations, e.g., $P_{o\overset{o}{o}o} =$

Table I: The minimal closed set of 14 Q's in the 2^{nd}-shell truncation approximation for random dimer filling on a cubic lattice (the dots separating lattice sites are included to clarify the 3D configurations)

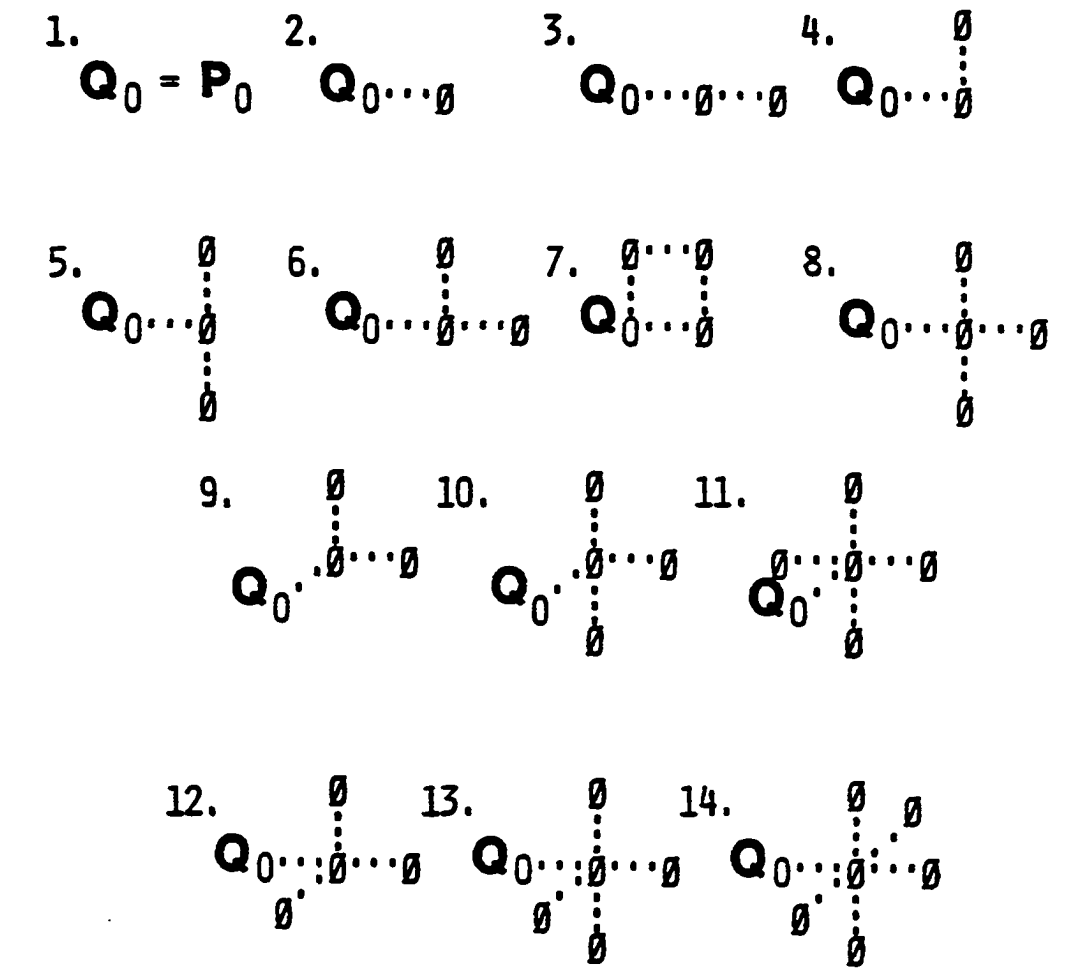

$P_o Q_{o\phi} Q_{o\phi\phi} Q_{\phi\phi\phi}^{o} = P_o Q_{o\phi} Q_{\phi\phi}^{o} Q_{\phi\phi o}^{\phi}$, without further approximation (agreement of the last two expressions for truncation solutions is proved in Ref. (15)). The probability P(0,6) of a single empty site surrounded by six filled sites can also be determined after first rewriting this expression in terms of P's for connected empty configurations using conservation of probability. Integration of the 2nd-shell equations yields the estimate $P_o^s \approx .08454$ ($\theta^s \approx .91546$). Various probabilities and conditional probabilities are plotted as functions of coverage $\theta = 1-P_o$ in Figs. 3 and 4 respectively. The latter clearly exhibits the shielding propensity of just a single empty site. Note that $Q_{o\phi\phi}^{\phi} - Q_{o\phi}^{\phi}$ and $Q_{o\phi\phi}^{\phi\phi} - Q_{o\phi}^{\phi\phi}$ are too small to show up graphically. We also mention that the 2nd-shell approximation exhibits "artificial shielding" in that $Q_{14}-Q_{11} \equiv 0$ using the labeling of Table I (a generic phenomenon for these types of truncation schemes[15]).

Except for P_o, saturation values for connected clusters of (n>2) empty sites are all zero. In contrast, those for P_{o-o}, $P_{o\overset{o}{-}}$, P_{o--o}, $P_{o\overset{o}{-}o}$, ... are nonzero and the 1st, 2nd and 4th can be reasonably estimated in the 2nd-shell approximation (here '-' indicates an unspecified site). To determine P_{o-o} ($P_{o\overset{o}{-}}$), one must include an equation for $Q_{o-\phi}$ ($Q_{o\overset{\phi}{-}}$) which couples to $Q_{\phi o\phi}$ ($Q_{\phi\overset{\phi}{o}}$) and some of the above 14 Q's. Since the equation for $Q_{\phi o\phi}$ ($Q_{\phi\overset{\phi}{o}}$) is closed with the original set of 14, P_{o-o} ($P_{o\overset{o}{-}}$) can be determined from integrating an extended set of 16 equations. To determine $P_{o\overset{o}{-}o}$, one must know $Q_{o\overset{\phi}{-}\phi}$ as well as $P_{o\overset{o}{-}}$. Its equation together with those for $Q_{\phi\overset{\phi}{o}\phi}$ and $Q_{\phi\overset{\phi}{o}\phi}$ close with the above 14 thus allowing integration. We

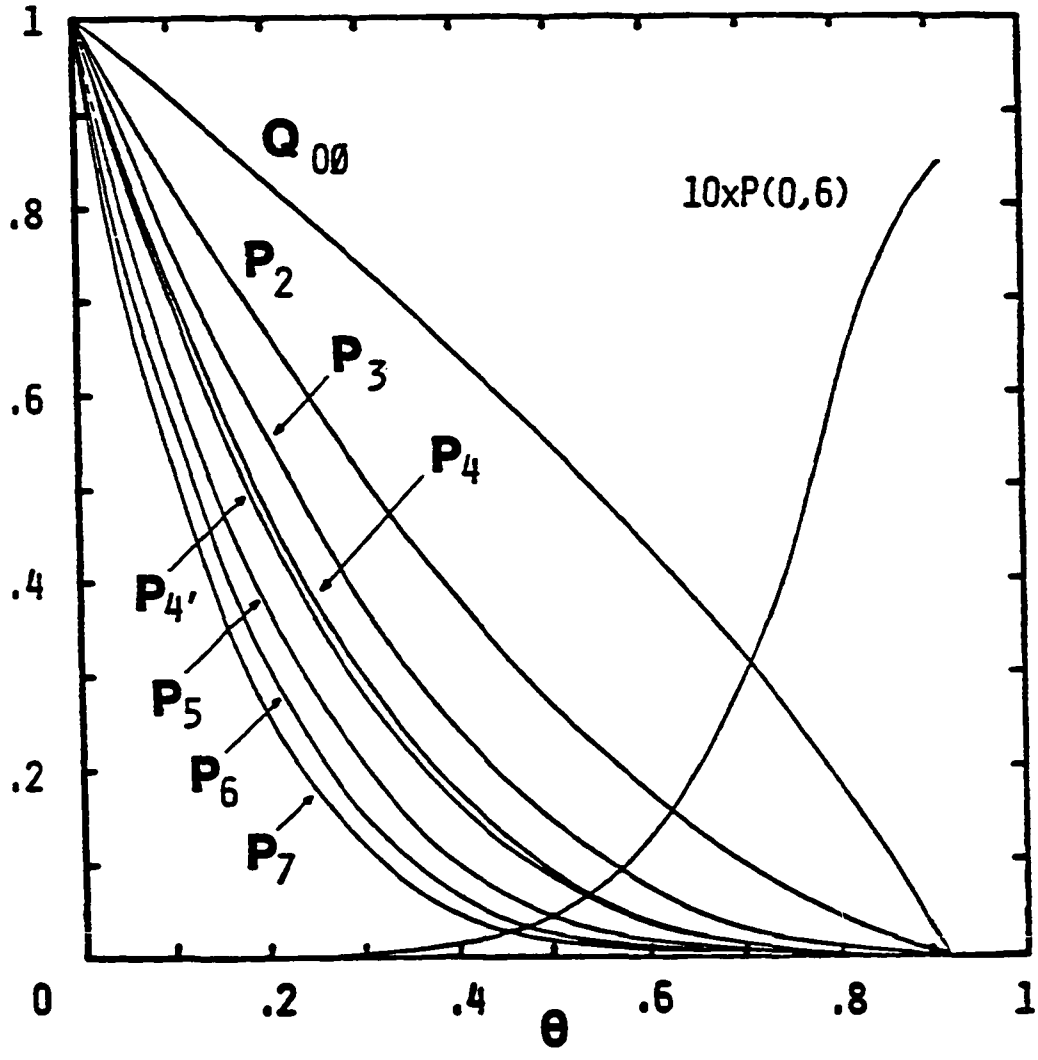

Figure 3: 2^{nd}-shell truncation values, as a function of coverage θ, for probabilities of a pair P_2, a linear (indistinguishable from a bent) triple P_3, a square P_4 or T-shaped P_4' quartet, and a cross-shaped quintet P_5 of empty sites. $P_6(P_7)$ corresponds to the 3D configuration 11(14) of Table I after replacing ϕ's with o's. $Q_{o\phi}$ and P(0,6) are defined in the text

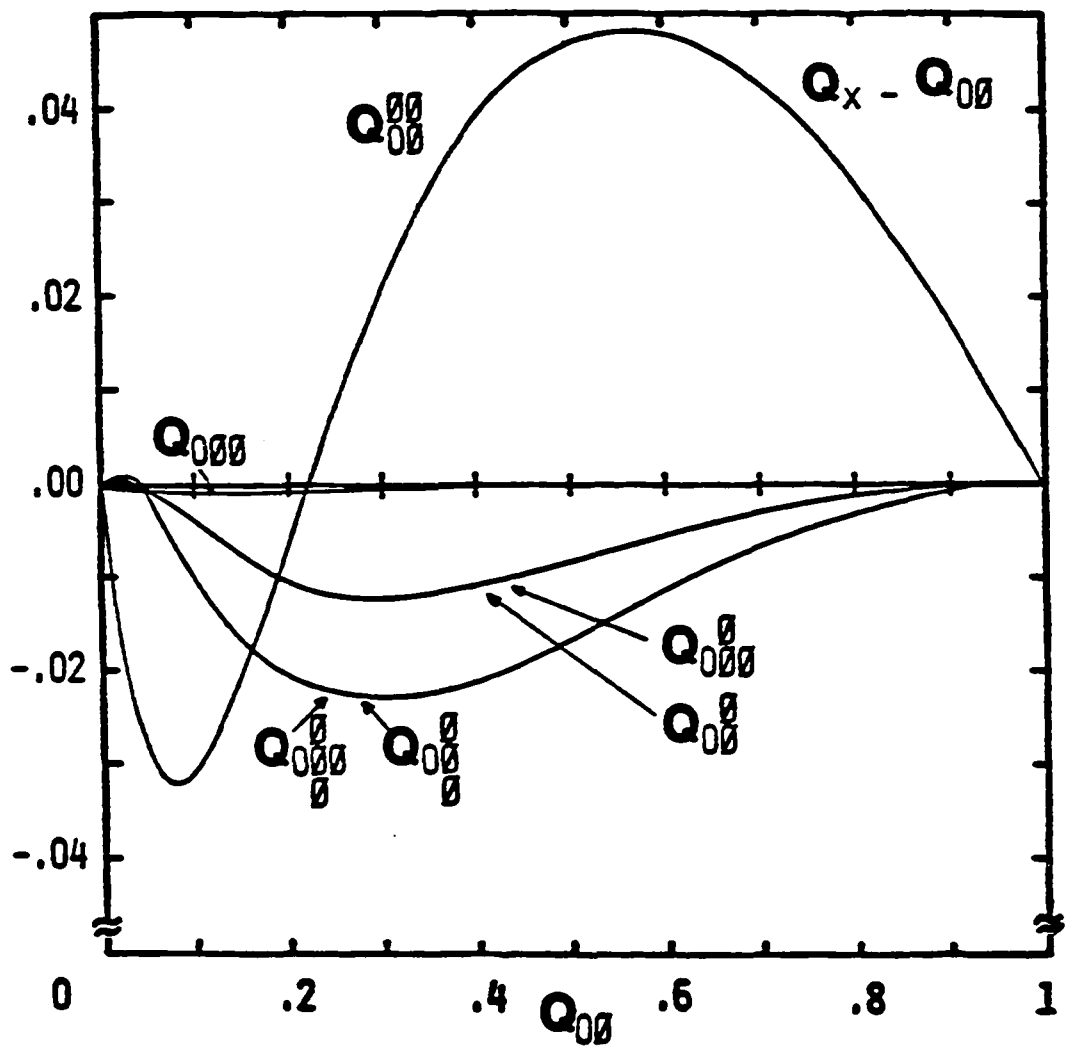

Figure 4: 2^{nd}-shell truncation values for deviations in conditional probabilities from $Q_{0\phi}$ plotted as a function of the natural parameter $Q_{0\phi}$

obtain the saturation values $P_{o\text{-}o} = .777\times10^{-2}$, $P_{o\overset{o}{-}} = .861\times10^{-2}$, $P_{o\overset{o}{-}o} = .227\times10^{-3}$. In Fig. 5, corresponding correlations are plotted as functions of θ.

Let us now sketch the formal density expansion method of solution[11,12]. Here we must start with the hierarchy for probabilities of configurations with all specified sites filled 'a'. This can be obtained from (2.13) using conservation of probability, i.e., $P_o \equiv 1 - P_a$, $P_{oo} \equiv 1 - 2P_a + P_{aa}$, ... where P_a ($\equiv \theta$, the coverage), P_{aa}, ... denote probabilities for a single, adjacent pair, ... of filled sites. This new hierarchy is, of course, equivalent to (2.13) and can be written down intuitively as follows:

$$\kappa^{-1}\, d/dt\, P_a = 6\, P_{oo} = 6(1 - 2P_a + P_{aa}) \tag{2.16a}$$

$$\kappa^{-1}\, d/dt\, P_{aa} = P_{oo} + 2P_{ooa} + 8P_{\overset{o}{\underset{a}{\diagup}}}$$

$$= 1 + 8P_a - 9P_{aa} - 2P_{a\text{-}a} - 8P_{a\overset{a}{-}} + 2P_{aaa} + 8P_{\overset{a}{\underset{a}{\diagup}}} \tag{2.16b}$$

$$\kappa^{-1}\, d/dt\, P_{aaa} = 2P_{aoo} + 2P_{aaoo} + 8P_{aa\overset{o}{\diagup}} + 4P_{a\overset{o}{\underset{a}{\diagup}}}$$

$$= 2P_a + 8P_{aa} + \ldots \tag{2.16c}$$

$$\vdots$$

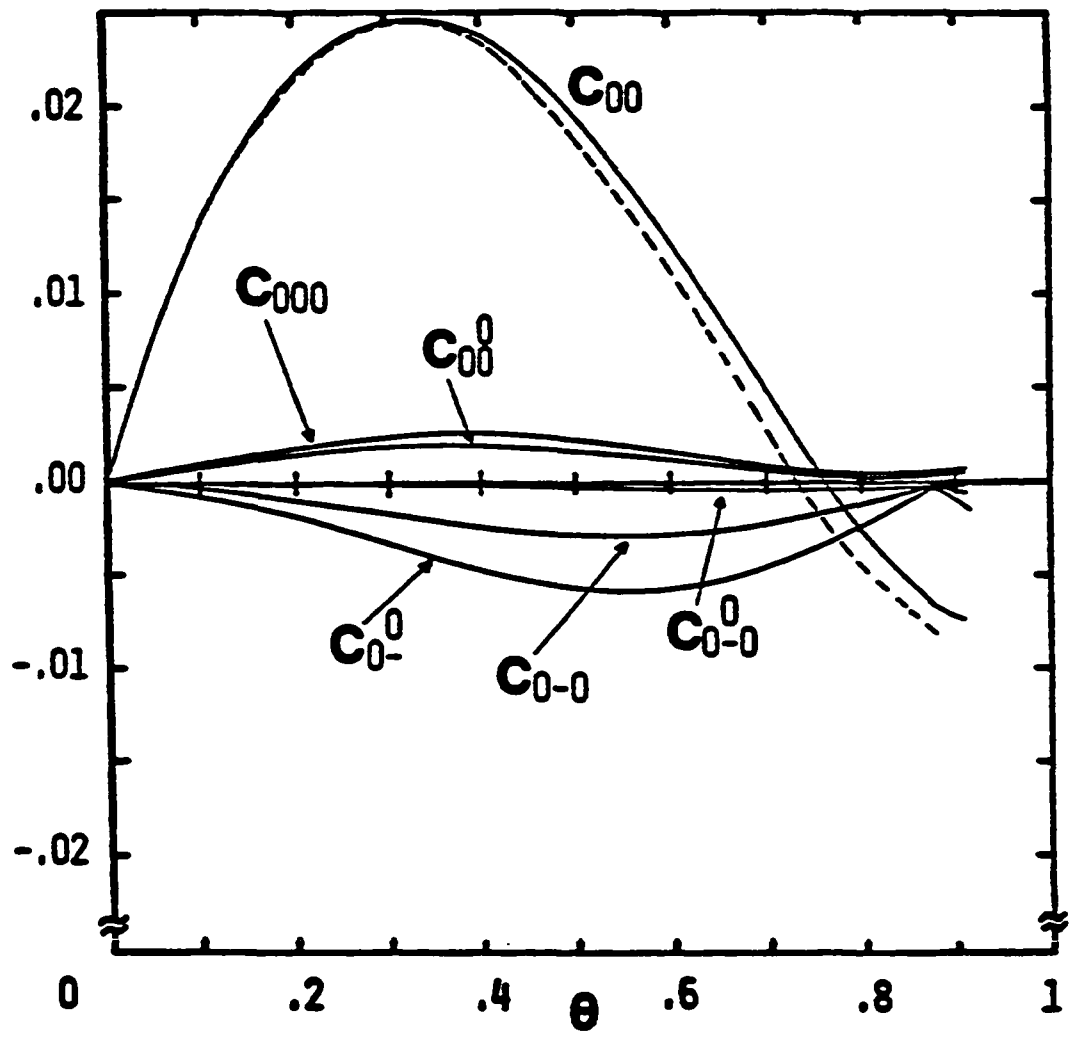

Figure 5: 2^{nd}-shell truncation values for the correlations $C_{oo} = P_{oo} - (P_o)^2$ (the dotted line gives 1^{st}-shell), $C_{o\bar{o}} = P_{o\bar{o}} - (P_o)^2$, $C_{o-o} = P_{o-o} - (P_o)^2$, $C_{ooo} = P_{ooo} - 2P_{oo}P_o - P_{o-o}P_o + 2P_o^3$, $C_{oo\bar{o}} = P_{oo\bar{o}} - \cdots$, $C_{o\bar{o}o} = P_{o\bar{o}o} - \cdots$

(Here, one should think of a dimer landing on the empty pairs shown on the r.h.s. to create the configuration on the l.h.s.). We now divide (2.16a) into the rest of (2.16) to obtain $d/d\theta\ P_{\cdots}$ [$= (d/dt\ P_{\cdots})/(d/dt\ P_a)$] equations which, after formally expanding denominators, have the form

$$d/d\theta\ P_{aa} = 1/6\ \{1 + 10\ P_a - 10\ P_{aa} - 2\ P_{a\text{-}a} - 8\ P_{a\underline{a}} + 2\ P_{aaa} + 8\ P_{\underline{a}aa}$$

$$+ (8\ P_a - 9\ P_{aa})(2\ P_a - P_{aa}) + \cdots\ \} \qquad (2.17a)$$

$$d/d\theta\ P_{aaa} = 1/6\ \{2\ P_a + 8\ P_{aa} + \cdots\ \} \qquad (2.17b)$$

$$\vdots$$

Next we postulate a Taylor expansion form $\sum_{p=0}^{\infty} B_p \theta^{n^*+p}$, with respect to the coverage (density) θ, for the solutions P_{aa}, P_{aaa}, $\cdots$ of (2.17), where B_p depend on the (filled) subconfiguration in question and n^* naturally equals the minimum number of dimers required to cover that configuration[12]. The coefficients B_p in these expansions are simply determined recursively after substitution into the $d/d\theta$ equations (2.17) and equating terms of equal power in θ. In particular, from (2.17a), it is immediate that $P_{aa} = 1/6\ \theta + \cdots$. More generally, this procedure yields

$$P_{aa} = \frac{1}{6}\theta + \frac{25}{36}\theta^2 + \frac{29}{324}\theta^3 + \frac{5}{216}\theta^4 + \cdots$$

$$P_{a\text{-}a} = \frac{35}{36}\theta^2 + \frac{5}{162}\theta^3 + \cdots, \quad P_{\underset{a}{a}} = \frac{17}{18}\theta^2 + \frac{5}{81}\theta^3 + \cdots$$

$$P_{aaa} = \frac{5}{18}\theta^2 + \frac{40}{81}\theta^3 + \cdots, \quad P_{\underset{aa}{a}} = \frac{5}{18}\theta^2 + \frac{39}{81}\theta^3 + \cdots$$

$$P_{aaaa},\ P_{\underset{aaa}{a}},\ P_{\underset{aa}{aa}} = \frac{1}{36}\theta^2 + \cdots,\ P_{\underset{aa}{\underset{a}{a}}} = \frac{1}{18}\theta^2 + \cdots$$

$$\vdots \qquad (2.18)$$

One can directly estimate (albeit rather poorly), the saturation coverage from the above expansion for P_{aa} by simply determining the appropriate root of $P_{oo}(\theta) = 1 - 2\theta + P_{aa}(\theta) = 0$. However a more sophisticated approach is now presented.

The 1^{st}-shell approximation for $Q_{o\phi}$ obtained from (2.12) after setting c=6 and $P_o \equiv 1-\theta$, suggests that we seek an expansion for $Q_{o\phi}$ in the form

$$Q_{o\phi} = (1 - \alpha) + \alpha(1 - \theta)^{2/3} + \beta\,\theta^2 + \gamma\,\theta^3 + \delta\,\theta^4 + \cdots \qquad (2.19)$$

which displays explicitly nonanalyticity outside the physical range of θ. The coefficients $\alpha, \beta, \cdots$ are obtained by expanding $P_{oo} \equiv (1 - \theta)\, Q_{o\phi}(\theta)$ as a power series in θ and matching coefficients with the expansion for $1 - 2\theta + P_{aa}(\theta)$ obtained from (2.18). This yields

$\alpha = 5/4$ recovering the 1^{st}-shell approximation,

$$\beta = 0,\ \gamma = 1/81 \text{ ("almost" canceling)},\ \delta = 19/1944,\ \cdots \qquad (2.20)$$

Values of P_0^s and θ^s associated with the partial sums of (2.19,20) are given in Table II along with their values from the truncation techniques.

The agreement of α with the 1^{st}-shell truncation value and the vanishing of β can be understood as follows. We first emphasize that the n^{th} coefficient in (2-19) is determined from the 1^{st}, 2^{nd}, $\cdots$ and n^{th} coefficients in the density expansion of P_{aa}. Second, we observe that using the corresponding expansion for P_{aa} for random dimer filling on a Bethe lattice with coordination number 6, one obtains $\alpha = 5/4$ and all remaining coefficients equal to zero (since the 1^{st}-shell approximation <u>is</u> the exact Bethe lattice solution[16]). Finally, we note that in determining the first two coefficients of P_{aa} in (2.18), we do not "see" that the lattice has closed loops since the small subconfigurations entering at this stage involve no closed loops and could equally well be associated with a Bethe lattice of coordination number c=6 as with a cubic lattice. Consequently, these coefficients have the Bethe lattice values.

Table II: Random Dimer Filling of a Cubic Lattice: Estimates of the saturation fraction of isolated empty sites P_0^S (and hence coverage $\theta^S = 1 - P_0^S$) from resummed density expansion and truncation techniques (cf. $P_0^S \approx .138$ in Ref. (2))

m^{th} partial sum	1 & 2 (1^{st}-shell)	3	4	2^{nd}-shell
P_0^S (θ^S)	.08944 (.91056)	.08441 (.91559)	.08070 (.91930)	.08454 (.91546)

III. DIMER FILLING OF LATTICES WITH A STOCHASTICALLY SPECIFIED DISTRIBUTION OF INACTIVE SITES (RECOMBINATION IN THE PRESENCE OF INERT DILUTENTS)

Consider now the random dimer filling of a lattice with a time-independent (stochastically specified) distribution of inactive sites on which a dimer cannot land. Thus we start with a suitable (time-independent) ensemble of inhomogeneous lattices including inactive sites and with each member of this associate an appropriate ensemble of irreversible fillings. All probabilities discussed below are implicitly evaluated with respect to this combined ensemble.

The site-type distribution can be specified by a set of time-independent, probabilities $\beta_{\{m\}}$ that all sites in the set $\{m\}$ are active. It is convenient to define the conditional probabilities $\gamma_{j,\{m\}} = \beta_{j+\{m\}}/\beta_{\{m\}}$ for site j to be active given that sites in $\{m\}$ are active. Typically $\gamma_{j,\{m\}}$ will be independent of sites in $\{m\}$ further than a certain distance from j, and for a random distribution, trivially $\gamma_{j,\{m\}} = \beta_j \equiv \beta$ for all j and $\{m\}$. These quantities together with the adsorption rate, κ, constitute the input to the hierarchial rate equations for this process. Exactly this type of formulation appears in the theoretical treatment of the kinetics of reactions involving binding to copolymers (i.e., 1D lattices) with (time-independent) stochastically specified site-type distributions[17].

Typically one assumes translation invariance of the site-type distribution. Then if $P_d \equiv \alpha$, say, denotes the probability that a site is

inactive (defective), P_0 that a site is active and empty, and P_a that a (necessarily active) site is filled, then clearly $P_d + P_0 + P_a = 1$. It is natural to ask what effect the inactive sites have on the final fraction of active and empty sites P_0^S. Clearly as α increases the fraction of active sites, $P_0 + P_a \equiv 1 - \alpha \equiv \beta$ decreases (to zero when $\alpha = 1$). However, increasing α also means there are more sites adjacent to inactive sites which we expect are less likely to fill (there are fewer ways a dimer can land covering these). Consequently the net effect is unclear (except for α near 1) and is analyzed below.

A. General Theory

The probabilities, $P_{\{m\}}$, for finding the sites in $\{m\}$ empty and active are naturally decomposed, here, as $P_{\{m\}} \equiv \beta_{\{m\}} f_{\{m\}}$ where, by definition, the quantities $f_{\{m\}}$ are (conditional) probabilities for finding sites in $\{m\}$ empty given they are active. Clearly the $P_{\{m\}}$ (still) satisfy (2.1), but here it is more convenient to deal directly with the infinite closed hierarchy for the $f_{\{m\}}$. These equations can be obtained by dividing (2.1) by $\beta_{\{m\}}$ or written down intuitively, and have the form

$$\kappa^{-1} \, d/dt \, f_{\{m\}} = - n_{\{m\}} f_{\{m\}} - \sum_{j \notin \{m\}} n_{j,\{m\}} \gamma_{j,\{m\}} f_{\{m\}+j} \quad . \qquad (3.1)$$

Note that $\gamma_{j,\{m\}} f_{\{m\}+j}$ gives the probability that the sites $\{m\}$, given active, are empty and that site j is active and empty (as is required for dimer filling). Of course, when $\beta = \beta_{\{m\}} = 1$ (no inactive sites), $f_{\{m\}} \equiv P_{\{m\}}$ and (3.1) automatically reduces to (2.1). For an alternative

perspective, consider random dimer filling of an initially partially (monomer) filled infinite, uniform lattice. Let $\beta_{\{m\}}$ now describe the stochastically specified distribution of initially empty sites, i.e., $P_{\{m\}} = \beta_{\{m\}}$ at t=0, where $P_{\{m\}}$, here, gives the probability that {m} is empty. Clearly (2.1) applies (being independent of initial conditions), and their solution here also solves the dimer filling problem on a "corresponding" defective lattice.

Equations (3.1) are extremely general not assuming any invariance of the defective site distribution ($\beta_{\{m\}}$) or site occupancy distribution ($f_{\{m\}}$). However, henceforth, we assume that $\beta_{\{m\}}$, and hence $f_{\{m\}}$ (for an initially empty lattice), are invariant under all space group operations on the lattice (so again we can regard {m} as representing and infinite class of subconfiguations of sites equivalent to {m} after translation). Furthermore, we assume that $\gamma_{j,\{m\}}$ depends only on the number of sites in {m} adjacent to j, so then one can write $\gamma_{j,\{m\}} \equiv \gamma_{n_{j,\{m\}}}$. Thus, for example, for a 1D lattice, if f_m denotes the probability that an m-tuple of active sites is empty, then (3.1) includes the infinite subhierarchy

$$\kappa^{-1} \, d/dt \, f_m = - (m-1) f_m - 2\gamma_1 f_{m+1} \quad , \quad m \geq 1 \quad , \tag{3.2}$$

where γ_1 denotes the conditional probability that a site is active given that its left (right) n.n. is active (and having no knowledge of the type of its right (left) n.n.).

The spectral analysis of (3.1) as a linear system is analogous to that of (2.1) (the spectrum is identical). Hierarchial truncation and

formal density expansion (with subsequent resummation) techniques again can be used to analyze various forms of these equations. Exact 1D truncation results as well as the corresponding 1^{st}-shell truncation approximation for a lattice of coordination number c are described below. Both truncation and density expansion methods are implemented in the next subsection to treat the cubic lattice case.

For a 1D lattice, defining $q_m = f_{m+1}/f_m$, one simply obtains from (3.2) the equations

$$\kappa^{-1} \, d/dt \, \ell n \, q_m = -1 - 2\gamma_1 (q_{m+1} - q_m) \quad , \quad m > 1 \tag{3.3}$$

which obviously have the solution $q_m = e^{-\kappa t}$, $m > 1$, noting that $q_m = 1$ at $t = 0$. Using this result to straightforwardly truncate (3.2) yields

$$f_0(t) \equiv f_1(t) = \exp\left[2\gamma_1 (e^{-\kappa t} - 1)\right] \quad , \tag{3.4}$$

thus predicting a saturation value of $f_0^s = e^{-2\gamma_1}$ (and $p_0^s = \beta f_0^s$). The latter result is well known from theoretical statistical analyses of intrasequence cyclization on stochastic binary copolymers whose site-type distribution satisfies 1^{st}-order Markov statistics[4,7,18].

Returning to the case of a general lattice with coordination number $c > 2$, it is straightforward to write equations for the quantities $q_{j,\{m\}} = f_{\{m\}+j}/f_{\{m\}}$ (note that these q's are ratios of, but <u>not</u> themselves,

conditional probabilities). The shielding condition of empty sites, as stated in Section II, applies directly to these f or q quantities. The n^{th}-shell truncation approximations can be implemented on the q equations in the same way as for the Q equations. For example, for a lattice with coordination number c and no closed loops of length three, the 1^{st}-shell equations are

$$\begin{aligned} -\kappa^{-1}\, d/dt\, \ell n\, f_0 &= c\, \gamma_1\, q_{0\phi} \\ -\kappa^{-1}\, d/dt\, \ell n\, q_{0\phi} &= 1 + (c-2)\, \gamma_1\, q_{0\phi} \end{aligned} \tag{3.5}$$

where γ_1 is the conditional probability that a site is active given that one of its n.n. is active (and not having any information about the type of the remaining c-1 n.n.). For c>2 and an initially empty lattice these have the solution

$$q_{0\phi} = \frac{1}{(c-2)\gamma_1}\left[\{1 + (c-2)\,\gamma_1\}\, f_0^{\frac{c-2}{c}} - 1\right] , \tag{3.6}$$

so, consequently, the saturation values of f_0 and P_0 are given by

$$P_0^s = \beta\, f_0^s \text{ and } f_0^s = \left(\frac{1}{1+(c-2)\gamma_1}\right)^{\frac{c}{c-2}} \sim 1 - c\,\gamma_1 + O(\gamma_1^2) \text{ as } \gamma_1 \to 0 \quad . \tag{3.7}$$

Note that these results are again exact for the corresponding Bethe lattice

problem. The effect of the introduction of defects on P_0^S is evident in the 1^{st}-shell identity

$$d/d\alpha\ P_0^S|_{\alpha=0} = (P_0^S|_{\alpha=0})/(c-1) \quad , \tag{3.8}$$

which follows from (3.7) assuming that $\gamma_1(\alpha) = \beta + 0(\alpha^2)$ as $\alpha \to 0$. Thus P_0^S initially increases as the inactive site concentration increases from zero. One can further show that, for a random distribution of defects (so $\gamma_1 = \beta$), this 1^{st}-shell estimate of P_0^S attains its maximum when $\alpha = 1/2$.

B. The Cubic Lattice

In this subsection, we restrict our attention to a lattice with a random distribution of inactive sites of concentration $\alpha \equiv 1-\beta$. In the 1^{st}-shell truncation approximation, we obtain

$$P_0^S = \frac{1-\alpha}{(5-4\alpha)^{3/2}} \text{ and } d/d\alpha\ P_0^S|_{\alpha=0} = \frac{1}{25\sqrt{5}} \approx .0179 \quad . \tag{3.9}$$

The minimal closed set of equations in the 2^{nd}-shell approximation contains 14 q's for the same configurations as shown in Table I. Other q's may be added. In Fig. 6 we have plotted 1^{st}- and 2^{nd}-shell estimates of P_0^S as a function of α. Numerical results for the 2^{nd}-shell also indicate that P_0^S has its maximum at $\alpha = 1/2$.

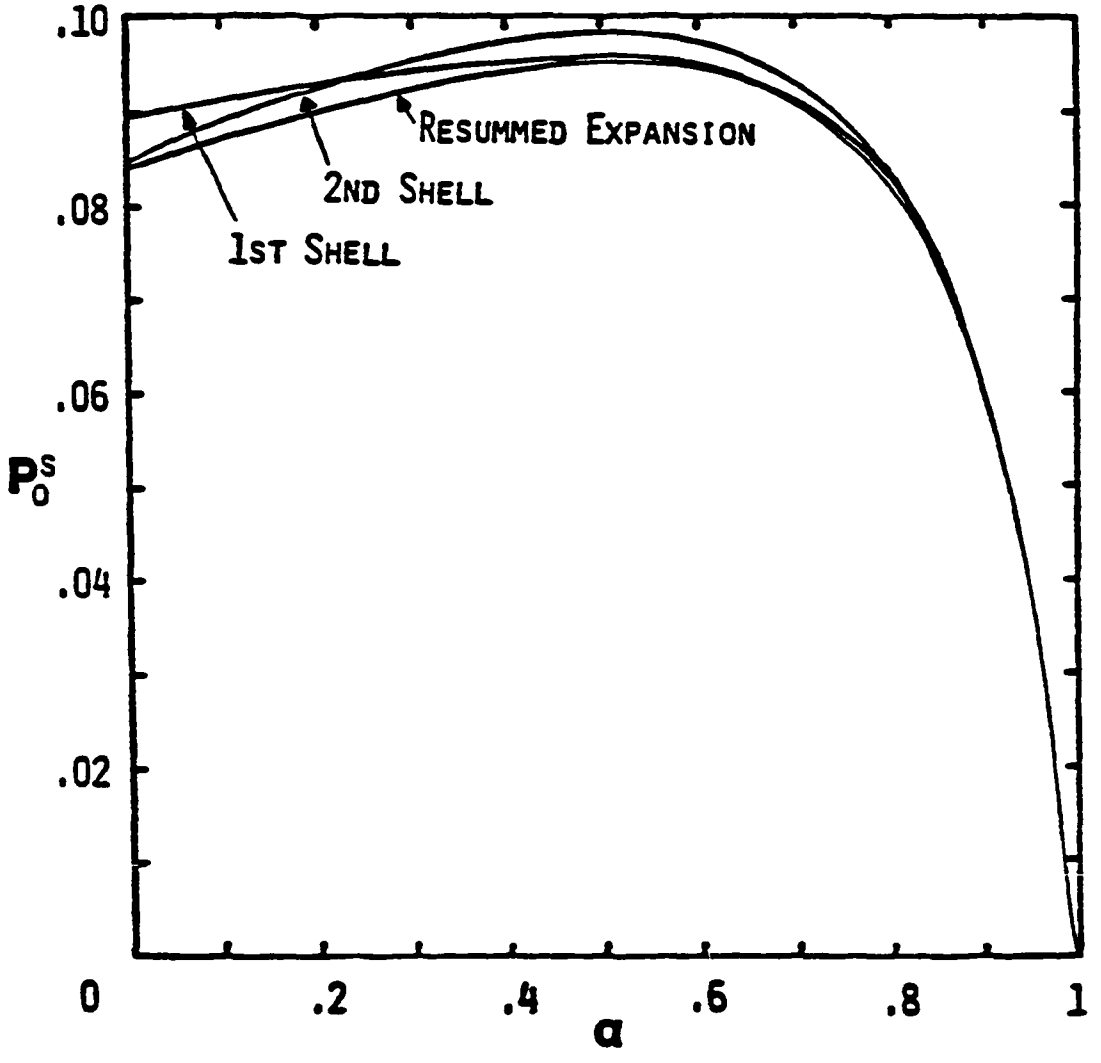

Figure 6: Estimates of the fraction of empty active sites at saturation for random dimer filling on a cubic lattice with a random distribution of nonadsorptive sites of concentration α

Density expansions of solutions are obtained by a procedure analogous to Section II. We start with the equations for probabilities, f, of configurations of sites, given to be active, which are in either an unspecified state 'x' or filled 'a'. For example, exploiting various lattices symmetries, and converting empty to unspecified/filled configurations using the relevant, more complicated form of conservation of probability yields

$$\kappa^{-1}\, d/dt\, f_a = 6\beta\, f_{oo} = 6\beta\,(1 - 2 f_{xa} + f_{aa}) \tag{3.10a}$$

$$\begin{aligned}\kappa^{-1}\, d/dt\, f_{xa} &= f_{oo} + \beta\, f_{xoo} + 4\beta\, f_{x\overset{o}{o}} \\ &= 1 - 2 f_{xa} + f_{aa} \\ &\quad + \beta\,(5 - f_{xax} - f_{xxa} - 4 f_{x\overset{x}{a}} - 4 f_{x\overset{a}{x}} + f_{xaa} + f_{x\overset{a}{a}})\end{aligned} \tag{3.10b}$$

$$\begin{aligned}\kappa^{-1}\, d/dt\, f_{aa} &= f_{oo} + 2\beta\, f_{ooa} + 8\beta\, f_{\overset{o}{o}a} \\ &= 1 - 2 f_{xa} + f_{aa} \\ &\quad + 2\beta\,(f_{xxa} - f_{xaa} - f_{axa} + f_{aaa} \\ &\qquad + 4 f_{\overset{x}{x}a} - 4 f_{\overset{x}{a}a} - 4 f_{\overset{a}{x}a} + f_{\overset{a}{a}a}) \\ &\quad \vdots\end{aligned} \tag{3.10c}$$

Of course $f_{xa} \neq f_a \equiv P_a/\beta \equiv \theta/\beta$ since knowledge that a site is active influences the probability that an adjacent (active) site is filled. Furthermore, from (3.10), we see that there is no simple relation between these two f's.

To obtain density expansions, one again first divides (3.10a) into the rest of (3.10) to obtain d/df_a equations and formally expand denominators. We postulate a Taylor expansion form for solutions where the lead power is the minimum number of dimers required to cover the filled sites in the corresponding configuration. Coefficients in these expansions are determined recursively after substitution into the d/df_a equations and matching terms of equal power in f_a. Note that determination of, say, the m^{th} coefficient of f_{aa} involves many more configurations than the corresponding calculation for P_{aa} in Section II. However, straightforward calculation yields

$$f_{aa} = \frac{1}{6\beta} f_a + \frac{25}{36} f_a^2 + \frac{1}{648}\left(87 - \frac{29}{\beta}\right) f_a^3 + \cdots$$

$$f_{xa} = \left(\frac{5}{6} + \frac{1}{6\beta}\right) f_a + \frac{5}{72}\left(1 - \frac{1}{\beta}\right) f_a^2 + \frac{35}{1296}\left(1 - \frac{1}{\beta}\right) f_a^3 + \cdots$$

$$f_{xxa} = \left(\frac{5}{6} + \frac{1}{6\beta}\right) f_a + \frac{1}{12\beta}\left(\frac{5}{6}\beta - \frac{2}{3} - \frac{1}{6\beta}\right) f_a^2 + \cdots$$

$$f_{x\bar{x}a} = \left(\frac{5}{6} + \frac{1}{6\beta}\right) f_a + \frac{1}{12\beta}\left(\beta - \frac{5}{6} - \frac{1}{6\beta}\right) f_a^2 + \cdots$$

$$f_{xax} = \left(\frac{2}{3} + \frac{1}{3\beta}\right) f_a + \frac{1}{12\beta}\left(\frac{2}{3}\beta - \frac{1}{3} - \frac{1}{3\beta}\right) f_a^2 + \cdots$$

$$f_{x\bar{x}a} = \left(\frac{2}{3} + \frac{1}{3\beta}\right) f_a + \frac{1}{6\beta}\left(\frac{2}{3}\beta - \frac{1}{2} - \frac{1}{6\beta}\right) f_a^2 + \cdots$$

$$f_{xaa},\ f_{\substack{x\\aa}} = \frac{1}{6\beta} f_a + \frac{1}{12\beta}\left(\frac{20}{3}\beta + \frac{11}{6} - \frac{1}{6\beta}\right) f_a^2 + \cdots$$

$$\vdots \qquad (3.11)$$

One can readily check agreement of (3.11) with (2.13) for $\beta=1$.

Resummation is again motivated by the 1^{st}-shell approximation, specifically (3.6) after setting $c=6$ and $f_0 = 1-f_a$, which suggests looking for $q_{0\phi}$ in the form

$$q_{0\phi} = (1 - \rho) + \rho\ (1 - f_a)^{2/3} + \zeta\ f_a^2 + \eta\ f_a^3 + \cdots \quad . \qquad (3.12)$$

Here $\rho, \zeta, \eta, \cdots$ are obtained by expanding $f_{00} \equiv (1 - f_a)\ q_{0\phi}$ as a power series in f_a and matching coefficients with the expansion for $1 - 2\ f_{xa} + f_{aa}$ obtained from (3.11). This yields

$$\rho = \frac{1+4\beta}{4\beta} \text{ recovering the } 1^{st}\text{-shell approximation,}$$

$$\zeta = 0, \quad \eta = \frac{1}{162}\left(3 - \frac{1}{\beta}\right) \text{ ("almost" canceling), } \cdots \quad . \qquad (3.13)$$

The agreement of ρ with the 1^{st}-shell value and the vanishing of ζ can be understood from Bethe lattice arguments indentical to those given in Section II. The value of f_0^s obtained from (3.12) by neglecting higher coefficients and setting $q_{0\phi} = 0$ satisfies

$$(f_0^s)^{2/3} = \frac{1}{1+4\beta}\left[1 - \frac{2}{81}(3\beta - 1)(1 - f_0^s)^3\right] \quad . \qquad (3.14)$$

The corresponding $P_0^s = \beta\ f_0^s$ is plotted in Fig. 6.

IV. DISCUSSION

The techniques used here appear to have produced a reliable description of the kinetics of random dimer filling of the 3D cubic lattice, at least for the probabilities of smaller configurations. In particular, fairly consistent values were obtained for the final fraction of empty sites, certainly improving on the previous estimates. Determination of, e.g., large separation spatial correlations is more difficult requiring an extended set of equations and a more refined truncation procedure. To our knowledge these calculations constitute the first explicit treatment of a nontrivial irreversible process on a 3D lattice exploiting the structure of the corresponding exact hierarchial rate equations. Finally we note that the techniques used here are quite general although, typically, application to other processes will be more complex.

ACKNOWLEDGEMENTS

Ames Laboratory is operated for the U.S. Department of Energy by Iowa State University under Contract No. W-7405-ENG-82. This work was supported by the Office of Basic Energy Sciences.

APPENDIX

The shielding property of separating walls of empty sites of thickness one is incorporated in a rather subtle way in the hierarchy. Rigorous proof must be based on the observation of self-consistency with the infinite Q hierarchy and requires development of an appropriately general (and complicated) notation for subconfigurations. Thus here, instead, we illustrate with some examples, the structural feature of these equations which leads to shielding. We consider only the 2D square lattice (for notational simplicity) concentrating on the identities $Q_{\circ\bullet\bullet\bullet\bullet\bullet\bullet\bullet\bullet\bullet\bullet} \equiv Q_{\circ\bullet\bullet\bullet\bullet\bullet\bullet\bullet\bullet\bullet}$ and

$Q_{\bullet\bullet\bullet\bullet\circ\bullet\bullet\bullet\bullet\bullet\bullet} \equiv Q_{\bullet\bullet\bullet\bullet\circ\bullet\bullet\bullet\bullet\bullet\bullet}$.

From (2.7) one obtains

$$-\kappa^{-1}\, d/dt\, \ell n\, Q_{\circ\bullet\bullet\bullet\bullet\bullet\bullet\bullet\bullet\bullet\bullet} = 1 + \sum_{ext.j} Q_{j,\bullet\bullet\bullet\bullet\bullet\bullet\bullet\bullet\bullet\bullet} - \sum_{ext.j} Q_{j,\bullet\bullet\bullet\bullet\bullet\bullet\bullet\bullet\bullet\bullet}$$

$$+ 3(Q_{\bullet\bullet\bullet\bullet\circ\bullet\bullet\bullet\bullet\bullet\bullet} - Q_{\bullet\bullet\bullet\bullet\bullet\bullet\bullet\bullet\bullet\bullet}) + 3(Q_{\bullet\bullet\bullet\bullet\circ\bullet\bullet\bullet\bullet\bullet\bullet} - Q_{\bullet\bullet\bullet\bullet\bullet\bullet\bullet\bullet\bullet\bullet})$$

$$-\kappa^{-1}\, d/dt\, \ell n\, Q_{\circ\bullet\bullet\bullet\bullet\bullet\bullet\bullet\bullet\bullet} = 1 + \sum_{ext.j} Q_{j,\bullet\bullet\bullet\bullet\bullet\bullet\bullet\bullet\bullet} - \sum_{ext.j} Q_{j,\bullet\bullet\bullet\bullet\bullet\bullet\bullet\bullet\bullet}$$

$$+ 3(Q_{\bullet\bullet\bullet\bullet\circ\bullet\bullet\bullet\bullet\bullet\bullet} - Q_{\bullet\bullet\bullet\bullet\bullet\bullet\bullet\bullet\bullet\bullet}) + 2(Q_{\bullet\bullet\bullet\bullet\circ\bullet\bullet\bullet\bullet\bullet\bullet} - Q_{\bullet\bullet\bullet\bullet\bullet\bullet\bullet\bullet\bullet\bullet})$$

$$+ 3(Q_{\bullet\bullet\bullet\bullet\bullet\bullet\bullet\bullet\circ\bullet} - Q_{\bullet\bullet\bullet\bullet\bullet\bullet\bullet\bullet\bullet\bullet}) \quad , \qquad (1)$$

where $\sum_{\text{ext.}j}$ represents a sum over empty sites j on the exterior of and adjacent to the closed shielding wall. The shielding condition, and in particular the first identity, is compatible with (1) noting pairwise cancellation of the terms in parentheses. The grouping of terms here (according to whether the 'o' site is inside or outside the shielding wall), when implemented throughout the Q hierarchy, demonstrates clearly self-consistency with shielding.

For the second identity, one naturally considers the equations

$$-\kappa^{-1}\, d/dt\, \ell n\, Q_{\bullet\bullet\phi\phi\phi\phi\phi\bullet\bullet} = 1 + [Q_{\bullet\bullet\phi\phi\phi\phi\phi\bullet\bullet} - Q_{\bullet\bullet\phi\phi\phi\phi\phi\bullet\bullet}]$$

$$+ 2[2Q_{\bullet\bullet\phi\phi\phi\phi\phi\bullet\bullet} - Q_{\bullet\bullet\phi\phi\phi\phi\phi\bullet\bullet}]$$

$$+ 2[Q_{\bullet\bullet\phi\phi\phi\phi\phi\bullet\bullet} - Q_{\bullet\bullet\phi\phi\phi\phi\phi\bullet\bullet}]$$

$$+ \cdots$$

$$+ (Q_{\bullet\bullet\phi\phi\phi\phi\phi\bullet\bullet} - Q_{\bullet\bullet\phi\phi\phi\phi\phi\bullet\bullet})$$

$$+ 2(Q_{\bullet\bullet\phi\phi\phi\phi\phi\bullet\bullet} - Q_{\bullet\bullet\phi\phi\phi\phi\phi\bullet\bullet})$$

$$+ \cdots$$

$$-\kappa^{-1}\ d/dt\ \ell n\ Q_{\cdots\phi\phi\phi\phi\phi\cdots} = 1 + [Q_{\cdots\phi\phi\phi\phi\phi\cdots} - Q_{\cdots\phi\phi\phi\phi\phi\cdots}]$$

$$+ 2[2Q_{\cdots\phi\phi\phi\phi\phi\cdots} - Q_{\cdots\phi\phi\phi\phi\phi\cdots}]$$

$$+ \cdots$$

$$+ (Q_{\cdots\phi\phi\phi\phi\phi\cdots} - Q_{\cdots\phi\phi\phi\phi\phi\cdots})$$

$$+ 2(Q_{\cdots\phi\phi\phi\phi\phi\cdots} - Q_{\cdots\phi\phi\phi\phi\phi\cdots})$$

$$+ \cdots \qquad (2)$$

again consistent with the shielding condition noting cancellation of terms in the second sets of parentheses and correspondence of those in the first sets.

Several other more obvious identities can be proved. For example, after applying shielding to the $Q_{\phi\phi\phi}$ equation, one obtains

$$-\kappa^{-1}\ d/dt\ \ell n\ Q_{\phi\phi\phi} = 4(1 - Q_{\phi\phi\phi}) \ , \qquad (3)$$

consistent with the physically obvious constraint (for any dimer filling process) that $Q_{\phi\phi\phi} \equiv 1$. More generally, for any closed, (empty) shielding

wall, one can always obtain a closed set of equations for various Q's with the conditioned 'o' site and conditioning 'ϕ' sites all inside this wall.

REFERENCES

1. A. M. Bass and H. P. Broida, Phys. Rev. 101, 1740 (1956).
2. J. L. Jackson and E. W. Montroll, J. Chem. Phys. 28, 1101 (1958); P. L. Chessin, J. Chem. Phys. 31, 159 (1959); S. Golden, J. Chem. Phys. 29, 61 (1958).
3. P. J. Flory, J. Am. Chem. Soc. 61, 1518 (1939).
4. E. R. Cohen and H. Reiss, J. Chem. Phys. 38, 680 (1963).
5. T. H. K. Barron and E. A. Boucher, Trans. Faraday Soc. 65, 3301 (1969).
6. R. B. McQuistan and D. Lichtman, J. Math. Phys. 9, 1680 (1968); T. H. K. Barron, R. J. Bawden and E. A. Boucher, J. Chem. Soc. 70, 651 (1974).
7. E. A Boucher, Prog. Polym. Sci. 6, 63 (1978).
8. P. D. Dawson and Y. K. Peng, Surf. Sci. 33, 565 (1972); W. D. Dong, Surf. Sci. 42, 609 (1974); D. R. Rossington and R. Borst, Surf. Sci. 3, 202 (1965); J. B. Peri, J. Chem. Phys. 69, 220 (1965).
9. R. B. McQuistan, D. Lichtman and L. P. Levine, Surf. Sci. 20, 401 (1970).
10. K. J. Vette, T. W. Orent, D. K. Hoffman and R. S. Hansen, J. Chem. Phys. 60, 4854 (1974).
11. D. K. Hoffman, J. Chem. Phys. 65, 95 (1976); D. Knodel and D. K. Hoffman, J. Chem. Phys. 69, 3438 (1978).
12. J. W. Evans, Physica A 123, 297 (1984).
13. R. S. Nord and J. W. Evans, J. Chem. Phys. 82, 2795 (1985).

14. A. Silberberg and R. Simha, Biopolymers 6, 479 (1968); Macromol. 5, 332 (1972); R. H. Lacombe and R. Simha, J. Chem. Phys. 61, 1899 (1974); A. Surda and I. Karasova, Surf. Sci. 109, 605 (1981); J. Luque and A. Cordoba, J. Chem. Phys. 76, 6393 (1982).

15. J. W. Evans, D. R. Burgess and D. K. Hoffman, J. Chem. Phys. 79, 5011 (1983).

16. J. W. Evans, J. Math. Phys. 25, 2527 (1984).

17. J. J. Gonzalez and P. C. Hemmer, Polymer Lett. Ed. 14, 645 (1976), J. Chem. Phys. 67, 2496 and 2509 (1977).

18. E. Merz, T. Alfrey and G. Goldfinger, J. Polym. Sci. 1, 75 (1946); H. J. Harwood, in "Reactions on Polymers", Ed. J. A. Moore, Nato Adv. Study Inst. Series (D. Reidel, Dordrecht, 1973).

PAPER IV:

CLUSTER-SIZE DISTRIBUTIONS FOR IRREVERSIBLE COOPERATIVE FILLING OF LATTICES I: EXACT ONE-DIMENSIONAL RESULTS FOR COALESCING CLUSTERS

CLUSTER-SIZE DISTRIBUTIONS FOR IRREVERSIBLE COOPERATIVE FILLING OF LATTICES I: EXACT ONE-DIMENSIONAL RESULTS FOR COALESCING CLUSTERS

R. S. Nord, D. K. Hoffman, and J. W. Evans

Ames Laboratory and Department of Chemistry
Iowa State University
Ames, Iowa 50011

ABSTRACT

We consider processes where the sites of an infinite, uniform lattice are filled irreversibly and cooperatively, with the rate of adsorption at a site depending on the state of its nearest neighbors (only). The asymmetry between empty and filled sites, associated with irreversibility, leads one to consider the closed infinite coupled hierarchies of rate equations for probabilities of connected, and singly-, doubly-, ••• disconnected empty subconfigurations, and results in an empty site shielding property. The latter allows <u>exact</u> solution, via truncation, of these equations in 1D, and is used here to determine probabilities of filled s-tuples, f_s ($f_1 \equiv \theta$ is the coverage), and thus of clusters of exactly s filled sites, $n_s \equiv f_s - 2f_{s+1} + f_{s+2}$, for $s \leq 13$ and 11 respectively. When all rates are nonzero so that clusters can coalesce, the f_s and n_s distributions decay exponentially as $s \to \infty$, and we can accurately estimate the asymptotic decay rate $\lambda(\theta) \equiv \lim_{s\to\infty} f_{s+1}/f_s \equiv \lim_{s\to\infty} n_{s+1}/n_s$, where $0 = \lambda(0) < \lambda(\theta) < \lambda(1) = 1$. Divergent behavior of the average cluster size, as $\theta \to 1$, is also considered. In addition, we develop a novel technique to <u>directly</u> determine the asymptotic decay rate, $\lambda(\theta)$, and indicate its extension to higher-dimensional irreversible cooperative filling (and to other dynamic processes on lattices).

I. INTRODUCTION

Consider processes where "filling" events occur irreversibly and, in general, cooperatively at a lattice of localized sites[1]. These have numerous important applications to the description of: (polymer analogous) reaction of small molecules at the sites along a polymer chain, and related intramolecular (e.g., cyclization) reactions[2,3] (1D lattices); immobile chemisorption[4], and reaction between attached groups on surfaces[5] (2D lattices); localized reactions in crystalline solids[6] (3D lattices). In every case, the characteristics of the "filled" cluster-size distribution are of basic interest.

The special case where single sites fill randomly (having trivial local statistics) has been analyzed extensively within the context of the random site percolation problem[7]. For random dimer filling of nearest-neighbor (NN) sites on a 1D lattice (first analyzed by Flory[8] in the context of a polymer cyclization reaction), some information on the filled cluster-size distribution is available from combinatorial analyses and simulations[9]. Filling of single sites on a 1D lattice, with NN cooperative effects, is the prototypical model for cooperative polymer analogous reactions[2,3]. Characterization of the site-type statistics of the resulting copolymer is of primary importance, however only limited exact results have peen presented for the filled cluster-size distributions[3,10]. A clear indication of the need for application of 2D irreversible filling models to chemisorption comes from the observation that, in several systems, <u>small</u> islands of presumably immobile, adsorbed

species are formed (rather than one large island, as anticipated from entropic considerations alone)[11]. There is also direct evidence of negligible surface diffusion rates in these systems[4]. More generally, irreversible cooperative filling provides a very natural extension of percolation analysis from random to correlated distributions, and, in fact, often constitutes a physically more realistic model.

Henceforth we shall concentrate on a basic class of cooperative processes where the sites of a lattice fill, $o \to a$, irreversibly with adsorption rates, k_i, depending only on the number $i = 0, 1, \cdots, z$ of filled nearest neighbor (NN) sites (z is the lattice coordination number). The final (stationary) state is not in equilibrium (and nontrivial if the lattice cannot fill completely) since the irreversible, immobile filling incorporates no equilibration mechanism.

Several avenues of investigation are available here. Analysis of Markov processes corresponding to the time evolution of such "infinite-particle systems" is being actively pursued using the abstract machinery of mathematical probability theory[12-14]. Existence of the dynamics and fundamental characteristics of the process are considered here. One immediate result, expected intuitively, is that probabilities for filled subconfigurations in the above filling process should be bounded below and above (at each time, t) by the corresponding trivial quantities for <u>random</u> filling at rates $k_\ell = \min_i k_i$ and $k_u = \max_i k_i$, respectively. This result, and its rigorous verification via "coupling methods", was pointed out by Liggett[15]. To illustrate its usefulness, we note that the probability, $f_{\{s\}}$, of any set {s} of s filled sites satisfies $[1 - \exp(-t\, k_\ell)]^s < f_{\{s\}} <$

$[1 - \exp(-t\, k_u)]^s$, suggesting large s exponential decay of f_s. Liggett[15] also notes that for 1D filling where $k_0 \leq k_1 \leq k_2$, if f_s refers to s consecutive filled sites, then a theorem of Harris[16] implies that $f_{s+t} \geq f_s f_t$, so $\lambda \equiv \lim_{s\to\infty} (-\log f_s/s)$ exists, and is nonzero (when $t > 0$) if $k_0 > 0$.

We emphasize that these irreversible filling models incorporate a complicated competition between irreversible birth and growth of clusters (nucleation can occur at any time during the process). In the regime where $0 < k_0 \ll k_i$, $i \geq 1$, the nucleation centers are, on average, well separated. Thus for 2 or 3D, it is natural to analyze the structure of individual clusters. Mathematical probability theory has already provided some powerful techniques to demonstrate the existence of a large-size asymptotic shape for clusters in a class of stochastic (single) cluster growth models[17-19]. These techniques and behavior should apply to the filling processes studied here, and we note, in particular, that when the k_i, $i \geq 1$, are equal, these individual clusters have (asymptotically round) Eden structure[17]. This cluster structure should be contrasted with the fractal-like behavior seen in Witten-Sander[20], Meakin-Witten[21], ... growth models (based on diffusive hopping and sticking mechanisms). In analysis of competitive cluster birth and growth, e.g., of the cluster-size distribution, comparison should be made with cluster-cluster aggregation models[22] also based on hopping and sticking mechanisms.

Our goal, here, is the exact quantitative determination of the probabilities, f_s, of s-tuples of consecutive filled sites in the 1D filling problem for arbitrary rates, and a range of s up to the asymptotic regime. This will provide estimates of the asymptotic exponential decay

rate, λ. (More direct methods for determination of λ are also of interest). For this reason an alternative approach, exploiting certain special features of irreversible filling, is adopted. We describe these filling processes using a set of master equations with the rates, k_i, as input. Since we deal only with infinite, uniform lattices here, it is convenient to recast these as an infinite hierarchy of rate equations for subconfiguration probabilities. These can be written down intuitively and include loss terms, corresponding to filling of each empty site in the subconfiguration, and gain terms, corresponding to creation of the subconfiguration by filling of appropriate sites in subconfigurations with one less filled site. For each case, we must account for all allowed configurations of the influencing, neighboring sites and multiply by the appropriate rates[1]. Throughout f_σ will denote the probability of a subconfiguration of sites, σ, each specified either empty 'o' or filled 'a'. Here we assume that the lattice is initially empty, and note that time evolution via the hierarchial equations preserves invariance of subconfiguration probabilities under all lattice space group operations (including translation and reflection).

There are several special features of the hierarchy associated with irreversibility, and the corresponding asymmetry between empty and filled sites. A closed subhierarchy can be obtained for very general (e.g., reversible) dynamical processes on lattices for probabilities of empty subconfigurations (by conservation of probability). However, for irreversible filling, there is a "minimal closed" subhierarchy involving just connected empty subconfigurations. Probabilities for disconnected

empty subconfigurations couple to those with the same or shorter separation(s), and thus indirectly back to those for less disconnected and connected empty subconfigurations[1]. One can also show that walls of empty sites of thickness two, that separate the lattice into disconnected regions, shield sites on one side from the influence of those on the other[1]. For a 1D lattice, these observations lead to exact solution of the hierarchy (as described below). However, in higher dimensions, exact solution is only possible for random filling, $k_i = k$, for all i (trivially), and "almost random" filling, $k_i = k$, for $i < z$; $k_z \neq k$[23].

The 1D version of this process was first treated in the early 1960's, where it was recognized that the minimal closed hierarchy involves only f_{o_n}, probabilities for empty n-tuples, o_n[24]. Exact solution followed from the observation that $f_{o_n} \equiv f_{oo}\, q^{n-2}$, for $n \geq 2$, where $q \equiv e^{-k_0 t}$, which is, of course, a consequence of the shielding property of an adjacent pair of empty sites[10,25,26]. Platé et al.[10] were the first to describe the method of exact determination of more general quantities such as spatial correlations, probabilities $f_s \equiv f_{a_s}$ of filled s-tuples, a_s (i.e., "pair connectivities" in percolation language[27]), and filled cluster probabilities, $n_s \equiv f_{oa_so} \equiv f_s - 2f_{s+1} + f_{s+2}$ (i.e., $n_s \equiv \Delta^2 f_s$, where $\Delta m_s = m_{s+1} - m_s$). They determined n_s for s = 1, 2, 3 only (which provided no insight into asymptotic behavior), and compared values with simulations[3,10]. We have recently presented a detailed quantitative analysis of the behavior of spatial correlations including their large-separation asymptotic decay[28]. The observed superexponential asymptotic

decay is characteristic of a larger class of "infinite-particle systems"[14].

In Section II, we briefly review the hierarchial structure and solution for monomer filling with NN cooperative effects on an infinite, uniform 1D lattice. Comparison is made of the exact equations solved here with corresponding approximate Smoluchowski-type equations. Such equations, which ignore cluster-cluster correlations, are often used to model coagulation processes[29]. Exact results for filled s-tuple, f_s, and filled cluster, n_s, size distributions for $s \leq 13$ and 11, respectively, are presented in Section III (obtained from simultaneous integration of hundreds of exactly truncated coupled equations). We show tnat the average cluster size without site weighting can be obtained directly, but not the variance or average size with site weighting (for which results are also presented). In Section IV, we present a novel new approach for extracting directly from the (suitably recast) hierarchial equations, quantities of prime interest pertaining to the asymptotics of the cluster-size distribution (here, the asymptotic exponential decay rate). The extension of this powerful approach to higher-dimensional filling processes (and even to other models) is indicated. Some conclusions are drawn and extensions discussed in Section V. Specifically, we give some results for the more complicated 1D monomer filling process with NN blocking and 2^{nd}-NN cooperative effects (where domain boundaries occur, just as in many 2D chemisorption systems).

II. HIERARCHIAL STRUCTURE AND SOLUTION FOR MONOMER FILLING OF AN INFINITE UNIFORM 1D LATTICE WITH NN COOPERATIVE EFFECTS

As indicated in the Introduction, the procedure for exact solution of this model reflects the special structure of the hierarchy associated with irreversibility, and the corresponding asymmetry of empty and filled sites. Since only empty sites shield, our truncation procedure operates directly on the closed subhierarchies for connected, singly-disconnected, ••• empty subconfigurations. Such important quantities as the filled s-tuple probabilities, f_s, cannot be obtained directly, but must be reconstructed from empty subconfiguration probabilities. Except for $f_1 \equiv f_a \equiv 1 - f_o$ and $f_2 \equiv f_{aa} = 1 - 2f_o + f_{oo}$, disconnected empty subconfiguration probabilities are required. For example, using reflection symmetry, one has

$$f_{aaaaa} \equiv 1 - 5f_o + 4f_{oo} + 3f_{o-o} + 2f_{o--o} + f_{o---o} - 3f_{ooo} - 4f_{oo-o} - f_{o-o-o} - 2f_{oo--o} + 2f_{oooo} + 2f_{ooo-o} + f_{oo-oo} - f_{ooooo} \ .$$

Since the procedure for obtaining exact solutions via hierarchy truncation is described in detail in Refs. (3,10,28), we only outline the basic ideas here. Probabilities for empty n-tuples satisfy the minimal closed subhierarchy[1,18,19],

$$- d/dt\ f_o = k_0\ f_{ooo} + 2k_1\ f_{aoo} + k_2\ f_{aoa}$$
$$= k_2\ f_o + 2(k_1 - k_2)\ f_{oo} + (k_0 - 2k_1 + k_2)\ f_{ooo} \quad , \quad (2.1a)$$

$$- d/dt\ f_{o_n} = (n-2)\ k_0\ f_{o_n} + 2(k_0\ f_{o_{n+1}} + k_1\ f_{ao_n})$$
$$= \{(n-2)\ k_0 + 2k_1\}\ f_{o_n} + 2(k_0 - k_1)\ f_{o_{n+1}}, \text{ for } n>2. \quad (2.1b)$$

A closed set of equations can similarly be obtained for $f_{o_m \overset{j}{\text{---}} o_n}$, for various j, m, n (where $\overset{j}{\text{---}}$ denotes j separating sites of unspecified occupancy). These f's couple through their rate equations to f's for subconfigurations with additional empty sites adjacent to the empty clusters (i.e., to f's in this class with separations j and j-1 and thus, indirectly, to the f_{o_n}). More generally, multiply disconnected empty configurations couple to f's for subconfigurations with additional empty sites adjacent to these empty clusters (and thus, indirectly, back to less disconnected, and connected empty subconfigurations).

The shielding property of adjacent pairs of empty sites (used to solve these hierarchies) is best expressed mathematically in terms of the conditional probabilities $q_{\sigma\sigma'} \equiv f_{\sigma+\sigma'}/f_{\sigma'}$ of (conditioned) σ given (conditioning) σ'. Empty/ filled conditioning sites $\bar{o}/\bar{a}$ will be denoted by ϕ/α for typographic convenience. For example, if ϕ_n denotes an empty n-tuple of conditioning sites, then one has that $q_{o\phi_n \overset{j}{\text{---}} \phi_m \text{---}\cdots} \equiv q_{o\phi\phi}$, for $n \geq 2$; $j, m \cdots > 0$, and that $q_{o\phi\phi}$ ($\equiv q$, say) $\equiv e^{-k_0 t}$ which is compatible with (2.1b). Thus one obtains

$$f_{o_n} = q_{o\phi_{n-1}} f_{o_{n-1}} = \cdots = q^{n-2} f_{oo} \quad , \quad \text{for } n>2 \quad , \tag{2.2a}$$

$$f_{o_n \overset{j}{\text{---}} o_m} = q_{o\phi_{n-1} \overset{j}{\text{---}} \phi_m} f_{o_{n-1} \overset{j}{\text{---}} o_m}$$

$$= \cdots = q^{n-2} f_{oo \overset{j}{\text{---}} o_m} \quad , \text{ for } n>2 \quad , \tag{2.2b}$$

(further reduction is possible if $m > 2$) thus providing finite closed sets of equations for q, f_{oo}, f_o, $f_{oo\underline{\ j\ }oo}$, $f_{oo\underline{\ j\ }o}$, and $f_{o\underline{\ j\ }o}$[10,28]. Clearly shielding further implies that the probability of any disconnected empty subconfiguration can be written in terms of q, f_{oo}, and probabilities of the type $f_{\sigma\underline{\ \ell\ }o\underline{\ m\ }o\text{---}\cdots\text{---}o\underline{\ r\ }\sigma'}$, where σ, $\sigma' = o$ or oo[30]. All of these can be obtained by integrating a finite closed coupled set of equations[28].

In the next section we present exact results for f_s, with $s \leq 13$, and thus for n_s, with $s \leq 11$. These have been obtained from the simultaneous integration of hundreds of exactly truncated equations for connected and disconnected empty subconfiguration probabilities of the type described above.

It should be realized that for the filling processes considered here, one can immediately write down an exact rate equation for any subconfiguration probability (though our exact truncation procedure has naturally led to emphasis on empty subconfigurations above). For example, we have that

$$d/dt\ f_s = d/dt\ f_{a_s} = k_2 \sum_{\substack{i+j=s-1 \\ i,j>1}} f_{a_i o a_j} + 2(k_1\ f_{ooa_{s-1}} + k_2\ f_{aoa_{s-1}}) \quad , \text{ for } s>2 \quad , \tag{2.3}$$

$$d/dt\ n_s = d/dt\ f_{oa_s o} = 2k_1\ f_{ooa_{s-1}o} + k_2 \sum_{\substack{i+j=s-1 \\ i,j>1}} f_{oa_i o a_j o} - 2(k_1\ f_{ooa_s o} + k_2\ f_{aoa_s o}) \quad , \text{ for } s>2 \quad . \tag{2.4}$$

and note that the loss term in (2.4) can be rewritten using the identity

$$f_{aoa_s o} = f_{oaoa_s o} + f_{aaoa_s o} = f_{oaoa_s o} + f_{oaaoa_s o} + f_{aaaoa_s o}$$
$$= \cdots = \sum_{i=1}^{\infty} f_{oa_i oa_s o} \quad . \tag{2.5}$$

One naturally compares (2.4,5) with simpler Smoluchowski-type coagulation equations[29] which also have a gain term, corresponding to formation of a cluster of size s from coagulation of two smaller ones of size i and j where i+j=s (rather than s-1 as above), and a loss term, corresponding to destruction of a cluster of size s by coagulation with any other cluster. However, in the Smoluchowski equations, these terms appear as sums of products of appropriately sized cluster probabilities, in contrast to (2.4,5) where cluster-cluster correlations are clearly accounted for. Such correlations are, of course, incorporated in our exact solutions.

A closer correspondence with the coagulation equations is achieved if one makes the so-called B approximation[10,31] (assume independence of lengths of consecutive blocks of filled and empty sites), in which case $q_{\sigma\overline{a\cdots o}\sigma'}$ is replaced by $q_{\sigma\overline{a\cdots o}}$, and $q_{\sigma\overline{o\cdots a}\sigma'}$ by $q_{\sigma\overline{o\cdots a}}$. Then (2.4) becomes

$$d/dt\ n_s = \frac{2f_{aoa}}{(f_{oa})^2}\left[1/2\left(2k_1\ n_0\ n_{s-1} + k_2 \sum_{\substack{i+j=s-1 \\ i,j\geq 1}} n_i\ n_j\right)\right.$$
$$\left. - (k_1 n_0 + k_2 \sum_{i=1}^{\infty} n_i)\ n_s\right] \quad , \tag{2.6}$$

where we have defined $n_0 \equiv f_{oa}\, f_{ooa}/f_{aoa}$ and used (2.5) in writing the loss term. These approximate equations, with the replacement $\sum_{i=1}^{\infty} n_i \equiv f_{oa}$, have been shown to give reasonable results for $s = 1, 2, 3$[10].

III. DETAILED CHARACTERIZATION OF THE FILLED CLUSTER-SIZE DISTRUBUTION

In this section, we present detailed results for the filled s-tuple and cluster-size distributions for 1D monomer filling with NN cooperative effects. In Fig. 1, we have displayed f_{s+1}/f_s and n_{s+1}/n_s as functions of s (for various θ), for the choice of rates $k_0:k_1:k_2 = 1:\rho:\rho^2$, with $\rho = 6$, 2, 1/2, 1/6. The more extreme cases $\rho = 20$, 1/20 are shown in Fig. 2. Other choices of nonzero rates produce similar results. It is clear that, for each θ, f_{s+1}/f_s approaches a constant, $\lambda(\theta)$ say, as $s \to \infty$, where $\lambda(\theta)$ ranges between zero and unity. (In fact f_{s+1}/f_s is very nearly constant, as a function of s, for moderate cooperativity.) Results presented below show that $\lambda(\theta) \sim \rho\theta$, as $\theta \to 0$, and that $1-\lambda(\theta)$ is asymptotically proportional to $(1-\theta)$, as $\theta \to 1$. Since the $n_s \equiv \Delta^2 f_s$ are 2^{nd}-order finite differences of the f_s, it follows that also $n_{s+1}/n_s \to \lambda(\theta)$, as $s \to \infty$, but that n_{s+1}/n_s is more sensitive to low s deviations than f_{s+1}/f_s (particularly when θ, and thus $\lambda(\theta)$, is close to unity). Since, in both cases, the convergence to asymptotic behavior is quite rapid, we can give accurate quantitative estimates of f_s and n_s for a large range of s.

Noting that $f_{s+1}/f_s \equiv q_{a\alpha_s}$, where α_s denotes a filled s-tuple of conditioning sites, and suggestively denoting $\lambda(\theta)$ by $q_{a\alpha_\infty}$, one has

$$f_{s+1} = \lambda(\theta)^s \prod_{i=1}^{s} \left[1 + \frac{q_{a\alpha_i} - q_{a\alpha_\infty}}{q_{a\alpha_\infty}}\right] \cdot \theta \quad . \tag{3.1}$$

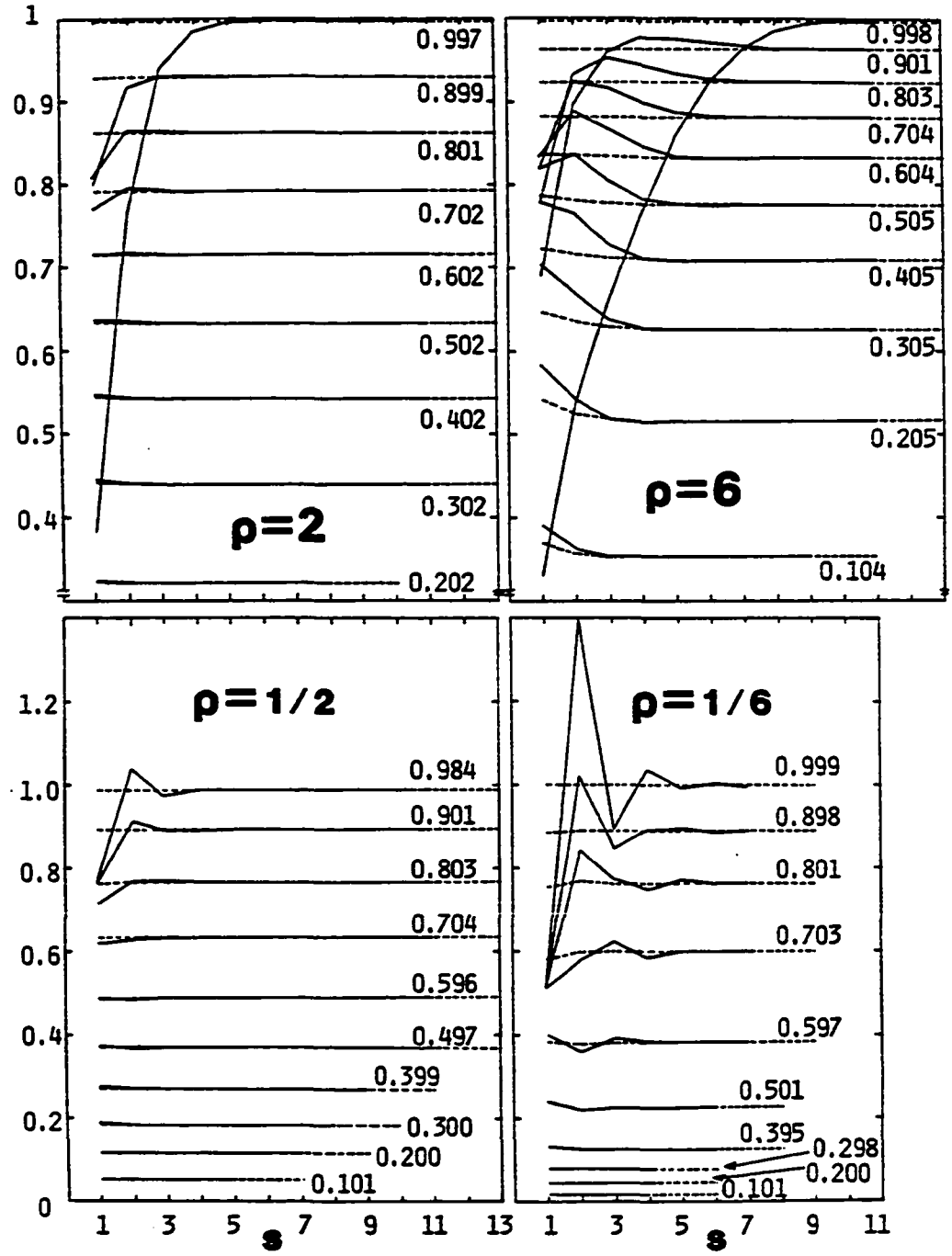

Figure 1: Ratios f_{s+1}/f_s (---) and n_{s+1}/n_s (——) as functions of s (for various θ, shown), for filling with NN cooperative effects with rates $k_0 : k_1 : k_2 = 1 : \rho : \rho^2$ and $\rho = 1/6, 1/2, 2, 6$

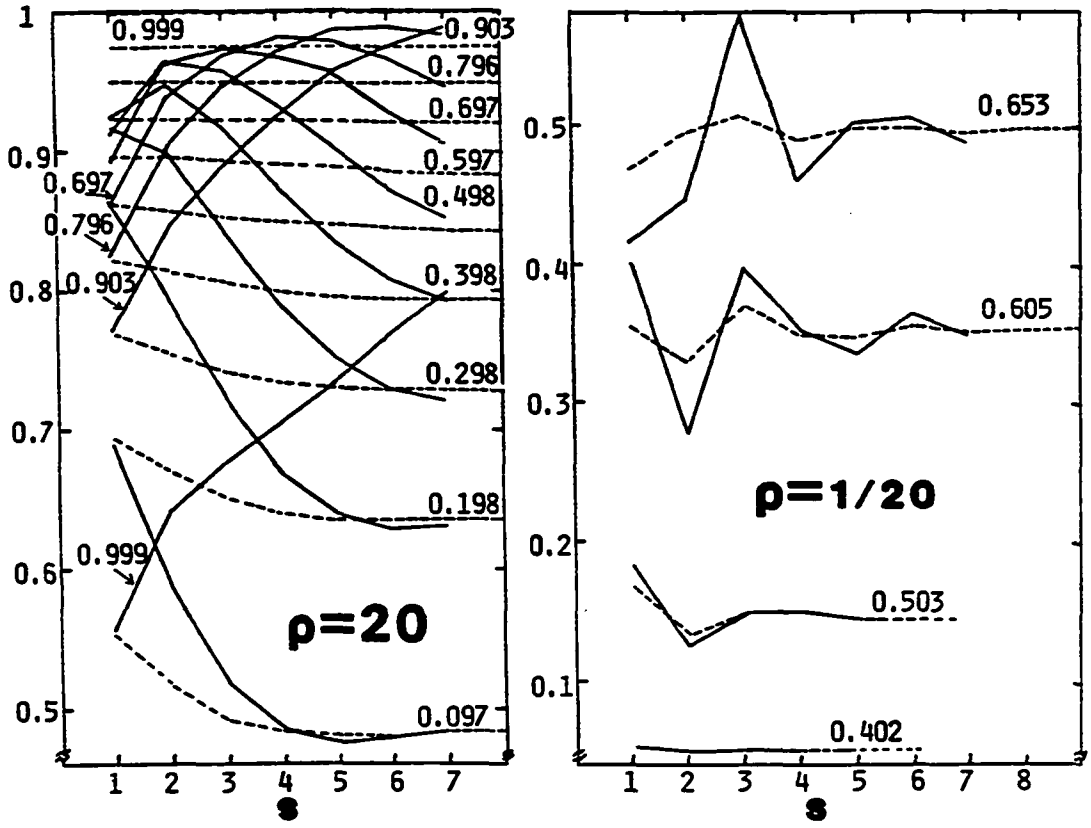

Figure 2: Ratios f_{s+1}/f_s (---) and n_{s+1}/n_s (——) (for various θ, shown), for filling with NN cooperative effects with $k_0 : k_1 : k_2 = 1 : \rho : \rho^2$ and $\rho = 1/20, 20$

Since numerical results indicate that the series $\sum_{i=1}^{\infty}(q_{a\alpha_i} - q_{a\alpha_\infty})$ is absolutely convergent (see Fig. 3), one concludes that the f_s (and thus the n_s) exhibit asymptotic (large s) exponential decay. Consequently, one can write

$$f_s \sim C(\theta)\,\lambda(\theta)^{s-1} \text{ and } n_s \sim C(\theta)[1 - \lambda(\theta)]^2\,\lambda(\theta)^{s-1}\ , \text{ as } s\to\infty\ , \qquad (3.2)$$

where an infinite product expression for the function $C(\theta)$ can be obtained from (3.1). We note that monotonic decrease of the f_s and n_s distributions is guaranteed by (3.2) for large s, since $\lambda(\theta) < 1$, and is only violated in the low ρ and s regime.

One nontrivial quantity, characteristic of the cluster-size distribution, which can be calculated immediately after solving the minimal closed hierarchy (2.1), is the average cluster size (without site weighting), n_{av}, given by

$$n_{av} \equiv \sum_{s=1}^{\infty} s\, n_s \,/\, \sum_{s=1}^{\infty} n_s \quad . \qquad (3.3)$$

Using the identity $n_s \equiv \Delta^2 f_s$, one can readily show that (cf. Ref. 27)

$$\sum_{s=1}^{\infty} n_s \equiv f_{oa} \equiv f_o - f_{oo}\ , \text{ and } \sum_{s=1}^{\infty} s\, n_s \equiv \theta\ , \qquad (3.4)$$

where $f_{oa} \equiv f_{ao}$ gives the fraction of sites corresponding to left (or

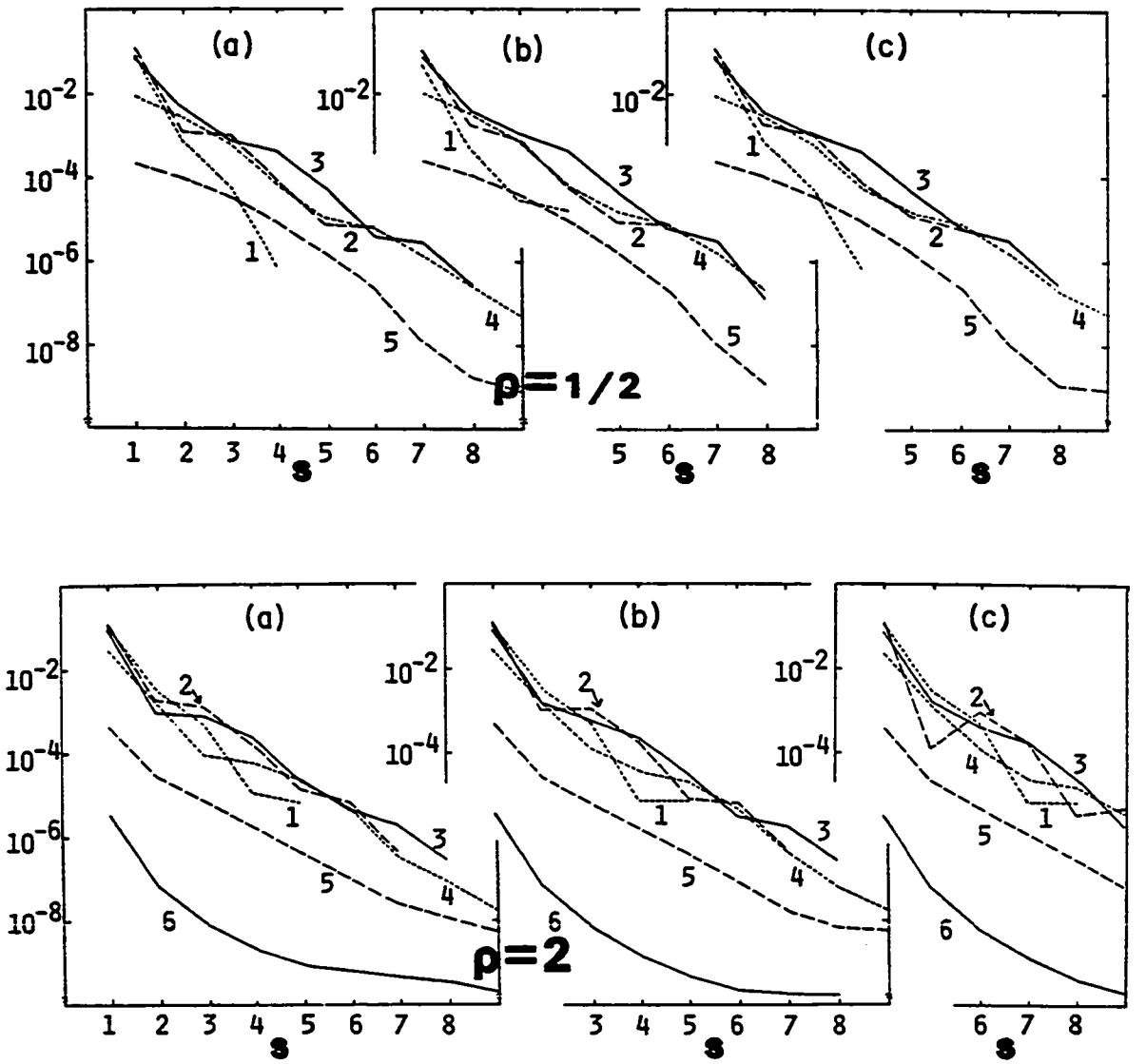

Figure 3: Quantities (A) $s|q_{\underset{\sim}{a}\alpha_s} - q_{\underset{\sim}{a}\alpha_\infty}|$, (B) $s|q_{\underset{\sim}{a}\alpha_s} - q_{\underset{\sim}{a}\alpha_{s-1}}|$, and (C) $s|q_{\alpha\underset{\sim}{a}\alpha_s} - q_{\alpha\underset{\sim}{a}\alpha_{s-1}}|$ as functions of s, for $k_0 : k_1 : k_2 = 1 : \rho : \rho^2$ with $\rho = 1/2$ (curves 1-5 correspond to $\theta = 0.2004$, 0.4971, 0.7041, 0.8999, 0.9834, respectively) and $\rho = 2$ (curves 1-6 correspond to $\theta = 0.2023$, 0.5020, 0.7014, 0.8992, 0.9973, 0.99997), respectively

right) ends of filled clusters, i.e., the cluster density. The identities (3.3,4) are obviously valid for any site occupancy statistics.

In Fig. 4, we have displayed $n_{av} \equiv \theta/f_{oa}$, as a function of θ, obtained from solution of (2.1) for a choice of rates $k_0:k_1:k_2 = 1:\rho:\rho^2$, with various ρ. For $\rho = 1$, it follows trivially from (3.3,4) that $n_{av} \equiv (1 - \theta)^{-1}$. The $\rho \to 0+$ limit deserves special comment. It has been recognized previously that, here, filling occurs in three stages, of sites with zero, one, and then two already filled NN, respectively, so $d/d\theta\ f_{oo}$ is piecewise constant with values -2, -1, 0, since two, one, then zero, empty pairs are destroyed for each site filled, respectively[1,26,32]. The stages end at coverages $(1-e^{-2})/2$, $(1+e^{-2})/2$, and 1, respectively. Thus in the first stage, one has $f_{oo} \equiv 1-2\theta$, so $f_{oa} = \theta$ and $n_{av} = 1$, which is obvious since all filled sites are isolated. In the second stage where $d/d\theta\ f_{oo} = -1$, f_{oa} is constant (obviously) with value $\theta^* \equiv (1-e^{-2})/2$, so $n_{av} \equiv \theta/\theta^*$. In the last stage, one has $f_{oo} \equiv 0$, so $n_{av} \equiv \theta/(1-\theta)$. It is also physically clear that $n_{av} \to \infty$, as $\rho \to \infty$, for fixed θ, since the $\rho \to \infty$ limit can be thought of as a single island growing (which thus has infinite size at any nonzero coverage).

Although the percolation threshold $\theta = \theta_c$ is always trivially <u>unity</u> in 1D, the nature of the divergence of n_{av}, as $\theta \to \theta_c$, depends nontrivially on the cooperativity, and is of particular interest here. Specifically, we wish to determine the critical exponent, ν, and coefficient, A, in the relation

$$n_{av} \sim A(\theta_c-\theta)^{-\nu}, \text{ as } \theta \to \theta_c \quad . \tag{3.5}$$

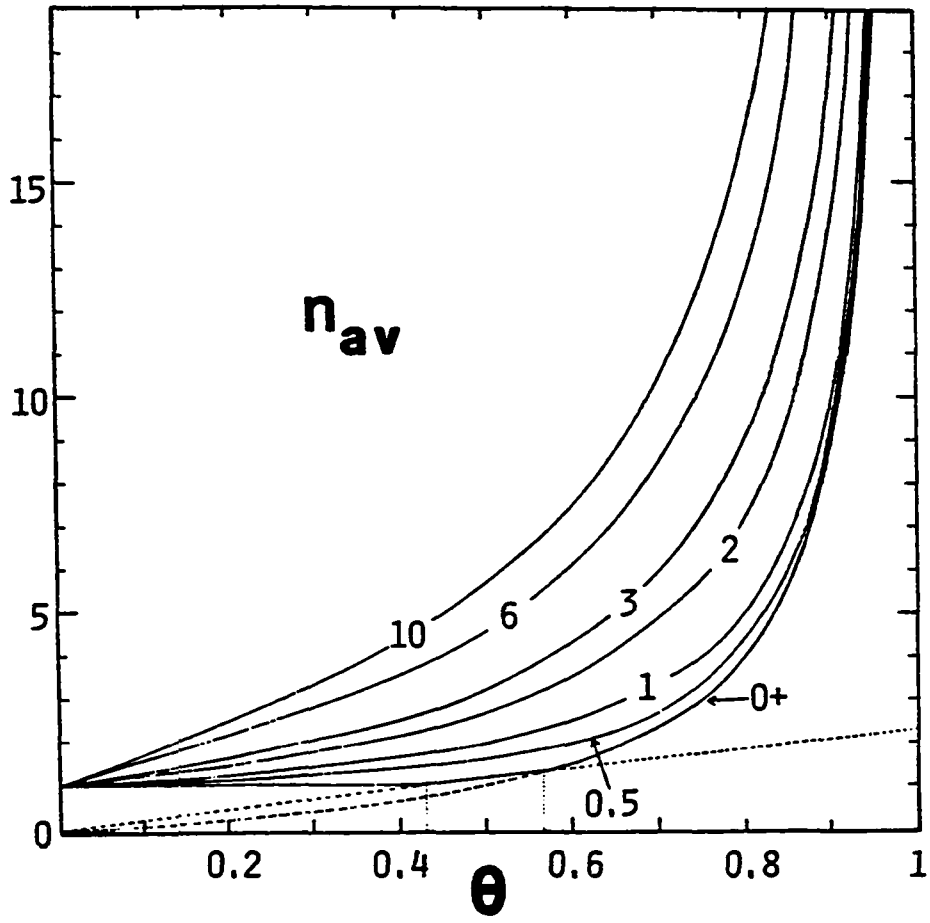

Figure 4: The average island size (without site weighting), $n_{av} \equiv \theta/f_{ao}$, as a function of coverage, θ, for filling with NN cooperative effects with $k_0 : k_1 : k_2 = 1 : \rho : \rho^2$ (and various ρ, shown)

First note that <u>if</u> f_{oo} goes to zero faster than f_o, <u>then</u> $f_{oa} \sim f_o \equiv 1 - \theta$, as $\theta \to \theta_c$, and thus we have A=1 and ν=1. This is trivially the case for random filling where $f_{oo} \equiv f_o^2$, so $n_{av} \equiv (\theta_c - \theta)^{-1}$. Furthermore, since we <u>never</u> have $f_{oo} \sim f_o$, as $\theta \to \theta_c$, it always follows that ν=1.

Explicit determination of both A and ν is easily achieved after expressing the solutions of (2.1) in terms of $q \equiv e^{-k_o t}$, and the reduced rates, $\rho_i = k_i/k_o$, as[26]

$$f_{oo} = q^{2\rho_1} \exp[2(1-\rho_1)(q-1)] \quad \text{and} \quad f_o \equiv 1-\theta = q^{\rho_2} G(q) \quad , \tag{3.6}$$

where

$$G(q) = 1 + \int_1^q du \exp[2(1-\rho_1)(u-1)][2(\rho_1-\rho_2)u^{2\rho_1-\rho_2-1} + (1-2\rho_1+\rho_2)u^{2\rho_1-\rho_2}],$$

$$\begin{aligned} &\to G(0), \text{ a finite constant, if } 2\rho_1 > \rho_2, \\ &\sim -\rho_2\, e^{2(\rho_1-1)}\, \ell n\, q, \text{ if } 2\rho_1 = \rho_2 \quad , \\ &\sim \frac{2\rho_2-2\rho_1}{\rho_2-2\rho_1}\, e^{2(\rho_1-1)}\, q^{2\rho_1-\rho_2}, \text{ if } 2\rho_1 < \rho_2 \quad , \end{aligned} \tag{3.7}$$

when $q \to 0$ (i.e., $t \to \infty$ or $\theta \to \theta_c = 1$). From these results, it follows immediately that

$$n_{av} \sim 1/f_{oa} \sim (\theta_c-\theta)^{-1} \sim e^{k_2 t}/G(0), \text{ as } \theta \to \theta_c (t \to \infty), \text{ for } 2\rho_1 > \rho_2 \ , \tag{3.8}$$

and

$$n_{av} \sim 1/f_{oa} \sim (\theta_c-\theta)^{-1} \sim e^{2-\rho_2}\, e^{k_2 t}/(k_2 t), \text{ as } \theta \to \theta_c (t \to \infty),$$
$$\text{for } 2\rho_1 = \rho_2 \ . \tag{3.9}$$

However, since $f_{oo} \sim \frac{\rho_2-2\rho_1}{2\rho_2-2\rho_1} f_o$ when $2\rho_1 < \rho_2$, one has that

$$n_{av} \sim 1/f_{oa} \sim \frac{2\rho_2 - 2\rho_1}{\rho_2} (\theta_c - \theta)^{-1} \sim \frac{\rho_2 - 2\rho_1}{\rho_2} e^{2(1-\rho_1)} e^{2k_1 t} ,$$

$$, \text{ as } \theta \to \theta_c (t \to \infty), \text{ for } 2\rho_1 < \rho_2 \quad . \qquad (3.10)$$

Thus, in contrast to the critical exponent, for $2\rho_1 < \rho_2$ the proportionality constant, A, differs from its random filling (or percolation) value of unity. The growth of the average cluster size is exponential in time, for large t, with exponent k_2 for $2\rho_1 > \rho_2$ (coalescence of clusters is the growth limiting step), and k_1 for $2\rho_1 < \rho_2$ (addition to clusters is the growth limiting step). As we shall sometimes use the choice of rates $k_0 : k_1 : k_2 = 1 : \rho : \rho^2$ ($\rho_1 = \rho_2^{1/2} = \rho$), we note that $2\rho_1 \gtrless \rho_2$ corresponds to $\rho \lessgtr 2$.

Finally, in this section, we consider the behavior of the site-weighted average cluster size

$$s_{av} \equiv \sum_{s=1}^{\infty} s^2 n_s / \sum_{s=1}^{\infty} s\, n_s , \qquad (3.11)$$

and of the variance of the cluster-size distribution (without site weighting)

$$\sigma^2 \equiv \sum_{s=1}^{\infty} (s^2 - n_{av}^2)\, n_s / \sum_{s=1}^{\infty} n_s \quad . \qquad (3.12)$$

The main complication here is that both quantities involve the nontrivial sum

$$\sum_{s=1}^{\infty} s^2 n_s = \theta + 2 \sum_{s=1}^{\infty} f_{s+1} \quad . \tag{3.13}$$

For numerical estimates of (3.13), it is convenient to use the identity

$$\sum_{s=1}^{\infty} f_{s+1} = [\lambda(\theta)\theta + \delta(\theta)]/[1 - \lambda(\theta)] \quad , \tag{3.14}$$

where $\delta(\theta) \equiv \sum_{s=1}^{\infty} (f_{s+1} - \lambda(\theta)\, f_s) = \sum_{s=1}^{\infty} f_s(q_{a\alpha_s} - q_{a\alpha_\infty})$. It follows that $|\delta(\theta)| < \sum_{s=1}^{\infty} |q_{a\alpha_s} - q_{a\alpha_\infty}|$, which our calculations indicate is rapidly convergent (see Fig. 3). Each term approaches zero as $\theta \to 1$, and if we reasonably assume that $\delta(\theta) \to 0$, as $\theta \to 1$, then one has

$$s_{av} \sim \sum_{s=1}^{\infty} s^2 n_s \sim 2[1 - \lambda(\theta)]^{-1}, \text{ as } \theta \to \theta_c = 1 \quad . \tag{3.15}$$

In Fig. 5, we have plotted the standard deviation of the cluster-size distribution in units of the average cluster size (both without site weighting), i.e.,

$$\sigma/n_{av} = \left(\sum_{s=1}^{\infty} s^2 n_s - \theta^2/f_{oa}\right)^{1/2} (f_{oa})^{1/2}/\theta \quad , \tag{3.16}$$

as a function of θ. Since it appears that $\sigma/n_{av} \to 1$, as $\theta \to 1$, we conclude that

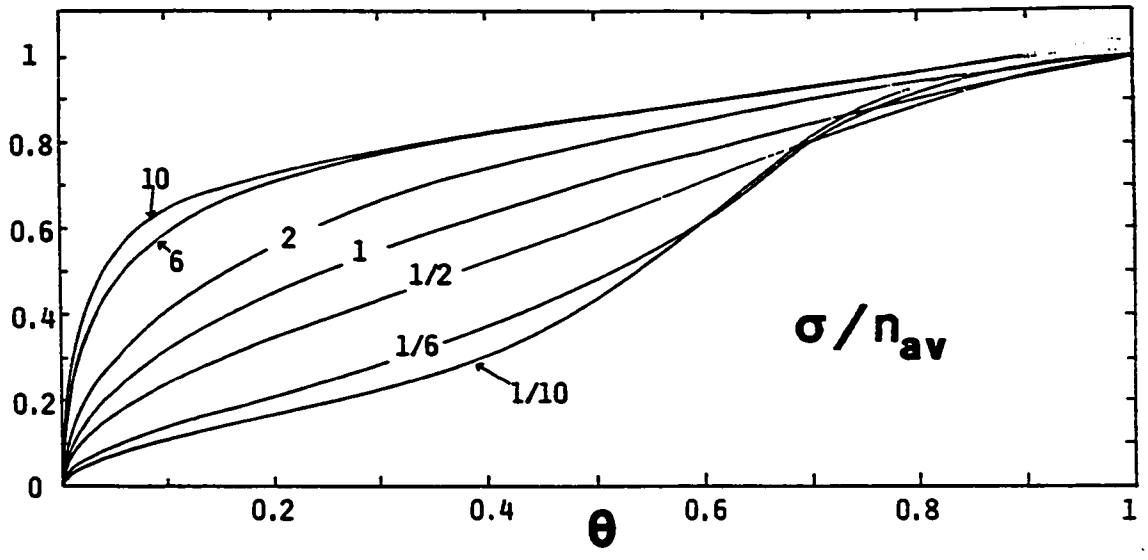

Figure 5: The standard deviation of the cluster-size distribution in units of the average cluster size (both without site weighting), σ/n_{av}, as a function of θ, for filling with NN cooperative effects with $k_0 : k_1 : k_2 = 1 : \rho : \rho^2$ (and various ρ, shown). Dotted lines, in the high θ regime, indicate presumed spurious behavior of the numerical integration for $\rho = 6$, 10 (the top line is for $\rho = 10$), and reasonable extrapolation for $\rho = 1/10$ (excessive computer time limits integration here)

$$s_{av} \sim \sum_{s=1}^{\infty} s^2 n_s \sim 2/f_{oa} \sim 2n_{av} \sim 2A(\theta_c-\theta)^{-1}, \text{ as } \theta\to\theta_c = 1 \quad , \qquad (3.17)$$

which, using (3.15), implies that (cf. Fig. 6 in the next section),

$$1 - \lambda(\theta) \sim f_{oa} \sim A^{-1}(\theta_c-\theta), \text{ as } \theta\to\theta_c = 1 \quad . \qquad (3.18)$$

Finally we note that for random filling, $\rho=1$, one has immediately from (3.13,14) that $\sum_{s=1}^{\infty} s^2 n_s = \theta(1+\theta)(1-\theta)^{-1}$ and so, together with $\sum_{s=1}^{\infty} s\, n_s = \theta$ and $\sum_{s=1}^{\infty} n_s = \theta(1-\theta)$, one concludes that $n_{av} \equiv (1-\theta)^{-1}$, $s_{av} \equiv (1+\theta)(1-\theta)^{-1}$ (see Ref. 27) and $\sigma/n_{av} \equiv \theta^{1/2}$.

IV. ASYMPTOTIC ANALYSIS OF THE CLUSTER-SIZE DISTRIBUTION

It is desirable to understand those structural features of the hierarchial equations which guarantee that f_{s+1}/f_s, $n_{s+1}/n_s \to \lambda(\theta)$, as $s\to\infty$, and to develop a technique for analyzing such quantities as $\lambda(\theta)$ more directly. The strategy adopted here, which achieves these goals, involves deriving equations satisfied directly by $\lambda(\theta)$ and related quantities, by taking appropriate limits of the (suitably recast) hierarchy equations.

Here we naturally start by considering the equation for $q_{a\alpha_s}$ conveniently expressed in the form

$$d/dt\ \ell n\ q_{a\alpha_s} = d/dt\ \ell n\ f_{s+1} - d/dt\ \ell n\ f_s \tag{4.1}$$

where, after some straightforward manipulation using (2.3), one has

$$d/dt\ \ell n\ f_{s+1} = 2(k_1\ q_{0\phi\alpha_s} + k_2\ q_{a\phi\alpha_s})\ q_{0\alpha_s}/q_{a\alpha_s} + k_2 \sum_{\substack{j+k=s \\ j,k>1}} [(q_{\alpha_j a\alpha_k})^{-1}-1]. \tag{4.2}$$

On letting $s\to\infty$, one obtains for $\lambda(\theta) \equiv \lim_{s\to\infty} q_{a\alpha_s} \equiv q_{a\alpha_\infty}$,

$$d/dt\ \ell n\ q_{a\alpha_\infty} = k_2[(q_{\alpha_\infty a\alpha_\infty})^{-1}-1] \quad , \tag{4.3}$$

where we have assumed that various limits exist, including $q_{\alpha_\infty a\alpha_\infty} \equiv$

$\lim_{j,k\to\infty} q_{\alpha_j a \alpha_k}$, and that, for $j + k = s$ and $j < k$, one has $q_{\alpha_j a \alpha_k} - q_{\alpha_j a \alpha_{k-1}} = o(1/s)$, as $s \to \infty$ (see Fig. 3). Calculations below support the validity of (4.3) and, thus, of these assumptions. One can check that, for random filling where $q_{a\alpha_\infty} \equiv q_{\alpha_\infty a \alpha_\infty} \equiv \theta$, (4.3) has the required solution $\theta = 1 - e^{-k_2 t}$. In general, one must continue to derive an equation for $q_{\alpha_\infty a \alpha_\infty}$ by considering $\lim_{j,k\to\infty} d/dt \ln q_{\alpha_j a \alpha_k}$. One thus obtains (after invoking appropriate assumptions regarding existence of, and appropriate convergence to certain limits)

$$d/dt \ln q_{\alpha_\infty a \alpha_\infty} = k_2[3(q_{\alpha_\infty a \alpha_\infty})^{-1} - 5 + 2q_{\alpha_\infty a \alpha_\infty}] - 2k_1[(q_{\alpha_\infty a - \alpha_\infty})^{-1} - 2 + q_{\alpha_\infty a \alpha_\infty}] + 2k_2 \sum_{i=1}^{\infty} [(q_{\alpha_\infty a \alpha_\infty})^{-1} - (q_{\alpha_\infty a \alpha_i - \alpha_\infty})^{-1}] \quad . \tag{4.4}$$

Continuing in this way, one obtains an infinite coupled set of equations for $\lambda(\theta) \equiv q_{a\alpha_\infty}, q_{\alpha_\infty a \alpha_\infty}, q_{\alpha_\infty a - \alpha_\infty}, q_{\alpha_\infty a \alpha_i - \alpha_\infty}, q_{\alpha_\infty a - - \alpha_\infty}, \cdots$.

Since all these quantities clearly have zero initial conditions, it then follows that their initial time rate of change, as prescribed by the above equations, are given in indeterminate form. For example,

$$d/dt \ln q_{a\alpha_\infty} \sim k_2/q_{\alpha_\infty a \alpha_\infty} \text{ (or } d/dt\, q_{a\alpha_\infty} \sim k_2\, q_{a\alpha_\infty}/q_{\alpha_\infty a \alpha_\infty}), \text{ at } t \to 0 \quad . \tag{4.5}$$

For all other q's where a central group of a single 'a' site, and several 'α' and '-' sites are bordered on either side by an α_∞, there are an

infinite number of indeterminate terms. Most of these can be "paired" (denoted pt below) as a rate k_i times a difference of reciprocals of q's both with i α-sites next to the a-site (cf. the last term in (4.4)). The form of the remaining terms depends on the state of the adjacent pair of sites on either side of 'a', and is thus completely enumerated by the following:

$$d/dt\ \ell n\ q_{\cdot\cdot\alpha\alpha a\alpha\alpha\cdot\cdot} \sim k_2/q_{\cdot\cdot\alpha a\alpha\alpha\alpha\cdot\cdot} + k_2/q_{\cdot\cdot\alpha\alpha a\alpha\alpha\cdot\cdot} + k_2/q_{\cdot\cdot\alpha\alpha\alpha a\alpha\cdot\cdot} - k_1/q_{\cdot\cdot\alpha a-\alpha\alpha\cdot\cdot} - k_1/q_{\cdot\cdot\alpha\alpha-a\alpha\cdot\cdot} + pt\ ,$$

$$d/dt\ \ell n\ q_{\cdot\cdot\alpha\alpha a\alpha-\cdot\cdot} \sim k_2/q_{\cdot\cdot\alpha a\alpha\alpha-\cdot\cdot} + k_2/q_{\cdot\cdot\alpha\alpha a\alpha-\cdot\cdot} + k_1/q_{\cdot\cdot\alpha\alpha\alpha a-\cdot\cdot} - k_1/q_{\cdot\cdot\alpha a-\alpha-\cdot\cdot} - k_0/q_{\cdot\cdot\alpha\alpha-a-\cdot\cdot} + pt\ ,$$

$$d/dt\ \ell n\ q_{\cdot\cdot-\alpha a\alpha-\cdot\cdot} \sim k_1/q_{\cdot\cdot-a\alpha\alpha-\cdot\cdot} + k_2/q_{\cdot\cdot-\alpha a\alpha-\cdot\cdot} + k_1/q_{\cdot\cdot-\alpha\alpha a-\cdot\cdot} - k_0/q_{\cdot\cdot-a-\alpha-\cdot\cdot} - k_0/q_{\cdot\cdot-\alpha-a-\cdot\cdot} + pt\ ,$$

$$d/dt\ \ell n\ q_{\cdot\cdot\alpha\alpha a-\cdot\cdot} \sim k_2/q_{\cdot\cdot\alpha a\alpha-\cdot\cdot} + k_1/q_{\cdot\cdot\alpha\alpha a-\cdot\cdot} - k_1/q_{\cdot\cdot\alpha a-\cdot\cdot\cdot} + pt\ ,$$

$$d/dt\ \ell n\ q_{\cdot\cdot-\alpha a-\cdot\cdot} \sim k_1/q_{\cdot\cdot-a\alpha-\cdot\cdot} + k_1/q_{\cdot\cdot-\alpha a-\cdot\cdot} - k_0/q_{\cdot\cdot-a-\cdot\cdot\cdot} + pt,$$

$$d/dt\ \ell n\ q_{\cdot\cdot-a-\cdot\cdot} \sim k_0/q_{\cdot\cdot-a-\cdot\cdot} + pt\ , \quad \text{as } t \to 0\ . \tag{4.6}$$

Here the dots indicate that the same configuration of 'α' and '-' sites, bordered by an α_∞, appears in each q.

It is clear that a choice of k's satisfying $q \sim kt$, as $t \to 0$, consistent with (4.6), is given by

$$q_{\bullet\bullet-a-\bullet\bullet} \sim k_0 t \;\; ; \;\; q_{\bullet\bullet\alpha a-\bullet\bullet} \;\; , \;\; q_{\bullet\bullet-a\alpha\bullet\bullet} \sim k_1 t \;\; , \;\; q_{\bullet\bullet\alpha a\alpha\bullet\bullet} \sim k_2 t \; . \quad (4.7)$$

Finally, returning to (4.5), we conclude that $q_{a\alpha_\infty} \sim k_1 t$, as $t \to 0$. This additional information allows us to consistently treat the initial indeterminacy in the q hierarchy under consideration here, thus obtaining a well-defined initial value problem. It is worth noting that these hierarchy equations are also clearly consistent with the anticipated behavior $q_{a\alpha_\infty}$, $q_{\alpha_\infty a\alpha_\infty}$, $\cdots \to 1$, as $t \to \infty$.

Exact solution of these hierarchial equations to determine, e.g., $\lambda(\theta) \equiv q_{a\alpha_\infty}$, is not feasible because of their complicated nonlinear structure. However to obtain approximate solutions, one could apply an n^{th}-order Markovian approximation wherein q's with the same conditioning configuration within n sites of 'a' are set equal (e.g., in such an approximation $q_{a\alpha_\infty}$, $q_{\alpha_\infty - - a\alpha_\infty}$, $q_{\alpha_\infty - - - a\alpha_\infty}$, $\cdots$ would be set equal for n=2). The resulting n=2 estimates of $\lambda(\theta) \equiv q_{a\alpha_\infty}$, shown in Fig. 6, are quite accurate for moderate cooperativity (except near $\theta=1$). We note, however, that better estimates of $\lambda(\theta)$ can be obtained from using the exact $q_{a\alpha\alpha}$, or better $q_{a\alpha\alpha\alpha}$ (except for extremes of cooperativity, and low θ).

This analysis is particularly significant, however, in that it provides a direct demonstration that for $k_2 \neq 0$, $\lambda(\theta) \equiv \lim_{s\to\infty} f_{s+1}/f_s$ exists

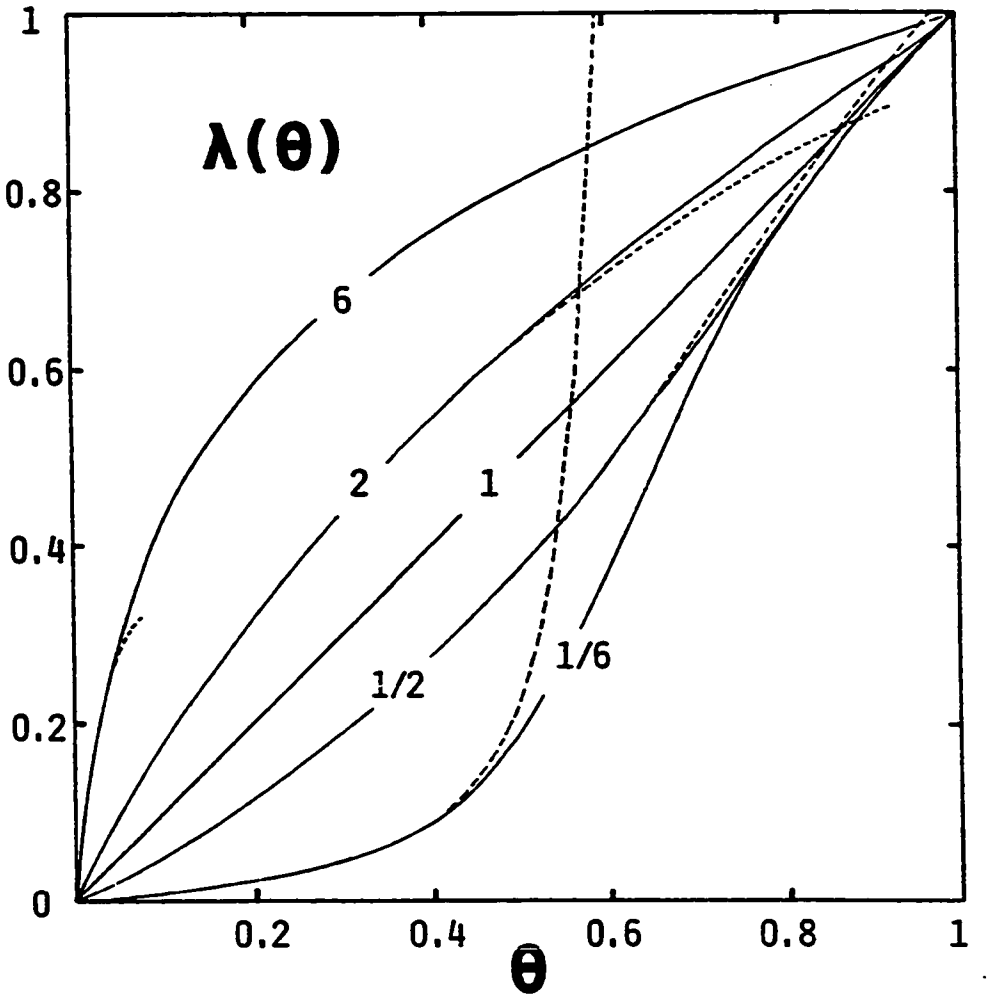

Figure 6: The asymptotic decay rate, $\lambda(\theta) = \lim_{s\to\infty} f_{s+1}/f_s$, as a function of coverage, θ, determined from exact calculation (——) and 2^{nd}-order Markovian trunction (---), for filling with NN cooperative effects with $k_0 : k_1 : k_2 = 1 : \rho : \rho^2$ (and various ρ, shown). Termination of the dashed lines indicates that certain probabilities in the Markovian truncation become unphysical at these points

as a well behaved function of θ, nonzero except when $\theta = 0$. It is also clear that the origin of this behavior is the appearance of O(s) creation terms (proportional to k_2) in the rate equation (3.4b) for f_s. (We can also conclude that if $k_2 = 0$, then $\lim_{s\to\infty} f_{s+1}/f_s \equiv 0$ for all θ; this case of noncoalescing clusters is treated in detail in the following paper[33].) As we shall see in the next section, this new-found insight can be used to predict the asymptotic behavior of the filled cluster-size distribution for other more complicated 1D filling processes. Perhaps the most important aspect of this analysis, is that the basic technique extends to <u>higher dimensions</u> (and even to other dynamic processes on lattices for which hierarchial rate equations apply) to provide some fundamental insights into the characteristics of the distribution of filled sites (see Appendix).

V. DISCUSSION AND EXTENSIONS

Here we have solved the master equations (in hierarchial form) to provide the first extensive, exact analytic investigation of the filled s-tuple and filled cluster-size distributions for a 1D irreversible, cooperative filling process (specifically, monomer filling with NN cooperative effects on an infinite, uniform lattice). The solution procedure, as outlined by Plate et al.[10], exploits shielding and coupling features of the hierarchy specific to irreversibility. Our calculations cover a sufficiently extensive range of size, s, to clearly demonstrate the transition to (large s) asymptotic exponential decay in the above distributions (when all rates, k_i, are nonzero). The analytic approach allows natural investigation of the coverage or time dependence of such quantities as the average cluster size, and asymptotic exponential decay rate, $\lambda(\theta)$. Further it facilitates a second important component of this work, specifically, development of a novel approach for extracting directly from the suitably recast hierarchial equations, asymptotic properties of the cluster-size distribution such as the exponential decay rate, $\lambda(\theta)$.

Clearly the asymptotic exponential decay in this model is associated with the occurrence of O(s) gain terms in the filled s-tuple, f_s, rate equation. This occurs provided $k_2 \neq 0$ so clusters can coalesce. More generally, for any 1D irreversible filling model where "clusters" of size s can be created by filling the gap between (coalescence of) "clusters" of size s_1 and s_2 (where $s_1 + s_2 = s-1$ and $0 < s_1 < s-1$), analogous calculations suggest one still has asymptotic exponential decay of the

"cluster"-size distribution. Liggett's arguments (see Introduction) support this claim as they apply to filling with arbitrary range cooperative effects, and all rates nonzero. The following results show that it has even more general validity.

For 1D monomer filling with NN blocking and 2^{nd}-NN cooperative effects (so now the rates, k_i, refer to the number i = 0, 1, 2 of filled 2^{nd}-NN), clusters of alternating empty and filled sites develop. We naturally let f_s (n_s) denote the probability of the configuration oaoa•••oaoao or, equivalently, aoa•••oaoa (ooaoa•••oaoaoo) where s a-filled sites appear. Here clusters can either grow together in phase (i.e., ••oaoaoooaoa••, where the center site will fill provided $k_2 \neq 0$, i.e., coalescence can occur), or out of phase (i.e., ••oaoaooaoa••, creating a permanent domain boundary)[34]. Exact hierarchial solution is again possible[34,35], but since an empty 4-tuple (rather than pair) of sites is required to shield, many more independent quantities exist, and must be determined from exactly truncated equations (specifically $q = f_{o_{n+1}}/f_{o_n} = e^{-k_0 t}$, $n>4$; f_{o_i}, $1 \leq i \leq 4$; and $f_{o_{j_1} \underbrace{\ell}\, o_{i_1} \underbrace{m}\, o_{i_2} \underbrace{n} \cdots \underbrace{r}\, o_{j_2}}$ where $1 \leq j_1, j_2 \leq 4$, $1 \leq i_1, i_2, \cdots \leq 3$). For $k_2 \neq 0$, this model does fit the above criteria for asymptotic exponential decay of f_s and n_s. This is confirmed from the results shown in Fig. 7, obtained from a very extensive exact truncation calculation. Furthermore, if $f_{s+1}/f_s \to \lambda(\theta)$, as $s \to \infty$, then the analogue of (4.3) becomes

$$d/dt \, \ell n \, \lambda(\theta) = k_2[(q_{\cdots\alpha\text{-}\alpha\text{-}a\text{-}\alpha\text{-}\alpha\cdots})^{-1} - 1] \quad . \tag{5.1}$$

The behavior of the average cluster size without site weighting,

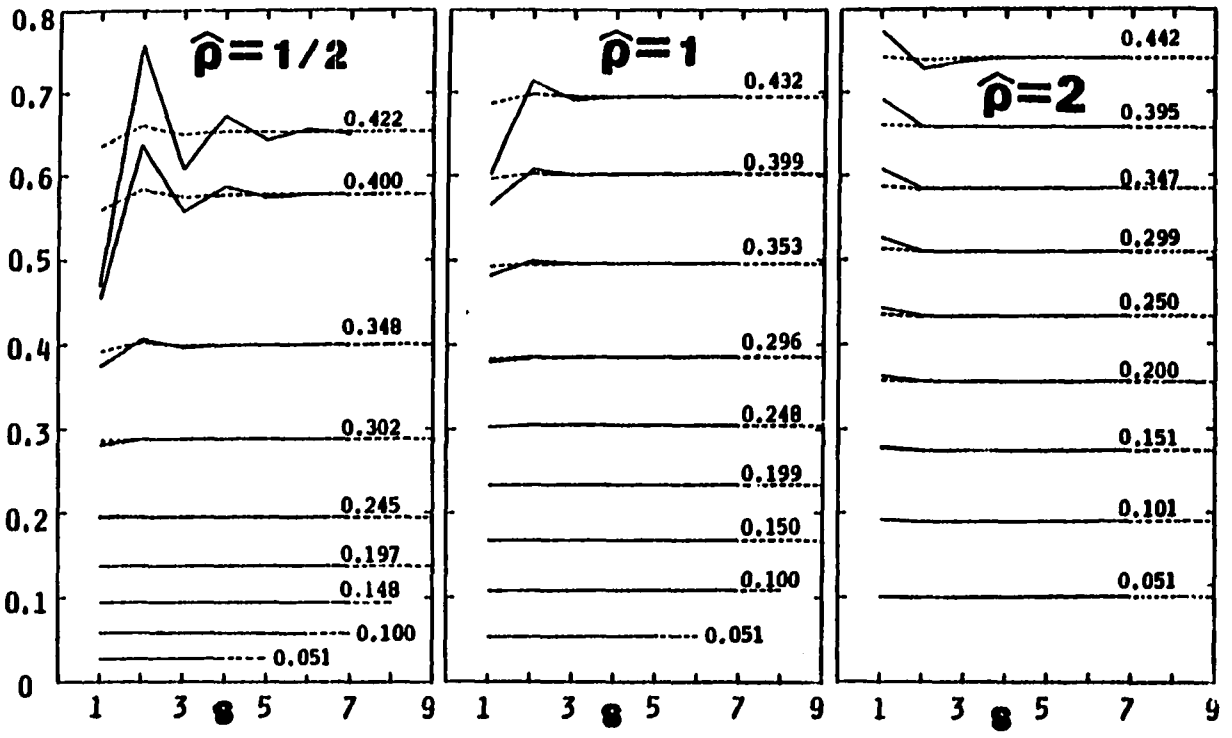

Figure 7: Ratios $\hat{f}_{s+1}/\hat{f}_s$ (---) and $\hat{n}_{s+1}/\hat{n}_s$ (——) (for various θ, shown), for filling with NN blocking and 2^{nd}-NN cooperative effects with rates $k_0 : k_1 : k_2 = 1 : \hat{\rho} : \hat{\rho}^2$ and $\hat{\rho} = 1/2, 1, 2$

straightforwardly determined[34] from $\hat{n}_{av} = \theta/f_{aoo}$, with $f_{aoo} \equiv f_{oo}-f_{ooo}$, is shown in Fig. 8. It is appropriate to recall the equivalence of this processes to 1D dimer filling with NN cooperative effects[34], and note the compatibility of our results with those from earlier simulations for 1D random dimer filling[9].

Finally we note the applicability of the technique of Section IV to higher-dimensional irreversible filling processes (see Appendix), and anticipate that it will be useful for consideration of a variety of other dynamic processes on lattices.

Our model could be modified so that nucleation is enhanced at (or confined to) a distribution of sites specified either defective or initially filled, making it similar to those used to describe irreversible kinetic gelation[36] (particularly if we consider bond rather than site filling). We leave such considerations till later work, but note that we expect the long-range connectivity transition of kinetic gelation to be in a different universality class from that of the filling processes considered here.

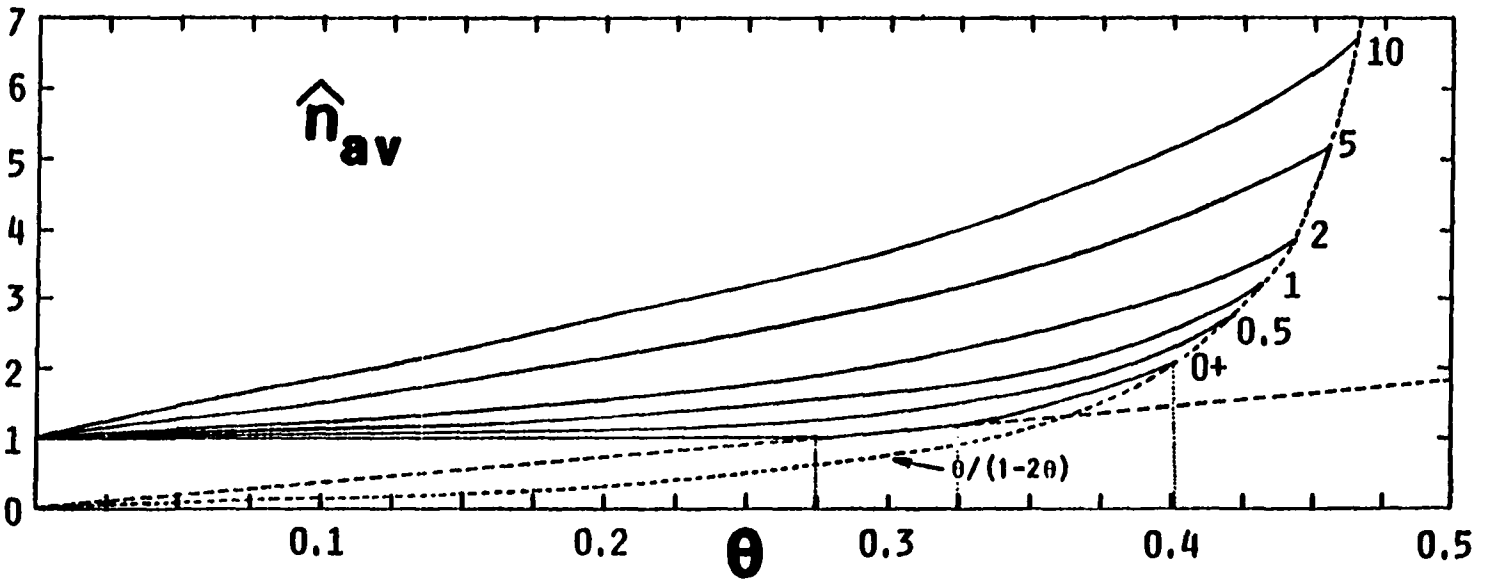

Figure 8: The average island size (without site weighting) $\hat{n}_{av} = \theta/f_{aoo}$, as a function of coverage, for filling with NN blocking and 2^{nd}-NN cooperative effects with $\hat{k}_0 : \hat{k}_1 : \hat{k}_2 = 1 : \hat{\rho} : \hat{\rho}^2$ (and various $\hat{\rho}$, shown). When $\hat{\rho} = 0+$, the process occurs in three stages corresponding to filling of sites where the number of filled 2^{nd}NN is zero [$0 < \theta < \theta_1 \approx 0.2746$, $n_{av} = 1$], one [$\theta_1 < \theta < \theta_2 \approx 0.3243$, $n_{av} = \theta/\theta_1$], and two [$\theta_2 < \theta < \theta_3 \approx 0.4011$, $\hat{n}_{av} = \theta(\theta_1 + \theta_2 - \theta)^{-1}$]. Since $f_{aoo}^{sat} = f_{oo}^{sat} = 1-2\,\theta^{sat}$, we have that $\hat{n}_{av}^{sat} = \theta^{sat}\,(1-2\,\theta^{sat})^{-1}$

ACKNOWLEDGEMENTS

Ames Laboratory is operated for the U.S. Department of Energy by Iowa State University under Contract No. W-7405-ENG-82. This work was supported by the Office of Basic Energy Sciences.

APPENDIX: IRREVERSIBLE COOPERATIVE FILLING ON A 2D SQUARE LATTICE

Consider the irreversible filling of sites on a square lattice with NN cooperative effects. Let k_i, $i = 0, 1, \cdots, 4$, denote the rates for filling sites with i (already) occupied NN. Rate equations can be written down intuitively for any subconfiguration probability[1]. For example, using the obvious notation for subconfigurations, one obtains

$$d/dt\, f_a = k_0\, f_{\substack{o\\ ooo\\ o}} + 4\, k_1\, f_{\substack{o\\ aoo\\ o}} + k_2\, \Big(2f_{\substack{o\\ aoa\\ o}} + 4f_{\substack{a\\ aoo\\ o}}\Big) + 4\, k_3\, f_{\substack{a\\ aoa\\ o}} + k_4\, f_{\substack{a\\ aoa\\ a}} \qquad (1)$$

$$d/dt\, f_{a_s} = \sum_{\substack{i+j=s-1\\ i,j\geq 1}} \Big(k_2\, f_{\substack{o\\ a_i o a_j\\ o}} + 2\, k_3\, f_{\substack{a\\ a_i o a_j\\ o}} + k_4\, f_{\substack{a\\ a_i o a_j\\ a}}\Big)$$

$$+ 2\, \Big(k_1\, f_{\substack{o\\ ooa_{s-1}\\ o}} + k_2\, f_{\substack{o\\ aoa_{s-1}\\ o}} + 2\, k_2\, f_{\substack{a\\ ooa_{s-1}\\ o}}$$

$$+ k_3\, f_{\substack{a\\ ooa_{s-1}\\ a}} + 2\, k_3\, f_{\substack{a\\ aoa_{s-1}\\ o}} + k_4\, f_{\substack{a\\ aoa_{s-1}\\ a}}\Big) \quad , \qquad (2)$$

where a_n here denotes a horizontal n-tuple of filled sites, and we have exploited various lattice group symmetries. Equation (2) should be compared with (2.3).

If we define $f_s \equiv f_{a_s}$, then again one can consider the behavior of f_{s+1}/f_s as $s\to\infty$. We naturally start by writing down the rate equation for

$q_{a\alpha_s} = f_{s+1}/f_s$ and verify that its structure is compatible with the existence of a finite, nonzero (except when $\theta=0$) limit $\lambda(\theta) = \lim_{s\to\infty} q_{a\alpha_s} \equiv q_{a\alpha_\infty}$, say (cf. Section IV). This is seen to be the case since, after taking the $s\to\infty$ limit, one obtains

$$d/dt \ln q_{a\alpha_\infty} = k_2 \left[\frac{1}{q_{\alpha_\infty a\alpha_\infty}} - 1\right] - 2(k_2-k_4)\left[\frac{q_{\alpha_\infty \bar{a}_{\alpha_\infty}}}{q_{\alpha_\infty a\alpha_\infty}} - q_{\alpha_\infty a_{\bar{\alpha}\alpha_\infty}}\right]$$

$$+ (k_2 - 2k_3 + k_4)\left[\frac{q_{\alpha_\infty a_{\bar{a}^{\alpha_\infty}}}}{q_{\alpha_\infty a\alpha_\infty}} - q_{\alpha_\infty a_{\bar{a}\alpha_\infty}}\right] \qquad (3)$$

where $q_{\alpha_\infty a\alpha_\infty} \equiv \lim_{i,j\to\infty} q_{\alpha_i a\alpha_j}$, $q_{\alpha_\infty a_{\bar{a}^{\alpha_\infty}}} \equiv \lim_{i,j\to\infty} q_{\alpha_i a_{\bar{a}^{\alpha_j}}}$, $\cdots$ and $q_{\alpha_i a\alpha_j} \equiv f_{a_{i+1+j}}/f_{a_i - a_j}$, $q_{\alpha_i a_{\bar{a}^{\alpha_j}}} \equiv f_{a_i a_{\bar{a}} a_j}/f_{a_i - a_j}$, $\cdots$ (assuming existence of, and appropriate convergence to these limits). Note that one can always factor these q's in terms of those with a single a-(filled, conditioned) site, e.g.,

$$q_{\alpha_i a_{\bar{a}^{\alpha_j}}} \equiv q_{\alpha_i a_{\bar{\alpha}^{\alpha_j}}}\, q_{\alpha_i a_{\bar{\alpha}^{\alpha_j}}} \quad \text{so} \quad q_{\alpha_\infty a_{\bar{a}^{\alpha_\infty}}} \equiv q_{\alpha_\infty a_{\bar{\alpha}^{\alpha_\infty}}}\, q_{\alpha_\infty a_{\bar{\alpha}^{\alpha_\infty}}} \quad . \qquad (4)$$

Support for the proposition that the limits $q_{\alpha_\infty a\alpha_\infty}$, $q_{\alpha_\infty a_{\bar{\alpha}^{\alpha_\infty}}}$, $\cdots$ exist and are nonzero (except when $\theta=0$), which is necessary for finite, nonzero $q_{a\alpha_\infty}$ to exist, comes from writing down equations for $q_{\alpha_i a\alpha_j}$, $q_{\alpha_i a_{\bar{\alpha}^{\alpha_j}}}$, $\cdots$

and examining the $i,j \to \infty$ limit. The resulting equations involving new, more complex q's with infinite numbers of filled conditioning sites, and thus an infinite hierarchy is generated in this fashion. Although the existence of well-behaved solutions is difficult to prove rigorously, it seems reasonable based on the structure of these equations, and particularly the capability to consistently handle the indeterminacy in the initial slopes.

The quantities describing the distribution of lengths of (horizontal) linear strings of filled sites are clearly the $n_s = f_{oa_s o} = f_s - 2f_{s+1} + f_{s+2}$. These, of course, will only reflect the distribution of cluster linear dimensions for fairly compact contiguous clusters. Since our arguments above indicate that $f_{s+1}/f_s \to \lambda(\theta)$, as $s \to \infty$, (compatible with Liggett's arguments described in the Introduction[15]) it follows that also $n_{s+1}/n_s \to \lambda(\theta)$, as $s \to \infty$. Thus for these nontrivial 2D filling processes, which are not amenable to exact solution, we anticipate that this distribution decays like $n_s \sim K(\theta)\, \lambda(\theta)^{s-1}$, as $s \to \infty$. To obtain estimates of $\lambda(\theta)$, which ranges from zero to unity as θ varies over this range, we could subject the above mentioned q hierarchy equations to Markovian-type truncation approximations. Of course, $\lambda(\theta) \equiv \theta$ for random filling, and we expect that these Markovian-type approximations will give reasonable estimates for weakly or moderately cooperative filling (cf. Section IV).

REFERENCES

1. J. W. Evans, D. R. Burgess and D. K. Hoffman, J. Chem. Phys. 79, 5011 (1983).
2. E. A. Boucher, Prog. Polym. Sci. 6, 63 (1978).
3. N. A. Platé and O. V. Noan, Adv. Polymer Sci. 31, 133 (1979).
4. R. Gomer, R. Wartman, and R. Lundy, J. Chem. Phys. 26, 1147 (1957); R. Gomer, Disc. Faraday Soc. 28, 23 (1959); Solid State Phys. 30, 94 (1975); R. Butz and H. Wagner, Surf. Sci. 63, 448 (1977).
5. J. B. Peri, J. Phys. Chem. 64, 220 (1965); J. B. Peri and M. Hensley, J. Phys. Chem. 72, 2926 (1968); M. Zamora and A. Cordoba, J. Phys. Chem. 82, 584 (1978).
6. G. J. M. Schmidt et al., "Solid State Photochemistry", Monographs in Modern Chemistry, Vol. 8 (Verlag Chemie, New York, 1976).
7. See, e.g., R. Zallen, "The Physics of Amorphous Solids", (Wiley, New York, 1983).
8. P. J. Flory, J. Am. Chem. Soc. 61, 1518 (1939).
9. T. H. K. Barron, R. J. Bawden and E. A. Boucher, J. Chem. Soc. 70, 651 (1974); F. Downton, J. R. Statistic Soc. B 23, 207 (1961); B. E. Blaisdell and H. Solomon, J. Appl. Prob. 7, 667 (1970).
10. N. A. Platé, A. D. Litmanovich, O. V. Noah, A. L. Toam and N. B. Vasilyev, J. Polym. Sci. 12, 2165 (1974).
11. M. G. Lagally, G.-C. Wang, and T.-M. Lu, CRC Crit. Rev. Solid State Sci. 7, 233 (1978); E. D. Williams, W. H. Weinberg, and A. C. Sobrero, J. Chem. Phys. 76, 1150 (1982).

12. T. M. Liggett, "The Stochastic Evolution of Infinite Systems of Interacting Particles", in Lecture Notes in Mathematics 598 (Springer, Berlin, 1976).

13. R. Durrett, Stoch. Proc. Applic. 11, 109 (1981); D. Griffeath, Stoch. Proc. Applic. 11, 151 (1981).

14. T. M. Liggett, "Interacting Particle Systems", Grundlehren der Mathematischen Wissenschaften, Vol. 276 (Springer, New York, 1985).

15. T. M. Liggett (Department of Mathematics, University of California at Los Angeles), private communication.

16. T. E. Harris, Ann. Prob. 5, 451 (1977); J. T. Cox, Ann. Prob. 12, 272 (1984).

17. M. Eden, in "Proceedings of the Fourth Berkeley Symposium on Mathematical Statistics and Probability", Vol. IV, Ed. J. Neyman (U. California Press, Berkeley, 1961).

18. D. Richardson, Proc. Camb. Phil. Soc. 74, 515 (1973).

19. R. Durrett and T. M. Liggett, Ann. Prob. 9, 186 (1981).

20. T. A. Witten and L. M. Sander, Phys. Rev. Lett. 47, 1400 (1982); Phys. Rev. B 27, 5686 (1983).

21. P. Meakin and T. A. Witten, Jr., Phys. Rev. B 28, 5632 (1983).

22. P. Meakin, Phys. Rev. Lett. 51, 1119 (1983); Phys. Rev. B 29, 2930 (1984); M. Kolb, R. Botet, and R. Jullien, Phys. Rev. Lett. 51, 1123 (1983); T. Vicsek and F. Family, Phys. Rev. Lett. 52, 1669 (1984). See also related articles in "Kinetics of Aggregation and Gelation", Ed. F. Family and D. P. Landau (North Holland, New York, 1984).

23. J. W. Evans and D. K. Hoffman, J. Stat. Phys. 36, 65 (1984).

24. J. B. Keller, J. Chem. Phys. 38, 325 (1963) and refs. therein; D. A. McQuarrie, J. P. McTague and H. Reiss, Biopolymers 3, 657 (1965).

25. R. L. Dobrushin, Probl. Peredachi Inf. 7, 57 (1971); L. G. Mityushin, Probl. Peredachi Inf. 9, 81 (1973).

26. N. O. Wolf, D. R. Burgess and D. K. Hoffman, Surf. Sci. 100, 453 (1980).

27. P. J. Reynolds, H. E. Stanley and W. Klein, J. Phys. A 10, L203 (1977).

28. J. W. Evans, D. R. Burgess and D. K. Hoffman, J. Math. Phys. 25, 3051 (1984).

29. See for example: F. Leyvraz and H. R. Tschudi, J. Phys. A 15, 1951 (1982); E. M. Hendricks, M. H. Ernst and R. M. Ziff, J. Stat. Phys. 31, 519 (1983).

30. When k_0, k_1, k_2 form an arthimetic progression, it has been noted (Ref. 10) that a single empty site shields, so, e.g., $f_{\underset{\sim}{0}_n} = f_0 q^{n-1}$, for $n>1$. [The proof uses that (2-1b) now also holds for n=1.] Here all empty subconfiguration probabilities factor in terms of q, f_0, and $f_{0\underline{\ell}0}$, so these determine all quantities.

31. E. Klesper, W. Gronski and V. Barth, Markromol. Chem. 160, 167 (1972); note that the "random statistics of blocks" described here is only approximately satisfied; J. J. Gonzalez and K. W. Kehr, Macromolecules 11, 996 (1978) and 12, 1231 (1979).

32. M. Higuchi and R. Senju, Polym. J. 3, 370 (1972).

33. J. W. Evans and R. S. Nord, Phys. Rev. A 31, 3831 (1985).

34. J. W. Evans and D. R. Burgess, J. Chem. Phys. 79, 5023 (1983).

35. E. A. Boucher, Trans. Faraday Soc. 69, 1839 (1973); J. J. Gonzalez, P. C. Hemmer, and J. S. Høye, Chem. Phys. 3, 228 (1974).

36. See for example: H. J. Herrmann, D. Staufer and D. P. Landau, J. Phys. A 16, 1221 (1983); R. B. Pandey, J. Stat. Phys. 34, 163 (1984).

PAPER V:

CLUSTER-SIZE DISTRIBUTIONS FOR IRREVERSIBLE COOPERATIVE FILLING OF LATTICES II: EXACT ONE-DIMENSIONAL RESULTS FOR NONCOALESCING CLUSTERS

CLUSTER-SIZE DISTRIBUTIONS FOR IRREVERSIBLE COOPERATIVE FILLING OF LATTICES II: EXACT ONE-DIMENSIONAL RESULTS FOR NONCOALESCING CLUSTERS

J. W. Evans and R. S. Nord

Ames Laboratory and Department of Chemistry
Iowa State University
Ames, Iowa 50011

ABSTRACT

We consider processes where the sites of an infinite, uniform, one-dimensional lattice are filled irreversibly and cooperatively, with the rates, k_i, depending on the number, $i = 0, 1, 2$, of filled nearest neighbors. Furthermore, we suppose that filling of sites with <u>both</u> neighbors already filled is <u>forbidden</u> so $k_2=0$. Thus clusters can nucleate and grow, but <u>cannot</u> coalesce. Exact truncation solution of the corresponding infinite hierarchy of rate equations for subconfiguration probabilities is possible. For the probabilities of filled s-tuples, f_s, as a function of coverage, $\theta \equiv f_1$, we find that $f_s/f_{s+1} = D(\theta)s + C(\theta,s)$, where $C(\theta,s)/s \to 0$, as $s\to\infty$. This corresponds to faster than exponential decay. Also if $\rho \equiv k_1/k_0$, then one has $D(\theta) \sim (2\rho\theta)^{-1}$, as $\theta\to 0$. The filled cluster-size distribution, n_s, has the same characteristics. Motivated by the behavior of these families of f_s/f_{s+1} versus s curves, we develop the natural extension of f_s to $s<0$. Explicit values for f_s, and related quantities, for "almost random" filling, $k_0=k_1$, are obtained from a direct statistical analysis.

I. INTRODUCTION

As in the preceding paper[1], we consider a class of filling processes where the sites of an infinite, uniform lattice fill, o→a, irreversibly with adsorption rates, k_i, depending on the number, i = 0, 1, ••• z, of (already) filled nearest neighbors (NN) to the site being filled (z is the lattice coordination number). Throughout f_σ will denote the probability of a subconfiguration, σ, of sites each specified empty 'o' or filled 'a'. For an infinite lattice, these satisfy an infinite hierarchy of rate equations which can be written down intuitively. The f_σ rate equation includes gain and loss terms corresponding to creation and destruction of σ, respectively, by single filling events, taking account of all allowed configurations of the influencing NN sites to the one being filled (and weighting with the appropriate rates)[1,2]. We shall assume that the lattice is initially empty, and note that time evolution via the hierarchial equations preserves invariance of f_σ's under all lattice space group operations (including translation and reflection). We shall sometimes also consider conditional probabilities $q_{\sigma\sigma'} \equiv f_{\sigma+\sigma'}/f_{\sigma'}$ of (conditioned) σ given (conditioning) σ'. For convenience, empty/filled conditioning sites $\bar{o}/\bar{a}$ will be denoted by ϕ/α. Also $o_n(a_n)$ will denote empty (filled) n-tuples of consecutive sites.

Here we focus on cases where some of the k_i are zero, in particular, where $k_i = 0$, for $i > i^*$, so the lattice will not fill completely. The saturation value of the coverage, θ, at infinite time, is denoted by $\theta^{sat} < 1$. Clearly $i^* = 1$ corresponds to random filling with NN blocking, so all

connected clusters of filled sites contain only one particle. The corresponding values of θ^{sat} have been determined exactly for a 1D lattice as $(1-e^{-2})/2 \approx 0.4323$[2,3], and approximately, via analytic methods, for a 2D hexagonal[4] (2D square[2]) lattice as 0.375 (0.365). When $i^* = 2$, so $k_2, k_3, \cdots = 0$ (and we set $\rho \equiv k_1/k_0$), the process involves competition between birth and growth of clusters, where the clusters cannot coalesce. Addition to clusters occurs at boundary sites with only one filled NN, so branched clusters develop in two or more dimensions (see Fig. 1). Such clusters should be compact (cf. Refs. 1,5) rather than fractal-like (cf. Ref. 6). The saturation coverage $\theta^{sat}(\rho)$, as a function of ρ, is shown in Fig. 2 for 1D linear, 2D hexagonal, and 2D square lattices. Note that $\lim_{\rho\to\infty} \theta^{sat}(\rho)$ gives the mean coverage within an individual (infinitely large) island provided that, at saturation, as $\rho\to\infty$, an infinitesimal fraction of lattice sites are at boundaries between clusters. When $i^* = z-1$ (i.e., $k_{z-1} = k_z = 0$), empty adjacent pairs of sites and single empty sites, surrounded by filled sites, remain at the end of the process. When $i^* = z$ (so only $k_z = 0$), then only isolated empty sites remain, and if $k_0 = k_1 = \cdots = k_{z-1}$ ("almost random" filling) then $\theta^{sat} = z/(z+1)$[2,7].

In this paper we consider, in detail, the 1D filling process where $k_0, k_1 \neq 0$, but $k_2 = 0$ (i.e., $i^* = z = 2$), so the growing contiguous clusters of filled sites cannot coalesce. Such a rate regime sometimes occurs in the consideration of irreversible cooperative reactions at the sites of a (1D) polymer chain[8]. The method of exact truncation solution of the hierarchial equations for arbitrary k_0, k_1, k_2, exploiting a shielding property of adjacent pairs of empty sites (see preceding paper and Refs.

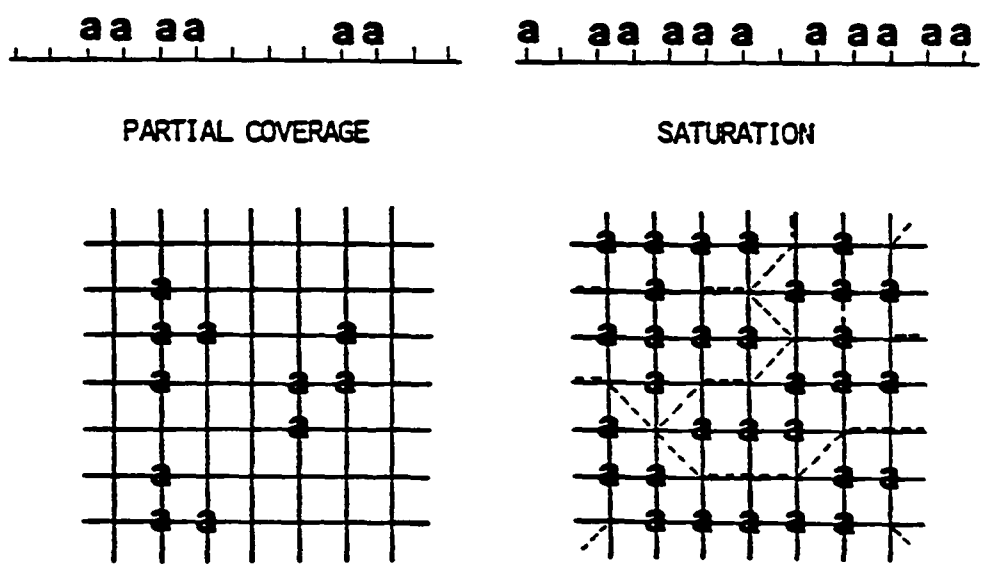

Figure 1: Growth of noncoalescing clusters where rates, k_i, for filling of sites with i filled NN are zero for $i > 2$. Illustrative partial coverage and saturation configurations are shown for a 1D linear and 2D square lattice

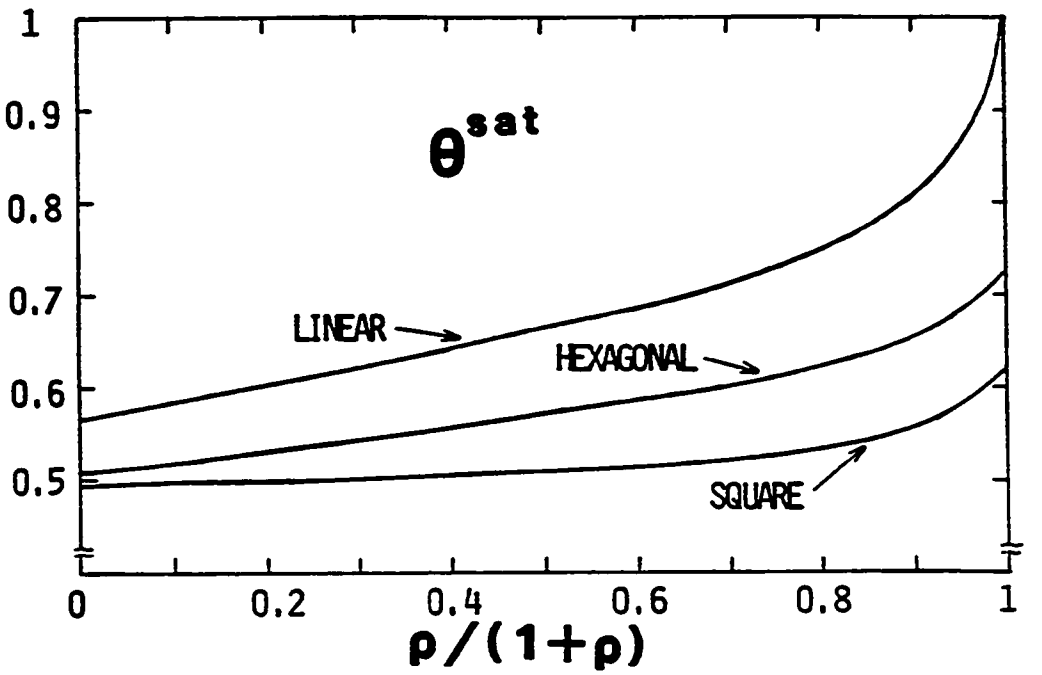

Figure 2: The saturation coverage $\theta^{sat}(\rho)$, for noncoalescing clusters grown as in Fig. 1 with rates $k_1/k_0 \equiv \rho$, $k_i/k_0 = 0$ for $i \geq 2$. Results for the 1D linear lattice are exact[2,3]. Results for the 2D hexagonal[4] and 2D square[2] lattices are obtained from approximate hierarchy truncation. (The truncated hexagonal lattice equations are identical to the exact $z = 3$ Bethe lattice equations, so the limitations of the corresponding results should be clear[4])

2,3,9), can be applied to this special case. Results presented here from such calculations clearly indicate a faster than exponential large size s decay of the filled s-tuple probabilities, $f_s \equiv f_{a_s}$, and of the (filled) cluster-size distribution, $n_s = f_{oa_so} = f_s - 2f_{s+1} + f_{s+2}$. Furthermore they suggest development of natural extensions of f_s and n_s to $s < 0$ to "complete the picture".

In Section II, we consider "almost random" filling, $k_0 = k_1$, $k_2 = 0$. We have noted previously[7] that a direct method of solution of the hierarchy (as an alternative to truncation) is available here. Furthermore, because of the relative simplicity of this single rate process, it is possible to directly determine the statistics. In Section III, we present extensive exact numerical calculations pertaining to the distribution of filled s-tuples (and, thus, the cluster-size distribution) for arbitrary k_0, k_1 (and $k_2 = 0$). The behavior of the average cluster size (without site weighting) is detailed. The structural features of the hierarchy leading to the observed "faster than exponential" asymptotic decay of f_s (or n_s) for large s are elucidated in Section IV. Specifically, we find that f_{s+1}/f_s, $n_{s+1}/n_s \sim (D(\theta)s)^{-1}$, as $s \to \infty$, and a novel method for the direct analysis of $D(\theta)$ is presented. Formal coverage (density) expansion techniques, appropriate to this process, have been developed previously, but we provide, for the first time, in Section V, examples of explicit (and generic) expressions for the first few expansion coefficients for probabilities of filled s-tuples of arbitrary size s. Since results of Section III show that f_s/f_{s+1} versus s curves approximate a family of straight lines nearly intersecting at some negative s value,

this motivates the development of a natural extension of f_s to $s<0$. Density expansions provide a natural mechanism to achieve this, and we indicate an alternative approach via extended truncation techniques. In Section VI, we summarize our findings, and present some corresponding results for a version of tne more complicated 1D process of monomer filling with NN blocking, and 2^{nd}-NN cooperative effects.

II. CLUSTER-SIZE DISTRIBUTION FOR 1D "ALMOST RANDOM" FILLING

$$k_0:k_1:k_2 = 1:1:0$$

For the special choice of rates $k_0 = k_1$ ($\equiv k$, say), $k_2 = 0$, corresponding to "almost random" filling, the process has some simplifying features which allow certain specialized methods of analysis to be implemented, as discussed below[2,7]. However, we expect (and shall see in Section III) that the qualitative features of the f_s (or n_s) distribution are preserved for $k_0 \neq k_1$ (and $k_2 = 0$).

The standard hierarchial truncation procedure for NN cooperative effects, which is based on the shielding property of empty pairs of sites and is used in the next section where $k_0 \neq k_1$, can of course be applied here[1-3,9]. Alternatively, one can exploit certain special features of "almost random" filling, specifically, that $f_{0_n} = e^{-nkt}$, $n \geq 2$, together with the highly restricted nature of the spatial correlations, to obtain exact solutions to the hierarchy (see Ref. 7). (Here the probability of any empty subconfiguration can be factored in terms of f_{0_n}, $f_{0\text{-}0}$, $f_{0\text{-}0\text{-}0}$, $f_{0\text{-}0\text{-}0\text{-}0}$, ...[7] (where - denotes a single site of unspecified state.)

A more direct and efficient approach for calculating subconfiguration probabilities for almost random filling follows from the observation that this process can be obtained from random filling (with rate k) by extracting, for each time t, the subensemble of "legal" fillings, where no site fills after both its NN are filled. To determine the probability, $f_{\{n\}}$, that the n sites {n} are filled at time t, it is convenient to introduce the extended set, $\{n^*\}$, including {n} and adjacent sites (so $n^* \geq$

n+2). Then clearly $f_{\{n\}}$ is given by the probability measure associated with those random fillings on $\{n^*\}$, with $\{n\}$ filled at time t, such that $\{n\}$ has filled legally. The calculation is simplest for the saturation value, $f^{sat}_{\{n\}}$, of $f_{\{n\}}$ which satisfies $f^{sat}_{\{n\}} = N_{\{n\}}/n^*!$, where $N_{\{n\}}$ is the number of ways (counting different orderings) of filling $\{n^*\}$, such that sites in $\{n\}$ fill "legally". The simplest and, here, most pertinent example is the saturation value of f_s, $f^{sat}_s = N_{s+2}/(s+2)!$, where N_{s+2} is the number of ways of filling s+2 sites by clustering around any of the s+2 possible nucleating sites. Clearly the number of ways of clustering about the i^{th} site in an m-site cluster is $\binom{m-1}{i-1}$, so $N_m = \sum_{i=1}^{m} \binom{m-1}{i-1} = 2^{m-1}$, and thus one has

$$f^{sat}_s = \frac{2^{s+1}}{(s+2)!} \quad , \quad \text{so} \quad f^{sat}_s/f^{sat}_{s+1} = \frac{s+3}{2} \ \text{(linear)} \quad . \tag{2.1}$$

We now expand on this calculation to obtain the probability, f_s, of a filled s-tuple at time t by considering various filling scenarios for the s sites of interest together with the ones on either end: (a) if both end sites are filled at time t, then we have exactly the same ordering constraints on filling as in the saturation calculation (2.1). Thus the contribution to f_s here is given by $P_{s+2} \equiv (1-e^{-kt})^{s+2}\, N_{s+2}/(s+2)!$. Here the first factor gives the random filling probability that s+2 sites are filled at time t, and the second accounts for ordering constraints; (b) if exactly one end site is empty at time t (probability $2e^{-kt}$), then the (conditional) probability that the other s+1 are filled is clearly P_{s+1}, so

that contribution to f_s here is $2e^{-kt} P_{s+1}$; (c) if both end sites are empty at time t (probability e^{-2kt}), then the (conditional) probability that the middle s are filled is clearly P_s, and the contribution to f_s here is $e^{-2kt} P_s$. Adding these contributions, we conclude that (see Ref. 10)

$$f_s \equiv f_{a_s} = \frac{2^{s+1}}{(s+2)!} [1 - e^{-kt}]^s [1 + s\, e^{-kt} + \frac{(s+1)(s+2)}{4} e^{-2kt}] \quad . \qquad (2.2)$$

The ratio, f_s/f_{s+1}, is plotted as a function of s (for various θ) in Fig. 3. This plot strongly motivates the extension of f_s to unphysical, $s<0$ as is automatically provided by (2.2), to "complete the picture". Note that (2.2) also implies that $f_s/f_{s+1} \sim \frac{1}{2}(1 - e^{-kt})^{-1} s + O(1)$, as $s \to \infty$.

Analogous calculations can be performed for probabilities of more complex subconfigurations such as those containing a filled s-tuple and a finite number of other filled sites (of fixed position relative to a_s), e.g., $f_s \equiv f_{a_s}$, f_{a_s-a}, f_{a_s-aa}, ···. These exhibit the same type of faster than exponential decay, when $s \to \infty$, as seen in (2.2). Clearly the most complicated part of these calculations is the combinatorics which are closely related to the saturation statistics. Thus below we list some more complicated examples illustrating the general characteristics of the combinatorial technique.

Consider first the saturation probability for a_s-a (where - denotes a single unspecified site). The appropriate extended configuration here consists of sites in a_s-a as well as the one to the left, i, in the gap, j, and to the right, k. Let M_s denote the appropriate number of ways of

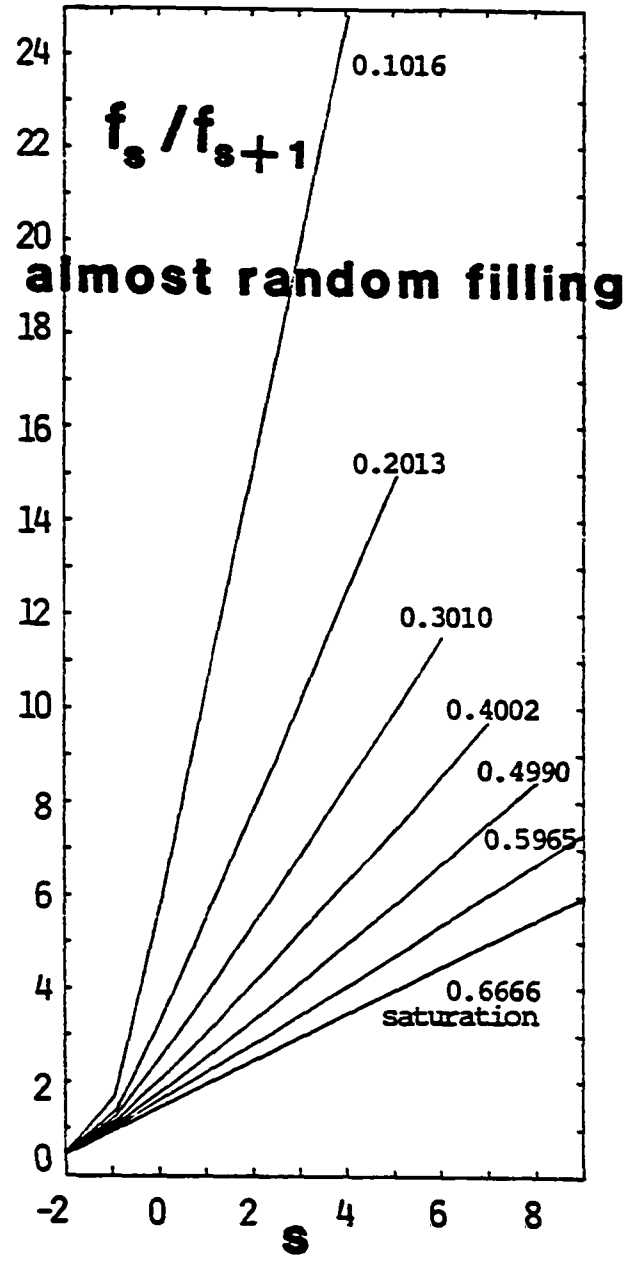

Figure 3: The ratio f_s/f_{s+1} as a function of s (for various θ, shown), for "almost random" filling ($k_0 : k_1 : k_2 = 1 : 1 : 0$)

filling this extended subconfiguration, so $f^{sat}_{a_s-a} = M_s/(s+4)!$, and let $N_{n,m} \equiv \binom{n+m}{m} N_n N_m$ denote the number of legal ways of filling <u>separated</u> clusters of n and m sites. Then in accordance with the rules prescribed above, M_s has contribution from when: (a) i fills last $[M_{s-1}]$; (b) the separated (s+1)-cluster (i, a_s) and 2-cluster (a, k) fill legally, then j fills $[N_{s+1,2}]$; (c) the (s+2)- cluster (i, a_s, k) fills, with a_s filling legally, and 'a' fills at sometime during this process, then k fills $[(s+3)\ N_{s+2}]$. Thus one obtains

$$M_s = M_{s-1} + N_{s+1,2} + (s+3)\ N_{s+2} = (s^2 + 5s + 8)\ 2^{s+1} \quad , \qquad (2.3)$$

where solution of the recursion relation (for <u>either</u> increasing <u>or</u> decreasing s) has used that $M_1 = 56$ (from a direct enumeration). From similar calculations, one can show that $f^{sat}_{a_s-aa} = P_s/(s+5)!$, where

$$P_s = P_{s-1} + N_{s+1,3} + M_s = \tfrac{1}{3}(s^3 + 9s^2 + 26s + 30)\ 2^{s+2} \quad , \qquad (2.4)$$

using $P_1 = M_2 = 176$, and that $f^{sat}_{a-a_s-a} = Q_s/(s+6)!$, where $Q_s = 2(s+5)[(s+4)\ M_{s-1} + M_s]$.

III. CLUSTER-SIZE DISTRIBUTION FOR 1D FILLING WITH NONCOALESCING CLUSTERS

$k_0:k_1:k_2 = 1:\rho:0$

Extensive calculations involving truncation of hierarchies for probabilities of connected and disconnected empty subconfigurations for this process lead to the results shown in Fig. 4 for f_s. Specifically, we have displayed f_s/f_{s+1} as a function of s (for various θ) and ρ = 1/5, 1/2, 2, 5. The behavior of the family of f_s/f_{s+1} vs. s curves (after connecting physical values for s = 1, 2, •••) suggests that we attempt to "naturally" extend f_s, and thus f_s/f_{s+1}, to nonphysical s = 0, -1, -2, •••. This is discussed in more detail in Section V and the Appendix where the special behavior of the cases ρ = 1/2 and ρ = 1 will be elucidated. It appears that, for each θ, f_s/f_{s+1} asymptotes to a line of constant slope, $D(\theta)$, as $s\to\infty$. It is clear, from Fig. 4, that $D(\theta)$ is infinite at $\theta=0$ and decreases monotonically with increasing θ.

Specifically, $D(\theta)$ is defined by the relation

$$f_s/f_{s+1} = D(\theta)s + C(\theta,s) \quad , \tag{3.1}$$

where $C(\theta,s)/s \to 0$, as $s\to\infty$. Equation (3.1) can be rewritten in the form

$$f_{s+1} = \theta/[D(\theta)^s s! \prod_{i=1}^{s} (1 + \frac{C(\theta,i)}{D(\theta)i})] \quad , \tag{3.2}$$

to clearly demonstrate the faster than exponential asymptotic decay. Note

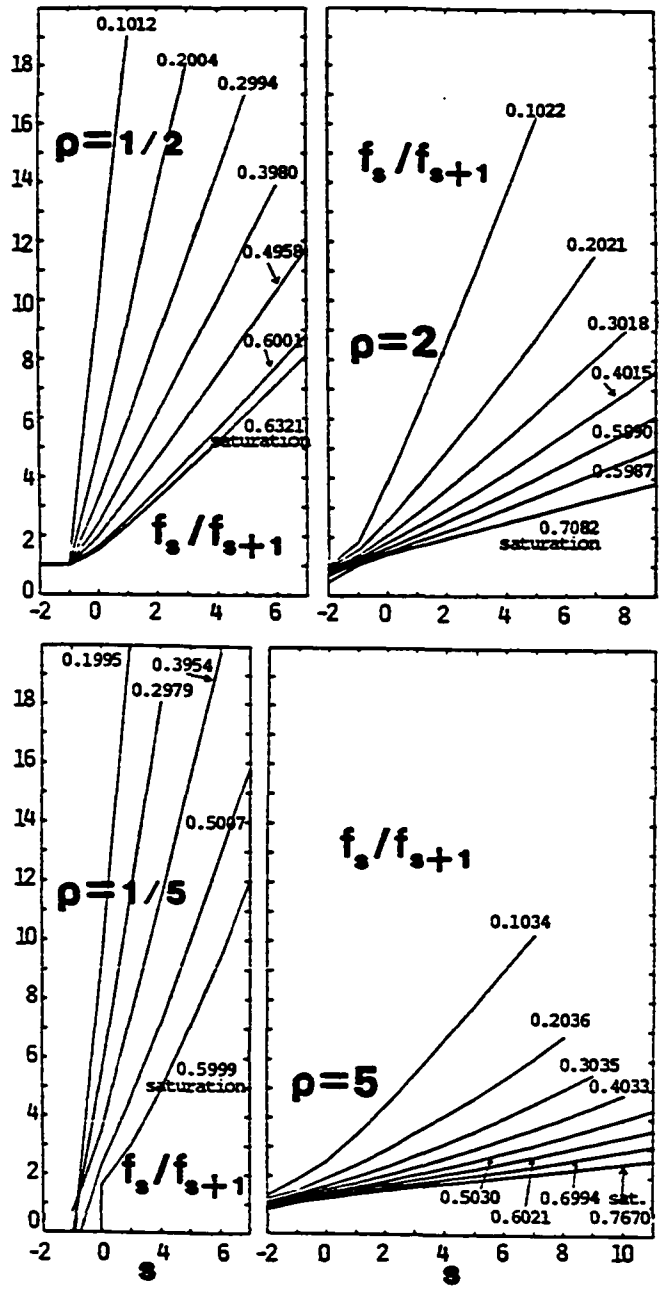

Figure 4: The ratios, f_s/f_{s+1}, as functions of s (for various θ, shown), for filling with NN cooperative effects with rates $k_0 : k_1 : k_2 = 1 : \rho : 0$ and $\rho = 1/5, 1/2, 2, 5$

that, typically, the factor $\prod_{i=1}^{s} \left(1 + \frac{C(\theta,i)}{D(\theta)i}\right)$ does <u>not</u> approach a constant as $s \to \infty$. [If $C(\theta,i) \sim C(\theta)$, as $i \to \infty$, then $\prod_{i=1}^{s} \left(1 + \frac{C(\theta,i)}{D(\theta)i}\right) \sim s^{C(\theta)/D(\theta)}$, as $s \to \infty$. For example, for "almost random" filling at saturation $\theta^{sat} = 2/3$, $D(\theta^{sat}) = 1/2$ and $C(\theta^{sat}) = 3/2$.] Clearly $n_s \equiv f_s - 2f_{s+1} + f_{s+2} \sim f_s$, as $s \to \infty$, exhibits the same behavior in this limit. To obtain the asymptotic behavior of f_s or n_s as a function of time, we must simply substitute the exact expression for $\theta = \theta(t)$ into (3.1,2)[1-3].

The large s asymptotic behavior of f_s (and n_s) exhibited here is quite different from the exponential decay characterizing cases where clusters can coalesce ($k_2 \neq 0$)[1]. The faster decay of the cluster-size distribution (or shift in weight to smaller clusters), when $k_2=0$, is not surprising since here smaller clusters cannot coalesce to form larger ones and, thus, remain frozen into the occupancy distribution.

Solution of the minimal closed hierarchy for f_{o_n}, using the shielding property of empty pairs, provides exact results for f_o, f_{oo} and $f_{o_n} = f_{oo}\, q^{n-2}$, for $n \geq 2$, where $q = e^{-k_0 t}$ [1-3,7]. Consequently, we can immediately determine the average cluster size (without site weighting)[1]

$$n_{av} \equiv \sum_{s=1}^{\infty} s n_s / \sum_{s=1}^{\infty} n_s \equiv \theta / f_{oa} \quad , \tag{3.3}$$

as a function of coverage or time, since $\theta \equiv 1 - f_o$, $f_{oa} \equiv f_o - f_{oo}$. At saturation $\theta = \theta^{sat}$, since $f_{oo} = 0$, one has [2] $n_{av}^{sat} = \theta^{sat}/(1-\theta^{sat})$. In

Fig. 5, we have shown n_{av}, as a function of θ, for various ρ. Note that $\rho \to 0+$ results in two stage filling of sites with zero, then one filled NN, respectively, and $n_{av} \to \infty$, as $\rho \to \infty$ (cf. Refs. (1,2)).

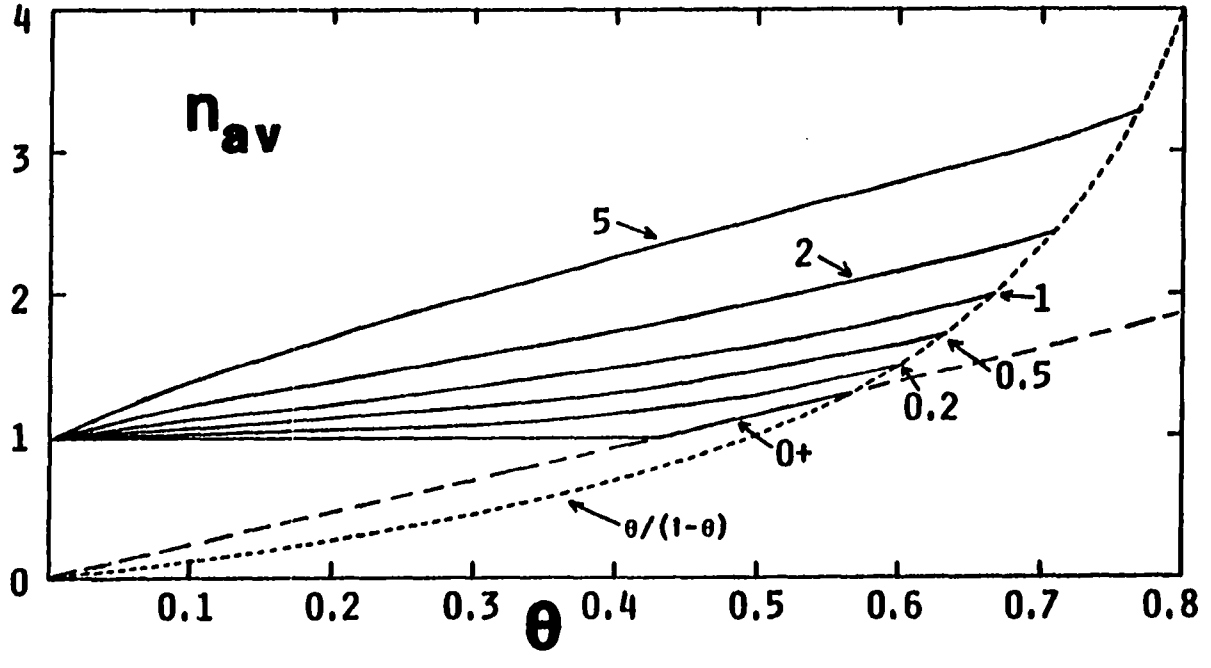

Figure 5: The average cluster size (without site weighting), $n_{av} \equiv \theta/f_{ao}$, as a function of coverage, θ, for filling with NN cooperative effects with rates $k_0 : k_1 : k_2 = 1 : \rho : 0$ (and various ρ, shown)

IV. ASYMPTOTIC ANALYSIS OF CLUSTER-SIZE DISTRIBUTION

It is desirable to understand those structural features of the hierarchy determining the asymptotic behavior of f_{s+1}/f_s, $n_{s+1}/n_s \sim (D(\theta)s)^{-1}$, as $s\to\infty$, here, and to develop a technique for determining asymptotic quantities, such as $D(\theta)$, more directly. The strategy adopted here is the same as that of the preceding paper[1], and involves taking appropriate limits of the suitably recast hierarchy equations. It will be convenient, in the following, to set $k_0 = 1$. This just corresponds to transforming to a chemical time scale, $t' = k_0 t$, and thus obviously does not affect the statistics.

The prime quantity of interest here is the asymptotic slope, $D(\theta)$. Thus one naturally attempts to obtain an equation satisfied by $D(\theta)$ directly. We begin by recasting the equation satisfied by $q_s \equiv q_{a\alpha_s} \equiv f_{s+1}/f_s$ in a suitable form motivated by the identity $q_s^{-1} - q_{s-1}^{-1} = D(\theta) + \Delta C(\theta,s)$. Here α_s denotes a filled s-tuple of conditioning sites, and $\Delta C(\theta,s) \equiv C(\theta,s) - C(\theta,s-1)$. Since

$$d/dt\ q_s^{-1} = -\ q_s^{-1}\ d/dt\ \ell n\ q_s = -\ q_s^{-1}[d/dt\ \ell n\ f_{s+1} - d/dt\ \ell n\ f_s]\ , \quad (4.1)$$

where $d/dt\ f_s = 2\rho f_{ooa_{s-1}} = 2\rho[f_{a_{s-1}} - f_{a_s} - f_{a-a_s} + f_{a_{s+1}}]$, one can show that

$$(2\rho)^{-1}\, d/dt\, (q_{s+1}^{-1} - q_s^{-1}) = (q_s^{-1} - q_{s+1}^{-1})\,[(q_s^{-1} - q_{s-1}^{-1}) - (g_s^{-1} - g_{s-1}^{-1})]$$
$$+ q_s^{-1}(q_{s+1} - q_s) - q_{s+1}^{-1}\,(q_{s+2} - q_{s+1})$$
$$- q_{s+1}^{-1}\,[(q_{s+1}^{-1} - 2q_s^{-1} + q_{s-1}^{-1}) - (g_{s+1}^{-1} - 2g_s^{-1} + g_{s-1}^{-1})] \quad . \tag{4.2}$$

In (4.2), we have set $g_s \equiv f_{s+1}/f_{a-a_s} \equiv q_s/q_{a-\alpha_s}$, so

$$g_s^{-1} = q_{a-\alpha_\infty}\, D(\theta)s + K(\theta,s) \quad , \tag{4.3}$$

where $K(\theta,s)/s \to 0$, as $s\to\infty$. The existence of a finite limit $q_{a-\alpha_\infty} \equiv \lim_{s\to\infty} q_{a-\alpha_s}$ is supported by exact numerical calculations (see Fig. 6), and will be discussed further below. In general, we anticipate that $q_{a-\alpha_\infty}$ varies monotonically from zero, when $\theta=0$, to unity, at saturation.

To procede further, we must make some additional assumptions about the behavior of $C(\theta,s)$ and $K(\theta,s)$. First we note that if $\Delta C(\theta,s) \to 0$, as $s\to\infty$, then $(q_{s+1}^{-1} - q_s^{-1}) \to D(\theta)$, as $s\to\infty$, and so (4.2) does, in fact, become an equation for $D(\theta)$ in the $s\to\infty$ limit. Second, we note that if $\Delta^2 C(\theta,s) \equiv C(\theta,s) - 2C(\theta,s-1) + C(\theta,s-2)$ and $\Delta^2 K(\theta,s)$ satisfy $s\Delta^2 C(\theta,s)$, $s\Delta^2 K(\theta,s) \to 0$, as $s\to\infty$, then the last term of (4.2) vanishes in this limit. Clearly one also has that $q_s^{-1}(q_{s+1} - q_s) \to 0$, as $s\to\infty$, from the assumption that $C(\theta,s)/s\to 0$, as $s\to\infty$. [We remark that $\Delta H(s) \to 0$, $s\Delta^2 H(s) \to 0$, as $s \to \infty$, are satisfied by any function $H(s) = k\, s^{\alpha}$ where $\alpha<1$, and since, from numerical

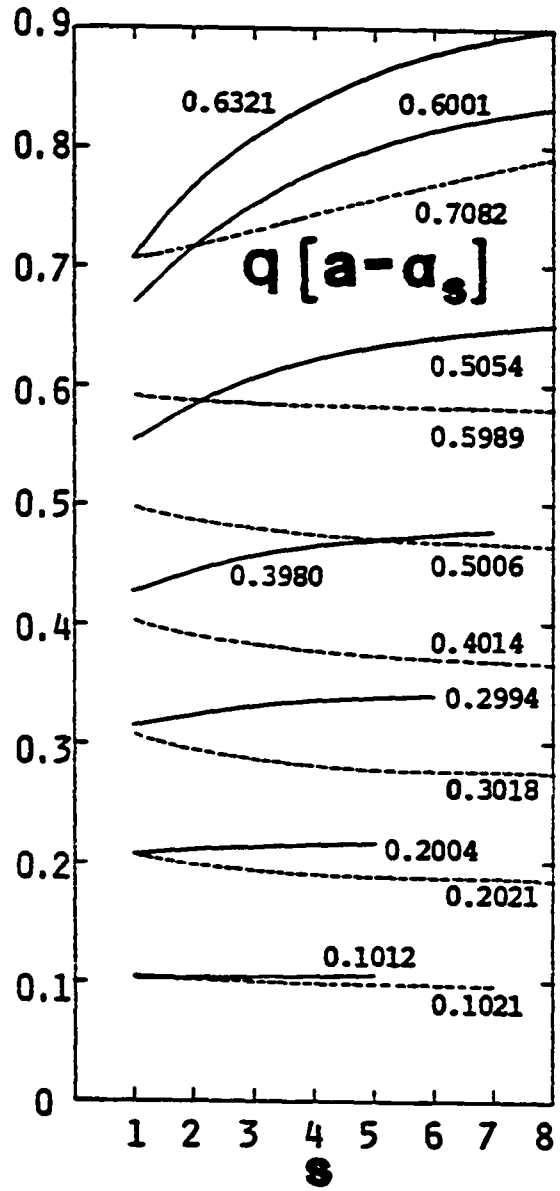

Figure 6: The quantity $q_{a-\underset{\sim}{\alpha}_s} \equiv f_{a-\underset{\sim}{a}_s}/f_{\underset{\sim}{a}_s}$ as a function of s (for various θ, shown) for rates $k_0 : k_1 : k_2 = 1 : \rho : 0$ with $\rho = 1/2$ (——) and $\rho = 2$ (---)

results, the functions $C(\theta,s)$ (see Fig. 7) and $K(\theta,s)$ (see Fig. 8) do not appear to have any oscillatory behavior, the above assumptions seem reasonable.] Thus we conclude that

$$d/dt\ D(\theta) = -2\rho D(\theta)^2\ (1 - q_{a\text{-}\alpha_\infty}) \quad , \tag{4.4}$$

which, since $D(0)^{-1} = 0$, is conveniently rewritten as

$$d/dt\ (D(\theta)^{-1}) = 2\rho(1 - q_{a\text{-}\alpha_\infty}) \quad . \tag{4.5}$$

The form of (4.5) is consistent with our assertion that $q_{a\text{-}\alpha_\infty} = 1$ at saturation. Since $q_{a\text{-}\alpha_\infty} = 0$, when $\theta = 0$, we conclude, from (4.5), that $D(\theta)^{-1} \sim 2\rho t$, as $t \to 0$, and since $d\theta/dt = f_{ooo} + 2\rho f_{aoo}$, so $\theta \sim t$ as $t \to 0$, it follows that

$$\theta D(\theta) \sim \frac{1}{2\rho} \quad , \quad \text{as } \theta \to 0 \quad . \tag{4.6}$$

One naturally continues to derive an equation for $q_{a\text{-}\alpha_\infty}$ by starting with

$$d/dt\ \text{ln}\ q_{a\text{-}\alpha_s} = d/dt\ \text{ln}\ f_{a\text{-}a_s} - d/dt\ \text{ln}\ f_{a_s} \tag{4.7}$$

Gain terms from filling of the disconnected a-site in $f_{a\text{-}a_s}$ present no

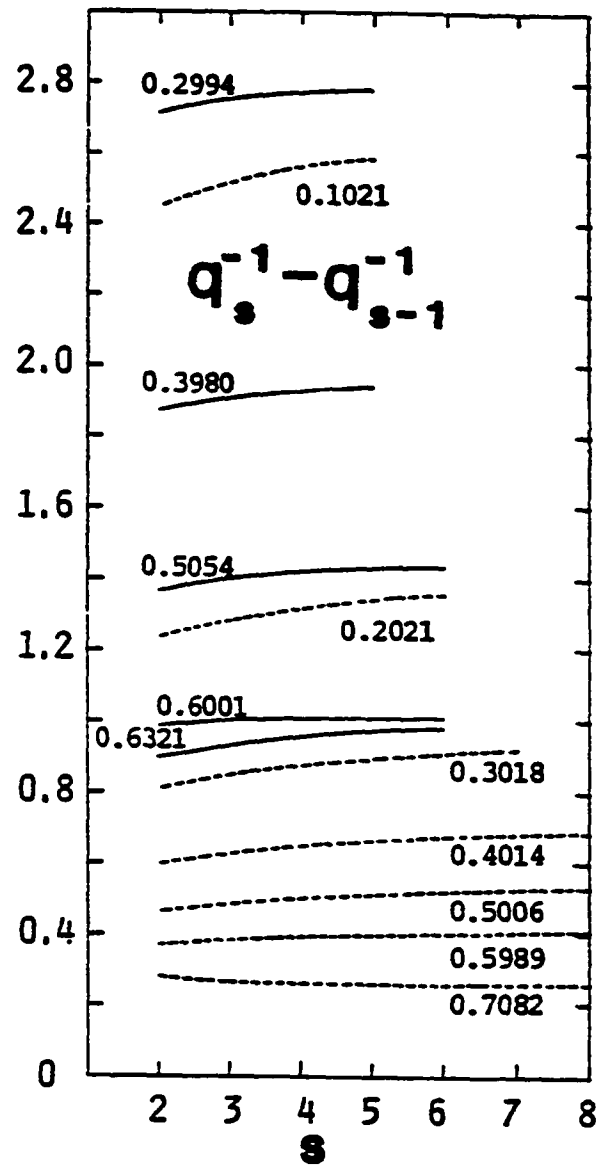

Figure 7: The quantity $q_s^{-1} - q_{s-1}^{-1} = \Delta C(\theta,s) + D(\theta)$ as a function of s, (for various θ, shown), for rates $k_0 : k_1 : k_2 = 1 : \rho : 0$ with $\rho = 1/2$ (——) and $\rho = 2$ (---)

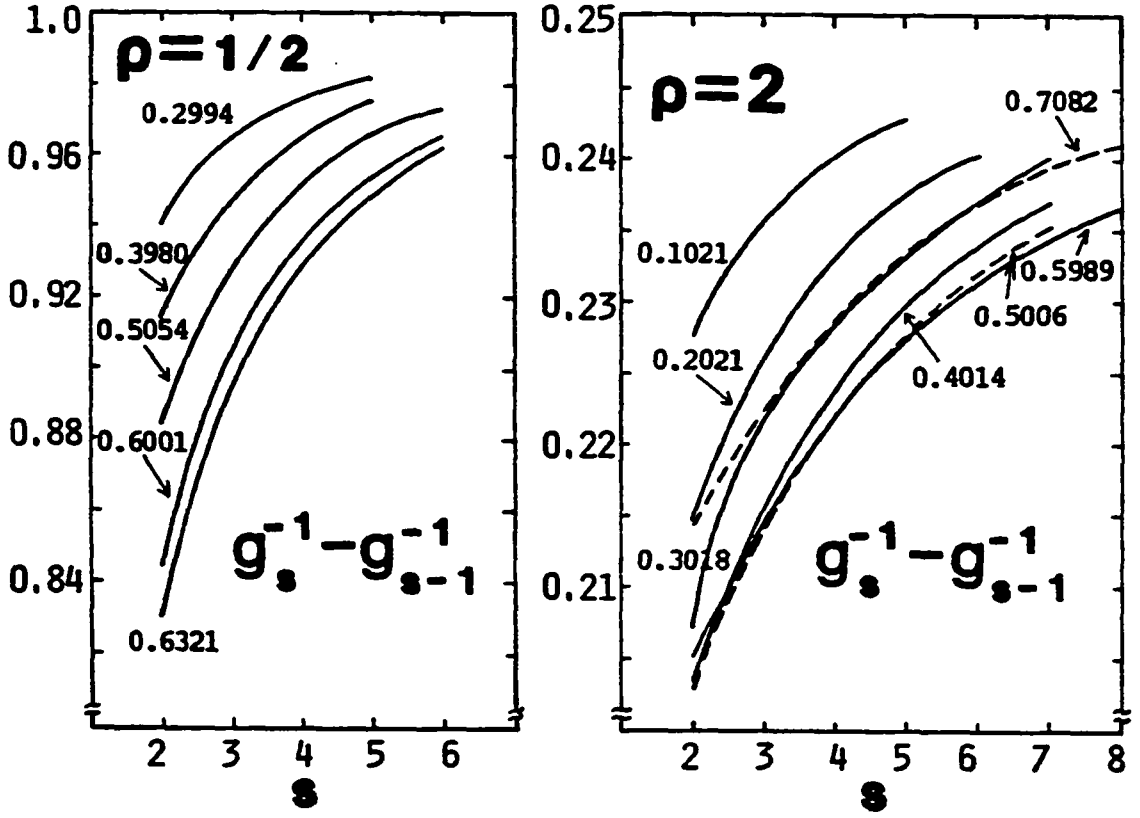

Figure 8: The quantity $g_s^{-1} - g_{s-1}^{-1} = \Delta K(\theta,s) + q_{a-\alpha_\infty} D(\theta)$ as a function of s (for various θ, shown), for rates $k_0 : k_1 : k_2 = 1 : \rho : 0$ with $\rho = 1/2, 2$

difficulty in the $s\to\infty$ limit, where they can be written in terms of $q_{a-\alpha_\infty}$, $q_{a--\alpha_\infty}$ and $q_{a\alpha-\alpha_\infty}$. The difference in gain terms from filling of the rightmost a_s-site in f_{a-a_s} and f_{a_s} approaches zero, as $s\to\infty$, provided $s(q_{\alpha-\alpha_{s-1}a} - q_{\alpha_{s-1}a})$, $s^2(q_{\alpha-\alpha_{s-1}a} - q_{\alpha_{s-1}a}) \to 0$, as $s\to\infty$. The latter can be easily verified for almost random filling at saturation, and seems reasonable in general. Corresponding cancellation of gain terms from filling of the leftmost a_s-site in f_{a-a_s} and f_{a_s}, as $s\to\infty$, is less clear. However direct verification is again possible for almost random filling at saturation, and truncation results suggest general validity. One should now continue to derive equations for such quantities as $q_{a--\alpha_\infty}$, $q_{\alpha a-\alpha_\infty}$, etc.

Finally we note that the above analysis of $q_{a-\alpha_\infty}$ can be circumvented by observing that Fig. 8 suggests $q_{a-\alpha_\infty} D(\theta)$ is (at worst, almost) constant, i.e., θ independent. Using (4.6) and assuming that $q_{a-\alpha_\infty} \sim \theta$, as $\theta\to 0$, it follows that this constant is $\frac{1}{2\rho}$. Substituting $q_{a-\alpha_\infty} = [2\rho D(\theta)]^{-1}$ into (4.5) and integrating yields

$$D^{-1}(t) = 2\rho(1-e^{-t}) \quad , \tag{4.8}$$

which is consistent with our exact numerical results (to within the substantial uncertainty of D values), and recovers the exact closed form results of Section II for "almost random" filling, $\rho=1$.

V. RESULTS FROM THE DENSITY EXPANSION TECHNIQUE

Formal density (coverage) expansion techniques have been developed which apply to general irreversible cooperative filling processes, including the one of interest here. (See Ref. (11) for a detailed discussion.) We now give the first demonstration of how these can be used to obtain explicit, and generic expressions for the first few expansion coefficients, for probabilities of filled s-tuples of arbitrary size, s. Again we set $k_0 = 1$, so $k_1 = \rho$.

One starts by writing down the hierarchial rate equations for subconfigurations with all sites specified filled and using conservation of probability to close this set. One thus obtains,

$$d/dt\ f_a = f_{ooo} + 2\rho f_{aoo}$$
$$= 1 + (2\rho-3)f_a + (2-2\rho)f_{aa} + (1-2\rho)f_{a-a} + (2\rho-1)f_{aaa}\ , \quad (5.1a)$$

$$d/dt\ f_s = d/dt\ f_{a_s} = 2\rho f_{oa_{s-1}}$$
$$= 2\rho[f_{s-1} - f_s - f_{a-a_{s-1}} + f_{s+1}] \quad , \quad \text{for } s \geq 2 \quad , \quad (5.1b)$$

$$\vdots$$

To obtain density expansions, we divide (5.1a) into the rest of (5.1) and formally expand the denominators to obtain $(d/dt)/(df_a/dt) = d/d\theta$ equations, e.g.,

$$d/d\theta\ f_s = 2\rho[f_{s-1} - f_s - f_{a-a_{s-1}} - (2\rho-3)\ f_{s-1}\ f_1 + \cdots] \quad . \qquad (5.2)$$

For the probability $f_{\{n\}}$ of n filled sites $\{n\}$, we postulate a density expansion of the form $f_{\{n\}} = \sum_{p=0}^{\infty} A_p^{\{n\}} \theta^{n+p}$. Then substitution into the d/dθ equations, and equating coefficients of equal powers of θ, yields a series of recursion relations for the coefficients $A_p^{\{n\}}$. For example, from (5.2), one immediately obtains

$$sA_0^s = 2\rho\ A_0^{s-1} \quad , \qquad (5.3a)$$

$$(s+1)\ A_1^s = 2\rho[A_1^{s-1} - A_0^s - A_0^{a-a_{s-1}} - (2\rho-3)\ A_0^{s-1}\ A_0^1] \quad , \qquad (5.3b)$$

$$\vdots$$

where $A_0^s \equiv A_0^{a_s}$.

In solving these relations, we need boundary values for s = 1, which come from the d/dθ versions [e.g., (5.2)] of the nongeneric equations [e.g., (5.1a)]. Using $A_p^1 = \delta_{p,0}$ (since $f_1 \equiv \theta$), (5.3a) can be solved to obtain

$$A_0^s = 2^{s-1}\ \rho^{s-1}/s! \quad . \qquad (5.4)$$

For any irreversible filling process, the lead coefficient in the expansion for some filled subconfiguration probability is given by the average of

products of reduced rates (i.e., rates scaled so that the rate for filling a site on an empty lattice is unity) corresponding to all possible ordered fillings creating the subconfiguration. (Each time a site is filled, an appropriate reduced rate factor is included.) The result (5.4) for A_0^s should now be clear in light of the analysis leading to (2.2), i.e., $A_0^s = N_s \rho^{s-1}/s!$. Clearly, zeroeth order coefficients for separated clusters factorize so $A_0^{a-a_s} = A_0^1 A_0^s = A_0^s$. Next (5.3b) can be solved, and one can continue to solve (successively more complex) recursion relations for coefficients of higher order (with respect to p), and for more complex subconfigurations, yielding, e.g.,

$$f_s = \frac{2^{s-1}\rho^{s-1}}{s!}\theta^s - [(s+4)\rho - (s+2)]\frac{(s-1)2^{s-1}\rho^{s-1}}{(s+1)!}\theta^{s+1}$$

$$+ [3(s^3 + 11s^2 + 30s + 8)\rho^2 - 6(s^3 + 8s^2 + 18s + 2)\rho$$

$$+ s(3s^2 + 17s + 32)]\frac{(s-1)2^{s-2}\rho^{s-1}}{3(s+2)!}\theta^{s+2} + \cdots \qquad (5.5a)$$

$$f_{a-a_s} = \frac{2^{s-1}\rho^{s-1}}{s!}\theta^{s+1} + [4\rho^2 - (s+1)(s^2 + 5s - 2)\rho$$

$$+ (s+1)(s^2 + 3s - 2)]\frac{2^{s-1}\rho^{s-1}}{(s+2)!}\theta$$

$$\vdots \qquad (5.5b)$$

Of course, results for "almost random" filling are obtained from (5.5) after setting $\rho=1$. Note that the relations (5.3) can be solved recursively for both increasing and decreasing s. In fact (5.5), with the convention that $(s!)^{-1} = 0$ for $s = -1, -2, \cdots$, incorporate the latter solutions and provide density expansions for unphysical $s\leq 0$ quantities (to be exploited below).

Clearly density expansions provide natural extensions of f_s, and related quantities, to unphysical $s\leq 0$ (as strongly motivated by Figs. 3 and 4 to make these plots more "complete"). A more fundamental and flexible formulation of this extension is based on the observation that the rate equations for such quantities as f_{a_s}, f_{a-a_s}, f_{o_n}, $f_{o_n a_s}$, $f_{o_n a_s o_m}$, $\cdots$ achieve a generic form when all of s, n, m, $\cdots \geq 2$. It is thus natural to extend the use of these generic equations to lower integral values of these labels, thus providing the basic defining rate equations for the unphysical quantities. Formal solution via density expansions of these extended equations automatically recovers such results as (5.5) for $s\leq 0$. However, the advantage of dealing directly with hierarchial rate equations for unphysical quantities is that one may be able to develop alternative closed form methods of solution, avoiding potential slow convergence problems[11] of density expansions. Such extended truncation methods are described in the Appendix, and have been applied to generate values for f_s, with $s\leq 0$, used in Fig. 4. We note, however, that the density expansion results were required here to provide initial values for various unphysical quantities, e.g., from (5.5a) one has $f_0 = \frac{1}{2\rho}$, $f_{-1} = \frac{3\rho-1}{2\rho^2}$, $f_{-2} = \frac{12\rho^2-15\rho+5}{4\rho^3}$, $\cdots$ at $t = 0$.

VI. DISCUSSION

We have considered irreversible, cooperative filling of an infinite, uniform, 1D lattice with rates, k_i, depending on the number, i, of filled NN, and $k_2 = 0$ (so clusters cannot coalesce). Exact truncation solution of the complicated infinite hierarchy of rate equations describing time evolution here demonstrates that probabilities for filled s-tuples, f_s, as well as the cluster-size distribution, n_s, exhibits faster than exponential decay for large s. This is not surprising when compared with the corresponding exponential decay characterizing processes with coalescing clusters. In fact, it is apparent from analyses analogous to that presented in Section IV, that for any 1D irreversible filling processes where no clusters coalesce, the same type of faster than exponential decay of the cluster-size distribution will occur. [Extension of this sort of analysis to higher-dimensional processes is also possible (cf. Ref. 1).]

To support the above proposition, we now present some results for 1D monomer filling with NN blocking and 2^{nd}-NN cooperative effects[12,13]. Here, if $\hat{k}_i$ denotes the filling rate with i filled 2^{nd}-NN, then $\hat{k}_2 = 0$ (and $\hat{\rho} \equiv \hat{k}_1/\hat{k}_0$), so clusters cannot coalesce. Thus both empty triples (••aoaoooaoa••) and empty pairs (••aoaooaoa••) remain at saturation marking boundaries between clusters. Here we let $\hat{f}_s$ denote the probability of the subconfiguration aoaoa•••oaoa, where s a-filled sites appear. In Fig. 9, we have plotted $\hat{f}_s/\hat{f}_{s+1}$ versus s, for various θ and $\hat{\rho} = 1/2, 1, 2$. Clearly $\hat{f}_s/\hat{f}_{s+1} \sim \hat{D}(\theta)s + o(s)$, as $s \to \infty$, and it appears that $\theta\hat{D}(\theta) \sim \frac{1}{2\hat{\rho}}$, as $\theta \to 0$, and $\hat{D}(\theta^{sat}) = 1/\hat{\rho}$. From a treatment analogous to that of Section IV (setting

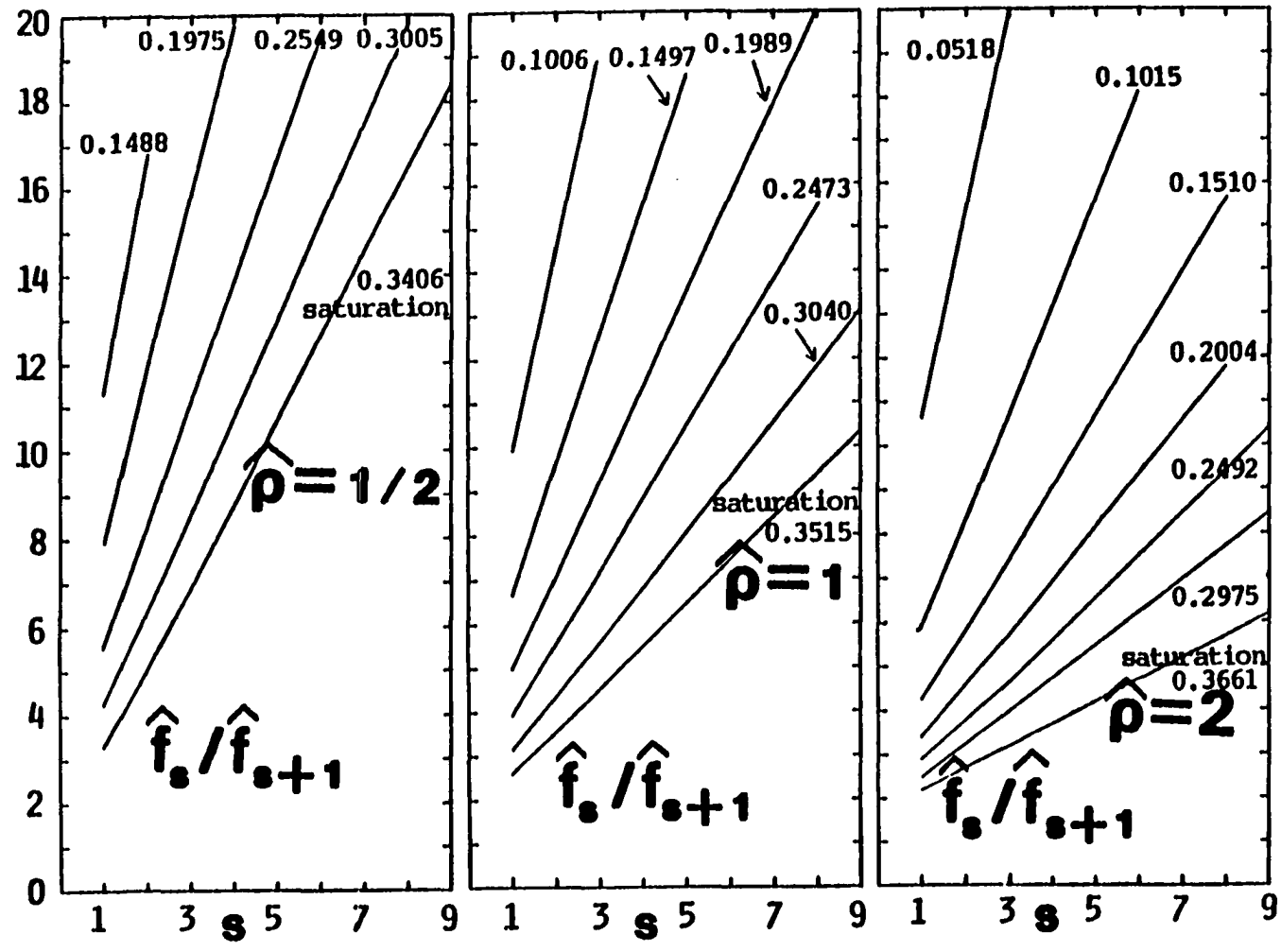

Figure 9: The ratio $\hat{f}_s/\hat{f}_{s+1}$ as a function of s (for various θ, shown), for filling with NN blocking and 2^{nd}-NN cooperative effects with rates $\hat{k}_0 : \hat{k}_1 : \hat{k}_2 = 1 : \hat{\rho} : 0$ and $\hat{\rho} = 1/2, 1, 2$

$\hat{k}_0 = 1$), one can show that

$$d/dt[\hat{D}(\theta)^{-1}] = 2\hat{\rho}(1 - q_{a-\alpha-\alpha-\alpha-\cdots} - q_{a--\alpha-\alpha-\alpha-\cdots}) \quad , \qquad (6.1)$$

which immediately confirms the postulated low-θ $\hat{D}$ behavior. Also the sum of the q's appearing in (6.1) is clearly unity at saturation, as required. If one assumes that these q's are identically equal, and that the product(s) $q\hat{D}$ are constant $(\frac{1}{2\hat{\rho}})$, then one obtains $\hat{D}(t)^{-1} = \hat{\rho}(1 - e^{-2t})$. This recovers the postulated saturation behavior, and is not inconsistent with our (uncertain) $\hat{D}$ estimates, but further analysis should be undertaken here. The behavior of the average cluster size[13], $\hat{n}_{av} \equiv \theta/f_{aoo}$, where $f_{aoo} = f_{oo} - f_{ooo}$, is shown in Fig. 10.

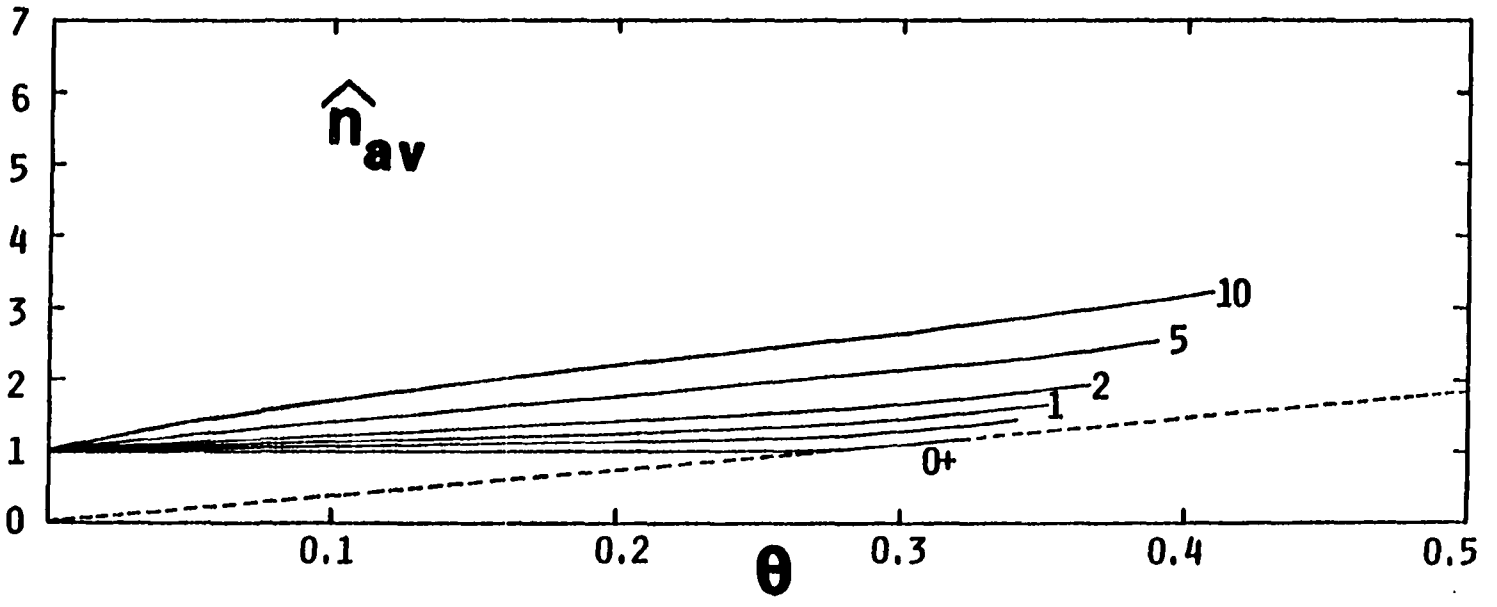

Figure 10: The average island size (without site weighting), $\hat{n}_{av} \equiv \theta/f_{aoo}$, as a function of coverage, for filling with NN blocking and 2nd-NN cooperative effects with $\hat{k}_0 : \hat{k}_1 : \hat{k}_2 = 1 : \rho : 0$ (and various $\hat{\rho}$, shown)

ACKNOWLEDGEMENTS

Ames Laboratory is operated for the U.S. Department of Energy by Iowa State University under Contract No. W-7405-ENG-82. This work was supported by the Office of Basic Energy Sciences.

APPENDIX: EXTENDED TRUNCATION TECHNIQUES; DETERMINATION OF f_s WITH $s < 0$

The primary goal here is determine exactly f_s, with $s<0$, by first obtaining f_{ooa_j}, with $j<-1$, and then integrating the generic equations

$$d/dt\ f_s = 2\rho f_{ooa_{s-1}} \quad , \quad \text{for integer } s \quad , \tag{1}$$

(setting $k_0=1$, so $k_1=\rho$). We first illustrate the appropriate extension of the shielding property of an adjacent pair of empty sites. Let us start with the generic hierarchial equations,

$$d/dt\ f_{o_m a_j o_n} = (4 - 4\rho - n - m)\, f_{o_m a_j o_n} + (\rho-1)\left[f_{o_{m+1} a_j o_n} + f_{o_m a_j o_{n+1}}\right] + \rho\left[f_{o_{m+1} a_{j-1} o_n} + f_{o_m a_{j-1} o_{n+1}}\right] \quad , \quad \text{for } m, n, j \geq 2 \quad , \tag{2}$$

and extend their application to $j = 1, 0, -1, -2, \cdots$ which, incidentally, closes this set of equations. Comparison of (2), for $j = 1$, with the $f_{o_m a o_n}$ equation provides one consistency relation satisfied by $f_{o_{m+1} a_0 o_n}$ and $f_{o_m a_0 o_{n+1}}$. Choice of initial conditions for the unphysical $f_{o_m a_j o_n}$, $j = 0, -1, \cdots$ follow from the analysis presented below. The main point that we wish to emphasize here is that equation (2), for $m, n \geq 2$ and j integer, is clearly compatible with the generalized (oo-Markovian) shielding property:

$$f_{o_m a_j o_n} = q^{m+n-4} f_{ooa_j oo} \quad , \quad \text{for } m, n \geq 2,\ j \text{ integral} \quad . \tag{3}$$

Extended generic equations for $f_{o_m a_j o}$ [$f_{o_m a_j}$] or the reflected quantity, with $m > 2$, couple to the extended set (2) and, together, they form a closed set. The main point for us is that these extended equations are compatible with the generalized (oo-Markovian) shielding property

$$f_{o_m a_j o} = q^{m-2} f_{ooa_j o} \quad [f_{o_m a_j} = q^{m-2} f_{ooa_j}] \quad ,$$

$$\text{for } m > 2 \quad , \quad j \text{ integral} \quad . \tag{4}$$

However, since $f_{o_m a_j} = f_{o_m a_j o} + f_{o_m a_j a} = f_{o_m a_j o} + f_{o_m a_{j+1} o} + f_{o_m a_{j+2}} = \cdots$, these quantities can alternatively (and consistently) be determined directly from $f_{o_p a_r o}$ and physical quantities.

Equating the r.h.s. of the generic $f_{o_m a_j o_n}$, $f_{o_m a_j o}$ and $f_{oa_j o}$ [$f_{o_m a_j}$ and f_{oa_j}] equations, for $j=1$, with those of the $f_{o_m a o_n}$, $f_{o_m a o}$ and f_{oao} [$f_{o_m a}$ and f_{oa}] equations, respectively, yields

$$\rho(f_{o_{m+1} a_0 o_p} + f_{o_m a_0 o_{p+1}}) = f_{o_{m+p+1}} \quad , \quad \text{for } m, p > 1 \quad , \tag{5a}$$

$$[\rho(f_{o_{m+1} a_0} + f_{o_m a_0 oo}) = f_{o_{m+2}} + \rho f_{o_{m+1} a} \quad , \quad \text{for } m > 1 \quad] \quad . \tag{5b}$$

Thus, using (3), we obtain from (5a)

$$f_{o_m a_0 o_n} \equiv \frac{1}{2\rho} f_{o_{m+n}} \quad , \quad \text{for } m + n > 3; \; m, n > 1 \quad . \tag{6}$$

Compatibility of (5a) and (5b) follows from the observation that

$$f_{o_m a_0} \equiv f_{o_m a_0 a} + f_{o_m a_0 o} \equiv f_{o_m a} + f_{o_m a_0 o} \equiv f_{o_m} - (1 - \tfrac{1}{2\rho})\, f_{o_{m+1}} ,$$

$$\text{for } m > 2 . \tag{7}$$

We naturally continue to compare expressions for $d/dt\, f_{o_m a_0 o_n}$ [$d/dt\, f_{o_m a_0 o}$] and $d/dt(\frac{1}{2\rho}\, f_{o_{m+n}})$ [$d/dt\, (\frac{1}{2\rho}\, f_{o_{m+1}})$] which, using (5a)[(8a)] and (3), implies that

$$f_{o_m a_{-1} o_n} = \frac{2\rho - 2}{(2\rho)^2}\, f_{o_{m+n-1}} , \quad \text{for } m, n > 2 , \tag{8a}$$

$$f_{o_m a_{-1} o} \equiv \frac{-1}{2\rho}\, f_{o_m} + \frac{1}{\rho}(1 - \tfrac{1}{2\rho})\, f_{o_{m+1}} , \quad \text{for } m > 2 . \tag{8b}$$

Consequently, one also has

$$f_{o_m a_{-1}} \equiv f_{o_m a_{-1} a} + f_{o_m a_{-1} o} \equiv f_{o_m a_0} + f_{o_m a_{-1} o}$$

$$\equiv (1 - \tfrac{1}{2\rho})[f_{o_m} - (1 - \tfrac{1}{\rho}) f_{o_{m+1}}] , \quad \text{for } m > 2 . \tag{9}$$

Repeating this procedure in the obvious way, and defining $f^o_m = q^{m-2} f_{oo}$, for all m[14], yields

$$f_{o_m a_{-j} o_n} = \frac{(2\rho-2)(2\rho-1)(2\rho)\cdots(2\rho+k-3)}{(2\rho)^{j+1}} f^{o}_{m+n-j} \ ,$$

$$\text{for } m,\ n \geq 2\ ,\ j \geq 0\ . \tag{10}$$

Rather complicated expressions also follow for $f_{o_m a_{-j}}$, for $m \geq 2$, $j \geq 2$, which can, however, readily be shown to contain the factor $(1 - \frac{1}{\rho})(1 - \frac{1}{2\rho})$, e.g.,

$$f_{o_m a_{-2}} = (1 - \tfrac{1}{\rho})(1 - \tfrac{1}{2\rho})[-f^{o}_{m-1}/(2\rho) + (1+\tfrac{1}{\rho})f^{o}_{m} - (1 - \tfrac{1}{\rho})f^{o}_{m+1}] \ ,$$

$$\text{for } m \geq 2. \tag{11}$$

Substituting (7, 9, 11, ...) for m=2 into (1) and integrating, using initial conditions from the density expansion (5.5a), determines $f_1 \equiv f_a$ (consistently), f_0, f_{-1}, ... One can easily check that $f_0 = 1 - (1 - \frac{1}{2\rho})\, f_{oo}$. Since $d/dt\ f_{-j} \propto (2\rho-1)(\rho-1)$, for $j \geq 1$, clearly such f_{-j} are constant when $\rho = 1$ ("almost random" filling), or 1/2 (where $k_0 : k_1 : k_2 = 1 : 1/2 : 0$ forms an arithmetic progression, and the distribution is o-Markovian[9]).

REFERENCES

1. R. S. Nord, D. K. Hoffman and J. W. Evans, Phys. Rev. A 31, 3820 (1985).

2. J. W. Evans, D. R. Burgess and D. K. Hoffman, J. Chem. Phys. 79, 5011 (1983).

3. J. B. Keller, J. Chem. Phys. 38, 325 (1963) and refs. therein; D. A. McQuarrie, J. P. McTague and H. Reiss, Biopolymers 3, 657 (1965).

4. J. W. Evans, J. Math. Phys. 25, 2527 (1984).

5. M. Eden, in "Proceedings of the Fourth Berkeley Symposium on Mathematical Statistics and Probability", Vol. IV, Ed. J. Neyman (U. of California Press, Berkeley, 1961); D. Richardson, Proc. Comb. Phil. Soc. 74, 515 (1973).

6. "Kinetics of Aggregation and Gelation", Ed. F. Family and D. P. Landau (North Holland, New York, 1984).

7. J. W. Evans and D. K. Hoffman, J. Stat. Phys. 36, 65 (1984).

8. P. A. Rempp, Pure Appl. Chem. 46, 9 (1976); N. A. Plate, in "Reactions on Polymers", Nato Adv. Study Inst. Series, ed. J. A. Moore (Reidel, Boston, 1973).

9. N. A. Platé and O. V. Noah, Adv. Polymer Sci. 31, 133 (1979) and refs. therein.

10. We are indebted to a referee who suggested the following formulation of "almost random" filling, and applied it to obtain (2.2). Let U_i, i = •• -1, 0, +1, •••, be independent random variables with exponential distributions of mean k^{-1} [$Pr(U_i>x) = e^{-kx}$]. Then the "almost random" filling model at time t is obtained by filling each site i unless either $U_i>t$, or $U_i>\max(U_{i-1}, U_{i+1})$. Probabilities of filled subconfigurations are straightforwardly obtained by evaluating the exponential measure of the corresponding region in U_i-space for an appropriate finite set of integers i.

11. J. W. Evans, Physica 123A, 297 (1984); D. K. Hoffman, J. Chem. Phys. 65, 95 (1976).

12. E. A. Boucher, Faraday Trans. II 69, 1839 (1973); J. J. Gonzalez, P. C. Hemmer and J. S. Høye, Chem. Phys. 3, 228 (1974).

13. J. W. Evans and D. R. Burgess, J. Chem. Phys. 79, 5023 (1983).

14. The quantities $f^o_m = q^{m-2} f_{oo}$ provide a "natural" extension of f_{o_m} to m<1, since they satisfy the generic equations $d/dt\ f^o_m = (2-2\rho-m) f^o_m + 2(\rho-1) f^o_{m+1}$' for all m.

PAPER VI:

RANDOM WALKS ON FINITE LATTICES WITH MULTIPLE TRAPS: APPLICATION TO PARTICLE-CLUSTER AGGREGATION

RANDOM WALKS ON FINITE LATTICES WITH MULTIPLE TRAPS: APPLICATION TO PARTICLE-CLUSTER AGGREGATION

J. W. Evans and R. S. Nord

Ames Laboratory and Department of Chemistry
Iowa State University
Ames, Iowa 50011

ABSTRACT

For random walks on finite lattices with multiple (completely adsorbing) traps, one is interested in the mean walk length until trapping, and in the probability of capture for the various traps (either for a walk with a specific starting site, or for an average over all nontrap sites). We develop the formulation of Montroll to enable determination of the large-lattice-size asymptotic behavior of these quantities. (Only the case of a single trap has been analyzed in detail previously.) Explicit results are given for the case of symmetric nearest-neighbor random walks on 2D square and triangular lattices. Procedures for exact calculation of walk lengths on a finite lattice with a single trap are extended to the multiple trap case to determine all the above quantities. We examine convergence to asymptotic behavior as the lattice size increases. Connection with Witten-Sander irreversible particle-cluster aggregation is made by noting that this process corresponds to designating all sites adjacent to the cluster as traps. Thus, capture probabilities for different traps determine the proportions of the various shaped clusters formed. (Reciprocals of) associated average walk lengths relate to rates for various irreversible aggregation processes involving a gas of walkers and clusters. Results are also presented for some of these quantities.

I. INTRODUCTION

Extensive results are available characterizing random walks on a finite lattice of N sites (with periodic boundary conditions) having a single (completely adsorbing) trap, ℓ_T[1-5]. The basic quantities of interest are the mean number of steps until trapping, $\langle n \rangle_\ell$, for walks starting from various lattice sites $\ell \neq \ell_T$ (the trap position). These, of course, have a natural interpretation as first passage times on a corresponding perfect lattice. The characteristics of the lattice-averaged walk length, $\langle n \rangle = (N-1)^{-1} \sum_{\ell \neq \ell_T} \langle n \rangle_\ell$, are of particular interest.

For sites, ℓ_T^*, adjacent to ℓ_T, one has that $\langle n \rangle_{\ell_T^*} = N-1$ for walks with jumps to neighboring sites only, independent of lattice structure[2]. For general $\ell = (\ell_1, \ell_2, \cdots)$ on a hypercubic lattice, where all sites except $\ell_T = (0,0,\cdots)$ have identical jump rates p(m) [for a jump of $(m_1, m_2, \cdots)$ lattice vectors], we define $\sigma_k^2 = \sum_k m_k^2\, p(m)$ and $\|\ell\| = (\sum_k \ell_k^2/\sigma_k^2)^{1/2}$. Then one has that

$$\langle n \rangle_\ell \sim \left(\frac{2}{\pi\sigma_1\sigma_2} \ln \|\ell\| + O(1)\right) N \quad , \quad \text{in 2D} \quad , \tag{1.1a}$$

$$\sim \left(u + O(\|\ell\|^{2-d})\right) N \quad , \quad \text{in } d > 3D \quad , \tag{1.1b}$$

for large $\|\ell\|$ ($\ll N$), where u^{-1} (= 0.340537... for a simple cubic lattice) is the probability of escape (i.e., nonreturn) for a walker starting at the origin on an infinite, perfect lattice. From (1.1), it is also clear

that[3]

$$\langle n \rangle \sim \frac{N \ell n\, N}{2\pi\sigma_1\sigma_2} \quad \text{in 2D} \quad , \quad \sim uN \quad \text{in } d>3D \quad , \tag{1.2}$$

where we have used that $\ell n \, \|\ell\| \sim \ell n \, N^{1/2}$ for most contributions in 2D. If S_n denotes the mean number of <u>distinct</u> sites visited by an n-step walk on an infinite perfect lattice, then one can show that (1.2) implies[6a] $S_{\langle n \rangle} \sim N$. This result, if also true for the corresponding finite lattice S_n, has the interpretation that the walker, on average, visits all distinct nontrapping sites once before being trapped.[6b] Another perspective on the behavior of $\langle n \rangle$ follows from assuming that the (average) probability for trapping on the n^{th} step is $(1 - 1/N)^{S_{n-1}} \, 1/N$, so that $\langle n \rangle \sim \sum_{n=1}^{\infty} n \, (1 - 1/N)^{S_{n-1}} \, 1/N$ (which has been shown to agree with (1.2) in d>3D)[7].

Efficient algorithms, exploiting lattice symmetry, have been developed to calculate $\langle n \rangle_{\ell}$ (and thus $\langle n \rangle$) directly and exactly for finite lattices (results for $N \sim 10^3$ are readily obtained)[8-10]. Such results for $\langle n \rangle$ have been compared with those obtained from the first few terms of large N asymptotic expansions whose first terms are given by (1.2). There is close agreement even for small lattice sizes. These techniques can be readily adapted to model modifications such as biased walks, and alternative boundary conditions.

Montroll has extended the above formulation to characterize a random walk in the presence of multiple (completely adsorbing) traps, denoted here by $L = \{\ell_T^1, \ell_T^2, \cdots, \ell_T^t\}$ for t traps[11]. Again the site-specific walk

lengths until trapping, $\langle n \rangle_\ell$, for $\ell \notin L$, and the average walk length, $\langle n \rangle = (N-t)^{-1} \sum_{\ell \notin L} \langle n \rangle_\ell$, are of particular interest. As the appropriate expressions for these quantities are rather complicated, little specific analysis has been given. The above discussion suggests that here, provided all trap separations are O(1), (1.2) should still hold in 2D. Consequently the influence of multiple traps (as compared with a single trap) will only be seen in the coefficient of the O(N) correction term. However for d>3D, $\lim_{N\to\infty} \langle n \rangle / N$ should be lowered from u by the presence of multiple traps. This behavior will be confirmed below. The above single trap procedures for direct calculation of $\langle n \rangle_\ell$ can be extended to the multiple-trap case, but ease of calculation is greatly enhanced by the presence of trap-lattice symmetries. The concept of lattice decimation[9], wherein successively larger regions of the lattice are replaced by traps, also provides some systematic simplifying features. For the multiple-trap case, trapping or capture probabilities for individual traps are nontrivial for walks starting from a specific site. (The trap-specific mean walk lengths are also nontrivial.) One can have traps of distinct symmetry for t>3, and, in this case, lattice averaged trapping probabilities become nontrivial and lattice averaged trap-specific walk lengths vary from $\langle n \rangle$. Finally we note that there has been some analysis of the case of a periodic array of traps (on a periodic lattice)[12].

This multiple-trap problem has obvious application to the description of particle-cluster aggregration where a single randomly walking particle, upon reaching a site adjacent to the immobile cluster, sticks (or coalesces) irreversibly (cf. the Witten-Sander model for the diffusion

limited aggregation of fractal-like clusters[13]). Here sites adjacent to the cluster are assigned as (completely adsorbing) traps, i.e., one decimates sites adjacent to the appropriate cluster shaped set of (trap) sites (see Fig. 1). We note that the cluster shape distribution in the Witten-Sander model is determined by the characteristics of an appropriate set of $N \to \infty$ trapping probabilities.[13] Calculation of site-specific walk lengths allows determination of the average over all sites external to the decimated cluster. (Reciprocals of) such average walk lengths relate to rates of destruction of immobile clusters, with a specific shape, by irreversible aggregation with walkers in a gas of random walkers and immobile clusters. Determination of shape-specific cluster creation rates requires more detailed knowledge of trap-specific capture probabilities.

Before outlining this contribution, we describe briefly work on other aspects of, and models for, multiple-trap problems. One can consider the effect of traps on the probability of return to tne origin (for finite or infinite lattice)[14]. Problems involving a random distribution of traps naturally arise in modeling exciton transport in photosynthetic processes. Processes where "regular" sites have a nonzero trapping probability were also considered here. There is a large body of work directed at analyzing transport/diffusion characteristics of walks on imperfect lattices[14].

In Section II, we first review Montroll's generating function formulation for walks on a finite lattice with multiple traps[11]. Expressions for trapping probabilities are introduced, and these together with Montroll's expressions for walk lengths are expressed in a simplified, more convenient form. Explicit expressions are given in cases of just a few

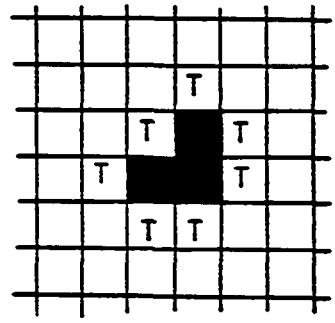

Figure 1: Aggregation with a bent trimer; adjacent sites which have been decimated to traps are denoted by T

traps. For lattice averaged walk lengths, we give some indication of behavior for large connected compact clusters of traps. Explicit large N asymptotic results are given in Section III for symmetric, nearest-neighbor random walks on a square lattice. There is also some discussion of the corresponding triangular lattice problem. In Section IV, we show how matrix techniques for exact calculation of walk lengths, on finite lattices with a single trap, extend simply to the multiple-trap case and can also be used to calculate trapping probabilities. The relationship of the matrix structure and (reduced) walk lengths for a decimated problem to those of the original problem is elucidated. Extensive numerical results are given for the case of a square lattice. Finally some concluding remarks are made in Section V, and application of these results to particle-cluster aggregation models is indicated.

II. GENERATING FUNCTION FORMULATION AND ANALYSIS OF THE MULTIPLE-TRAP PROBLEM

The development presented here is based on that of Montroll[11]. The set of t traps is denoted by $L = \{\ell_T^1, \ell_T^2, \cdots \ell_T^t\}$. The most basic quantity for this process is the probability, $P_n(\ell)$, that the walker is at site ℓ after n steps, given that it started at ℓ^0, so $P_0(\ell) = \delta_{\ell,\ell^0}$. The corresponding generating function is given by $P(\ell) = \sum_{n=0}^{\infty} z^n P_n(\ell)$. Since clearly $\sum_{\ell} P_n(\ell) = 1$, for all n, one has that $\sum_{\ell} P(\ell) = (1 - z)^{-1}$.

The probability of trapping (or capture) at $\ell_T^i \equiv \ell^i$ is trivially $P_\infty(\ell^i) \equiv \lim_{n\to\infty} P_n(\ell^i)$. Since one has

$$(1-z)\, P(\ell^i) \equiv \sum_{n=1}^{\infty} z^n [P_n(\ell^i) - P_{n-1}(\ell^i)] \equiv P_\infty(\ell^i) + (1-z) \sum_{n=1}^{\infty} z^n [P_n(\ell^i) - P_\infty(\ell^i)], \tag{2.1}$$

it follows that

$$P_\infty(\ell^i) = \lim_{z\to 1} (1-z)\, P(\ell^i) \quad . \tag{2.2}$$

Since the probability of trapping at ℓ^i on the n^{th} step is $P_n(\ell^i) - P_{n-1}(\ell^i)$, we conclude that the mean walk length, $\langle n \rangle_{\ell^0 \to \ell^i}$, from ℓ^0 to ℓ^i is given by

$$\langle n \rangle_{\ell^0 \to \ell^i} = \frac{\sum_{n=1}^{\infty} n[P_n(\ell^i) - P_{n-1}(\ell^i)]}{\sum_{n=1}^{\infty} [P_n(\ell^i) - P_{n-1}(\ell^i)]} = \frac{\frac{\partial}{\partial z}\{(1-z)\ P(\ell^i)\}_{z=1}}{P_\infty(\ell^i)} \quad . \qquad (2.3)$$

It is now clear that the mean walk length from ℓ^0 for capture at any trap is[11]

$$\langle n \rangle_{\ell^0} = \frac{\partial}{\partial z}\{(1-z)[P(\ell^1) + P(\ell^2) + \cdots + P(\ell^t)]\}_{z=1} \quad . \qquad (2.4)$$

Montroll has provided expressions for $P(\ell)$ in terms of the generating function, $G(\ell)$, for random walks (starting at the origin) on a corresponding perfect lattice, as[11]

$$P(\ell) = G(\ell - \ell^0) + \sum_{k=1}^{t} [(1-z)\ G(\ell - \ell^k) + \delta_{\ell,\ell^k}]\ P(\ell^k) \quad . \qquad (2.5)$$

A simultaneous set of equations is provided by (2.5) for the $P(\ell^k)$. Solving these by Cramer's rule yields[11]

$$P(\ell^k) = (1-z)^{-1} \begin{vmatrix} G_{11} & \cdots & G_{1\,k-1} & G_{10} & G_{1\,k+1} & \cdots & G_{1t} \\ G_{21} & & G_{2\,k-1} & G_{20} & G_{2\,k+1} & & G_{2t} \\ G_{31} & & G_{3\,k-1} & G_{30} & G_{3\,k+1} & & G_{3t} \\ \vdots & & \vdots & \vdots & \vdots & & \vdots \end{vmatrix} \Big/ \det\{G_{ij}\} \ , \qquad (2.6)$$

where $G_{ij} = G(\ell^i - \ell^j) = G_{ji}$, and i,j in $\det\{G_{ij}\}$ run from 1 through t.

Equation (2.6) allows calculation of various quantities for a walker starting at a specific site, ℓ^0. Corresponding averages over $\ell^0 \notin L$ can be obtained in terms of

$$\bar{P}(\ell^k) = \frac{1}{N-t} \sum_{\ell^0 \notin L} P(\ell^k) \quad . \tag{2.7}$$

Since $\sum_{\ell^0 \notin L} G_{j0} = \sum_{\ell^0} G_{j0} - \sum_{k=1}^{t} G_{jk}$, and $\sum_{\ell_0} G_{j0} = \sum_n z^n \sum_{\ell^0} G_n(\ell^j - \ell^0) = (1-z)^{-1}$, we conclude that

$$(1-z)\bar{P}(\ell^k) = \frac{-1}{N-t} + \frac{1}{(N-t)(1-z)} \begin{vmatrix} G_{11} & \cdots & G_{1\,k-1} & 1 & G_{1\,k+1} & \cdots & G_{1t} \\ G_{21} & & G_{2\,k-1} & 1 & G_{2\,k+1} & & G_{2t} \\ \vdots & & \vdots & \vdots & \vdots & & \vdots \end{vmatrix}$$

$$/ \det \{G_{ij}\}. \tag{2.8}$$

To reduce these expressions further, it is necessary to analyze in more detail the generating function, $G(\ell)$, for random walks on a perfect lattice. For a finite periodic d-dimensional lattice where $N=L^d$, one has that

$$G(\ell) = \frac{1}{L^d} \left(\prod_{j=1}^{d} \sum_{k_j=0}^{L-1} \right) \exp(2\pi i \ell \cdot k/L)/[1-z\lambda(2\pi k/L)] \quad , \tag{2.9}$$

where $\lambda(\theta) = \sum_{\ell} p(\ell) \exp(i\ell\cdot\theta)$, so

$$G(\ell) = \frac{1}{N(1-z)} + \Phi(\ell,z) \quad , \tag{2.10}$$

and $\Phi(\ell,1)$ is finite. Previous detailed analysis has shown that[2]

$$\Phi(0,z) \sim \{c_1 \ell n\, N + c_2 + c_3 N^{-1} + \cdots\} + O(1-z)^{1/2} \quad , \quad \text{in 2D} \quad , \qquad (2.11a)$$

where $c_1 = (2\pi\sigma_1\sigma_2)^{-1}$ for a square lattice, and the first few c_i have been calculated for various 2D lattices. One can also deduce from previous work that

$$\Phi(0,z) \sim \{u + c_2 N^{-1/d} + \cdots\} + O(1-z) \quad , \quad \text{in } d>3D \quad . \qquad (2.11b)$$

Given these results, we naturally make the decomposition $\Phi(\ell,z) = \Phi(0,z) + \varepsilon(\ell,z)$, and express quantities of interest in terms of $\Phi(0,z)$ and $\varepsilon_{ij} = \varepsilon(\ell^i-\ell^j,z)$ as $z\to 1$.

The first step is to exhibit explicitly, through $G(0)$ factors, any $z\to 1$ singular behavior in the determinants appearing in (2.6) and (2.8). We thus note that

$$\begin{vmatrix} G_{11} & \cdots & G_{1\,k-1} & 1 & G_{1\,k+1} & \cdots \\ G_{21} & & G_{2\,k-1} & 1 & G_{2\,k+1} & \\ \vdots & & \vdots & & \vdots & \end{vmatrix} = \begin{vmatrix} \varepsilon_{11} & \cdots & \varepsilon_{1\,k-1} & 1 & \varepsilon_{1\,k+1} & \cdots \\ \varepsilon_{21} & & \varepsilon_{2\,k-1} & 1 & \varepsilon_{2\,k+1} & \\ \vdots & & \vdots & \vdots & \vdots & \end{vmatrix} \text{(non-singular)}, \qquad (2.12a)$$

$$\begin{vmatrix} G_{11} & \cdots & G_{1\,k-1} & G_{10} & G_{1\,k+1} & \cdots \\ G_{21} & & G_{2\,k-1} & G_{20} & G_{2\,k+1} & \\ \vdots & & \vdots & \vdots & \vdots & \end{vmatrix}$$

$$= G(0)\begin{vmatrix} \varepsilon_{11}-\varepsilon_{10} & \cdots & \varepsilon_{1\,k-1}-\varepsilon_{10} & 1 & \varepsilon_{1\,k+1}-\varepsilon_{10} & \cdots \\ \varepsilon_{21}-\varepsilon_{20} & & \varepsilon_{2\,k-1}-\varepsilon_{20} & 1 & \varepsilon_{2\,k+1}-\varepsilon_{20} & \\ \vdots & & \vdots & \vdots & \vdots & \end{vmatrix}$$

$$+ \begin{vmatrix} \varepsilon_{11} & \cdots & \varepsilon_{1\,k-1} & \varepsilon_{10} & \varepsilon_{1\,k+1} & \cdots \\ \varepsilon_{21} & & \varepsilon_{2\,k-1} & \varepsilon_{20} & \varepsilon_{2\,k+1} & \\ \vdots & & \vdots & \vdots & \vdots & \end{vmatrix}, \qquad (2.12b)$$

and

$$\det\{G_{ij}\} = G(0)\left\{\begin{vmatrix} 1 & \varepsilon_{12} & \cdots & \varepsilon_{1t} \\ 1 & \varepsilon_{22} & & \varepsilon_{2t} \\ \vdots & \vdots & & \vdots \end{vmatrix} + \begin{vmatrix} \varepsilon_{11} & 1 & \varepsilon_{13} & \cdots & \varepsilon_{1t} \\ \varepsilon_{21} & 1 & \varepsilon_{23} & & \varepsilon_{2t} \\ \vdots & \vdots & \vdots & & \vdots \end{vmatrix} + \cdots \right.$$

$$\left. + \begin{vmatrix} \varepsilon_{22} & \cdots & \varepsilon_{1\,t-1} & 1 \\ \varepsilon_{21} & & \varepsilon_{2\,t-1} & 1 \\ \vdots & & \vdots & \vdots \end{vmatrix}\right\} + \det\{\varepsilon_{ij}\} \quad . \qquad (2.13)$$

Note that the symmetric sum over determinants (2.12a), or over those constituting the coefficient of G(0) in (2.12) equals

$$\begin{vmatrix} 1 & \varepsilon_{12}-\varepsilon_{11} & \cdots & \varepsilon_{1t}-\varepsilon_{11} \\ 1 & \varepsilon_{22}-\varepsilon_{21} & \cdots & \varepsilon_{2t}-\varepsilon_{21} \\ \vdots & \vdots & & \vdots \end{vmatrix} = \begin{vmatrix} \varepsilon_{11}-\varepsilon_{12} & 1 & \varepsilon_{13}-\varepsilon_{12} & \cdots & \varepsilon_{1t}-\varepsilon_{12} \\ \varepsilon_{12}-\varepsilon_{22} & 1 & \varepsilon_{23}-\varepsilon_{22} & & \varepsilon_{2t}-\varepsilon_{22} \\ \vdots & \vdots & \vdots & & \vdots \end{vmatrix}$$

$$= \cdots \ (\equiv S_t, \text{ say}). \qquad (2.14)$$

It now follows that

$$P_\infty(\ell^k) = \begin{vmatrix} \varepsilon_{11}-\varepsilon_{10} & \cdots & \varepsilon_{1\,k-1}-\varepsilon_{10} & 1 & \varepsilon_{1\,k+1}-\varepsilon_{10} & \cdots \\ \varepsilon_{21}-\varepsilon_{20} & & \varepsilon_{2\,k-1}-\varepsilon_{20} & 1 & \varepsilon_{2\,k+1}-\varepsilon_{20} & \cdots \\ \vdots & & \vdots & \vdots & \vdots & \end{vmatrix} / S_t \quad , \qquad (2.15)$$

$$\bar{P}_\infty(\ell^k) = \frac{N}{N-t} \begin{vmatrix} \varepsilon_{11} & \cdots & \varepsilon_{1\,k-1} & 1 & \varepsilon_{1\,k+1} & \cdots \\ \varepsilon_{21} & & \varepsilon_{2\,k-1} & 1 & \varepsilon_{2\,k+1} & \cdots \\ \vdots & & \vdots & \vdots & \vdots & \end{vmatrix} / S_t - \frac{1}{N-t} \quad , \qquad (2.16)$$

where the ε_{ij} are now evaluated at z=1. Thus one has for a single trap (t=1) trivially $P_\infty(\ell^1) = \bar{P}_\infty(\ell^1) = 1$, for a pair of traps (t=2)

$$P_\infty(\ell^1) = \frac{\varepsilon_{12}+\varepsilon_{20}-\varepsilon_{10}}{2\varepsilon_{12}} \quad , \quad P_\infty(\ell^2) = \frac{\varepsilon_{12}+\varepsilon_{10}-\varepsilon_{20}}{2\varepsilon_{12}} \quad , \qquad (2.17)$$

so $\bar{P}_\infty(\ell^1) = \bar{P}_\infty(\ell^2) = 1/2$ (as must be the case since both traps are equivalent), and for a triple of traps (t=3)

$$S_3 \cdot P_\infty(\ell^1) = \varepsilon_{23}(\varepsilon_{12}+\varepsilon_{13}-\varepsilon_{23}) + \varepsilon_{23}(\varepsilon_{20}+\varepsilon_{30}-2\varepsilon_{10}) + (\varepsilon_{12}-\varepsilon_{13})(\varepsilon_{30}-\varepsilon_{20}) \quad , \qquad (2.18)$$

$$S_3 \cdot \bar{P}_\infty(\ell^1) = \varepsilon_{23}(\varepsilon_{12}+\varepsilon_{13}-\varepsilon_{23}) + \frac{1}{N-3}[\varepsilon_{23}(\varepsilon_{12}+\varepsilon_{13}-2\varepsilon_{23}) + (\varepsilon_{12}-\varepsilon_{13})^2] \quad , \qquad (2.19)$$

where $S_3 = 2(\varepsilon_{12}\varepsilon_{23} + \varepsilon_{13}\varepsilon_{23} + \varepsilon_{12}\varepsilon_{13}) - \varepsilon_{12}^2 - \varepsilon_{13}^2 - \varepsilon_{23}^2$, and corresponding expressions for traps ℓ^2 and ℓ^3 are obtained by permutation of indices. For the special case of a connected triple of traps where ℓ^1 and ℓ^2, ℓ^2 and ℓ^3 are adjacent, so $\varepsilon_{12} = \varepsilon_{23} = \varepsilon_{NN}$ (= -1, as shown below), and $\varepsilon_{13} = -1 - \rho$, one has that

$$\bar{P}_\infty(\ell^{1,3}) : \bar{P}_\infty(\ell^2) = 1 + \rho/(N-3) : (1-\rho) - 2\rho/(N-3) \quad . \tag{2.20}$$

Note that it is possible for ℓ^2 and ℓ^3 to also be adjacent (ρ=0) on a triangular lattice wherein (2.20) shows that the $\bar{P}_\infty(\ell^i)$ are equal (as required).

For a multiple-trap problem where all sites within hopping range of a particular trap, ℓ_T^{isol}, are <u>also</u> traps, it is clear that the walker can never reach ℓ_T^{isol}, and thus $P_\infty(\ell_T^{isol}) = \bar{P}_\infty(\ell_T^{isol}) = 0$. Such a condition obviously implies complicated relationships between the ε_{ij} for associated geometrical configurations. In the next section we consider one such simple example.

Let us now consider the mean walk length, $\langle n \rangle_{\ell^0}$, from a specific starting site ℓ^0, and the average walk length $\langle n \rangle = (N-t)^{-1} \sum_{\ell^0 \notin L} \langle n \rangle_{\ell^0}$. From (2.4), (2.6) and (2.12-14), one has that

$$\langle n\rangle_{\ell 0} = \frac{\partial}{\partial z}\left\{ \frac{G(0)\cdot S_t + \sum_{k=1}^{t} \begin{vmatrix} \varepsilon_{11} & \cdots & \varepsilon_{1\,k-1} & \varepsilon_{10} & \varepsilon_{1\,k+1} & \cdots \\ \varepsilon_{21} & & \varepsilon_{2\,k-1} & \varepsilon_{20} & \varepsilon_{2\,k+1} & \\ \vdots & & \vdots & \vdots & \vdots & \end{vmatrix}}{G(0)\cdot S_t + \det\{\varepsilon_{ij}\}} \right\}_{z=1}$$

$$= -N\left\{ \sum_{k=1}^{t} \begin{vmatrix} \varepsilon_{11} & \cdots & \varepsilon_{1\,k-1} & \varepsilon_{10} & \varepsilon_{1\,k+1} & \cdots \\ \varepsilon_{21} & & \varepsilon_{2\,k-1} & \varepsilon_{20} & \varepsilon_{2\,k+1} & \\ \vdots & & \vdots & \vdots & \vdots & \end{vmatrix} - \det\{\varepsilon_{ij}\} \right\} / S_t \quad , \tag{2.21}$$

where the ε_{ij} are evaluated at z=1. Thus for a single trap (t=1), one has that $\langle n\rangle_{\ell 0} = -\varepsilon_{10} N$, and for a pair of traps (t=2), $\langle n\rangle_{\ell 0} = \frac{1}{2}(\varepsilon_{12} - \varepsilon_{10} - \varepsilon_{20})N$. The result for t=1 is particularly elucidating in providing a direct physical interpretation for the ε_{ij} at z=1. This result also follows trivially from previous first passage time analyses[2] which further lead us to conclude that, for nearest-neighbor sites, $\varepsilon_{ij} = \varepsilon_{NN} = -1$, and that $\varepsilon_{ij} \sim \frac{-\ell n \|i-j\|}{\pi\sigma_1\sigma_2}$ for a 2D square lattice, $\sim -u$ in d>3D, for $\|i-j\|$ large (cf. (1.1)).

From (2.4), (2.8) and (2.13-14), one has that

$$\langle n\rangle = \frac{1}{N-t}\frac{\partial}{\partial z}\left\{\frac{(1-z)^{-1}S_t}{G(0)\cdot S_t + \det\{\varepsilon_{ij}\}}\right\}_{z=1}$$

$$= \frac{N}{N-t}\left(N\Phi(0,1) + N \det\{\varepsilon_{ij}\}/S_t\right) \quad , \tag{2.22}$$

where the ε_{ij} are evaluated at z=1. For a single trap (t=1), (2.22)

reduces to $\langle n\rangle = \frac{N}{N-1}(N\Phi(0,1))$, i.e., only the first term contributes (cf. Refs. (3,9)), so the second provides the correction associated with the introduction of additional traps (and thus will be negative). For a pair of traps (t=2), (2.22) becomes $\langle n\rangle = \frac{N}{N-2}(\Phi(0,1) + 1/2\ \varepsilon_{12})N$, and for a triple (t=3), $\langle n\rangle = \frac{N}{N-3}(N\Phi(0,1) + 2\varepsilon_{12}\varepsilon_{13}\varepsilon_{23}/S_3)N$, in which $2\varepsilon_{12}\varepsilon_{13}\varepsilon_{23}/S_3$ reduces to $-1/2(1 + \tilde{\varepsilon}/4)^{-1}$ for a connected triple where $\varepsilon_{ij} = \tilde{\varepsilon}$ for the (possibly) nonadjacent pair of traps. We can also deduce from (2.22) that in 2D, $\langle n\rangle \sim c_1\ N\ \ell n\ N$, as in the single trap case, and that corrections effect the O(N) term, and that in d>3D, $\langle n\rangle \sim [u + \det\{\varepsilon_{ij}\}/S_t]N$, so corrections affect the dominant large-N behavior.

It is appropriate to note, at this point, that characterization and enumeration of the ε_{ij}-product terms in such determinant quantities as $\det\{\varepsilon_{ij}\}$ and S_t is quite easily achieved using ideas from flow graph theory, and specifically the Coates graph[15] (see Appendix A).

We are particularly interested in characterizing the behavior of the correction term to the average walk length, $\det\{\varepsilon_{ij}\}/S_t$, for a large number of traps (particularly when these form a connected cluster). To illustrate this behavior in 2D, consider the case of a symmetric nearest-neighbor random walk on a square lattice, where $\sigma_1 = \sigma_2 = 2^{-1/2}$. First consider a linear string of m (roughly) equally spaced traps of total span t (see Fig. 2). We let t become large while holding m>2 fixed, so the separation between adjacent traps is $\sim t/m$. Thus one has $\varepsilon_{ij} \sim -2/\pi\ \ell n(|i-j|\ t/m)$, assuming that the traps are labeled from left to right 1, 2, 3, ..., and so to leading order, for large t, and m fixed, the $\varepsilon_{ij} \sim -2/\pi\ \ell n\ t$ are

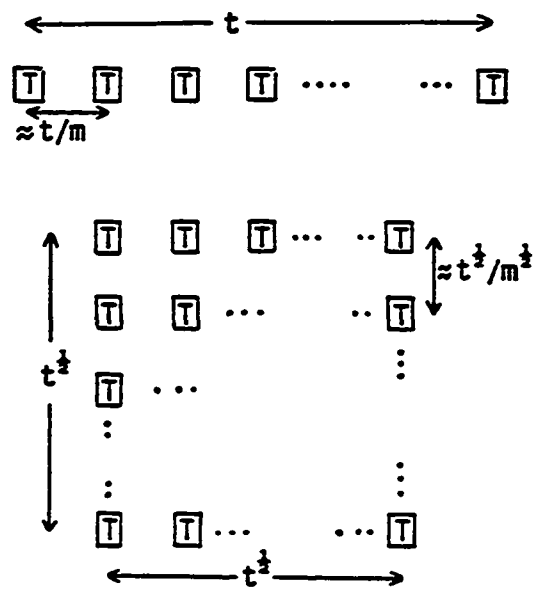

Figure 2: A linear string (square array) of m roughly equally spaced traps of total linear span t ($t^{1/2}$)

equal. It is then a simple matter to show that[16] $\det\{\varepsilon_{ij}\} \sim (-1)^{m+1}(m-1)(-\frac{2}{\pi}\ell n\ t)^m$ and $S_t \sim (-1)^{m-1}m(-\frac{2}{\pi}\ell n\ t)^{m-1}$, so $\langle n\rangle \sim N\Phi(0,1) - N\frac{m-1}{m}\frac{2}{\pi}\ell n\ t$, for large t. For <u>any</u> m, this result clearly provides an upper bound on the large t behavior of the average walk length for a string of t contiguous traps. In fact calculations following indicate that for a linear string of t contiguous traps (t-lin), one has

$$\langle n\rangle_{t\text{-}lin} \sim N\Phi(0,1) - \frac{2}{\pi}N\ell n\ t \quad . \tag{2.23}$$

For comparison, one naturally considers $\langle n\rangle$ for a square array of m traps of <u>total</u> horizontal/vertical span $t^{1/2}$ (see Fig. 2). Similar arguments to those above show that $\varepsilon_{ij} \sim -\frac{2}{\pi}\ell n\ t^{1/2} = -\frac{1}{\pi}\ell n\ t$, and $\langle n\rangle \sim N\Phi(0,1) - N\frac{m-1}{m}\frac{1}{\pi}\ell n\ t$, for t large and m fixed. This leads to the speculation that for a contiguous square array of t traps (t-sq), $\langle n\rangle_{t\text{-}sq} \sim N\Phi(0,1) - \frac{1}{\pi}N\ell n\ t$, and, more generally, that for a general contiguous <u>compact</u> array of t traps

$$\langle n\rangle \sim N\Phi(0,1) - \frac{2}{\pi}N\ell n\ Perim \quad , \tag{2.24}$$

for large t, where Perim is a suitably defined perimeter function. Validity of these relationships is investigated in the next section.

The expressions for trap-specific walk lengths are, in general, more complex. Of course for a single trap (t=1), these are given by (2.21) and (2.22) with t=1. For a pair of traps (t=2), one has

$$P_\infty(\ell^1)\ \langle n\rangle_{\ell^0\to\ell^1} = \frac{\partial}{\partial z}\left\{\frac{G(0)(-\varepsilon_{12}-\varepsilon_{20}+\varepsilon_{10}) - \varepsilon_{12}\varepsilon_{20}}{G(0)(-2\varepsilon_{12}) - \varepsilon_{12}^2}\right\}_{z=1}$$

$$= \frac{\partial}{\partial z}\left\{\frac{\varepsilon_{12}+\varepsilon_{20}-\varepsilon_{10}}{2\varepsilon_{12}}\right\}_{z=1} + \frac{1}{2}\langle n\rangle_{\ell^0} \quad , \qquad (2.25)$$

and $P_\infty(\ell^2)\ \langle n\rangle_{\ell^0\to\ell^2}$ follows from interchanging 1 and 2 on the r.h.s. of (2.25). One can straightforwardly show that $\frac{\partial}{\partial z}\varepsilon_{ij}$ at $z=1$ is bounded with respect to N in $d>3$D, but not in 2D. The average walk length to trap ℓ [given by $\frac{\partial}{\partial z}(1-z)\,\vec{P}(\ell^i)_{z=1}/\vec{P}_\infty(\ell^i)$] for t=2 becomes $\frac{1}{N-2}\frac{\partial}{\partial z}\left\{\frac{(1-z)^{-1}(-\varepsilon_{12})}{G(0)(-2\varepsilon_{12})-\varepsilon_{12}^2}\right\}_{z=1}$ = $\langle n\rangle$ for both ℓ^1 and ℓ^2 (as required, since ℓ^1 and ℓ^2 are equivalent). Corresponding expressions for $t>3$ can be easily obtained, but are rather complicated.

III. LARGE-N ASYMPTOTIC RESULTS FOR SYMMETRIC NEAREST-NEIGHBOR RANDOM WALKS ON A SQUARE LATTICE

As demonstrated in the previous section, the quantities of interest here can be obtained from the behavior of $\Phi(0,z)$ and the ε_{ij}, as $z \to 1$. For symmetric nearest-neighbor random walks on a square lattice, these are determined from the appropriate structure function, $\lambda(\theta_1,\theta_2) = \frac{1}{2}(\cos\theta_1 + \cos\theta_2)$. From Montroll's analysis[3], we have that

$$\Phi(0,1) = \frac{1}{\pi} \ell n\, N + 0.195056 - 0.1170\, N^{-1} - 0.051\, N^{-2} + O(N^{-3}) \ . \quad (3.1)$$

Our primary task is thus to determine, for z=1 (assumed implicitly below), the $\varepsilon_{ij} \equiv \varepsilon(r,s)$, say, where r(s) denotes the horizontal (vertical) separation in lattice vectors between the sites i and j. Clearly we have that $\varepsilon(r,s) = \varepsilon(s,r)$, the $\varepsilon(\pm r,\pm s)$ are equal, and we already know that $\varepsilon(1,0) = -1$, and that $\varepsilon(r,s) \sim -\frac{1}{\pi} \ell n\, (r^2+s^2)$, for large $r^2 + s^2$.

Here we are content to determine the $\varepsilon(r,s)$ to leading order in $N = L^2$, as illustrated by the (Euler-McLauren formula based) decomposition

$$\varepsilon(r,s) = L^{-2} \sum_{k_1 k_2 = 0}^{L-1} \frac{\exp[2\pi i(rk_1+sk_2)]-1}{1-\frac{1}{2}[\cos(\frac{2\pi k_1}{L}) + \cos(\frac{2\pi k_2}{L})]} = \varepsilon_0(r,s) + O(N^{-1/2}) \ , \quad (3.2)$$

$$\text{where } \varepsilon_0(r,s) = -\frac{2}{\pi^2} \int_0^\pi d\theta_1 \int_0^\pi d\theta_2 \ \frac{1-\cos(r\theta_1)\cos(s\theta_2)}{2-\cos\theta_1-\cos\theta_2} \ . \quad (3.3)$$

It is obvious that $\varepsilon_0(1,0) + \varepsilon_0(0,1) = -\frac{2}{\pi^2}\int_0^\pi \int_0^\pi d\theta_2 \cdot 1 = -2$, so $\varepsilon_0(1,0) = \varepsilon_0(0,1) = -1$, as required. All of the $\varepsilon_0(r,s)$ can be evaluated exactly as demonstrated below[17].

One can easily show that

$$\varepsilon_0(r,0) = -\frac{2}{\pi}\int_0^\pi d\theta_1 \frac{1-\cos(r\theta_1)}{(1-\cos\theta_1)^{1/2}(3-\cos\theta_1)^{1/2}}$$

$$= -\frac{2}{\pi}\int_{-1}^{+1} dx \frac{F_{|r|-1}(x)}{(1+x)^{1/2}(3-x)^{1/2}} \quad , \tag{3.4}$$

where $F_r(x) = (1-T_{r+1}(x))/(1-x)$ is an r^{th}-order polynomial (T_r denotes the first kind of Tschebysheff polynomial of order r). A recursive formula relating $\int dx\, x^n/(a+bx+cx^2)^{1/2}$ for different n, allows exact evaluation of (3.4). Note that making the transformation $\phi = r\theta_1$ in the first expression for $\varepsilon_0(r,0)$, and expanding $(1-\cos\frac{\phi}{r})^{1/2} = 2^{-1/2}\frac{\phi}{r}(1+0(\frac{\phi}{r})^2)$ shows that $\varepsilon_0(r,0) \sim -2\,\ell n\, r/\pi$, as $r\to\infty$ (as required). To evaluate

$$\delta\varepsilon_0(r,s) \equiv \varepsilon_0(r,s) - \varepsilon_0(r,0) = \frac{2}{\pi^2}\int_0^\pi d\theta_1 \int_0^\pi d\theta_2 \frac{\cos(r\theta_1)[\cos(s\theta_2)-1]}{2-\cos\theta_1-\cos\theta_2} \tag{3.5}$$

(which is clearly bounded as $r\to\infty$, for fixed s), we start by rewriting $\cos(s\theta_2)-1 = H_1(\cos\theta_1, \cos\theta_2)(2-\cos\theta_1-\cos\theta_2) + H_2(\cos\theta_1)$. For $|s|<|r|$, only the H_2 term contributes to (3.5) which can be rewritten as a single integral of the form

$$\delta\varepsilon_0(r,s) = -\frac{1}{\pi}\int_{-1}^{+1} dx \frac{T_{|r|}(x)}{(1+x)^{1/2}(3-x)^{1/2}} G_{|s|}(x) \text{ , for } |s|<|r| \text{ , } \quad (3.6)$$

where $G_1(x) = 1$, $G_2(x) = 6-2x$, $G_3(x) = 25-20x+4x^2$, ... Clearly (3.6) can be evaluated exactly.

In Table I, we have presented transcendental forms for several $\varepsilon_0(r,s)$ and, in Table II, a more extensive set of numerical values which should be compared with the asymptotic behavior $-\frac{1}{\pi}\ell n(r^2+s^2)$. Note the monotonic increase in magnitude of with $\varepsilon_0(r,s)$ with increasing r^2+s^2, as must be the case given their relationship to site-specific walk lengths for a single trap (here $\langle n\rangle_{\ell^0} = -\varepsilon_{10}N \sim -\varepsilon_0(r,s)N$, as $N\to\infty$, where $\ell^0 = (r,s)$).

In Fig. 3 we have shown, for various starting sites, the $N\to\infty$ values of the probability, $P_\infty(\ell^1)$, that the walker is captured by the end trap ℓ^1 in a pair, and linear triple of traps. Clearly as the starting site becomes far removed from the cluster of traps, these site-specific probabilities converge to the lattice average trapping probability, $\bar{P}_\infty(\ell^1)$. This follows from (2.15), (2.16) and the logarithmic behavior of the ε_{ij} for large $\|i-j\|$. To illustrate the latter quantities, we consider the cases of linear [bent] connected triples of traps ℓ^1, ℓ^2, ℓ^3, where the central one is ℓ^2, and use (2.19) to show that as $N\to\infty$,

$$\bar{P}_\infty(\ell^{1,3}) = \frac{\pi}{8} \approx 0.3927 \left[\tfrac{1}{4}(1-\tfrac{1}{\pi})^{-1} \approx 0.3667\right] \text{ ,}$$

$$\bar{P}_\infty(\ell^2) = 1-\frac{\pi}{4} \approx 0.2146 \left[(\tfrac{1}{2}-\tfrac{1}{\pi})(1-\tfrac{1}{\pi})^{-1} \approx 0.2665\right] \text{ .} \quad (3.7)$$

Table I: Transcendental forms for $\varepsilon_0(r,s)$ for random walks on a 2D square lattice

r \ s	1	2	3	4
0	-1	$\frac{8}{\pi} - 4$	$\frac{48}{\pi} - 17$	$\frac{736}{3\pi} - 80$
1	$-\frac{4}{\pi}$	$1 - \frac{8}{\pi}$	$8 - \frac{92}{3\pi}$	$49 - \frac{160}{\pi}$
2	$1 - \frac{8}{\pi}$	$-\frac{16}{3\pi}$	$-1 - \frac{8}{3\pi}$	$12 - \frac{472}{15\pi}$

Table II: Numerical values for $\varepsilon_0(r,s)$ for random walks on a 2D square lattice

r \ s	0	1	2	3
0	0.000000	-1.000000	-1.453521	-1.721125
1	-1.000000	-1.273240	-1.546479	-1.761503
2	-1.453521	-1.546479	-1.697653	-1.848826
3	-1.721125	-1.761503	-1.848826	-1.952301
4	-1.907975	-1.929582	-1.983849	-2.055775
5	-2.051609	-2.065000	-2.101213	-2.152758
6	-2.168462	-2.177598	-2.203243	-2.241436
7	-2.267041	-2.273688	-2.292725	-2.321919
8	-2.352328	-2.357386	-2.372051	-2.394983
9	-2.427497	-2.431478	-2.443111	-2.461548
10	-2.494702	-2.497919	-2.507367	-2.522487
11	-2.555475	-2.558128	-2.565952	-2.578561
12	-2.610940	-2.613167	-2.619750	-2.630419
13	-2.661953	-2.663848	-2.669464	-2.678603
14	-2.709176	-2.710809	-2.715655	-2.723568
15	-2.753134	-2.754555	-2.758780	-2.765696
16	-2.794249	-2.795498	-2.799213	-2.805309
17	-2.832867	-2.833975	-2.837265	-2.842679
18	-2.869267	-2.870271	-2.873193	-2.878041
19	-2.903660	-2.904648	-2.907196	-2.911610

0.552	0.552	0.544	0.520	0.480	0.456	0.448	0.448
0.568	0.576	0.576	0.546	0.454	0.424	0.424	0.432
0.584	0.608	0.637	0.637	0.363	0.363	0.392	0.416
0.593	0.634	0.727	ℓ_T^1	ℓ_T^2	0.273	0.366	0.407

0.463	0.464	0.455	0.427	0.377	0.340	0.324	0.322	0.325
0.483	0.494	0.497	0.465	0.356	0.297	0.289	0.297	0.309
0.504	0.534	0.572	0.581	0.285	0.205	0.236	0.270	0.295
0.515	0.565	0.677	ℓ_T^1	ℓ_T^2	ℓ_T^3	0.181	0.151	0.288

Figure 3: Infinite lattice trapping probabilities for the leftmost trap, ℓ_T^1, in a pair, and linear triple of traps

In Table III we have presented trapping probabilities for all members of linear strings of traps of length m, (so t=m) for $1 \leq m \leq 20$.

It is also interesting to consider trapping probabilities for decimated linear strings of traps. Here the results can be interpreted in the context of particle-cluster aggregation as describing what proportion of the linear and various branched clusters are formed by aggregation with a linear cluster. For example, for aggregation with a dimer (adjacent pair), as $N \to \infty$, 42.73% (57.27%) of the trimers formed are linear (bent). A more extensive set of results for aggregation with m-mers (so $t=3m+2$), for $1 \leq m \leq 16$, is shown in Table IV.

It is obvious, particularly in the context of the above example, that a trap for which all nearest neighbors are also traps cannot be reached by the walker, and thus has zero trapping probability (see the remarks in Section II). Obviously this is true for the simpler $N \to \infty$ form of trapping probabilities, and reflects rather complicated relationships between the $\varepsilon_0(r,s)$. The simplest example is a decimated single trap, ℓ^1 ($m=1$ above), where one has that

$$\frac{N-5}{N} S_5 P_\infty(\ell^1) - \frac{1}{N} = \begin{vmatrix} 1 & \varepsilon(1,0) & \varepsilon(1,0) & \varepsilon(1,0) & \varepsilon(1,0) \\ 1 & 0 & \varepsilon(1,1) & \varepsilon(2,0) & \varepsilon(1,1) \\ 1 & \varepsilon(1,1) & 0 & \varepsilon(1,1) & \varepsilon(2,0) \\ 1 & \varepsilon(2,0) & \varepsilon(1,1) & 0 & \varepsilon(1,1) \\ 1 & \varepsilon(1,1) & \varepsilon(2,0) & \varepsilon(1,1) & 0 \end{vmatrix}$$

$$= \varepsilon(2,0)^2[\varepsilon(2,0)^2 - 4\varepsilon(2,0)\varepsilon(1,0) + 8\varepsilon(1,1)\varepsilon(1,0) - 4\varepsilon(1,1)^2]$$

$$\longrightarrow 0 \quad , \quad \text{as } N \to \infty \quad . \tag{3.8}$$

Table III: Random walks on a square lattice of N sites with a linear string of m traps. $N \to \infty$ values of lattice averaged probabilites for capture in a trap on the left (or right) end, and 2nd, 3rd, 4th,... from that end, respectively

m	Trapping Probabilities									
1	1.000000									
2	0.500000									
3	0.392699	0.214602								
4	0.332474	0.167526								
5	0.293202	0.141012	0.131571							
6	0.265127	0.123834	0.111039							
7	0.243802	0.111640	0.097654	0.093810						
8	0.226903	0.102432	0.088119	0.082546						
9	0.213088	0.095169	0.080904	0.074512	0.072654					
10	0.201520	0.089255	0.075204	0.068427	0.065593					
11	0.191652	0.084318	0.070557	0.063618	0.060243	0.059224				
12	0.183103	0.080118	0.066675	0.059695	0.056013	0.054396				
13	0.175604	0.076487	0.063369	0.056416	0.052562	0.050579	0.049964			
14	0.168957	0.073308	0.060509	0.053624	0.049678	0 047465	0.046460			
15	0.163011	0.070494	0.058004	0.051208	0.047221	0.044861	0.043600	0.043201		
16	0.157652	0.067981	0.055787	0.049091	0.045095	0.042643	0.041209	0.040543		
17	0.152789	0.065719	0.053805	0.047217	0.043232	0.040724	0.039172	0.038320	0.038048	
18	0.148349	0.063668	0.052020	0.045541	0.041582	0.039042	0.037409	0.036426	0.035962	
19	0.144275	0.061798	0.050402	0.044033	0.040108	0.037553	0.035865	0.034787	0.034185	0.033991
20	0.140516	0.060085	0.048926	0.042665	0.038780	0.036222	0.034497	0.033351	0.032647	0.032311

Table IV: Random walks on a square lattice of N sites which irreversibly aggregated with a linear cluster of m sites. $N \to \infty$ values of lattice averaged probabilities for sticking besides the left (or right) end site, for sticking above the left (or right) end site, and above those 2nd, 3rd, ... from that end, respectively

m	Trapping Probabilities								
1	0.250000	0.250000							
2	0.213656	0.143172							
3	0.190489	0.122353	0.064806						
4	0.173952	0.108973	0.054051						
5	0.161316	0.099422	0.047410	0.045021					
6	0.151218	0.092134	0.042814	0.039443					
7	0.142889	0.086318	0.039388	0.035588	0.034522				
8	0.135854	0.081528	0.036702	0.032719	0.031125				
9	0.129803	0.077486	0.034519	0.030472	0.028599	0.028046			
10	0.124521	0.074012	0.032697	0.028648	0.026624	0.025759			
11	0.119855	0.070983	0.031145	0.027127	0.025021	0.023971	0.023650		
12	0.115692	0.068309	0.029801	0.025832	0.023686	0.022522	0.022003		
13	0.111947	0.065924	0.028622	0.024712	0.022551	0.021316	0.020669	0.020466	
14	0.108552	0.063779	0.027577	0.023730	0.021568	0.020290	0.019558	0.019222	
15	0.105455	0.061837	0.026640	0.022860	0.020708	0.019403	0.018614	0.018186	0.018050
16	0.102616	0.060065	0.025796	0.022081	0.019945	0.018626	0.017798	0.017306	0.017075

Reduction of this determinant to polynomial form (which was simplified by symmetries and Coates graph techniques) is unnecessary if one notes that, as $N\to\infty$, all rows sum to -3, guaranteeing a vanishing $N\to\infty$ limit.

Finally we consider site-specific walk lengths, $\langle n\rangle_{\ell^0}$, and corresponding lattice averages, $\langle n\rangle$, for various connected arrays of traps. Let (r,s) denote the position of ℓ^0. Then for a single trap at the origin $(0,0)$, $\langle n\rangle_{\ell^0} = -\epsilon_{10}N \sim |\epsilon_0(r,s)|N$, as $N\to\infty$, so the dominant $N\to\infty$ behavior can be read off from Tables I and II. For an adjacent pair of traps at $(0,0)$ and $(0,1)$, one has $\langle n\rangle_{\ell^0} \sim \frac{1}{2}(|\epsilon_0(r,s)| + |\epsilon_0(r-1,s)| - 1)N$, as $N\to\infty$, for which some values are shown in Fig. 4. For t traps, we have from (2.22) and (3.1) that

$$\langle n\rangle = \frac{N}{N-t}[N\,\Phi(0,1) - \delta\,N + O(N^{1/2})]$$

$$= \frac{N}{N-t}[\frac{1}{\pi}\,N\,\ell n\,N + (0.195056 - \delta)N + O(N^{1/2})] \quad , \tag{3.9}$$

and here we shall provide δ values for a range of trap configurations.

For an adjacent pair of traps one has $\delta = 1/2$, and for a connected linear [bent] triple of traps $\delta = \pi/4 \approx 0.785398$ $[\frac{\pi}{2}(\pi - 1)^{-1} \approx 0.733471]$. In Table V, we have displayed δ values for linear strings of m traps with $1\le m\le 20$ (so $t=m$), and in Table VI, δ values obtained from decimating a string of m traps (to produce $2m+2$ extra traps, so $t=3m+2$) are displayed for $1\le m\le 16$. In both cases we have also given values of $\Delta_m = [\delta_m - \delta_{m-1}]/[\ell n(t+\alpha) - \ell n(t-1+\alpha)]$ for a few choices of α, in order to estimate $\Delta = \lim_{m\to\infty} \Delta_m$

1.5040	1.4006	1.30516	1.13380	1.13380
1.4163	1.2732	1.12207	1.00000	1.00000
1.3455	1.1540	0.90986	0.63662	0.63662
1.3145	1.0873	0.72676	T	T

Figure 4: The coefficient γ in $\langle n \rangle_{\ell} \sim \gamma N$, as $N \to \infty$, for random walks on a lattice with an adjacent pair of traps

Table V: Random walks on a square lattice of N sites with a linear string at m traps. Values of δ_m in $\langle n \rangle = \frac{n}{N-t}[\phi(0,1) - \delta_m N + O(N^{1/2})]$, and of $\Delta_m = [\delta_m - \delta_{m-1}]/[\ell n(t+\alpha) - \ell n(t+\alpha-1)]$ (cf. $\frac{2}{\pi} = 0.636620$) are shown

m	δ_m	Δ_m $\alpha = -1$	$\alpha = 0$	$\alpha = -0.287389$
1	0.000000			
2	0.500000		0.721348	0.570230
3	0.785398	0.411742	0.703878	0.620575
4	0.983258	0.487983	0.687773	0.630481
5	1.134376	0.525295	0.677223	0.633601
6	1.256553	0.547526	0.670118	0.634903
7	1.359076	0.562320	0.665083	0.635558
8	1.447386	0.572881	0.661343	0.635924
9	1.524943	0.580815	0.658473	0.636158
10	1.594079	0.586978	0.656185	0.636297
11	1.656444	0.591920	0.654337	0.636400
12	1.713246	0.595970	0.652811	0.636476
13	1.765395	0.599335	0.651515	0.636519
14	1.813596	0.602191	0.650416	0.636557
15	1.858404	0.604631	0.649458	0.636576
16	1.900267	0.606773	0.648651	0.636616
17	1.939546	0.608613	0.647905	0.636613
18	1.976543	0.610264	0.647271	0.636636
19	2.011507	0.611703	0.646676	0.636626
20	2.044650	0.612996	0.646147	0.636620

Table VI: Random walks on a square lattice of N sites after decimating a linear string of m traps (producing 2m+2 extra traps, so t = 3m+2). Values of δ_m and Δ_m (cf. Table V) are shown

m	δ_m	Δ_m $\alpha = 2$	$\alpha = 2.5$	$\alpha = 3$
1	1.000000			
2	1.175138	0.608790	0.696888	0.784867
3	1.306508	0.588724	0.654655	0.720540
4	1.412524	0.581478	0.634621	0.687743
5	1.501803	0.579167	0.623889	0.668599
6	1.579115	0.578980	0.617690	0.656393
7	1.647402	0.579769	0.613950	0.648127
8	1.708618	0.581015	0.611650	0.642282
9	1.764132	0.582456	0.610233	0.638009
10	1.814945	0.583981	0.609403	0.634824
11	1.861809	0.585487	0.608931	0.632375
12	1.905308	0.586968	0.608727	0.630485
13	1.945902	0.588380	0.608684	0.628989
14	1.983964	0.589756	0.608794	0.627831
15	2.019797	0.591063	0.608985	0.626907
16	2.053651	0.592284	0.609215	0.626146

(which is independent of α). This corresponds to fitting δ_m to the asymptotic behavior $\delta_m \sim \Delta \, \ell n[\beta(m+\alpha)]$. Note that Perim = 2(m+1) [2(m+3)] corresponds to the standard choice of perimeter function for the linear string [decimated linear string] of m traps. Our speculation that $\Delta = 2/\pi$ (see the previous section) is supported by the results for the linear string of traps, and not inconsistent with results for the decimated string. In the former case we have chosen an optimal α value, so $\Delta_{20} = 2/\pi$, and checked that the Δ_m varies slowly from $2/\pi$ as m is reduced from 20. For a decimated single trap (m=1,t=5), the result δ=1, obtained previously in Ref. 9, follows trivially from the observation[2] that the mean walk length for return to the origin on a perfect finite lattice is N (cf. (4.6)). For a general decimated linear string of traps, reduction in the average walk length with increasing string length, reflects the increase in the rate of destruction by irreversible aggregation with random walkers of corresponding immobile linear clusters (in the same walker/cluster gas environment).

A limited set of results for the 2D triangular lattice, analogous to those discussed in this section, are presented in Appendix B.

IV. EXACT ANALYSIS OF RANDOM WALKS ON FINITE LATTICES WITH MULTIPLE TRAPS

Here we consider only symmetric nearest-neighbor random walks on a finite 2D square lattice (of N sites) with periodic boundary conditions, and one or more completely adsorbing traps. Extension to more complicated walks is straightforward. For the case of a single trap, there are extensive previous calculations for the site-specific mean walk length (providing the lattice-averaged walk length) until trapping. We start by demonstrating the straightforward extension to the case of multiple traps, $L = \{\ell_T^1, \ell_T^2, \cdots, \ell_T^t\}$, where analysis is always based on the intuitively obvious set of equations

$$\langle n\rangle_\ell = 1/4 \sum_m{}' \left(\langle n\rangle_m + 1\right) \quad , \quad \ell \notin L \quad . \tag{4.1}$$

Here the sum is over sites adjacent to ℓ, and we set $\langle n\rangle_{\ell_T^i} = 0$. The average walk length is again calculated from $\langle n\rangle = (N-t)^{-1} \sum_{\ell \notin L} \langle n\rangle_\ell$.

We use the example of an adjacent pair of traps on a lattice of size $N = L^2$, with L even, for illustration. Reflection symmetry about horizontal axes through the traps guarantees equivalence of various sites. Nonequivalent ones can be labeled as shown in Fig. 5 for L=14. (The reason why we did not choose a more conveniently shaped (L)x(L-1) lattice is because we want to compare with the asymptotic large $N=L^2$ results of the previous section.) The equations (4.1) for this case, rewritten in matrix form, become

$$\underline{\underline{A}} \cdot \begin{bmatrix} \langle n\rangle_1 \\ \langle n\rangle_2 \\ \vdots \\ \vdots \end{bmatrix} = \begin{bmatrix} 1 \\ 1 \\ \vdots \\ \vdots \end{bmatrix} , \tag{4.2}$$

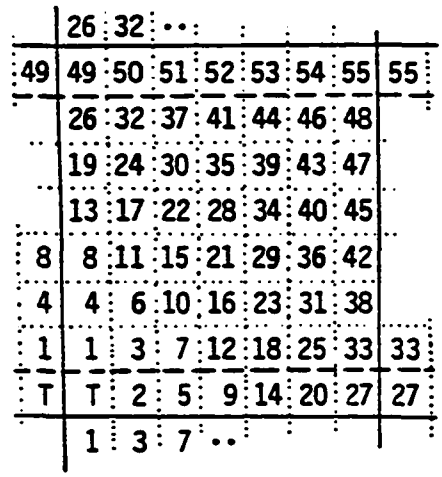

Figure 5: Equivalent site labeling for one quadrant of an 14x14 square lattice with an adjacent pair of traps

where the "fundamental" matrix $\underline{\underline{A}}$ satisfies $\underline{\underline{A}} \equiv \underline{\underline{I}} + \underline{\underline{\Delta}}$ with (cf. Fig. 5)

$$\underline{\underline{\Delta}} \equiv \left[\begin{array}{cc:cccccccc:c}
-\frac{1}{4} & 0 & -\frac{1}{4} & -\frac{1}{4} & 0 & 0 & 0 & 0 & 0 & 0 & \cdots \\
0 & 0 & -\frac{2}{4} & 0 & -\frac{1}{4} & 0 & 0 & 0 & 0 & 0 & \cdots \\
\hdashline
-\frac{1}{4} & -\frac{1}{4} & 0 & 0 & 0 & -\frac{1}{4} & -\frac{1}{4} & 0 & 0 & 0 & \\
-\frac{1}{4} & 0 & 0 & -\frac{1}{4} & 0 & -\frac{1}{4} & 0 & -\frac{1}{4} & 0 & 0 & \\
0 & -\frac{1}{4} & 0 & 0 & 0 & 0 & -\frac{2}{4} & 0 & -\frac{1}{4} & 0 & \\
\hdashline
0 & 0 & -\frac{1}{4} & -\frac{1}{4} & 0 & 0 & 0 & 0 & -\frac{1}{4} & -\frac{1}{4} & \\
\vdots & \vdots & & & & & & & & & \\
\end{array}\right] \qquad (4.3)$$

Solution of (4.2) is obtained by matrix inversion. If additional equivalent sets of sites in the above case are decimated (to create a multiple-trap problem preserving the symmetry of the two-trap problem), the corresponding matrices are obtained from $\underline{\underline{A}}$ (or $\underline{\underline{\Delta}}$) by removing the rows and columns corresponding to the additional traps. For example $\underline{\underline{A}}(m) = \{(\underline{\underline{A}})_{ij}$, for $i,j>m\}$ corresponds to decimating sites labeled 1, 2, ..., m-1 (so $\underline{\underline{A}}(1) \equiv \underline{\underline{A}}$). The similarly defined $\underline{\underline{\Delta}}(3)$ and $\underline{\underline{\Delta}}(6)$ submatrices are indicated above in (4.3).

Results from these calculations applied to determination of the average walk length, $\langle n \rangle$, for various lattice sizes $N=L^2$, are presented for linear strings of m traps (so t=m) with $1 \leq m \leq 9$ in Table VII, for a bent triple of traps in Table VIII, and after decimating a linear string of m traps (where $t = 3m+2$) with $1 \leq m \leq 9$ in Table IX. Values of δ obtained from

Table VII: Random walks on an LxL square with a linear string of m traps. Values of the average walk length, $\langle n \rangle$ (and δ_m, where $\langle n \rangle = \frac{N}{N-m}$ $[\frac{1}{\pi} N \ln N + (0.195056-\delta_m)N]$ $N=L^2$), for various L

L	m=1		m=3		m=5		m=7		m=9	
	$\langle n \rangle$	δ_1	$\langle n \rangle$	δ_3	$\langle n \rangle$	δ_5	$\langle n \rangle$	δ_7	$\langle n \rangle$	δ_9
3	9.00000	0.005565	4.00000	0.598158						
5	31.6667	0.003656	14.0909	0.723656	10.0000	0.899656				
7	71.6154	0.002150	35.4367	0.754940	22.4861	1.021787	18.6667	1.107330		
9	130.604	0.001358	69.5359	0.767180	45.3801	1.068188	33.6910	1.213860	30.0000	1.264635
11	209.937	0.000926	117.667	0.773263	79.6320	1.090683	58.7271	1.264333	47.6161	1.357352
13	310.649	0.000668	180.867	0.776732	126.193	1.103341	94.4457	1.292251	75.0153	1.407714
⋮										
31	2290.61	0.000115	1539.83	0.783877	1209.66	1.129003	1000.48	1.347705	849.613	1.505388
33	2638.78	0.000101	1787.56	0.784055	1412.78	1.129636	1174.91	1.349050	1002.86	1.507711
35	3013.97	0.000089	2056.00	0.784204	1633.83	1.130163	1365.46	1.350169	1170.90	1.509643
37	3416.45	0.000079	2345.46	0.784329	1873.11	1.130606	1572.43	1.351110	1354.04	1.511267
39	3836.41	0.000070	2656.22	0.784435	2130.88	1.130983	1796.11	1.351909	1552.56	1.512644

	m=2		m=4		m=6		m=8	
	$\langle n \rangle$	δ_2	$\langle n \rangle$	δ_4	$\langle n \rangle$	δ_6	$\langle n \rangle$	δ_8
4	11.0476	0.473433	6.66667	0.765098				
6	32.2790	0.488900	17.9257	0.893117	14.0000	1.011651		
8	67.7156	0.493878	39.9223	0.934070	27.7455	1.125989	24.0000	1.190745
10	118.859	0.496112	73.8282	0.952176	51.6703	1.175227	40.3159	1.290021
12	186.870	0.497309	120.740	0.961814	86.5650	1.200899	66.5156	1.340745
⋮								
30	1678.41	0.499567	1247.96	0.979863	1007.90	1.247899	843.749	1.431160
32	1951.25	0.499619	1460.95	0.980274	1187.07	1.248952	999.315	1.433143
34	2246.93	0.499662	1692.92	0.980615	1383.03	1.249823	1170.14	1.434782
36	2565.76	0.499698	1944.16	0.980900	1596.08	1.250552	1356.53	1.436154
38	2908.04	0.499728	2214.98	0.981141	1826.52	1.251169	1558.77	1.437312

Table VIII: Random walks on an LxL square lattice with a bent triple of traps. <n> and δ as in Table VII

L	<n>	δ
3	3.27273	0.652030
5	14.7107	0.701838
7	37.4129	0.717080
9	73.2098	0.723504
11	123.434	0.726781
13	189.136	0.728674
15	271.184	0.729863
17	370.318	0.730660
19	487.184	0.731218
21	622.354	0.731625
26	949.614	0.732166
27	1142.60	0.732351

Table IX: Random walks on an LxL square lattice after decimating a linear string of m traps (so t = 3m+2). <n> and δ_m as in Table VII

L	m=1 <n>	m=1 δ_1	m=3 <n>	m=3 δ_3	m=5 <n>	m=5 δ_5	m=7 <n>	m=7 δ_7	m=9 <n>	m=9 δ_9
3	2.000000	0.795689								
5	9.20000	0.925256	4.79121	1.112333						
7	25.7622	0.961750	14.5592	1.203436	10.5918	1.292695				
9	53.2678	0.976819	32.8320	1.243564	22.8104	1.371346	19.1673	1.424412		
11	93.0383	0.984465	60.8790	1.264211	43.3107	1.413953	33.8708	1.494888	30.4489	1.53027
13	146.129	0.988869	99.7446	1.276164	73.1172	1.438828	56.7396	1.537908	47.6819	1.59422
⋮										
33	1556.51	0.998265	1231.27	1.301777	1027.68	1.492046	879.327	1.630593	763.888	1.73822
35	1795.84	0.998457	1429.13	1.302301	1199.17	1.493130	1031.21	1.632465	900.049	1.74112
37	2054.46	0.998618	1643.82	1.302743	1385.93	1.494042	1197.17	1.634041	1049.36	1.74355
39	2332.66	0.998756	1875.62	1.303118	1588.24	1.494818	1377.52	1.635380	1212.12	1.74562

L	m=2 <n>	m=2 δ_2	m=4 <n>	m=4 δ_4	m=6 <n>	m=6 δ_6	m=8 <n>	m=8 δ_8
4	3.00000	0.983848						
6	11.5145	1.086955	7.33583	1.211196				
8	28.8027	1.125083	18.3286	1.295132	14.5389	1.362690		
10	56.2993	1.142974	37.6889	1.336803	27.9939	1.436976	24.4716	1.479838
12	95.1789	1.152752	66.5454	1.359804	49.6669	1.479992	40.4350	1.546898
⋮								
32	1268.86	1.171972	1034.38	1.405090	873.278	1.565258	751.489	1.686170
34	1475.64	1.172332	1210.04	1.405938	1027.15	1.566843	888.439	1.688747
36	1700.17	1.172635	1401.53	1.406649	1195.51	1.568171	1038.84	1.690904
38	1942.73	1.172890	1609.15	1.407250	1378.65	1.569294	1203.98	1.693407

setting $\langle n \rangle$ equal to $\frac{1}{\pi} N \ell n N + (0.195056 - \delta)N$ are also listed, and their convergence to the $N \to \infty$ asymptotic values, given in Section III, should be noted.

We now turn our attention to evaluation of site-specific trapping probabilities for a general set of t traps, L. If P_{ℓ}^{i} denotes the probability that a walker, starting at ℓ, is trapped at ℓ_T^i, then one obviously has that

$$P_{\ell}^{i} = \frac{1}{4} \sum_{m}{}' P_{m}^{i} \quad , \quad \ell \notin L \quad , \tag{4.4}$$

where $P_{\ell_T^j}^{i} = \delta_{i,j}$. Equation (4.4) implies that $\left(\sum_{i=1}^{t} P_{\ell}^{i} \right) = \frac{1}{4} \sum_{m}{}' \left(\sum_{i=1}^{t} P_{m}^{i} \right)$ which, together with the imposed boundary conditions, is consistent with the requirement that $\sum_{i=1}^{t} P_{\ell}^{i} = 1$, for all ℓ. The lattice-averaged trap-specific capture probabilities P^i are again calculated from $P^i = (N-t)^{-1} \sum_{\ell \notin L} P_{\ell}^{i}$. For the above example of an adjacent pair of traps, the P_{ℓ}^{i} are not invariant with respect to reflection in a vertical line through the traps, so the matrix $\underline{\underline{A}}$ is not appropriate. A larger matrix accounting for the lower symmetry must be introduced. However full symmetry is preserved in the important case where sites labeled 1 and 2 (in Fig. 5) are also decimated and we consider only $P_{\ell}^{1,2}$. Here the appropriate matrix is $\underline{\underline{A}}(3)$, and one has that

$$\underline{\underline{A}}(3) \cdot \begin{bmatrix} P_3^1 \\ P_4^1 \\ P_5^1 \\ P_6^1 \\ \vdots \end{bmatrix} = \frac{1}{4}\begin{bmatrix} 1 \\ 1 \\ 0 \\ 0 \\ \vdots \end{bmatrix} , \quad \underline{\underline{A}}(3) \cdot \begin{bmatrix} P_3^2 \\ P_4^2 \\ P_5^2 \\ P_6^2 \\ \vdots \end{bmatrix} = \frac{1}{4}\begin{bmatrix} 1 \\ 0 \\ 1 \\ 0 \\ \vdots \end{bmatrix} . \qquad (4.5)$$

As mentioned previously, these $P_\ell^{1,2}$ and the corresponding lattice averages, give the proportion of bent to linear trimers formed by aggregation with a dimer (adjacent pair of filled sites).

Another useful application of the P_ℓ^i is in relating the walk lengths $\langle n\rangle_\ell$ to those corresponding to decimating <u>all</u> neighboring sites to the original set of traps L. We denote the enlarged set of t' traps by L', the corresponding walk lengths by $\langle n\rangle'_\ell$, and the corresponding trapping probabilities by $P_\ell'^m$, for $m \in L'$ and $\ell \notin L'$. Note that $P_\ell'^m = 0$ for $m \in L$. It is clear that

$$\langle n\rangle'_\ell = \langle n\rangle_\ell - \sum_{m\in L'-L} P_\ell'^m \langle n\rangle_m \quad , \qquad (4.6)$$

since, to reach L, the walker must first reach one of the sites, m, in L'-L (with probability $P_\ell'^m$), and then the additional mean walk length from m to L is $\langle n\rangle_m$. Using (4.6) to calculate the average walk length, $\langle n\rangle' = (N-t')^{-1} \sum_{\ell\notin L'} \langle n\rangle'_\ell$, for the decimated case, one obtains

$$\langle n\rangle' = \frac{N-t}{N-t'}\left(\langle n\rangle - \sum_{m\in L'-L} P'^m \langle n\rangle_m\right) + \frac{t'-t}{N-t} \sum_{m\in L'-L} \left(P'^m - \frac{1}{t'-t}\right)\langle n\rangle_m \, , \qquad (4.7)$$

where $P'^m \equiv (N-t')^{-1} \sum_{\ell \in L'} P'^m_\ell$ are the lattice-averaged capture probabilities. That is, given the $\langle n \rangle_\ell$, we need only calculate the P'^m to determine $\langle n \rangle'$.

Returning to the example of an adjacent pair of traps, walk lengths for the case where neighboring sites 1 and 2 are decimated can be obtained from (4.6) as

$$\langle n \rangle'_j = \langle n \rangle_j - (P^1_j \langle n \rangle_1 + P^2_j \langle n \rangle_2)$$

$$= \sum_i [(\underline{\underline{A}}^{-1})_{ji} - P^1_j (\underline{\underline{A}}^{-1})_{1i} - P^2_j (\underline{\underline{A}}^{-1})_{2i}] \quad , \quad \text{for } j>3 \quad . \qquad (4.8)$$

An alternative and more complete understanding of this result comes from the observation that (see Appendix C)

$$(\underline{\underline{A}}(3)^{-1})_{ji} = (\underline{\underline{A}}^{-1})_{ji} - P'_j (\underline{\underline{A}}^{-1})_{1i} - P^2_j (\underline{\underline{A}}^{-1})_{2i} \quad , \quad \text{for } i,j>3 \ , \qquad (4.9)$$

and, thus, that the sum in (4.8) can be taken over $i>3$ only (rather than $i>1$). Equation (4.9) is characteristic of the general relationship between inverses of fundamental matrices for the original and decimated problems. Each row of the decimated inverse is obtained from the corresponding row of the original inverse after subtracting a trapping probability weighted average of rows (in the original inverse) corresponding to sites decimated to traps. This result generalizes the procedure given by Walsh and Kozak for some simple special cases[19].

Finally we consider the mean walk lengths, $\langle n\rangle_{\ell}^{i}$, for a walker starting at site ℓ to be adsorbed at trap ℓ_T^i. Clearly one has that

$$P_{\ell}^{i}\,\langle n\rangle_{\ell}^{i} = \frac{1}{4}\sum_{m}{}' P_{m}^{i}(\langle n\rangle_{m}^{i} + 1) \quad , \quad \ell \notin L \quad , \tag{4.10}$$

which can be solved for the $\langle n\rangle_{\ell}^{i}$ given knowledge of the P_{ℓ}^{i} from (4.4). Equation (4.10) implies that $(\sum_{i=1}^{t} P_{\ell}^{i}\langle n\rangle_{\ell}^{i}) = \frac{1}{4}\sum_{m}{}' [(\sum_{i=1}^{t} P_{m}^{i}\,\langle n\rangle_{m}^{i}) + 1]$ consistent with the requirement that $\langle n\rangle_{\ell} \equiv \sum_{i=1}^{t} P_{\ell}^{i}\,\langle n\rangle_{\ell}^{i}$ (cf. (4.1)). We can now also calculate trap-(i)-specific lattice average walk lengths

$$\langle n\rangle^{i} \equiv \frac{1}{N-t}\sum_{\ell\notin L} P_{\ell}^{i}\,\langle n\rangle_{\ell}^{i} \,/\, P^{i} \quad , \tag{4.11}$$

which satisfy $\langle n\rangle = \sum_{i=1}^{t} P^{i}\,\langle n\rangle^{i}$, as required.

Finally we return to the example of a decimated pair of traps (where the decimated sites adjacent to the pair are denoted by 1 and 2 as in Fig. 5). In Table X, we have given values for $\langle n\rangle^{1}$ and $\langle n\rangle^{2}$ for a range of lattice sizes. These can be interpreted as lattice-averaged walk lengths for the formation of bent and linear trimers, respectively.

Table X: Random walks on an LxL square lattice after decimating an adjacent pair of traps (producing six additional traps, four on the sides and two on the ends). Values of the corresponding trap-specific average walk lengths are given for various L

L	<n> side	<n> end
4	3.00000	3.00000
6	11.6082	11.3790
8	28.8432	28.7467
10	56.2841	56.3201
12	95.1143	95.2663
14	146.294	146.548
16	210.632	210.976
18	288.824	289.248
20	381.481	381.978
22	489.149	489.713
24	612.322	612.947
26	751.447	752.129
28	906936	907.671
30	1079.17	1079.96

V. CONCLUSIONS

We have shown that the formulation of Montroll can be developed to provide explicit results for the large lattice size (N) asymptotic behavior of trapping probabilities and walk lengths on a lattice with multiple traps. Procedures for exact calculation of these quantities on finite lattices ($N \lesssim 10^3$) were developed. A simple characterization of the reduction of walk lengths for a decimated problem (as compared with the original) leads to an elucidation of the relationship of the matrix structure for the two problems. All of the finite square lattice results presented here are for LxL (square) rather than rectangular lattices. However, the techniques of analysis described here readily extend to the latter case and results for symmetric nearest-neighbor random walks for some corresponding δ values (as defined by $\langle n \rangle = \frac{N}{N-t}\left[\frac{1}{\pi} N \ln N + (0.195056-\delta)N\right]$) are shown in Fig. 6.

These results for $N\to\infty$ trapping probabilities are particularly significant in the context of Witten-Sander particle-cluster aggregation,[13] where it is clear that these determine the shape distribution of clusters formed. This applies in the standard case where the cluster nucleates around a single filled site as well as to generalizations, where a (nearby) pair, triple, ... of filled sites act as nucleation centers.[20]

For another application, we consider a process where a gas of random walkers irreversibly aggregate forming immobile clusters (a Brownian aggregation process). Mean-field-type kinetic equations for the cluster-

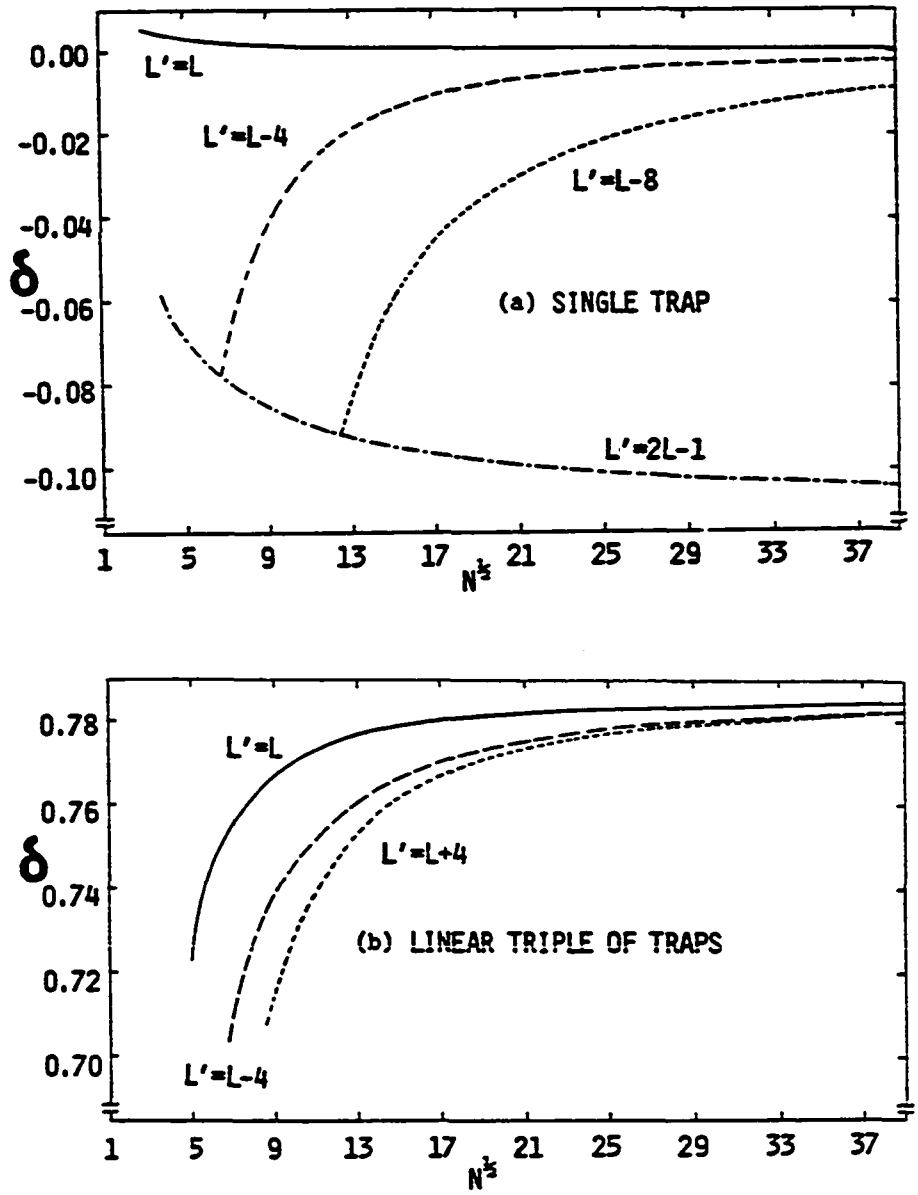

Figure 6: Values of δ in $\langle n \rangle = \frac{N}{N-t}\left[\frac{1}{\pi} N \ell n\, N + (0.195056-\delta)N\right]$ are shown for random walks on various LxL' square lattices (of N = LxL' sites) with (a) a single trap, (b) a linear triple of traps aligned with the side of length L. When $L \to \infty$ with L-L' constant, δ converges to the L = L' value. The deviation from this limit when, e.g., $L \to \infty$ with L' = 2L-1, is exactly accounted for by a change in c_2 in (2.11a)

size (and shape) distribution in this process are based on identification of appropriate rates for formation and destruction of clusters by aggregation with individual walkers (at the simplest level, ignoring the effect of a walker irreversibly linking two smaller clusters to form a larger one). Each of the former rates is naturally related to (the reciprocal of) the average walk length for a random walk on a suitable sized (N_t) lattice with an appropriate decimated cluster of traps. This time-dependent size, N_t, is naturally related to the reciprocal of the density, ρ_c, of clusters of one or more atoms. To see this, one thinks of dividing the lattice into regions of size $N_t = 1/\rho_c$ about each such cluster, and considering the fate (i.e., the average walk length) of an additional "test" walker artificially confined to one such region. To assess the validity of this scheme for determining rates, we have performed direct simulations involving a single walker on a lattice with several immobile clusters [where destruction rates are taken as the capture probabilities divided by the average walk length (for capture anywhere)]. These indicate that a choice of equal-sized (N_t) regions, for all clusters overestimates (underestimates) destruction rates for larger (smaller) clusters, so a larger (smaller) region should be associated with larger (smaller) clusters. In fact, it appears that the sizes of these regions should be chosen so as to equalize average walk lengths, and then (for comparison with the walker–multiple-cluster simulations) destruction rates are taken as the fraction of the total unoccupied area associated with regions surrounding clusters of the size and shape under consideration, divided by this equalized walk length. Corresponding

shape-specific creation rates involve an additional appropriate capture probability factor. The resulting kinetic equations do not have the standard Smoluchowski form[21] because of the complicated functional dependence of average walk lengths on N. Such equations will be investigated in later work.

The analysis here can be extended to include the effect of attractive or repulsive interactions in particle-cluster aggregation[22] by introducing more traps surrounding the cluster or introducing trapping probabilities less than unity, respectively. A further natural extension involves calculation of (complete) walk-length distributions (rather than just the means). Its use in the analysis of simple single-cluster growth models has already been suggested[23]. These distributions could also be applied to the development of non-Markovian kinetic equations for Brownian aggregation. Finally we remark on the need for a more sophisticated analysis of the appropriate t×t determinant structure for a large number of traps, t, in order to provide a more detailed understanding of the basic quantities of interest in this regime. For example, we would like quantitative estimates of the shielding effect by the arms of fractal clusters (from trapping close to the cluster nucleus).

ACKNOWLEDGEMENTS

The work of J. W. Evans was supported by the Ames Laboratory Applied Mathematical Sciences Program. Ames Laboratory is operated for the U.S. Department of Energy by Iowa State University under Contract No. W-7405-ENG-82. This work was supported by the Office of Basic Energy Sciences.

APPENDIX A: DETERMINANTS VIA COATES GRAPHS

Evaluation of $\det\{g_{ij}\}$, where $1 \le i,j \le t$, can be achieved by first constructing a Coates flow graph, G, involving points 1, 2, $\cdots$, t where each nonzero g_{ij} is represented by a directed bond from i to j, with "transmittance" g_{ij}. If H is a subgraph of G, then $\pi(H)$ denotes the product of transmittances, and c(H) the number of one way circuits. Then one has that[14]

$$\det\{g_{ij}\} \equiv \det G = (-1)^t \sum_{H \in S} (-1)^{c(H)} \pi(H) \quad ,$$

where S is the set of spanning subgraphs in which each (disconnected) component is a one way circuit. The simplest application of this result here is the determination of $\det\{\varepsilon_{ij}\}$ where $\varepsilon_{ij} = \varepsilon_{ji}$ and $\varepsilon_{ii} = 0$. Some examples are given in Fig. 7. Examples for the more complicated determination of $\begin{vmatrix} 1 & \varepsilon_{12} & \varepsilon_{13} & \cdots \\ 1 & \vdots & \vdots & \\ \vdots & \vdots & \vdots & \end{vmatrix}$ are shown in Fig. 8. Here summation over permutations of labels, leads to expressions for S_t.

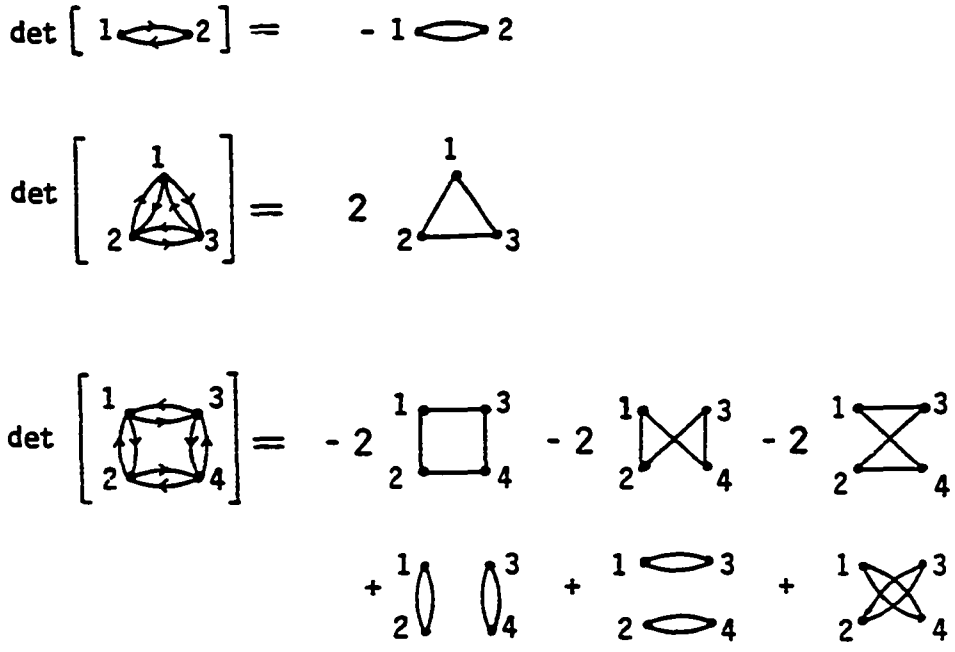

Figure 7: Diagramatic representation of det $\{\varepsilon_{ij}\}$ for t = 2,3,4,... . Each line on the r.h.s. represents a factor of ε_{ij}. Factors of 2 are associated with circuits of more than two points since the flow can have two directions (flow arrows can be dropped since $\varepsilon_{ij} = \varepsilon_{ji}$)

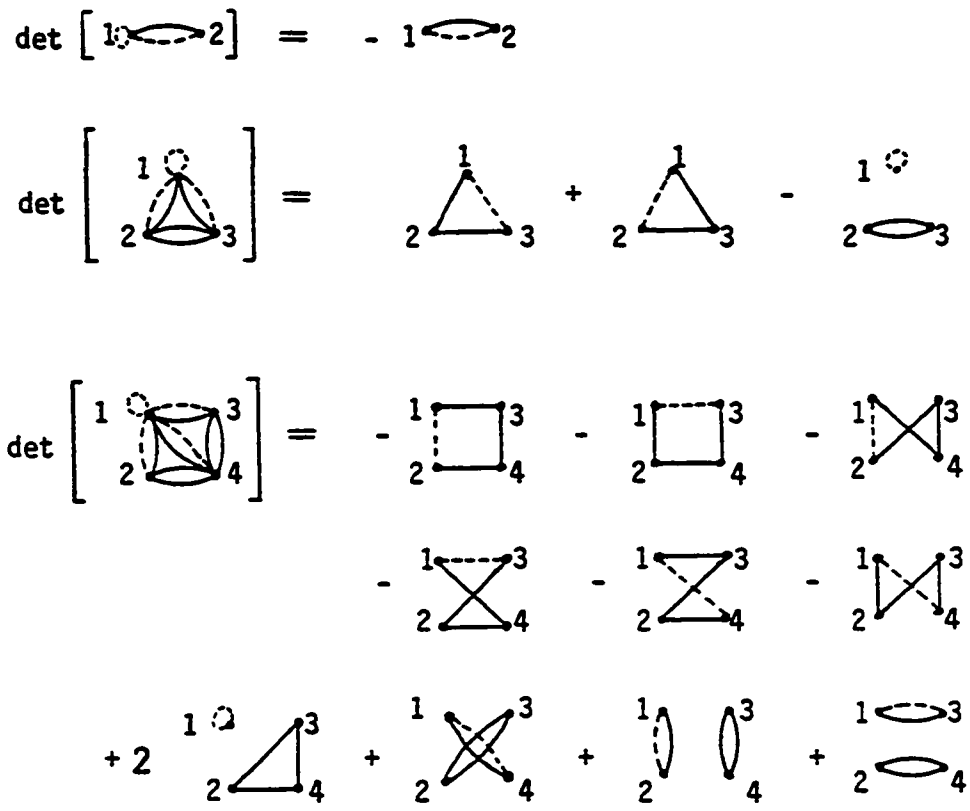

Figure 8: Diagramatic representation of $\begin{vmatrix} 1 & \varepsilon_{12} & \varepsilon_{13} \cdots \\ 1 & \varepsilon_{22} & \varepsilon_{23} \cdots \\ \vdots & \vdots & \vdots \end{vmatrix}$

for t = 2,3,4,.. Each line on the r.h.s. represents a factor of ε_{ij}. Dashed lines representing factors of unity transmittance are included for completeness only, and can be ignored

APPENDIX B: RANDOM WALKS ON A TRIANGULAR LATTICE WITH TRAPS

It is convenient to shear the triangular lattice, as described by Montroll[3], so that its sites superimpose those of a square lattice (see Fig. 9). Again we set $\varepsilon_{ij} = \varepsilon_0(r,s) + O(N^{-1/2})$, where r(s) denotes the horizontal (vertical) separation, in lattice vectors, between sites i and j. Here we determine only the dominant $N\to\infty$ behavior, $\varepsilon_0(r,s)$, of $\varepsilon(r,s)$ which is given in terms of the triangular lattice structure function $\lambda(\theta_1,\theta_2) = \frac{1}{3}[\cos\theta_1+\cos\theta_2+\cos(\theta_1-\theta_2)]$, as

$$\varepsilon_0(r,s) = \frac{1}{(2\pi)^2}\int_{-\pi}^{+\pi} d\theta_1 \int_{-\pi}^{+\pi} d\theta_2\, [\cos(r\theta_1)\cos(s\theta_2) - \sin(r\theta_1)\sin(s\theta_2) - 1]/[1-\lambda(\theta_1,\theta_2)].$$

It is a straightforward matter to show that[24]

$$\varepsilon_0(r,0) = -\frac{3}{2\pi}\int_{-\pi}^{\pi} d\theta_1 \frac{1-\cos(r\theta_1)}{(1-\cos\theta_1)^{1/2}(7-\cos\theta_1)^{1/2}}$$

$$= -\frac{3}{\pi}\int_{-1}^{+1} dx \frac{F_{|r|-1}(x)}{(1+x)^{1/2}(7-x)^{1/2}} \quad ,$$

where $F_r \equiv (1 - T_{r+1})/(1-x)$, as previously. Clearly $\varepsilon_0(r,0) \sim -\frac{2}{\pi}\,\text{ln}\, r$ from analogous arguments to those given in Section III. A more complicated analysis shows that[21]

$$\varepsilon_0(r,1) = \frac{3}{4\pi}\int_{-\pi}^{+\pi} d\theta_1 K_r(\cos\theta_1) - \frac{3}{4\pi}\int_{-\pi}^{+\pi} d\theta_1 \frac{2+K_r(\cos\theta_1)(3-\cos\theta_1)}{(1-\cos\theta_1)^{1/2}(7-\cos\theta_1)^{1/2}} \quad ,$$

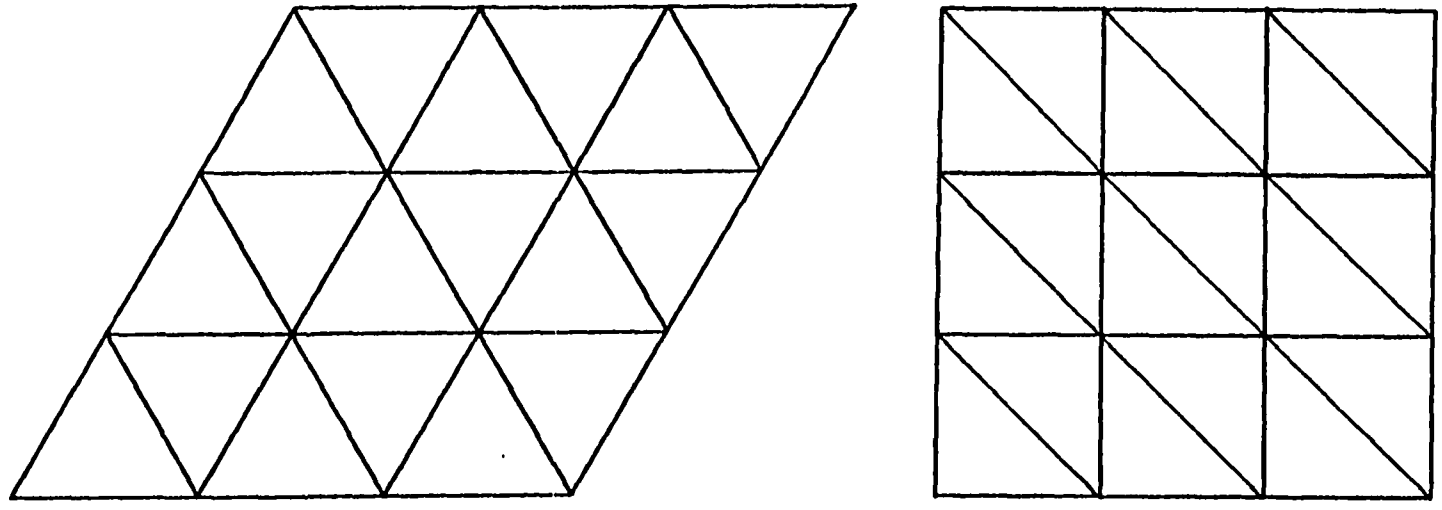

Figure 9: Shearing of a triangular lattice so that its sites are superimposed on those of a square lattice

where $K_r(\cos\theta) = \frac{\sin(r\theta)\sin\theta}{1+\cos\theta} - \cos(r\theta) = \text{sgn } r\ (1-x)\ U_{|r|-1}(x) - T_{|r|}(x)$, with $x=\cos\theta$, sgn r = -1, 0, 1 for $r < 0$, $= 0$, > 0 respectively, and U_r denoting the r^{th}-order Tschebysheff polynomial of the second kind. The second integral can be reexpressed as

$$-\frac{3}{2\pi}\int_{-1}^{+1} dx\ \frac{\text{sgn } r\ (1-x)U_{|r|-1}(x)-\tilde{F}_{|r|}(x)}{(1+x)^{1/2}(7-x)^{1/2}} \quad ,$$

where $\tilde{F}_r(x) \equiv [(3-x)T_r(x)-2]/(1-x)$ is an r^{th}-order polynomial.

Clearly these integrals for $\varepsilon_0(r,0)$ and $\varepsilon_0(r,1)$ can be evaluated exactly, and one obtains, e.g.,

$$\varepsilon_0(1,0) = -1,\ \varepsilon_0(2,0) = -8 + 6\sqrt{12}/\pi,\ \varepsilon_0(3,0) = -81 + 72\sqrt{12}/\pi,\ \cdots$$

$$\varepsilon_0(0,1) = -1,\ \varepsilon_0(1,1) = 2 - 3\sqrt{12}/\pi,\ \varepsilon_0(2,0) = 15 - 15\sqrt{12}/\pi,\ \cdots\ .$$

From Fig. 9, it is also obvious that there are various equivalences between the $\varepsilon_0(r,s)$. For example, one must have that $\varepsilon_0(1,0) = \varepsilon_0(0,1) = \varepsilon_0(-1,0) = \varepsilon_0(0,-1) = \varepsilon_0(1,-1) = \varepsilon_0(-1,1)$, and $\varepsilon_0(-j,k) = \varepsilon_0(j-k,k)$. Such equalities are not transparent in the above expressions, however it is obvious, using the basic defining expression for $\varepsilon_0(r,s)$, that the six ε_0's for nearest-neighbor sites (listed above) sum to -6. These results are used in the following calculations.

For a linear, bent, triangular triple of connected traps ℓ^1, ℓ^2, ℓ^3 (where ℓ^2 is central) we obtain from (2.20) that, as $N\to\infty$, $\bar{P}_\infty(\ell^{1,3}):\bar{P}_\infty(\ell^2) =$

1:$-6+6\sqrt{12}/\pi$, 1:$72\sqrt{12}/\pi-79$, 1:1 respectively (so $\bar{P}_\infty(\ell^1,3) \approx .3823, .3715, .3333$, and $P_\infty(\ell^2) \approx .2355, .2571, .3333$, respectively). For a trap, ℓ^1, surrounded by six other traps, the determinant associated with $\bar{P}_\infty(\ell^1)$, as $N\to\infty$, can be shown to vanish since all of its rows sum to -7 (cf. (3.8)). The change from single trap behavior in the average walk length, $\langle n\rangle$, is reflected by $\delta = -\det\{\varepsilon_{ij}\}/S_t$ (cf. (2.22)). As $N\to\infty$, we have that $\delta = 1/2$ for an adjacent pair of traps, and $\delta = \pi(3\sqrt{12}-2\pi)^{-1}, \frac{2\pi}{3}(2\pi-\sqrt{12})^{-1}, 2/3$ for a linear, bent, triangular connected triple of traps, respectively.

APPENDIX C: INVERSES OF DECIMATED FUNDAMENTAL MATRICES

Let $\underline{\underline{A}}$ denote the "fundamental" matrix for some multiple-trap problem, and $\underline{\underline{\tilde{A}}}$ the "fundamental" matrix for some corresponding decimated problem. We shall thus write

$$\underline{\underline{A}} = \begin{bmatrix} \underline{\underline{B}} & \underline{\underline{C}} \\ \underline{\underline{D}} & \underline{\underline{\tilde{A}}} \end{bmatrix} \quad \text{and} \quad \underline{\underline{A}}^{-1} = \begin{bmatrix} \underline{\underline{X}} & \underline{\underline{Y}} \\ \underline{\underline{Z}} & \underline{\underline{U}} \end{bmatrix} .$$

Then from the standard relations $\underline{\underline{U}} = (\underline{\underline{\tilde{A}}} - \underline{\underline{D}}\underline{\underline{B}}^{-1}\underline{\underline{C}})^{-1}$ and $\underline{\underline{Y}} = -\underline{\underline{B}}^{-1}\underline{\underline{C}}\underline{\underline{U}}$, one has that $\underline{\underline{\tilde{A}}}^{-1} = \underline{\underline{U}} + \underline{\underline{\tilde{A}}}^{-1}\underline{\underline{D}}\underline{\underline{Y}}$ or

$$(\underline{\underline{\tilde{A}}}^{-1})_{ji} = (\underline{\underline{U}})_{ji} + \sum_k \left[\sum_m (\underline{\underline{\tilde{A}}}^{-1})_{jm} (\underline{\underline{D}})_{mk}\right] (\underline{\underline{Y}})_{ki} .$$

Finally from (4.4) (or (4.5)), one can straightforwardly make the identification

$$p_j^k \equiv \sum_m (\underline{\underline{\tilde{A}}}^{-1})_{jm} (\underline{\underline{D}})_{mk} ,$$

for the probability of capture at trap ℓ_T^k for a walker starting at site j.

REFERENCES

1. E. W. Montroll, Proc. Symp. Appl. Math., Am. Math. Soc. 16, 193 (1964).
2. E. W. Montroll and G. H. Weiss, J. Math. Phys. 6, 167 (1965).
3. E. W. Montroll, J. Math. Phys. 10, 753 (1969).
4. M. N. Barber and B. W. Ninham, "Random and Restricted Walks" (Gordon and Breach, New York, 1970).
5. G. H. Weiss and R. J. Rubin, "Random Walks: Theory and Selected Applications", in Adv. Chem. Phys. 52, 363 (1983).

6a. K. E. Shuler, H. Silver and K. Lindenberg, J. Stat. Phys. 15, 393 (1976).

6b. For this result to be valid, one would require that infinite square lattice behavior, $S_n \sim \pi n/\ell n\ n$, as $n\to\infty$, also applies to an LxL(=N site) square lattice (with periodic boundary conditions) for $n=O(N\ \ell n\ N)$. Clearly, the finite and infinite lattice S_n are equal for $0 \leq n \leq L-1$, and thereafter the former is smaller, approaching N as $n\to\infty$. For either a finite or infinite perfect lattice, one has that $S(z) = \sum_{n=0}^{\infty} z^n=(1-z)^{-2}G(0,z)^{-1}$, where G(0,z) is the corresponding generating function.[2] For an N-site square lattice $G(0,z) = N^{-1}(1-z)^{-1}+\Phi(0,z)$ (see (2.10)), and one can easily show that[2] $\Phi(0,z) \sim -\pi^{-1}\ell n(1-z)$, for $1 \gg 1-z \gg N^{-1}$, and that[3] $\Phi(0,z)\sim -\pi^{-1}\ell n\ N+c_1+c_2N^{-1} + \ldots + O(1-z)^{1/2}$, for $1 \gg N^{-1} \gg 1-z$. This suggests that the first (infinite lattice) form of $\Phi(0,z)$ is also valid for $1-z = O(N^{-1})$, and thus that the infinite lattice form of S_n is valid for $n \lesssim O(N)$.

7. H. B. Rosenstock, J. Math. Phys. 11, 487 (1970).

8. J. J. Ten Bosch and Th. W. Ruijgrok, J. Theor. Biol. 4, 225 (1963); R. S. Knox, J. Theor. Biol. 21, 244 (1968); J. W. Sanders, Th. W. Ruijgrok and J. J. Ten Bosch, J. Math. Phys. 12, 534 (1971).

9. C. A. Walsh and J. J. Kozak, Phys. Rev. Lett. 47, 1500 (1981); Phys. Rev. B 26, 4166 (1982).

10. P. A. Politowicz and J. J. Kozak, Phys. Rev. B 28, 5549 (1983).

11. E. W. Montroll, in Proceedings of the International Conference on Statistical Mechanics 1968, J. Phys. Soc. Japan, Suppl. 26, 6 (1969).

12. E. W. Montroll and B. J. West, in "Fluctuation Phenomena", Studies in Statistical Mechanics Vol. VII, Ed. E. W. Montroll and J. L. Lebowitz (North Holland, Amsterdam, 1979).

13. T. A. Witten and L. M. Sander, Phys. Rev. Lett. 47, 1400 (1982); Phys. Rev. B 27, 5686 (1983). Here each walker is introduced randomly at a large distance from the aggregating cluster and either walks in and sticks to the cluster or wanders out too far and is destroyed (before the next walker is introduced). In the large distance limit, trapping probabilities are clearly the same as the $N \to \infty$ lattice-averaged trapping probabilities obtained from our calculations (where almost all walkers have come in from an infinite distance).

14. See for example: S. Kirkpatrick, Rev. Mod. Phys. 45, 574 (1974); S. Kivelson, Phys. Rev. B 21, 5755 (1980); H. Scher and C. H. Wu, Proc. Nat. Acad. Sci. 78, 22 (1981).

15. F. Nielsen, in "Applications of Graph Theory" Ed. R. J. Wilson and L. W. Beineke (Academic, New York, 1979).

16. Note that if $\alpha_{ij} = 1 + \delta_{ij}a_i$, then $\det\{\alpha_{ij}\} = \prod_k a_k(1 + \sum_{k'} \frac{1}{a_{k'}})$.

17. A more detailed asymptotic analysis could follow that of Montroll[3]. One can straighforwardly show that the contribution to $\epsilon(r,s)$ from $k_1 = 0$ in (3•2) is given by $\frac{1}{3}(1 - 6s/L + 6s^2/L^2 - 1/L^2) + O(1-z)^{1/2}$.

18. $\frac{1}{\pi}\int_0^{\pi} d\theta\ (a + b\cos\theta)^{-1} = (a^2-b^2)^{-1/2}$, for $a^2>b^2$ and $a>b$.

19. The procedure outlined in Ref. 9 where a simple average is taken over all trap rows only applies in special cases where all trapping probabilities are equal.

20. T. A. Witten and P. Meakin, Phys. Rev. B 28, 5632 (1983).

21. R. Botet and R. Julien, J. Phys. A 17, 2517 (1984); R. K. Ziff in "Kinetics of Aggregation and Gelation," Ed. F. Family and D. Landau (Elsevier, Amsterdam, 1984).

22. P. Meakin, Phys. Rev. A 27, 604 and 1495 (1983); J. Chem. Phys. 79, 2426 (1983).

23. H. B. Rosenstock and C. L. Marquardt, Phys. Rev. B 22, 5797 (1980).

24. $\frac{1}{2\pi}\int_{-\pi}^{+\pi} d\theta(a + b\sin\theta + c\cos\theta)^{-1} = (a^2-b^2-c^2)^{-1/2}$, and
$\frac{1}{2\pi}\int_{-\pi}^{+\pi} d\theta\ \frac{A + B\sin\theta + C\cos\theta}{a + b\sin\theta + c\cos\theta} = \frac{Bb+Cc}{b^2+c^2} + (A - \frac{Bb+Cc}{b^2+c^2}a)(a^2-b^2-c^2)^{-1/2}$,
for $a^2>b^2+c^2$ and $a>c$.

MONTE CARLO SIMULATIONS

In order to test the accuracy of certain of our approximate truncation results, we have performed some Monte Carlo simulations of processes of interest. The particular systems we have chosen to look at are random dimer, linear and bent trimer, and square tetramer filling of a square lattice, from Paper I, and random dimer filling of a cubic lattice from Paper III.

To perform a naive Monte Carlo simulation of these random filling processes, a large lattice (referred to as the atomic lattice) is initially stored in the computer with all sites specified "empty". The computer's random number generator is then used to randomly pick a group of lattice sites which has the same configuration as the filling species. If these sites are all empty, a filling event occurs and these sites are now specified to be "filled". If one or more of the selected sites were already filled, no filling event can take place. The computer then randomly selects a new group of sites and the procedure is repeated until an arbitrary cutoff point is reached (typically, failing to fill the selected group of sites a certain number of consecutive times).

Here, we have chosen a more sophisticated approach where the filling processes were carried out on the event lattice, rather than on the atomic lattice, as monomer filling with a suitable blocking range (for a description of the event lattice see refs. (1) and (3) and Section V of Paper I). An illustration of 2D dimer filling on the atomic and event lattices is given in Fig. 2. The event lattice is initially stored, in the computer, with all sites specified "fillable". The computer then randomly

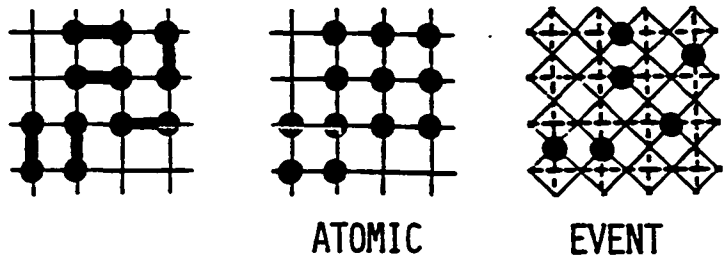

Figure 2: The atomic and event lattice pictures of dimer filling of a square lattice

picks a single site. If this site is fillable, then a filling event occurs and this site and an appropriate group of neighboring sites are specified "unfillable". If the site is unfillable, no filling event occurs. The event lattice is preferred over the atomic lattice since, to test whether or not a filling event can take place at any particular location, it is only necessary to test the state of a single site rather than a group of sites. The computer routine randomly tests and subsequently fills sites until it tests N consecutive times without filling any sites, where N is the number of sites in the lattice. At this point it tests all lattice sites to determine where filling is still possible and randomly fills these. During this last filling stage we lose our time scale, but since we are only interested in the final ($t\to\infty$) number of filling events, this is immaterial. To obtain the saturation coverage from the event lattice description, multiply the number of filling events by the number of lattice sites filled, in the atomic lattice description, during each filling event (e.g., by 2 for dimer filling, by 3 for trimer filling, ...) and then divide by the total number of sites in the lattice.

In order to minimize the effects due to finite lattice size, the simulations were all carried out on lattices with periodic (cyclic) boundary conditions. The lattice size, N, was also varied in order to detect any dependance of the saturation coverage, θ^{sat}, upon N. 50 trials were run at each lattice size. Typically, trials were run at approximately 9 different lattice sizes with N varying from 400 to as large as 160,000.

In order to obtain θ^{sat} for the infinite lattice we performed a weighted linear regression of θ^{sat} vs. d/L where d is the lattice dimension

and L is the length of one side (the number of sites in the lattice, $N = L^d$). For 1D a-mer filling, Mackenzie[18] showed that $\sigma^2 = (1 + a/N)(a/N) A_2(a)$ where $A_2(a)$ is some function of a and σ^2 is the variance. For the infinite lattice ($N \gg a$) this result simplifies to $N\sigma^2 = aA_2(a)$. Calculations by Page[7] support Mackenzie's work. Wolf[1] showed that $N\sigma^2 \approx$ const for 1D dimer filling and his arguments can be straightforwardly extended to higher dimensions (the observation that $N\sigma^2 \approx$ const was also made by Jodrey and Tory[67] for the random packing of d-dimensional hypercubes). Therefore, we expect for the processes considered here that $\sigma^2 \propto 1/N$. Consequently, we weight each data point by N.

After calculating the linear regression we found that in every case the magnitude of the slope was less than the uncertainty in the slope. Consequently, we also calculated the weighted mean for each case and found it to be effectively as good a fit to the data (similar reduced chi square and no systematic trend in the residuals). Therefore, we feel the linear regression is unnecessary, and that the periodic boundary conditions effectively eliminate the edge effects (this conclusion is in agreement with the results of Jodrey and Tory[67]). The weighted means of the saturation coverage are given in Table I (with ±'s presented as 95% confidence limits, calculated using only the point representing the mean for each different lattice size) along with the results from our most accurate truncation scheme.

From Table I one can immediately see the accuracy of the truncation results for the more compact species. Only for the linear trimer (which requires the thickest shielding wall) is the error greater than 1% (as was

anticipated in Section VI of Paper I). These results clearly demonstrate the reliability of the techniques which we have employed here.

Table I: Saturation coverage estimates from Monte Carlo simulations and truncation techniques for various random filling processes

Filling Species	Lattice	Saturation Coverage	
		Monte Carlo	Truncation
Dimer	square	0.90687 ± 0.00014	0.9068
Linear Trimer	square	0.84659 ± 0.00015	0.8366
Bent Trimer	square	0.83330 ± 0.00023	0.83334
Square Tetramer	square	0.74788 ± 0.00011	0.748
Dimer	cubic	0.91838 ± 0.00018	0.91546

CONCLUSIONS

Summary of Main Results

In this thesis we have been concerned with various aspects of the mathematical modeling of irreversible, random and cooperative processes on lattices. The main contributions which have been made can be summarized as follows:

(a) For random dimer, trimer, and tetramer filling of infinite 2D lattices, we have demonstrated that the hierarchial truncation techniques can produce accurate estimates of the time dependence of the probabilities for various small configurations and estimates of the saturation coverage (see Paper I).

(b) We have generated 2D random dimer filling results which are the most accurate, and extensive, available. They provide sufficient insight into the shielding propensity of sites to motivate and justify a "shortest unshielded path" truncation procedure (see Paper I).

(c) We have provided the first analysis of, and specific results for, 2D random trimer filling (see Paper I).

(d) We have developed a sophisticated treatment of processes involving competitive, irreversible (immobile), random filling of monomers, dimers, ... on 2D lattices. These are the first such results for non-trivial, competitive, irreversible lattice processes in 2D (see Paper II).

(e) A reliable description of the kinetics of random dimer filling of the 3D cubic lattice (focusing on probabilities of smaller subconfigurations) has been obtained, including estimates of the saturation

coverage. This is the first time that a nontrivial irreversible process on a 3D lattice has been explicitly treated by exploiting the structure of the corresponding exact hierarchial rate equations (see Paper III).

(f) We have explicitly analyzed the effect of a stochastically specified distribution of inactive sites on a random filling process (see Paper III).

(g) We have provided the first extensive, exact analytic investigation of the filled cluster-size distribution for a 1D irreversible, cooperative filling process. Our calculations cover a large enough size range to determine the asymptotic decay behavior (see Papers IV and V).

(h) A novel approach for the direct extraction of asymptotic properties of the cluster-size distribution from the suitably recast hierarchial equations has been developed. This technique may also prove to be applicable to higher-dimensional irreversible filling processes (see Paper IV).

(i) We have developed the formulation of Montroll[68] to provide explicit results for the large-lattice-size asymptotic behavior of trapping probabilities and average walk lengths for a single random walker on a lattice with multiple traps. Procedures for exact calculation of these quantities on finite lattices were developed as well (see Paper VI).

(j) We have performed Monte Carlo simulations of certain processes of interest in order to test the accuracy of our approximate truncation results. The results of our simulations clearly demonstrate the reliability of the truncation technques which we have employed here.

Extensions

There still remains much room for additional improvements, extensions, and applications of the models used here. A brief description of present and future work, some of which is nearly completed, follows.

Many extensions of earlier 1D results to two (and higher) dimensions are possible. Some basic problems to be considered include the analysis of the large separation behavior of the two-point correlations, the effect of limited mobility, and the extension of the asymptotic cluster-size distribution analysis in higher dimensions. Preliminary development of the long range correlations for the 2D random dimer filling problem has already been made[17] and in Paper IV the extension of the asymptotic cluster-size distribution analysis has been clearly outlined.

Improvement upon our approximate truncation techniques is a goal, particularly if we wish to consider the filling of large species, or filling with more extreme or longer range cooperative effects. In Paper I we presented the "shortest unshielded path" (s.u.p.) truncation which served to reduce the number of equations at a particular truncation order by truncating conditioning sites which had only a small influence on the conditioned site of interest. However, these new configurations tend to be more disconnected and seem to cause some problems in the numerical integration routine near saturation. As a result we have since combined a higher order s.u.p. truncation with a lower order sever truncation to truncate only those sites which both truncations would remove. This hybrid truncation, thus, still removes those distant conditioning sites (which do not significantly influence the conditioned site, but greatly increase the

number of equations), and keeps all of the closer conditioning sites which lead to compact, connected configurations whose probability rate equations are easily integrated. Further refinements are still necessary, but this new truncation shows some promise.

Some additional higher-dimensional features which have not been addressed in detail include the effects of the lattice coordination number and the effects due to the shape of the filling species (e.g., bent vs. linear trimers).

Another effect which needs to be expanded upon in higher dimensions is the effect of an edge or a corner; the former can be applied to the study of terraces in 2D, and both can be used to study finite size effects. Issues which need addressing include the distance dependence of the dissipation of edge effects and the effects of finite size on infinite lattice results. Edge effects also play an important role in processes involving multiple-layer adsorption.

The effects of simultaneous vs. sequential filling mechanism, when the filling species occupies more than a single site, need to be addressed. Since Page[7] first pointed out the difference between conventional (simultaneous) and end-on (sequential) filling, no explicit acknowledgement that a difference exists has appeared in the literature prior to our work. Indeed, confusion on the point has led to difficulties and discrepancies in comparison of results (see ref. (33) and the Discussion section of Paper II).

A more general extension of these techniques is to continuous space filling problems (e.g., disk or sphere packing) as opposed to the discrete

lattice cases already considered. This type of extension has been successfully implemented in 1D by Wolf[1]. These problems should provide insights into the structure of liquids, crystals, and absorbates on surfaces. For instance, Feder[69] has proposed 2D sequential disk packing as a model for protein adsorption and for particles in a biological membrane.

There are many logical extensions to our work on random walks. The application to the Brownian aggregation process (a process where a gas of random walkers irreversibly aggregate to form immobile clusters) where growth rates are related to (average) walk lengths is a prime example. A natural extension of this is to calculate the complete walk-length distribution (rather than just the average) and use this to obtain more accurate rates. The use of the complete walk-length distribution in the analysis of single-cluster growth models has previously been suggested[70].

Additional areas to be pursued include extending the analyses to include complications such as attractive or repulsive forces between clusters and walkers[71] or the effect of limited mobility within a cluster which can lead to cluster rearrangement.

REFERENCES

1. N. O. Wolf, Ph. D. Thesis, Iowa State University, 1979.

2. I. Oppenheim, K. E. Shuler and G. H. Weiss, Stochastic Processes in Chemical Physics: The Master Equation (MIT Press, Cambridge, Mass., 1977).

3. D. R. Burgess, Ph. D. Thesis, Iowa State University, 1982.

4. J. W. Evans, D. R. Burgess and D. K. Hoffman, J. Chem. Phys. 79, 5011 (1983).

5. N. A. Platé, A. D. Litmanovich, O. V. Noah, A. L. Toam and N. B. Vasilyev, J. Polym. Sci. 12, 2165 (1974).

6. P. J. Flory, J. Am. Chem. Soc. 61, 1518 (1939).

7. E. S. Page, J. Roy. Stat. Soc. B 21, 364 (1959).

8. E. R. Cohen and H. Reiss, J. Chem. Phys. 38, 680 (1963).

9. R. B. McQuistan and D. Lichtman, J. Math. Phys. 9, 1680 (1968); R. B. McQuistan, J. Math. Phys. 10, 2205 (1969).

10. A. Maltz and E. E. Mola, J. Math. Phys. 22, 1746 (1981).

11. B. Widom, J. Chem. Phys. 44, 3888 (1968); J. Chem. Phys. 58, 4043 (1973).

12. W. H. Olson, J. Appl. Prob. 15, 835 (1978).

13. T. H. K. Barron and E. A. Boucher, Trans. Faraday Soc. 65, 3301 (1969).

14. T. H. K. Barron, R. J. Bawden and E. A. Boucher, Trans. Faraday Soc. 70, 651 (1974).

15. F. Downton, J. Roy, Stat. Soc. B 23, 207 (1961).

16. K. J. Vette, T. W. Orent, D. K. Hoffman and R. S. Hansen, J. Chem. Phys. 60, 4854 (1974).

17. J. W. Evans, D. R. Burgess and D. K. Hoffman, J. Math. Phys. 25, 3051 (1984).

18. J. K. Mackenzie, J. Chem. Phys. 37, 723 (1962).

19. M. Gordon and I. H. Hillier, J. Chem. Phys. 38, 1376 (1963).

20. E. A. Boucher, Chem. Phys. Lett. 17, 221 (1972); J. Chem. Phys. 59, 3848 (1973); Faraday Trans. II 69, 1839 (1973).

21. I. R. Epstein, Biophysical Chemistry 8, 327 (1978); Biopolymers 18, 765 (1979).

22. A. Maltz and E. E. Mola, Surf. Sci. 115, 599 (1982); J. Chem. Phys. 79, 5141 (1983).

23. N. O. Wolf, J. W. Evans and D. K. Hoffman, J. Math. Phys. 25, 2519 (1984).

24. F. Gornick and J. L. Jackson, J. Chem. Phys. 38, 1150 (1963).

25. J. L. Jackson and E. W. Montroll, J. Chem. Phys. 28, 1101 (1958).

26. J. K. Roberts, Nature 135, 1037 (1935); Proc. Roy. Soc. A 152, 473 (1935); Proc. Roy. Soc. A 161, 141 (1937); Proc. Camb. Phil. Soc. 34, 399 (1938).

27. D. R. Rossington and R. Borst, Surf. Sci. 3, 202 (1965).

28. J. B. Peri, J. Chem. Phys. 69, 220 (1965).

29. J. B. Peri and A. L. Hensley, Jr., J. Phys. Chem. 72, 2926 (1968).

30. P. T. Dawson and Y. K. Peng, Surf. Sci. 33, 565 (1972).

31. W. D. Dong, Surf. Sci. 42, 609 (1974).

32. E. L. Fuller, S. Ebey and V. R. R. Uppuluri, "Statistical Modelling of Adsorption Processes on Catalyst Surfaces: Preliminary Report", ORNL-5231, Oak Ridge National Laboratory, Oak Ridge, Tenessee (1976).

33. B. E. Hayden and D. F. Klemperer, Surf. Sci. 80, 401 (1979).

34. R. B. McQuistan, D. Lichtman and L. P. Levine, Surf. Sci. 20, 401 (1970).

35. B. E. Blaisdell and H. Solomon, J. Appl. Prob. 7, 667 (1970); J. Appl. Prob. 19, 382 (1982).

36. J. B. Keller, J. Phys. Chem. 37, 2584 (1962); J. Chem. Phys. 38, 325 (1963).

37. T. Alfrey, Jr. and W. G. Lloyd, J. Chem. Phys. 38, 318 (1963).

38. C. B. Arends, J. Chem. Phys. 38, 322 (1963).

39. D. A. McQuarrie, J. P. McTague and H. Reiss, Biopolymers 3, 657 (1965).

40. B. H. Zimm and J. K. Bragg, J. Chem. Phys. 31, 526 (1959).

41. N. Gō, J. Phys. Soc. Jap. 22, 413 (1967); J. Phys. Soc. Jap. 22, 416 (1967).

42. R. Kikuchi, Ann. Phys. 10, 127 (1960).

43. G. Schwarz, Ber. Bunsenges. Phys. Chem. 75, 40 (1971).

44. R. L. Dobrushin, Probl. Peredachi Inf. 7, 57 (1971).

45. L. G. Mityushin, Probl. Peredachi Inf. 9, 81 (1973).

46. J. J. Gonzalez, P. C. Hemmer and J. S. Høye, J. Chem. Phys. 3, 228 (1974).

47. J. J. Gonzalez and P. C. Hemmer, J. Polym. Sci., Polym. Lett. 14, 645 (1976).

48. P. C. Hemmer and J. J. Gonzalez, J. Polym. Sci. 15, 321 (1977).

49. J. J. Gonzalez and P. C. Hemmer, J. Chem. Phys. 67, 2496 (1977); J. Chem. Phys. 67, 2509 (1977).

50. J. J. Gonzalez, Macromolecules 11, 1074 (1978).

51. M. Higuchi and R. Senju, Polym. J. 3, 370 (1972).

52. J. W. Evans and D. R. Burgess, J. Chem. Phys. 70, 5023 (1983).

53. J. W. Evans, D. K. Hoffman and D. R. Burgess, J. Chem. Phys. 80, 963 (1984).

54. B. Mellein and E. E. Mola, J. Matn. Phys. 26, 514 (1985); B. Mellein, J. Math. Phys. 26, 1769 and 2930 (1985).

55. J. W. Evans and D. K. Hoffman, Phys. Rev. B 30, 2704 (1984).

56. J. W. Evans, J. Math. Phys. 25, 2527 (1984).

57. J. W. Evans and D. K. Hoffman, J. Stat. Phys. 36, 65 (1984).

58. R. Rosei, F. Ciccacci, R. Memeo, C. Mariani, L. S. Caputi and L. Papagno, J. Catalysis 3, 19 (1983).

59. D. K. Hoffman, J. Chem. Phys. 65, 95 (1976).

60. J. W. Evans, Physica 123A, 297 (1984).

61. D. Knodel and D. K. Hoffman, J. Chem. Phys. 69, 3438 (1978).

62. D. J. Dwyer, G. W. Simmons and R. P. Wei, Surf. Sci. 64, 617 (1977).

63. N. O. Wolf, D. R. Burgess and D. K. Hoffman, Surf. Sci. 100, 453 (1980).

64. J. J. Gonzalez and K. W. Kehr, Macromolecules 11, 996 (1978).

65. E. Klesper, W. Gronski and V. Barth, Makromol. Chemie 150, 223 (1971); Makromol. Chemie 160, 167 (1972).

66. T. A. Witten and L. M. Sander, Phys. Rev. Lett. 47, 1400 (1982); Phys. Rev. B 27, 5686 (1983).

67. W. S. Jodrey and E. M. Tory, J. Statist. Comput. Simul. 10, 87 (1980).

68. E. W. Montroll, in Proceedings of the International Conference on Statistical Mechanics, 1968 [J. Phys. Soc. Jpn., Suppl. 26, 6 (1969)].

69. J. Feder, J. Theor. Biol. 87, 237 (1980).

70. H. B. Rosenstock and C. L. Marquardt, Phys. Rev. B 22, 5797 (1980).

71. P. Meakin, Phys. Rev. A 27, 604 (1983); Phys. Rev. A 27, 1495 (1983); J. Chem. Phys. 79, 2426 (1983).

ACKNOWLEDGMENTS

I would like to thank Dr. David Hoffman, my major professor, for the support and guidance he has given me throughout my graduate career. I greatly admire and respect him and hope to pass along to my future students what I have learned from him. Dr. Jim Evans has been an outstanding person to be associated with and I gratefully acknowledge his immeasurable contribution to the work presented here. I have appreciated the support of the other members of Dr. Hoffman's group during my graduate study (Dave Burgess, Bob Cole, C. K. Chan, Thom Hendrixson, and David Sanders), as well of that of the other graduate students (with a special thanks to Bob Crackel) and faculty. Finally, I would like to acknowledge the support and help provided me by my family. In particular, I wish to thank my wife, Janet, for her caring and support through these years and my parents whose faith and encouragement have helped me to attain my goals throughout my life.